
# PERFORMANCE MODELLING AND VALIDATION OF BIOMASS GASIFIERS FOR TRIGENERATION PLANTS

**Maria Puig Arnavat**

**Dipòsit Legal: T. 1718-2011**

Maria Puig Arnavat

# PERFORMANCE MODELLING AND VALIDATION OF BIOMASS GASIFIERS FOR TRIGENERATION PLANTS

DOCTORAL THESIS

Supervisors
Prof. Dr. Alberto Coronas
Dr. Joan Carles Bruno

Department of Mechanical Engineering

UNIVERSITAT ROVIRA I VIRGILI

Tarragona, October 2011

UNIVERSITAT
ROVIRA I VIRGILI
DEPARTAMENT D'ENGINYERIA MECÀNICA
Escola Tècnica Superior d'Enginyeria Química (ETSEQ).
Av. Països Catalans 26. 43007 Tarragona (Spain)

Los abajo firmantes, Dr. Alberto Coronas, Catedrático de Universidad del área de Máquinas y Motores Térmicos y Dr. Joan Carles Bruno, Profesor Agregado, del Departament d'Enginyeria Mecànica de la Universitat Rovira i Virgili de Tarragona

**HACEN CONSTAR:**

Que el trabajo titulado: "PERFORMANCE MODELLING AND VALIDATION OF BIOMASS GASIFIERS FOR TRIGENERATION PLANTS" presentado por la Sra. Maria Puig Arnavat para optar al grado de Doctor de la Universitat Rovira i Virgili, ha sido realizado bajo su dirección inmediata en el CREVER – Grup de recerca d'Enginyeria Tèrmica Aplicada del Departament d'Enginyeria Mecànica de la Universitat Rovira i Virgili, que todos los resultados han sido obtenidos en las experiencias realizadas por dicho doctorando y que cumple los requisitos para poder optar a la Mención Europea.

Y para que así conste a los efectos oportunos, firmamos este documento.

Tarragona, 09 de Septiembre de 2011

# ACKNOWLEDGEMENTS

Acknowledgments are like a window to show the human side of all this work, and a fair opportunity to say everybody involved in this process thanks. Mentioning all people who deserve my gratitude without leaving someone out is quite a difficult task, but I will try to do my best.

First I would like to express my gratitude to my advisers Prof. Alberto Coronas and Dr. Joan Carles Bruno for the opportunities given and their support. I also acknowledge the financial support received from the European Comission under the European Project Polycity (Energy networks in sustainable communities) (TREN/05FP6EN/S07.43964/51381) and the mobility grant funded by Spanish Ministry of Education.

I would like also to thank Dr. Manuel Campoy (University of Seville), Luís Monge (Taim-Weser) and Dr. Alfredo Hernández (Universidad Autónoma del Estado de Morelos) for their contribution to this thesis in the form of helpful information and discussions.

Thanks to Dr. Ulrik Henriksen, Dr. Jesper Ahrenfeldt and their research group at Risø National Laboratory for Sustainable Energy. They received me with great hospitality in Denmark during my research stay. They have always been available for discussions, questions and comments. My time in Denmark was also made enjoyable in large part due to the friends I met and that became a part of my life. Special thanks to Igor for the wonderful chats, support, encouragement and friendship.

Further thanks are due to all colleagues from CREVER, who have influenced this work and who have contributed to create a very pleasant atmosphere at work. I am also in debt with my friends who have always been by my side. Special thanks to Sergi for his support and encouragement to start and perseverate in this adventure. In addition, I wish also to dedicate special words of gratitude to David who has contributed to this thesis in many ways. He knew when to listen, when to question and when to encourage. His support and patience have been crucial to come to the end of this challenge.

Finally, I would like to thank my parents and sister for being the source of motivation and support for me throughout my entire academic career. They have encouraged me during these years despite being difficult to understand what I was doing.

# ABSTRACT

A reliable, affordable and clean energy supply is of major importance for society, economy and the environment. In this context, modern use of biomass is considered a very promising clean energy option for reduction of greenhouse gas emissions and energy dependency. Biomass gasification has been considered the enabling technology for modern biomass.

Cogeneration has been used for many years for biomass gasification and several plants have been implemented. However, little work has been done on trigeneration plants producing heat, cold and electricity. Trigeneration plants are of great interest for warm climate and developing countries that usually have a high cooling demand. For this reason, simple and reliable simulation tools are needed to give a better understanding of the whole process and as preliminary tools to evaluate the potential of trigeneration biomass gasification plants in a certain location.

The main objective of this thesis is to develop a simplified but rigorous biomass gasification trigeneration plant model for the simulation, design and preliminary evaluation of trigeneration plants. To achieve this goal, different models for biomass gasification process have been reviewed and studied as well as different implemented biomass gasification plants configurations. A modified thermodynamic equilibrium model has been developed to account for real processes that do not achieve equilibrium. It has been validated using published experimental showing good agreement between experimental and predicted data. In addition, this model offers the opportunity to evaluate the influence of variations of the fuel and operating conditions in producer gas quality. Besides this model, two artificial neural network models, based on published experimental data, have also been developed: one for BFB gasifiers and the other for CFB gasifiers. These ANN models provide better results compared with the modified equilibrium model and have proven the great potential they have in this field. In addition, they can be easily extended and improved when more data is available.

Because the absorption chiller is a key element in the trigeneration plant a new approach to the characteristic equation method has been developed to reduce the operating characteristics of absorption chillers into easier to handle simple algebraic equations that allow the model to be integrated in simulation and optimization programs.

These previous developed models have been included in the model of the small-medium scale (250 $kW_e$ - 2 $MW_e$) biomass gasification trigeneration plant. The trigeneration plant accounts for a downdraft or fluidised bed gasifier, heat recovery unit, clean-up section and an ICE coupled with an absorption chiller. The three different configurations considered differ in how heat from exhaust gases and cooling water from the engine jacket is recovered and used in the absorption chiller. For this reason three different absorption chillers have been implemented: a single-effect hot water driven absorption chiller, a double-effect exhaust gases driven absorption chiller and a double-effect steam driven absorption chiller. These configurations have been applied to a case study of the polygeneration plant ST-2 foreseen in Cerdanyola del Vallés in the framework of European Project Polycity.

# RESUMEN

Un suministro de energía fiable, asequible y limpia es de gran importancia para la sociedad, la economía y el medio ambiente. En este contexto, la biomasa se considera una opción prometedora para la obtención de energía limpia, la reducción de las emisiones de gases de efecto invernadero y la dependencia energética.

Durante  años se han estudiado e implementado diferentes plantas de cogeneración con gasificación de biomasa. Sin embargo, poco se ha hecho con plantas de trigeneración para la producción de calor, frío y electricidad. Las plantas de trigeneración son de gran interés para los países en desarrollo y los de clima cálido. Por esta razón, es necesario el desarrollo de herramientas de simulación simple y fiable que permitan una mejor comprensión del proceso y que puedan usarse en la evaluación preliminar y estudio del potencial de este tipo de plantas.

El objetivo principal de esta tesis es el desarrollo de un modelo sencillo pero riguroso de plantas de trigeneración con gasificación de biomasa para su simulación, diseño y evaluación preliminar. Para lograr este objetivo, se han revisado y estudiado los diferentes modelos propuestos para el proceso de gasificación de biomasa, así como diferentes configuraciones de plantas. Se ha desarrollado un modelo modificado de equilibrio termodinámico para aplicarlo a los procesos reales que no alcanzan el equilibrio. El modelo se ha validado con datos experimentales publicados y se ha obtenido un buen ajuste entre datos predichos y datos reales. Además, ofrece la oportunidad de evaluar la influencia de las variaciones de la biomasa y las condiciones de operación en la calidad del gas producido. En paralelo, también se han desarrollado dos modelos de redes neuronales  basados en datos experimentales publicados: uno para gasificadores BFB y otro para gasificadores CFB. Estos modelos ofrecen mejores resultados que el modelo de equilibrio modificado. Además, pueden ser fácilmente ampliados y mejorados cuando hay más datos disponibles.

La enfriadora de absorción es un elemento clave en la modelización de la planta de trigeneración. Por este motivo,  se ha desarrollado un método basado en la ecuación característica para modelizar su funcionamiento a carga parcial; usando ecuaciones algebraicas sencillas, fáciles de manejar y que pueden integrarse en programas de simulación y optimización.

Los diferentes modelos desarrollados anteriormente se han integrado en el modelo global de la planta de trigeneración con gasificación de biomasa de pequeña-mediana escala (250 $kW_e$ – 2 $MW_e$). El modelo integra diferentes unidades como el gasificador (downdraft o lecho fluidizado), una unidad de recuperación de calor, la sección de limpieza y un motor de combustión interna acoplado a una máquina de absorción. Las tres configuraciones propuestas difieren en cómo se recupera el calor de los gases de escape y de las camisas del motor para su uso en la máquina de absorción. Por esta razón, se han considerado tres máquinas de absorción diferentes: simple efecto con agua caliente y doble efecto con gases de escape directos o con vapor. Estas configuraciones se han aplicado a un caso de estudio de la planta de poligeneración ST-2 prevista en Cerdanyola del Vallés, en el marco del Proyecto Europeo Polycity.

## CONTRIBUTIONS IN JOURNALS

Puig-Arnavat, M.; López-Villada, J.; Bruno, J.C.; Coronas, A. (2010) Analysis and parameter identification for characteristic equations of single- and double-effect absorption chillers by means of multivariable regression. International Journal of Refrigeration, 33:70 – 78.

Puig-Arnavat, M.; Bruno, J.C.; Coronas, A. (2010) Review and analysis of biomass gasification models. Renewable and Sustainable Energy Reviews, 14: 2841 – 51.

Puig-Arnavat, M.; Bruno, J.C.; Coronas, A. (2011) Modified thermodynamic equilibrium model for biomass gasification: study of the influence of operating conditions. Energy and Fuels, in preparation.

Puig-Arnavat, M.; Bruno, J.C.; Coronas, A. (2011) Artificial neural network models for biomass gasification process. Bioresource Technology, in preparation.

## CONTRIBUTIONS IN CONGRESSES, CONFERENCES AND SYMPOSIUMS

Simader, G.; Barthel, C.; Wohlauf, G.; Lezsovits, F.; Coronas, A.; Bruno, J.C.; Puig-Arnavat, M.; Quince N. (2009) Raising the Efficiency of Boiler installations (BOILeff) ECEEE 2009 Summer Study, 1-6 June, La Colle sur Loup, France

Simader, G.; Trnka, G.; Zach, F; Coronas, A.; Bruno, J.C.; Puig-Arnavat, M.; Quince N.; Barthel, C.; Wohlauf, G.; Lezsovits, F.; (2009) Raising the Efficiency of Boiler installations (BOILeff) 5$^{th}$ International Conference on Energy Efficiency in Domestic Appliances and Lighting (EEDAL'09), 16-18 June, Berlin, Germany.

Puig-Arnavat, M.; Quince, N.; Bruno, J.C.; Coronas, A. (2009) Raising the efficiency of boiler installations through the BOILEFF project: the experience of Spain. 8$^{th}$ International Conference on Sustainable Energy Technologies (SET2009), 31 August – 3 September, Aachen, Germany.

Puig-Arnavat, M.; López-Villada, J.; Montero, I.A.; Bruno, J.C.; Coronas, A. (2009) Simulación de plantas de frío solar utilizando ecuaciones carcterísticas para el modelado de enfriadoras por absorción. V Congeso Ibérico y III Congreso Iberoamericano de Ciencias y Técnicas del Frío (CYTEF 2009), 23-25 September, Castellón, Spain.

Puig-Arnavat, M.; Bruno, J.C.; Coronas, A. (2010) Model validation and simulation of a biomass gasifier integrated in a 6 MWe engine cogeneration plant of an alcohol distillery. 23 rd International Conference on Efficiency, Cost, Optimization, Simulation & Environmental Impact of Energy Systems – ECOS 2010, 14-17 June, Lausanne, Switzerland.

Puig-Arnavat, M.; Bruno, J.C.; Coronas, A. (2010) Comparative analysis of biomass gasification models. Simposio Internacional sobre Energías Renovables y Sustentabilidad. UNAM. 9-10 August, Temixco, Mexico.

Bruno, J.C.; Ortiga, J.; López-Villada, J.; Puig-Arnavat, M.; Coronas, A. (2010) Renewable district heating and cooling concepts with large scale trigeneration within the Spanish Polycity project. Polycity Final Conference: Visions of Sustainable Urban Energy Systems. 15-17 September, Stuttgart, Germany.

Puig-Arnavat, M. (2011) Biomass gasification for district cooling applications. 3rd International Symposium Solar and Renewable Cooling, 10 February, Stuttgart, Germany.

## COLLABORATION IN CHAPTERS IN BOOKS

Polycity – Energy networks in sustainable cities. Ursula Eicker (Ed.) Chapter 4: Energy supply - concepts and performance and Chapter 8: Knowledge transfer. Karl Krämer Verlag Stuttgart (Germany). ISBN 978-3-7828-4051-4

## PARTICIPATION IN PROJECTS

POLYCITY - Energy Networks in sustainable cities. European Commission - VI Framework Program (TREN/05FP6EN/S07.43964/51381). May 2005 – May 2011.

BOILEFF - Raising the efficiency of boilers installations. Intelligent Energy Europe (EIE/06/134/SI2.448721). February 2007 - October 2009.

## PARTICIPATION IN PROJECTS DERIVERABLES

POLYCITY PROJECT:

- DR 4.13 Polygeneration conference in Tarragona: organisation, providing conference manuals and project flyers, press releases. Date: 05/11/2007
- DD 2.4: General DE 2 report, describing the selected systems and summarising the most relevant findings as input for dissemination products developed in T 1. Date: 05/05/2008
- DT 1.11 Training modules for university teaching/young scientists. Date: 05/05/2009
- DD 2B.2 Report on integrated thermal cooling technologies. Date: 22/02/2010
- DD 4.5 Energy performance report. Date: 28/02/2010
- DD 4.3 Environmental performance report. Date: 29/04/2010
- DD 4.4 Economic performance report. Date: 05/05/2010

BOILEFF PROJECT:

- Deliverable 2.1: Summary report on studies and field test reports dealing with boiler efficiency in practice.
- Deliverable 2.5: Documentation of 75 audited heating systems in Austria, Germany, Hungary, Greece and Spain.
- Deliverable 3.4 and 3.5: List of installers and boiler owners interested to participate in the Boileff field test.
- Deliverable 5.2: List of participating boiler owners that take part in DHQUI and GPQU programs
- Deliverable 5.3: List of boilers and consumed energy before the replacement
- Deliverable 6.3: Revised versions of DHQUI and GPQU – Validation of DHQUI and GPQU.
- Deliverable 6.1: Technical evaluation report
- Deliverable 6.2: Evaluation report on success factors for a broad market introduction of DHQUI and GPQU.
- Deliverable 6.4: Advice to the boiler industry, what can / should be changed by the boiler regulation.

# TABLE OF CONTENTS

# TABLE OF CONTENTS

# TABLE OF CONTENTS

# LIST OF FIGURES

# LIST OF FIGURES

# LIST OF FIGURES

## LIST OF FIGURES

# LIST OF TABLES

# LIST OF TABLES

# LIST OF TABLES

# NOMENCLATURE

## Abbreviations

ANN: Artificial Neural Network
BFB: Bubbling Fluidised Bed
BM: Black-box Model
CFB: Circulating Fluidised Bed
CFDM: Computational Fluid Dynamics Model
CHP: Combined Heat and Power
CRF: Char reactivity factor
CV: Calorific Value
DFB: Dual Fluidised Bed
DHC: District Heating and Cooling
EFB: Empty Fruit Bunch
EFGT: Externally Fired Gas Turbine
EM: Equilibrium Model
FICFB: Fast Internal Circulating Fluidised Bed
FM: Fluidization Models
HNN: Hybrid Neural Network
ICE: Internal Combustion Engine
IGCC: Integrated Gasification Combined Cycle
HHV: Higher Heating Value (MJ/kg or MJ/$Nm^3$)
LHV: Lower Heating Value (MJ/kg or MJ/$Nm^3$)
MCFC: Molten Carbonate Fuel Cells
MFNN: Multilayer Feedforward Neural Network
MSW: Municipal Solid Waste
ORC: Organic Rankine Cycle
PANER: Plan de Acción Nacional en Materia de Energías Renovables (2011-2020)
PER: Plan Energías Renovables (2005-10)
QET: Quasi-equilibrium Temperature
RDF: Refuse Derived Fuel
RES: Renewable Energy Sources
RMSE: Root Mean Square Error
SOFC: Solid Oxide Fuel Cells
ST: Steam Turbine

# NOMENCLATURE

## Variables and parameters

a: Output of the ANN

a': Characteristic parameter (-)

a'': Characteristic parameter (-)

A': Enthalpy Coefficient (-)

AF ratio : Air to fuel ratio ($Nm^3$ air/kg fuel)

Ash: Ash content in biomass (wt % d.b.)

B: Isostere slope in a Dühring chart (-)

b1: Bias vector of the ANN input layer

b2: Bias vector of the ANN output layer

C: Carbon mass fraction in biomass (wt % d.b.)

C': Enthalpy coefficient (-)

COP: Coefficient of performance (-)

$COP_{ref}$: coefficient of performance according to the different scenarios proposed for TPES (-)

$C_p$: Specific heat capacity (kJ/ kg·K)

e': Characteristic parameter (-)

e'': Characteristic parameter (-)

ER: Equivalence ratio (-)

$f_{abs}$: Absorption chiller factor (-)

$F_{gr}$: Relative fuel/air ratio

FC: Fixed carbon content of biomass (% wt d.b.)

G': Enthalpy coefficient (-)

H: Hydrogen mass fraction in biomass (%)

$h_v$: Enthalpy of water vaporization (MJ/kg)

$h_f$: Enthalpy of formation (MJ/kg; kJ/kg; kJ/kmol)

$h_i$: Specific enthalpy (kJ/kg)

I: Relative influence of an input variable on the output variable of the ANN (%)

IW: Weights' matrix of the ANN input layer

$K_1$: Equilibrium constant for water gas shift reaction

$K_2$: Equilibrium constant for methane reaction

LW: Weights' matrix of the output layer

m: Mass flow rate (kg/h or kg/s)

MC: Biomass relative moisture content (wt % w.b.)

N: Nitrogen mass fraction in biomass (wt % d.b.)

O: Oxygen mass fraction in biomass (wt % d.b.)

P: Pressure (kPa)

$\bar{p}_i$ : normalised data input vector for the ANN

$p_i$: data input vector for the ANN

## NOMENCLATURE

PES: Primary energy savings (%)

R: Ideal gas constant (kJ/ ·kmol)

$R^2$: Correlation coefficient

Q: Heat flux (kW)

r: Atoms of sulphur in biomass substitution formula (-)

$R^2$: Correlation coefficient

REE: Electrical equivalence performance (%)

S: Sulphur mass fraction of biomass (wt % d.b.)

s: Characteristic parameter (kW/K)

s': Characteristic parameter (-)

s'': Characteristic parameter (-)

r': Characteristic parameter (-)

r'': Characteristic parameter (-)

t: Output target of the ANN

T: Temperature

TPES: Trigeneration primary energy savings (%)

UA: heat transmission (kW/K)

VM: Volatile mater content of biomass (% wt d.b.)

W: Power output (kW)

x: Atoms of hydrogen in biomass substitution formula (-)

y: Atoms of oxygen in biomass substitution formula (-)

z: Atoms of nitrogen in biomass substitution formula (-)

$\Delta_a$, $\Delta_b$, $\Delta_c$ and $\Delta_d$: constants for each group of organic compound used for tar enthalpy calculation using Jackob's method

$\Delta$n: difference of moles between products and reactants of a reaction

**Subscripts**

A: Absorber

0: Initial

b: Biomass

C, O, N, H, S: Carbon, Oxygen, Nitrogen, Hydrogen, Sulphur

C: Condenser

ch: Chilled water

cw: Cooling water

e: Electric

E: Evaporator

G: Generator

g: Gas

hex: Heat exchanger

hw: Hot water

# NOMENCLATURE

i: Number of neurons in the ANN input layer

in: Inlet

j: Number of neurons in the ANN hidden layer

k: Number of neurons in the ANN output layer

loss: Solution heat exchanger loss

min: Minimum

o: Outlet

p: Pyrolysis

ref: Reference

refr: Refrigerant

strong: Strong solution of absorption chillers

th: Thermal

u: Different heat exchanger units of absorption chillers (evaporator, condenser, absorber, generator)

weak: Weak solution in absorption chillers

**Greek symbols**

α: Characteristic parameter (-)

$\eta_{CPH,e}$: Electrical efficiency of the cogeneration system (%).

$\eta_{CPH,heat}$: Heat efficiency of the cogeneration system (%)

$\eta_g$: Carbon conversion efficiency (%)

$\eta_{CG}$: Cold gas efficiency (%)

$\eta_{HG}$: Hot gas efficiency (%)

$\eta_{ref,e}$: Efficiency reference value for separate electricity production (%).

$\eta_{ref,e^*}$: Efficiency reference value for separate electricity production according to the different scenarios proposed for TPES calculation (%).

$\eta_{ref,heat}$: Efficiency reference value for separate heat production (%)

$\eta_{ref,heat^*}$: Efficiency reference value for separate heat production according to the different scenarios proposed for TPES calculation (%)

$\eta_t$: Overall efficiency of the trigeneration system (%)

τ: Internal arithmetic mean temperature of absorption chillers (ºC)

ω: Logarithmic mean temperature difference divided by arithmetic mean temperature difference (-)

$\Delta G^o_T$: Standard Gibbs function of reaction (kJ/kmol)

$\Delta g^o_{f,T}$: Standard Gibbs function of formation at given temperature (kJ/kmol)

ΔΔt: Characteristic temperature difference (K)

$\Delta\Delta t_{min}$: Minimum temperature difference (K)

# Chapter 1

# Introduction and objectives: energy production from biomass

## 1.1 INTRODUCTION

The awareness about depletion of fossil fuels, energy dependency, environmental pollution, greenhouse gas emissions and global climate change; together with the potential of biomass to supply large amount of useful energy with reduced environmental impacts have converted biomass in one of the most promising renewable energy sources. Among all biomass conversion technologies, this thesis focuses on biomass gasification that has the advantage over combustion of more efficient and better controlled heating, higher efficiencies in power production and the possibility to be applied for chemicals and fuel production. This chapter includes a brief description of characteristics, actual use and energy potential of biomass, as well as an overview of the main processes for biomass conversion into energy. Afterwards, a special attention is paid to biomass gasification, discussing the reactions occurring in the process as well as different reactor designs and producer gas conditioning. The different technologies for power generation from biomass gasification are also reviewed as well as the studies and implemented co- and trigeneration plants. Finally, the objectives and structure of the thesis are also presented.

## 1.2 BIOMASS GENERAL CHARACTERISTICS

The term of “biomass” covers a broad range of materials that can be used as fuel or raw materials and which have in common that they are all derived from recently living organisms (Highman and Van der Burgt, 2008). This definition clearly excludes traditional fossil fuels since, although they also derive from plant (coal) or animal life (oil and gas); it has taken millions of years to convert them into their current form.

Sources of biomass include various natural and derived materials, such as woody and herbaceous species, woody wastes (e.g. from forest thinning and harvesting, timber production and carpentry residues), agricultural and industrial residues, waste paper, municipal solid waste, sawdust, grass, waste from food processing, animal wastes, aquatic plants and industrial and energy crops grown for biomass. For political purposes, some other materials (such as tires, manufactured from either synthetic or natural rubbers) may be included under the general definition of biomass even though the material is not strictly biogenic (Klass, 1998). There is also a potential overlap between what is classified as waste and what as biomass.

Although biomass is not a major industrial fuel, it supplies 15-20% of the total fuel use in the world (Highman and Van der Burgt, 2008). It is used mostly in non-industrialised economies for domestic heating and cooking. In industrialised countries, the use of biomass as a fuel is largely restricted to the use of by-products from forestry and the paper and sugar industries. Nonetheless, its use in industrialised countries is being encouraged as part of strategy for $CO_2$ abatement.

It is the inherent properties of the biomass source what determines both the choice of conversion process and any subsequent processing difficulties that may arise. Equally, the choice of biomass source is influenced by the form in which the energy is required. Dependent on the energy conversion process selected, particular material properties become important during subsequent processing. The main material properties of interest, during subsequent processing as an energy source, relate to:

- Moisture content (intrinsic and extrinsic)
- Calorific value (CV)
- Proportions of fixed carbon and volatiles
- Ash/residue content

- Alkali metal content
- Cellulose/lignin ratio

For dry biomass conversion processes, the first five properties are of interest, while for wet biomass conversion processes, the first and last properties are of prime concern.

In Table 1.1 the physical, chemical and fuel properties of biomass and coal fuels are presented. Additional information is given by several researchers on typical composition of different biomass fuels (Ebeling and Jenkins, 1985; Jenkins et al., 1998, van der Drift et al., 2001; Demirbas, 2004). Also, Phyllis database (2000) contains complete and detailed information on the composition of several biomass and waste compounds.

Table 1.1: Physical, chemical and fuel properties of biomass and coal fuels (source: Demirbas, 2004)

| **Property** | **Biomass** | **Coal** |
|---|---|---|
| Fuel density (kg/m$^3$) | ~500 | ~1300 |
| Particle size | ~ 3 mm | ~100 μm |
| C content (wt% of dry fuel) | 42-54 | 65-85 |
| O content (wt% of dry fuel) | 35-45 | 2-15 |
| S content (wt% of dry fuel) | Max. 0.5 | 0.5-7.5 |
| $SiO_2$ content (wt% of dry ash) | 23-49 | 40-60 |
| $K_2O$ content (wt% of dry ash) | 4-48 | 2-6 |
| $Al_2O_3$ content (wt% of dry ash) | 2.4-9.5 | 15-25 |
| $Fe_2O_3$ content (wt% of dry ash) | 1.5-8.5 | 8-18 |
| Ignation temperature (K) | 418-426 | 490-595 |
| Dry heating value (MJ/kg) | 14-21 | 23-28 |

## 1.3 BIOMASS CONVERSION

Biomass raw materials usually have to be converted in some way to solid, liquid or gaseous fuels that can be used to provide heat, generate electricity or drive vehicles. This conversion is generally achieved by some type of mechanical, thermochemical or biological processes:

- Mechanical processes are not strictly conversion processes since they do not change the nature of the biomass. They are commonly used in the treatment of

woody biomass and waste. The sorting and compaction of waste, the processing of woody residues into bundles, pellets and chips, the cutting of straw and hay into pieces, and the squeezing of oil out of plants in a press are all examples of mechanical processes. Such processes are often used to pre-treat a biomass resource for further conversion.

- Biological processes (Figure 1.1) use some type of biochemical process to achieve biomass conversion; the most important ones that produce useful fuels or heat are mainly aerobic decomposition, anaerobic digestion, hydrolysis and fermentation.
- Thermochemical processes (Figure 1.2) are the most commonly used conversion processes and biomass conversion is achieved by heat. These processes include combustion, pyrolysis, liquefaction and gasification.

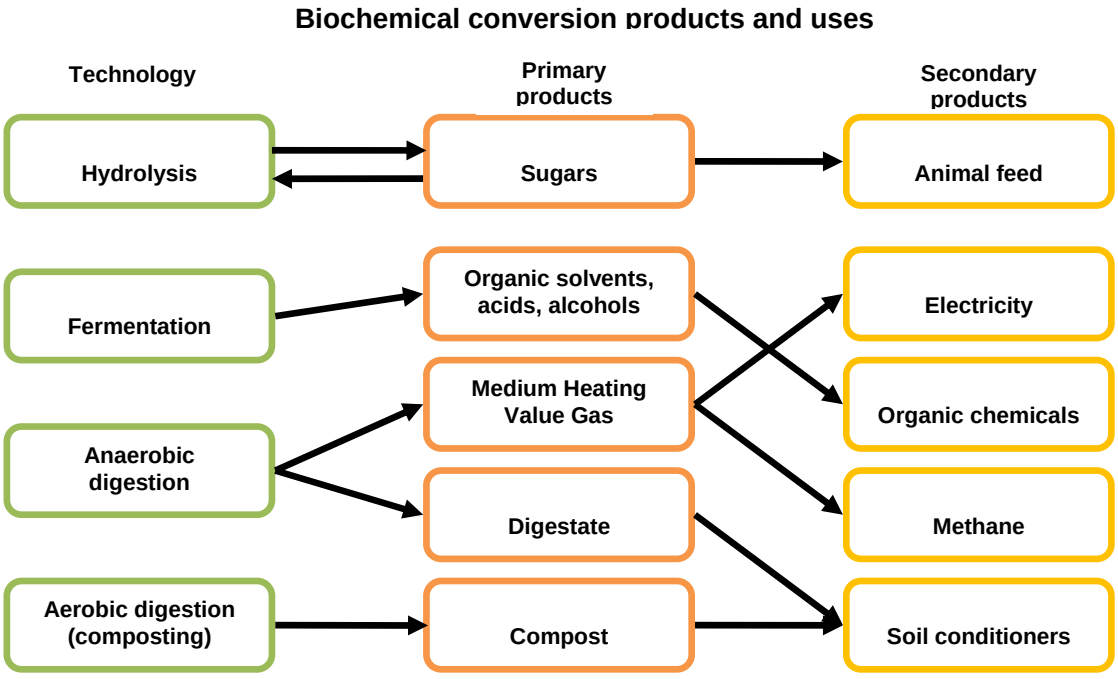


Figure 1.1: Biochemical conversion processes, products and uses (Source: EC, 2005).

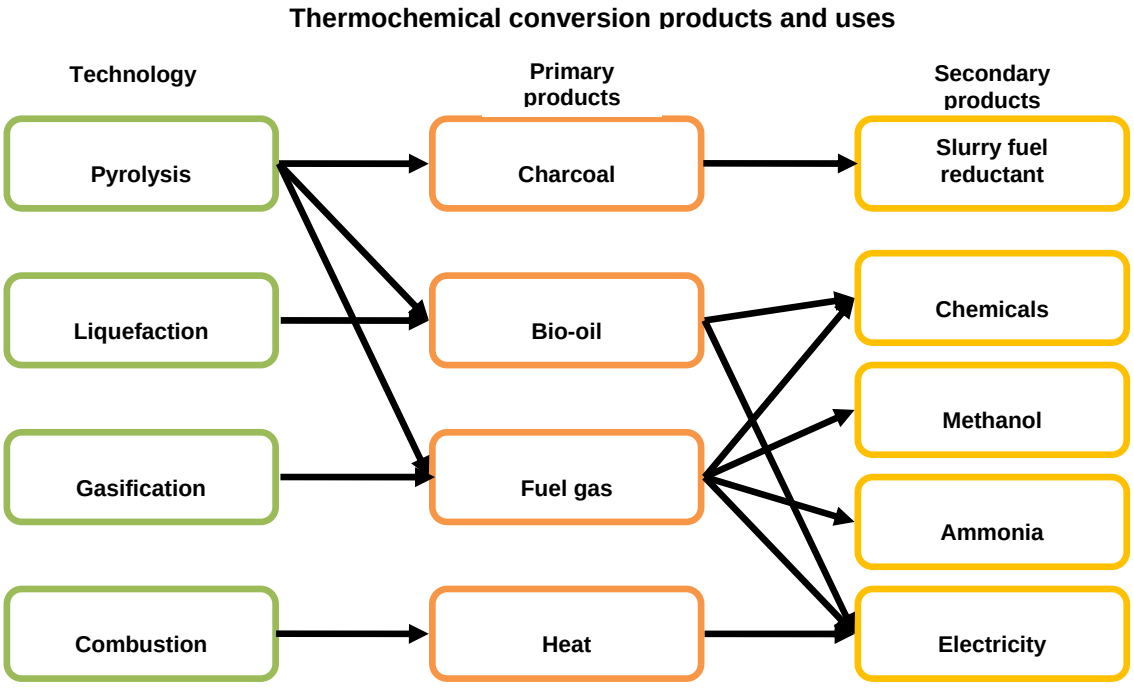


Figure 1.2: Thermochemical conversion processes, products and uses (Source: EC, 2005).

## 1.4 ACTUAL AND POTENTIAL USES OF BIOMASS RESOURCES

The contribution of renewable energies to the energy supply system remains relatively low, although by 2020 renewable energy should account for 20% of the EU's final energy consumption (8.5% in 2005). The European plan on climate change consists of a range of measures adopted by the members of the European Union to fight against climate change. The plan was launched in March 2007, and after months of tough negotiations between the member countries, it was adopted by the European Parliament on December 2008. The plan include the so-called “three 20 targets (20-20-20)”, but in reality it consisted in four proposals. These aims were:

- To reduce emissions of greenhouse gases by 20% by 2020.
- To increase energy efficiency to save 20% of EU energy consumption by 2020.
- To reach 20% of renewable energy in the total energy consumption in the EU by 2020.
- To reach 10% of biofuels in the total consumption of vehicles by 2020.

Figure 1.3 and Figure 1.4 show the European Union (EU-27) electricity and heat production in 2008, breakdown by different energy sources. It can be observed how biomass represented 2% and 10% of the total production of electricity and heat, respectively.

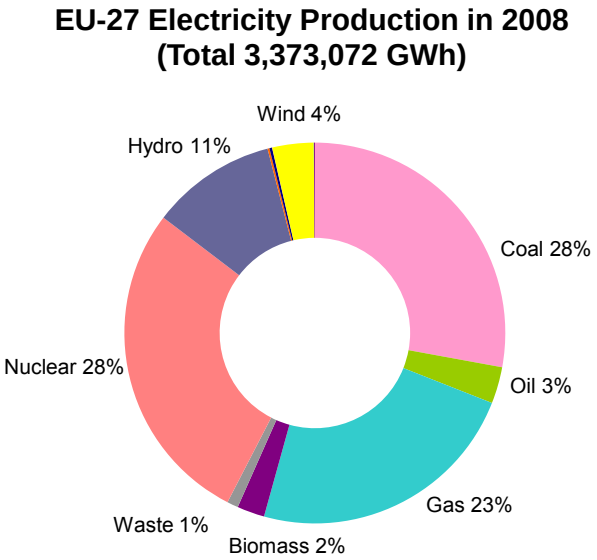


| Electricity production 2008 (GWh) | |
|---|---|
| Coal | 940260 |
| Oil | 105107 |
| Gas | 786472 |
| Biomass | 78802 |
| Waste | 31677 |
| Nuclear | 937236 |
| Hydro | 358672 |
| Geothermal | 5732 |
| Solar PV | 7433 |
| Solar thermal | 16 |
| Wind | 118734 |
| Tide | 513 |
| Other sources | 2418 |

Figure 1.3: EU-27 Electricity production in 2008 (source: International Energy Agency www.iea.org).

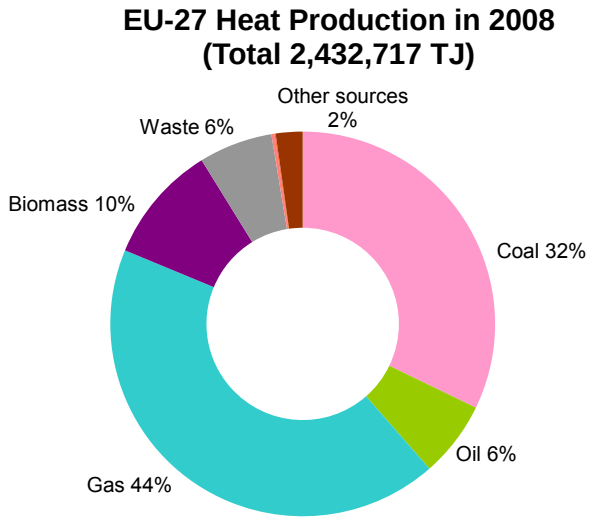


| Heat production 2008 (TJ) | |
|---|---|
| Coal | 782654 |
| Oil | 155240 |
| Gas | 1038608 |
| Biomass | 242263 |
| Waste | 150659 |
| Nuclear | 6311 |
| Geothermal | 2169 |
| Solar Thermal | 58 |
| Other sources | 54755 |

Figure 1.4: Heat production in 2008 (source: International Energy Agency www.iea.org).

Among the renewable resources represented in Figure 1.5 and Figure 1.6, it can be seen how biomass represents an important share in the renewable electricity and heat production of year 2008 (in %).

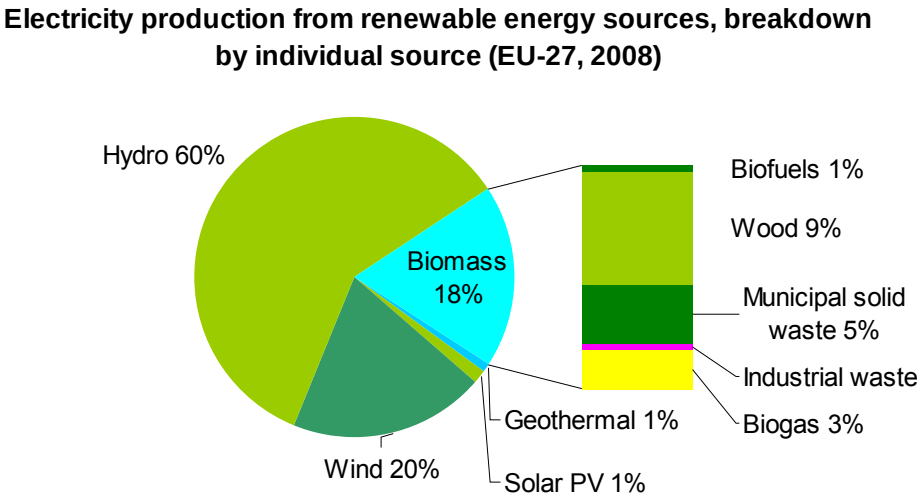


Figure 1.5: EU-27 Electricity production in 2008 from renewable energy sources, breakdown by different energy sources (source: International Energy Agency www.iea.org)

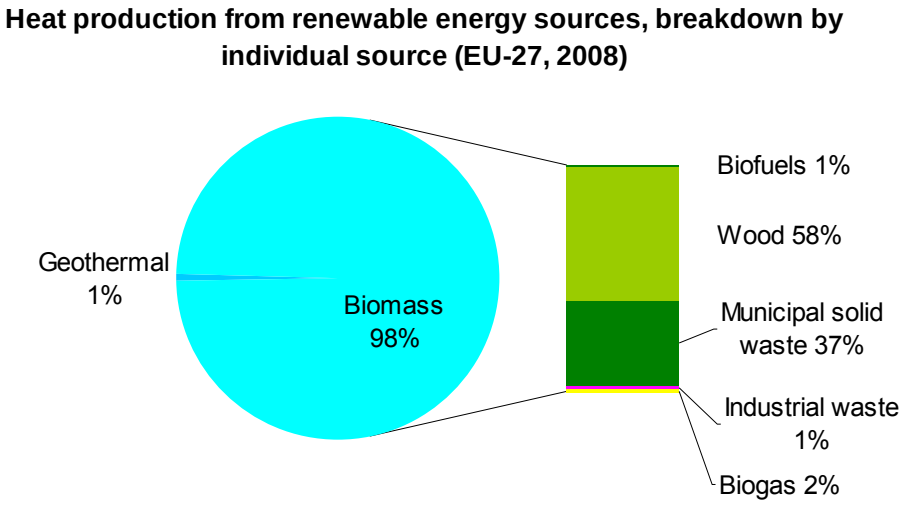


Figure 1.6: EU-27 Heat production in 2006 from renewable energy sources, breakdown by different energy sources (source: International Energy Agency www.iea.org)

The main benefits of the use of biomass over conventional fuels can be summarized as follows (Flamos et al., 2011):

- Renewable and recyclable energy source
- Widespread availability in Europe and abroad
- Decreased reliance on imported energy sources
- Less waste directed to landfills
- Can be stored and used on demand
- Reduced $CO_2$, sulphur dioxide ($SO_2$), and other emissions
- Source of many business opportunities
- Opportunities for technology exports
- Contribution to a balanced growth of agriculture, employment opportunities, and population retention in rural areas

In addition to the many benefits common to any renewable energy use, biomass is the only other naturally available energy containing carbon resource known that is large enough to be used as a substitute for fossil fuels (Jager-Waldau and Ossenbrink 2003). In addition, bioenergy is unique in its potential to service all three of the major energy demand sectors for heat, electricity, and transport fuels. Moreover, biomass has a great potential to provide feed stocks to make a wide range of chemicals and materials or bio-products.

For these reasons, the role of bioenergy in achieving EU energy targets is crucial. However, its complexity and inter-sectorial nature, along with limited attention by policy makers compared to that given to photovoltaics and wind, are some of the reasons that have resulted to lower growth of bioenergy compared to other RES. Other reasons are relatively high costs of the technologies of upgrading; the investment costs can be twice as high compared to fossil-fired plants (the low energy density requires larger plant sizes, the wide variety of fuel characteristics and the objective to achieve a clean combustion require higher efforts in conversion and clean-up technology). There is also a high effort necessary for transportation and storage of biofuels because of the low energy density and a reliable market for biofuels has not yet been established (Maniatis et al., 2002).

Even though in nearly all of the EU-countries less than 50% of the available biomass resources are currently used, the estimated potential of biomass in the EU is large

enough to reverse this situation and boost the growth of the industry, but only if appropriate policy measures are put into place. An estimation of the potential of biomass resources in UE can be found in the work of Esteban and Carrasco (2011). They compared several recent studies with their own study and the results obtained are presented in Table 1.2. The differences observed between authors, are due to different methodological elements and assumptions that sometimes have not been completely explained in the relevant publications.

Table 1.2: Comparison between different assessments on biomass resources on 11 countries of UE (Source: Esteban and Carrasco, 2011).

| | ES | FR | IT | GR | PT | SE | AT | DK | FI | DE | PL |
|---|---|---|---|---|---|---|---|---|---|---|---|
| **Agri-residues (PJ/year)** | | | | | | | | | | | |
| Nikolau et al. (2003) | 126.0 | 412.0 | 163.3 | 69.0 | 25.8 | 5.5 | 9.0 | 28.9 | 9.7 | 130.0 | 125.0 |
| EEA (2006)[a] | 296.8 | 530.9 | 673.0 | 66.9 | 112.9 | 372.0 | 125.4 | 96.1 | 255.0 | 622.8 | 305.1 |
| RENEW (2007)[b] | 128.5 | 573.4 | 230.4 | 73.0 | 18.9 | 14.9 | 42.3 | 38.7 | 17.2 | 189.0 | 133.7 |
| Esteban and Carrasco (2011) | 228.6 | 886.6 | 301.5 | 85.8 | 30.3 | 55.4 | 67.5 | 145.5 | 19.9 | 757.6 | 184.4 |
| **Forest residues (PJ/year)** | | | | | | | | | | | |
| Nikolau et al. (2003) | 60.6 | 296.0 | 98.5 | 21.6 | 48.4 | 119.2 | 193.0 | 18.0 | 146.0 | 227.0 | 32.0 |
| EEA (2006) | 71.1 | 530.9 | 234.1 | n.a. | 8.4 | 92.0 | 137.9 | 4.2 | 71.1 | 263.3 | 83.6 |
| RENEW (2007) | 66.9 | 106.0 | 31.9 | n.a. | 13.4 | 120.3 | 37.0 | 4.7 | 94.9 | 116.5 | 49.3 |
| Esteban and Carrasco (2011) | 90.6 | 147.3 | 76.2 | 20.7 | 12.2 | 198.2 | 50.0 | 7.0 | 131.9 | 81.1 | 39.0 |

Conversion values applied: LHV agri-residues 17.5 GJ/Mg. LHV forest residues 19 GJ/Mg.
[a] Includes waste agricultural, agroindustrial wood industry and municipal organic.
[b] Includes only straw.

### 1.4.1 Biomass policies in Spain

In Spain, primary energy consumption decreased by 8.3% in 2009 compared to the previous year, while the primary consumption of renewable energy increased 12.6% (about 1,400 ktoe) reaching a consumption of 12.3 million toe in 2009. Renewable energies continue the trend of previous year, increasing in absolute terms while there is a decreasing of primary energy consumption. Now, their contribution to the primary energy consumption is 9.4%. Likewise, the share of renewable energies on the gross final energy consumption in year 2009, new indicator of contribution of RES in accordance with Directive 2009/28/EC for the promotion of renewable energy, reached 12.2% (10.3% in 2008) (MITYC, 2009).

The “Plan for Renewable Energy (PER) 2005–2010’’ (IDAE, 2005) defined concrete objectives for each kind of renewable energy (Table 1.3). According to the PER,

renewables must have covered, in 2010: 12% of the primary energy consumption of the country and 30.3% of the gross electricity consumption, following the Directive 2007/71/EC. In addition, they should have covered 5.8% of petrol and diesel consumed in the transport sector, following the Directive 2003/30/EC on the promotion of the use of biofuels (3.4% in 2009) with a binding minimum level for biodiesel of 3.9% of diesel (2.5% in 2009) and a binding minimum level for bioethanol of 3.9% of gasoline consumed (2.5% in 2009).

As a result of PER 2005-2010, Spain has become the world's second largest producer of wind energy (16.7 GW installed at the end of 2008), behind Germany, and ahead of United States. Photovoltaic energy has also characterized a similar industrial development (more than 3 GW of solar PV installed at the end of 2008) and emerging technologies like concentrated solar power also had ambitious targets of 0.5 GW for 2010 (Labriet et al., 2010). However, biomass has not developed as fast as expected (nor for electricity neither for heating purposes).

Due to the slow development of biomass technologies in the PER 2005-2010, only 510 MW (39%) were installed at the end of year 2010 out of the 1317 MW foreseen initially; their weight on the renewable energy mix has been reduced from 47.78% to 3% in the new Spanish 2011-2020 Renewable Energies Plan (Plan de Acción Nacional en Materia de Energías Renovables - PANER 2011-2020) (IDAE, 2011) (Table 1.3).

Table 1.3: Comparison of targets of the Spanish renewable energy plan (PER 2005-2010 (IDAE, 2005)) for biomass with those of the new renewable energies plan (PANER 2011-2020 (IDAE, 2011)).

| | **Target 2010 (PER 2005-2010)** | | **Estimated August 2010** | | **Target 2020 (PANER 2011-2020)** | |
|---|---|---|---|---|---|---|
| | Power (MW) | Output (GWh) | Power (MW) | Output (GWh) | Power (MW) | Output (GWh) |
| **Electricity generation** | | | | | | |
| **Biomass** | | | | | | |
| **- Biomass power stations** | 1,317 | 8,980 | 596 | 3,719 | 1,350 | 8,100 |
| **- Biogas** | 235 | 1,417 | 156 | 799 | 400 | 2,600 |
| **Thermal Uses** | | ktoe | | ktoe | | ktoe |
| **Biomass** | | | | | | |
| **- Solid biomass** | | 4,070 | | 3,550 | | 4,850 |
| **- Biogas** | | | | 33 | | 100 |

Despite of the reduction of biomass technologies objectives, the currently installed power for biomass in Spain, compared with the energy potential, indicate that there is

still an important unused potential for electricity generation from biomass (Gómez et al., 2010a, 2010b).

## 1.5 BIOMASS GASIFICATION

Gasification is a partial thermal oxidation, which results in a high proportion of gaseous products (carbon dioxide, water, carbon monoxide, hydrogen, and gaseous hydrocarbons), small quantities of char (solid product), ash and condensable compounds (tars and oils). Steam, air or oxygen, are supplied to the reaction as oxidising agents.

The gas produced can be standardised in its quality and is easier and more versatile to use than the original biomass e.g. it can be used to power gas engines and gas turbines, or used as a chemical feedstock to produce liquid fuels. Gasification adds value to low or negative-value feedstock by converting them to marketable fuels and products.

From a chemical point of view, the process of biomass gasification is quite complex. Broadly speaking, the gasification process consists of the following stages (McKendry, 2002a and 2002b; Li, 2002; Kishore, 2008):

- Drying. In this stage, the moisture content of the biomass is reduced. Typically, the moisture content of biomass ranges from 5% to 35%. Drying occurs at about 100-200ºC with a reduction in the moisture content of the biomass of <5%.
- Devolatilisation (pyrolysis). This is essentially the thermal decomposition of the biomass in the absence of oxygen or air. In this process, the volatile matter in the biomass is reduced. This results in the release of hydrocarbon gases from the biomass, due to which the biomass is reduced to solid charcoal. The hydrocarbon gases can condense at a sufficiently low temperature to generate liquid tars.
- Oxidation. This is a reaction between solid carbonised biomass and oxygen in the air, resulting in formation of $CO_2$. Hydrogen present in the biomass is also oxidised to generate water. A large amount of heat is released with the

oxidation of carbon and hydrogen. If oxygen is present in substoichiometric quantities, partial oxidation of carbon may occur, resulting in the generation of carbon monoxide.

- Reduction. In the absence (or substoichiometric presence) of oxygen, several reduction reactions occur in the 800-1000ºC temperature range. These reactions are mostly endothermic.

A schematic presentation of these processes is shown in Figure 1.7.

Gasification has the advantage over combustion of more efficient and better controlled heating, higher efficiencies in power production and the possibility to be applied for chemicals and fuel production (Faaij, 2007). Biomass gasification offers the opportunity compared with biomass combustion of more efficient conversion processes for power generation like combined cycles. Power generation by means of a gas turbine combined cycle system can have an efficiency as much as twice the efficiency of biomass combustion processes, which uses a steam cycle alone. In addition, biomass gasification can virtually eliminate the need for water if generating power without a steam turbine (Peterson and Haase, 2009). Furthermore, gasification works best as an efficient means of converting low value-residual biomass (such as municipal solid waste) into higher value products including power, steam, hydrogen, and basic chemicals.

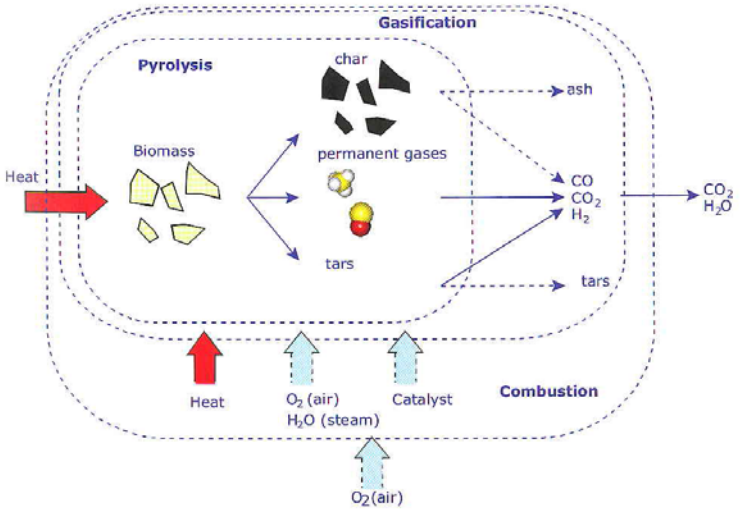


Figure 1.7: Schematic presentation of gasification as one of the thermal conversion processes (source: Stassen et al., 2002)

### 1.5.1 Gasification reactions

The important chemical reactions taking place in the gasifier can be encapsulated as:

- Oxidation reactions:

  $C + ½\ O_2 \leftrightarrow CO + 123.1\ kJ/mol$ (1)

  $C + O_2 \leftrightarrow CO_2 + 393.8\ kJ/mol$ (2)

  $CO + ½\ O_2 \leftrightarrow CO_2 + 283.9\ kJ/mol$ (3)
- Boudouard reaction:

  $C + CO_2 + 172.6\ kJ/mol \leftrightarrow 2CO$ (4)
- Water gas reaction:

  $C + H_2O + 131.4\ kJ/mol \leftrightarrow CO + H_2$ (5)
- Methanation reaction:

  $C + 2H_2 \leftrightarrow CH_4 + 74.9\ kJ/mol$ (6)

The oxidation reactions are exothermic and provide, by auto-thermal gasification, the heat necessary for the endothermic reactions in the drying, pyrolysis and reduction zones. Gasifiers self-sufficient in heat are termed autothermal and if they require heat, allothermal, but autothermal processes are the most common. The last of the presented oxidation reactions also produces heat, which is beneficial to the gasification process, but it is not desired because it reduces the heating value of the producer gas.

The most important reduction reactions are the water gas reaction and the Boudouard reaction. These heterogeneous endothermic reactions increase the gas volume of CO and $H_2$ at higher temperatures and lower pressures (a high pressure suppresses the gas volume). Besides these reactions several other reduction reactions take place of which one the most important is the methanation reaction.

The above presented reactions are heterogeneous reactions, and the following two equations present the homogeneous reactions that can be obtained by subtracting Boudouard reaction from Water gas reaction and subtracting Water gas reaction from Methanation reaction as:

- Water-gas shift reaction

  $CO + H_2O \leftrightarrow CO_2 + H_2 + 41.2\ kJ/mol$ (7)
- Methane reforming reaction

$$CH_4 + H_2O + 206.3\ kJ/mol \leftrightarrow CO + 3H_2 \quad (8)$$

In practice, the equilibrium composition of the gas will only be reached in cases where the reaction rate and the time for reaction are sufficient. The water gas shift equilibrium determines to a large extent the final gas composition and depends on the temperature. The reaction rate decreases with falling temperature. Below 700ºC, the water gas shift reaction proceeds so slowly that the product gas composition is said to be “frozen”. Once formed, the gaseous products do not further react with each other. In fluidised bed and entrained flow gasifiers all the above reactions occur simultaneously on top of the primary decomposition reactions.

Three product gas qualities can be produced from gasification by varying the gasifying agent, the method of operation and the process operating conditions (McKendry, 2002c):

| | | |
|---|---|---|
| Low CV | 4-6 MJ/Nm$^3$ | Using air and steam/air |
| Medium CV | 12-18 MJ/Nm$^3$ | Using oxygen and steam |
| High CV | 40 MJ/Nm$^3$ | Using hydrogen and hydrogenation |

Low calorific value gas is used directly in combustion or in an engine fuel, while medium/high calorific value gases can be utilised as feedstock for subsequent conversion into basic chemicals, principally methane and methanol. As the use of oxygen for gasification is expensive, air is normally used for processes up to about 50 $MW_{th}$. The disadvantage is that the nitrogen introduced with the air dilutes the product gas.

### 1.5.2 Effect of feedstock properties on the gasifier performance

The characteristics of the biomass feedstock have a significant effect on the performance of the gasifier, especially the following ones:

- Moisture content: Fuel with moisture content above about 30% makes ignition difficult and reduces the CV of the product gas due to the need to evaporate the additional moisture before combustion/gasification can occur. High moisture content reduces the temperature achieved in the oxidation zone, resulting in the

incomplete cracking of the hydrocarbons released from the pyrolysis zone. Increased levels of moisture and the presence of CO produce $H_2$ by the water gas shift reaction and in turn the increased $H_2$ content of the gas produces more $CH_4$ by direct hydrogenation. The gain in $H_2$ and $CH_4$ of the product gas does not however compensate for the loss of energy due to the reduced CO content of the gas and therefore gives a product gas with a lower CV.

- Ash content: High mineral matter can make gasification impossible. The oxidation temperature is often above the melting point of the biomass ash, leading to clinkering/slagging problems and subsequent feed blockages. Clinker is a problem for ash contents above 5%, especially if the ash is high in alkali oxides and salts which produces eutectic mixtures with low melting points.
- Elemental composition: The elemental composition of the fuel is important with respect to the heating value and the emission levels in almost all applications. The production of nitrogen and sulphur compounds is generally small in biomass gasification because of the low nitrogen and sulphur content in biomass.
- Heating value: The heating value is determined by the elemental composition, the ash content of the biomass and in particularly on the fuel moisture content. On a dry and ash free basis, most biomass species have a heating value of about 19 MJ/kg.
- Volatile compounds: Besides operating conditions, reactor designs, etc. the amount of volatiles has an impact on the tar production levels in gasifiers. The gasifier must be designed to destruct tars and the heavy hydrocarbons released during the pyrolysis stage of the gasification process.
- Bulk density and morphology: The bulk density refers to the weight of material per unit of volume. Biomass of low bulk density is expensive to handle, transport and store. The particle size of the feedstock material depends on the hearth dimensions but is typically 10–20% of the hearth diameter. Larger particles can form bridges which prevent the feed moving down, while smaller particles tend to clog the available air voidage, leading to a high pressure drop and the subsequent shutdown of the gasifier.

Feedstock pre-treatment/preparation is required for almost all types of biomass materials because of a large variety in physical, chemical and morphological characteristics. The degree of pre-treatment of the biomass feedstock depends on the

gasification technology used. Fuel requirements for different gasifier types are presented in Table 1.4.

Table 1.4: Fuel requirements versus gasifier design (source: Knoef, 2005)

| Gasifier type | Downdraft | Updraft | Fluid bed | Entrained flow |
|---|---|---|---|---|
| Size (mm) | 20 -100 | 5 -100 | 10 -100 | < 1 |
| Moisture content (% w.b.) | < 1520 | < 50 | < 40 | < 15 |
| Ash content (% d.b.) | < 5 | < 15 | < 20 | < 20 |
| Morphology | Uniform | Almost uniform | Uniform | Uniform |
| Bulk density (kg/m$^3$) | > 500 | > 400 | > 100 | > 400 |
| Ash melting point (ºC) | > 1250 | > 1000 | > 1000 | < 1250 |

### 1.5.3 Gasification types. Reactor designs

Reactor designs have been investigated for more than a century, which resulted in the availability of several designs at small and large scale. Gasifiers can be classified in different ways (Rauch, 2003):

- According to the gasification agent: air-blown, oxygen or steam gasifiers.
- According to heat for gasification: autothermal (heat is provided by partial combustion of biomass) or allothermal (heat is supplied from an external source).
- According to pressure in the gasifier: atmospheric or pressurised
- According to the design of the reactor: fixed bed, fluidised bed, entrained flow or twin-bed

Despite these classifications, there are basically four major types of gasifiers existing in the industry: downdraft and updraft gasifiers, which are in the fixed bed category; and fluidized bed gasifiers, which consist of bubbling fluidized bed biomass gasifiers (BFB) and circulating fluidized biomass bed gasifiers (CFB).

#### 1.5.3.1 Gasification in fixed bed reactors

These reactors are rather easy to construct and operate and are widely available, especially in developing countries. They are suitable for small scale applications but have, in general, limited scale-up properties. There are mainly two types of fixed bed gasifiers, depending on whether the gasification agent is feed from the top of the reactor, as the biomass (downdraft), or from the bottom and therefore counter-current to the biomass flow (updraft):

- Updraft gasifier

  This is the simplest type of gasifier (Figure 1.8). Biomass moves counter-currently to the gas flow, and passes through the drying zone, the pyrolysis zone, the reduction zone and the oxidation zone.

  The major advantages of this type of gasifier are its simplicity, high charcoal burn-out and internal heat exchange leading to relatively low gas exit temperatures and high gasification efficiencies. Because of the internal heat exchange, the fuel is dried in the top of the gasifier and therefore fuels with high moisture content (up to 60% w.b.) can be used. Furthermore, this type of gasifier can even process relatively small sized fuel particles and accepts some size variation in the fuel feedstock.

  Major drawbacks are the high amounts of tar and pyrolysis products, because the pyrolysis gas is not combusted. This is of minor importance if the gas is used for direct heat applications, in which the tars are simply burnt. In case the gas is used for power production, extensive gas cleaning is required.

- Downdraft gasifier

  In downdraft reactor (Figure 1.8), the fuel and the gas move in the same direction. The same zones can be distinguished as in the updraft gasifier, although the order is somewhat different.

  Downdraft gasifiers produce the lowest level of tar and are therefore the best option for engine applications. Scaling-up of this type of gasifier is however limited. At low load levels, the temperature is decreasing and more tars are

produced because the tar cracking becomes less efficient but the advantage is the lower content of particles in the gas. At high load levels, the tar cracking capability is higher which results in lower tar levels. However, more particles are entrained with the gas. At too high load levels, the residence time for tar cracking becomes too short which will increase the tar level again, along with the particle level.

Drawbacks of the downdraft gasifier are the high amounts of ash and dust particles in the gas. This leads also to a relative high temperature of the leaving gases resulting in lower gasification efficiency. Downdraft gasifier demand a relatively strict requirements of the fuel like moisture content less than 25% (w.b.) and of uniform size in the range of 4-10 cm to realise regular flow, no blocking in the throat, enough “open space” for the pyrolysis gases to flow downwards and to allow heat transport from the hearth zone upwards. This type of gasifiers is used in power production applications in a range from 80 up to 500 $kW_e$ approximately.

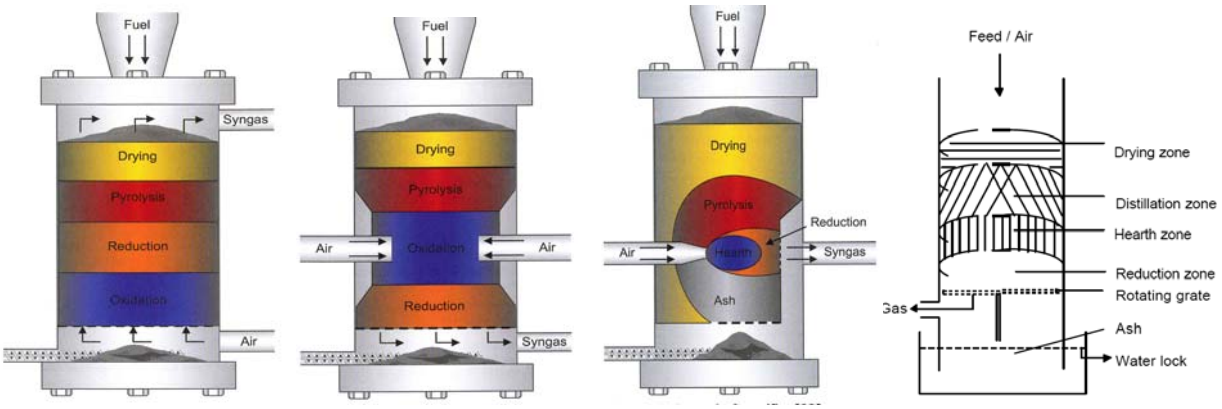


Figure 1.8: From left to right: updraft, downdraft, crossdraft and open core gasifiers (source: Knoef, 2005)

Other designs for fixed bed gasifiers are:

- Open core gasifiers (Figure 1.8): especially designed to gasify fine materials with low bulk density, for example rice husks.
- Crossdraft gasifier (Figure 1.8): adapted for the use of charcoal that reaches very high temperatures (1500ºC and higher) in the hearth zone which can lead to material problems.

- Double fire gasifier: a combination of downdraft and updraft gasification. In the upper part of the gasifier the fuel is converted by means of a downdraft but a certain amount of unreacted charcoal accumulates in the reduction zone. The purpose of two-zone gasification is to use updraft gasification to convert this residual fuel in the grate area completely into producer gas.
- Staged fixed bed gasification systems: based on the separation of the partial processes of thermo-chemical conversion (drying, pyrolysis, oxidation, reduction) in separated reactors. The separation of the process steps permits a greater influence on the partial steps.

Some major characteristics of updraft, downdraft, crossdraft and opencore gasifiers are presented in Table 1.5. Because of the variety of gasifier designs, which have been developed for each type of gasifier, the mentioned data are only rough indications. The efficiency of a gasifier reactor can be expressed on cold or hot gas basis. Cold gas efficiency ($\eta_{CG}$) is the chemical energy content of the producer gas divided by the energy content of the biomass while the hot gas efficiency ($\eta_{HG}$) is the chemical and heat energy content of producer gas divided by the energy content of the biomass. In well-insulated reactors, the hot gas efficiency can be close to 100%.

Table 1.5: Some characteristics of fixed bed gasifiers (Knoef, 2005)

| | **Downdraft** | **Updraft** | **Crossdraft** | **Open core** |
|---|---|---|---|---|
| Fuel (wood) | | | (charcoal) | |
| - moist. Cont. (% w.b.) | 12 (max. 25) | 43 (max. 60) | 10 – 20 | 7 – 15 (max.15) |
| - ash content (% d.b.) | 0.5 (max. 6) | 1.4 (max. 25) | 0.5 – 1.0 | 1 – 2 (max. 20) |
| - size (mm) | 20 – 100 | 5 – 100 | 5 – 20 | 1 – 5 |
| Gas exit temp. (ºC) | 700 | 200 – 400 | 1250 | 250 – 500 |
| Tars (g/Nm$^3$) | 0.015 – 0.5 | 30 – 150 | 0.01 – 0.1 | 2 – 10 |
| Sensitivity to load fluctuations | Sensitive | Not sensitive | Sensitive | Not sensitive |
| $\eta_{HG}$ full load (%) | 85 – 90 | 90 – 95 | 75 – 90 | 70 – 80 |
| $\eta_{CG}$ full load (%) | 65 – 75 | 40 – 60 | 70 – 85 | 35 – 50 |
| Producer gas LHV (MJ/Nm$^3$) | 4.5 – 5.0 | 5.0 – 6.0 | 4.0 – 4.5 | 5.5 – 6.0 |

### 1.5.3.2 Gasification in fluidised bed reactors

Fluidised-bed reactors function with a fluidised mix of bed material and biomass. The gasification medium flows in through the nozzle bottom and fluidises the bed material.

This can be inert, as for example quartz sand or also catalytically active with regard to the conversion of organic contaminants in the crude gas through possible after-reactions in the gas phases. For this purpose, substances like dolomite or olivine can be used. The air passes upwards through the bed, and when the point where the pressure drop equals the gravity force of the particles, the particles become suspended and termed fluidised at the minimum fluidisation velocity. This is an important parameter in designing fluid bed reactors. Further increase of the air velocity causes the particles to move more and more vigorously resembling a boiling liquid.

Due to the intense mixing the different zones (drying, pyrolysis, oxidation, reduction) cannot be distinguished like at fixed bed gasifiers; the temperature is uniform throughout the bed. Contrary to fixed bed gasifiers the air-biomass ratio can be changed, and as a result the bed temperature can be controlled, usually between 700 to 900ºC.

The advantages of fluidised bed reactors in comparison with fixed bed reactors are (Knoef, 2005):

- Compact construction because of high heat exchange and reaction rates due to the intensive mixing in the bed.
- Flexible to changes in fuel characteristics such as moisture and ash content; ability to deal with fluffy and fine grained materials with high ash contents and/or low bulk density.
- Relatively low ash melting points are allowed due to the low reaction temperatures.

But the drawbacks are (Knoef, 2005):

- High tar and dust content of the produced gas.
- High producer gas temperatures containing alkali metals in the vapor state.
- Incomplete carbon burn out.
- Complex operation because of the need to control the supply of both air supply and solid fuel.
- The need for power consumption for the compression of the gas stream.

The main fluidised bed reactor designs are:

- Bubbling fluidised bed (BFB)

  The BFB gasifier (Figure 1.9) is well known and commonly used because of its robust properties. The BFB utilizes the minimum fluidisation velocity of the bed material to achieve fluidisation state and has a distinct interface between the freeboard above the bed surface and fluidised bed reaction zone. Tar production is ~ 1% to 2% because the unit operates like a continuous stirred thermal reactor, so there is some biomass and tar slip.

- Circulating fluidised bed (CFB)

  The CFB gasifier (Figure 1.9) has no distinct interface between the fluidised sand bed and the freeboard. It uses a velocity higher than the minimum fluidisation velocity and requires a cyclone separator to transport the elutriated bed material back to the gasifier. CFB operates with higher superficial velocities, typically in the range of 2-5 m/s, whereas the velocity in the BFB is only 0.5-2 m/s, maintaining the ratio of fuel to fluidization gas (Gómez-Baera and Leckner, 2010). This type of gasifier increases the rate of gasification, has a high conversion rate of tar and is suitable for large scale power generations. The carbon burn out in circulating fluidised bed gasifiers is considerably better than in bubbling fluidised beds.

- Dual fluidised bed (DFB)

  This system has two chambers (a gasifier and a combustor). Biomass is fed into the CFB/BFB gasification chamber, and converted to nitrogen free syngas and char using steam. The char is burnt in air in the CFB/BFB combustion chamber, heating the accompanying bed particles. This hot bed material is then fed back into the gasification chamber, providing the indirect reaction heat. This reactor operates at temperatures below 900ºC to avoid ash melting and sticking.

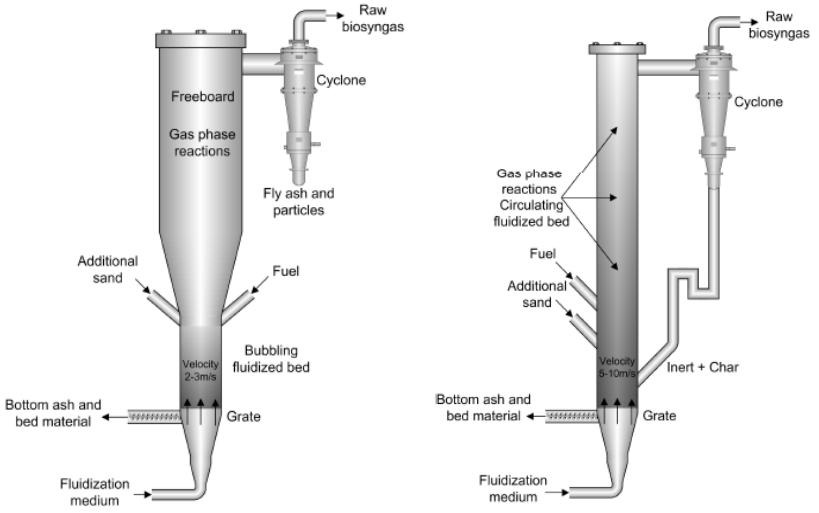


Figure 1.9: Diagram of a bubbling fluidised bed gasifier (left) and a circulating fluidised bed gasifier (right) (source: Knoef, 2005)

In the following table (Table 1.6) the general operating conditions of the four main types of gasifiers are presented and compared.

Table 1.6: Operating conditions of different types of gasifiers (source: Stassen et al., 2002)

| | **Downdraft** | **Updraft** | **BFB** | **CFB** |
|---|---|---|---|---|
| T (ºC) | 700 – 1200 | 700 – 900 | < 900 | < 900 |
| Tars | Low | High | Moderate | Moderate |
| Control | Easy | Very easy | Moderate | Moderate |
| Scale ($MW_{th}$) | < 5 | < 20 | 10 – 100 | 20 - ?? |
| Feedstock | Very critical | Critical | Less critical | Less critical |

### 1.5.4 Gas cooling

The purpose of gas cooling is to lower the producer gas temperature to fulfil the requirements and necessary producer gas temperatures due to the optimal operation conditions of the present gas treatment step. In demonstration facilities the reactor discharge (500-800°C) is cooled down to a level of about 600-100 °C, e.g. to be able to carry out dry particle filtration with ceramic filters or fabric filters respectively. For gas utilisation a temperature range of below 40°C is required to attain a volumetric efficiency in the gas engine that is as high as possible – therefore adequate cooler and chillers have to be installed, which allows to decrease the producer gas temperature on

a certain stable level as well as which allows to fall below the dew point of the producer gas. The gas cooling requires well founded design of the various heat exchangers according to the application requirements of wood gas and its efficient usage in internal combustion engines (ICE).

### 1.5.5 Gas conditioning

The producer gas leaving the gasifier will contain undesired particulates, tars and other contaminants which can cause problems in the downstream application. Depending on the feedstock, the type of gasifier used and other factors the composition of the produced gas will vary. Despite the type of application in which the produced gas is meant to be used, it must meet the requirement of the specific application. For a direct combustion system the raw gas may be used with little clean-up but for use in a gas turbine extensive clean-up may be needed. It would be preferable to design gasifiers that minimize the contaminants but since the forming of these contaminants is somewhat inevitable additional gas cleaning must be considered (Stevens, 2001). There are five primary contaminants that have to be regarded (Stevens, 2001):

- Particulates
- Alkali compounds
- Tars
- Nitrogen-containing compounds
- Sulphur

Particulates are solid-phase materials entrained in the product gas leaving the gasifier. They include inorganic ash, unconverted biomass in the form of char or material from the gasifier bed. Particulates are unwanted in the product gases since they can cause erosion on downstream equipment which leads to a shortened time of operation (Stevens, 2001). Depending on the desired application requirements for particulate removal varies but for use in gas turbine levels below 15 mg/Nm$^3$, with a particle size below 5 μm is needed. The most common systems for particular removal are the following (Stevens, 2001): cyclonic filters, barrier filters, electrostatic filters and wet scrubbers.

Biomass can contain large amounts of alkali compounds. This is problematic since some of these contaminants can vaporize at fairly low temperatures of about 700°C. Therefore these alkali vapours cannot be separated by filtration. When the gas temperature then is lowered the vapours will start to condensate and form particles which finally deposit on cooler surfaces of the downstream equipment. If the gas is to be used in a gas turbine, such build-up must be avoided otherwise it may cause imbalance which in turn can lead to breakdown of the machinery (Stevens, 2001). To remove alkali vapours today's gasification system has to cool the product gas below 600°C. By doing so the alkali vapours condensate to solid particulates. After that, previously described filtration techniques can be used to remove the alkali compounds. Consideration of the alkalis possibilities to cause corrosion on metallic or ceramic filters although has to be taken into account (Stevens, 2001).

Tar is a general term which describes a wide range of oxygenated organic elements. These elements are produced by partial reaction of the biomass fuel. The tars occur in the gas stream in the form of vapour or aerosols. The presence of tar can be accepted if the product gas is to be used in e.g. burner because then cooling and condensation of the tar can be evaded. The tar then contributes to the calorific value of the fuel. If the gas is intended for applications with higher demands on the product gas even small concentrations of tar can cause a problem. Tars can easily condensate on cool equipment which can result in plugging and fouling. Also at temperatures above about 400°C the tars can undergo reactions forming solid char and coke that can plug the equipment (Stevens, 2001).

Removal of the tar is essential in systems where cooling of the gas occurs before use, because the condensation of tar on pipes and other equipment will cause problems. Besides the operational problems, tar also means that the gasification efficiency is reduced. Therefore it is also important to choose a gasification technology that minimizes tar production. Two different approaches on removing tar is to either physically removing the tar, using techniques resembling that of particulate removal, or catalytic or thermal processing. These two approaches are discussed below and summarised in Figure 1.10.

- Tar physical removal

It requires that the product gas is cooled, allowing the tars to condensate. At present, tars are most frequently removed from the gas stream by cooling the product gas to allow tar condensation into aerosol droplets and then removing the droplets using technologies similar to those for particulate removal. These technologies include wet scrubbers, electrostatic precipitators, or cyclones. Particulates are removed separately from tars. While it is possible to remove both simultaneously, the condensation of sticky tars on particulate surfaces can lead to plugging and fouling of gas conditioning equipment.

The most effective way to physically remove tars is to use wet scrubbers and electrostatic precipitators. But waste usually consists of water mixed with tar components, thus a convenient waste water treatment process is required. In addition, it should be taken into consideration that tars formed during the gasification process at temperatures less than 800ºC can be handled using standard safety practices, while tars formed at temperatures above 800ºC are much more hazardous to human health.

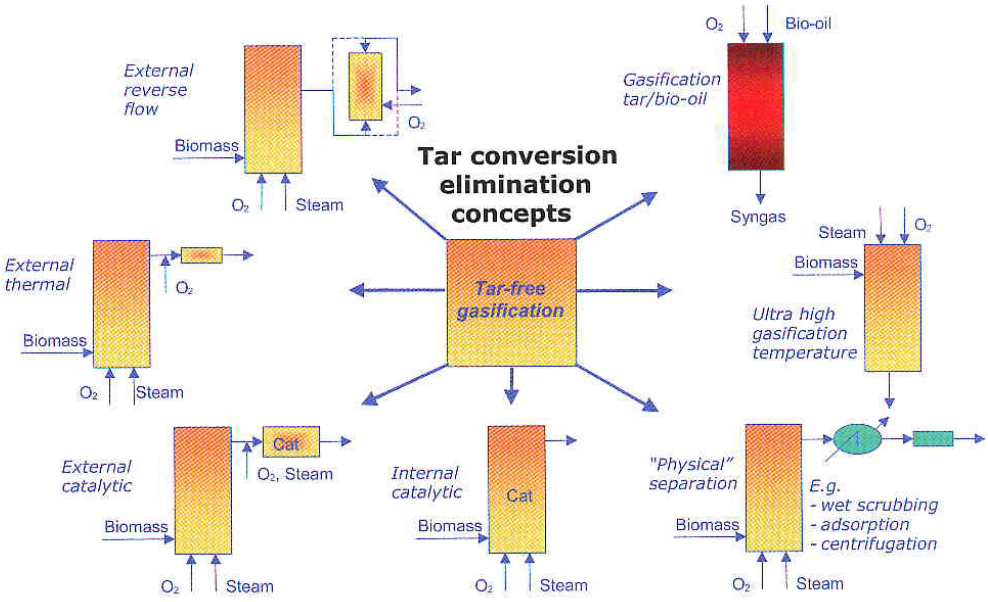


Figure 1.10: Different tar conversion or elimination concepts (source: Stassen et al., 2002).

- Catalytic and thermal tar destruction

In these processes, tars thermally decompose to form additional product gas and sometimes char. Tar destruction can be accomplished with thermal energy alone at above about 1200 °C or with catalysts at moderate temperatures of 750-900 °C.

Three main groups of catalysts have been evaluated for elimination of tar in the producer gas (Sutton, 2001):

- Naturally occurring catalysts such as dolomite and olivine
- Stable metals such as nickel and alkali metals
- Alkalis such as KO, $KHCO_3$ and $K_2CO_3$

While catalysts facilitate tar destruction at intermediate temperatures, tars can also be cracked thermally without catalysts at higher temperatures, typically 1200 °C or higher. The temperature where the cracking takes place is dependent on the kind of tar produced from the gasification process, but it is in the temperature range 900ºC to 1300ºC (Brand and Henriksen, 2000). The problems with operating at such high temperatures are reduction in the heating value of the product gas (Brand and Henriksen, 2000) and higher heat losses. Thus, economical and operational considerations make thermal cracking of tar less attractive in larger-scale gasifiers.

Ammonia is the primary contamination originating from nitrogen in the biomass. It is formed from protein and other nitrogen-containing components. In pressurized gasification there is a higher ammonia production because of the equilibrium considerations. Ammonia in the product gas is unwanted due to the formation of $NO_x$ when the product gas is burned. For this reason, it has to be removed with either catalytic destruction or wet scrubbing. The formation of $NO_x$ in gasifiers is not a big problem since the temperatures at which gasification occurs are low in comparison with combustion (Stevens, 2001).

If the biomass contains sulphur it can be converted to hydrogen sulphide or sulphur oxides when gasified. However, most of the different biomass fuels contain very low shares of sulphur (<0.1% in wood) although refused derived fuels (RDF) can contain higher levels. So, with most biomasses the concentrations of hydrogen sulphide and sulphur oxides are below clean-up requirements for most applications (Stevens, 2001).

## 1.6 POWER GENERATION FROM BIOMASS GASIFICATION

The gaseous products from biomass gasification can be used to generate heat and/or electricity, or they can potentially be used in the synthesis of liquid transportation fuels, $H_2$, or chemicals. The main technologies able to use producer gas to generate power and/or heat are:

- Internal combustion engines (ICE)
- Steam turbines
- Gas turbines
- Externally fired gas turbines (EFGT)
- Combined cycle systems (IGCC)
- Fuel cells
- Stirling engines

Table 1.7 summarises the efficiency (based on LHV) and suitable size for plants that use different technologies with producer gas as fuel.

Table 1.7: Efficiency (LHV) and suitable size for plants that use producer gas as fuel. The size is limited by the available gasifiers and by the fact that biomass is a local source of energy.

| Configuration | Efficiencies (%) | | | Nominal Capacity (MW) | Reference |
|---|---|---|---|---|---|
| | Thermal recovery | Electrical conversion | Overall Cogeneration | | |
| Engines | | | | | |
| - Gas engine | | | | 0.01 – 10 | Bauen (2004) |
| - Small gas engine | 50 | 20 – 32 | 74 – 82 | 0.01 – 0.5 | Demirbas (2006) |
| - Large gas engine | 50 | 26 – 36 | 76 – 86 | 0.5 – 3 | Demirbas (2006) |
| - Diesel engines | 50 | 23 – 38 | 73 – 88 | 0.01 – 3 | Demirbas (2006) |
| Steam turbine | - | 15 – 35<br>17 – 34<br>30 – 35<br>15 – 24 | - | 1 – 100<br>10 – 100<br>5 – 25<br>> 5 | Bauen (2004)<br>Demirbas (2006)<br>IEA (2007)<br>Meshram & Mohan (2007) |
| Gas turbine | | ~ 30 | | 0.1 – 10 | Bauen (2004) |
| - Small gas turbine | 50 | 24 – 31 | 74 – 81 | 0.8 – 10 | Demirbas (2006) |
| - Large gas turbine | 50 | 26 – 31 | 78 – 81 | 10 – 100 | Demirbas (2006) |
| Combined cycle (Brayton + Rankine) | | 47 – 52<br>30 – 40<br>45 – 55 | | 1 – 100<br>10 – 30 | Bauen (2004)<br>IEA (2007)<br>Meshram & Mohan (2007) |
| Combined cycle (Gas engine + Rankine) | | 40 – 50 | | 1 – 10 | Bauen (2004) |
| Fuel cell system | | 35 – 60 | | 0.01 – 1 | Larminie and Dicks (2003) |
| Stirling engine | | 11 – 20 | | < 0.1 | IEA (2007) |

Several experiments on part-load behaviour have shown that ICE provide a slightly better part load efficiency than microturbines (Alanne and Saari, 2004; Wang et al., 2004). In comparison to that, stirling engine and EFGT part load efficiency seems to decrease more significantly, although only few results have been published so far (Obernberger et al., 2003; Traverso et al., 2005; Traverso et al., 2003).

Discussing maintenance efforts and interval cycles, it can be stated that microturbines and stirling engines are significantly easier to maintain. Both technologies can run up to 10,000-15,000 hours continuously and normally need only one day of maintenance per year (Obernberger et al., 2003; Vincent and Strenziok, 2007; Wiltsee and Emerson, 2003). In comparison to that, conventional internal combustion engines need significantly more maintenance, and especially in biomass applications their oil lubrication suffers from the solubility of $H_2S$ and they require frequent oil changes (Alanne and Saari, 2004; Vincent and Strenziok, 2007; Wiltsee and Emerson, 2003). Product gas impurities represent an important factor regarding availability, operation and the service life of ICE operated CHP plants. Values recommended by the manufacturers of gas utilisation facilities as the permissible upper limits of such contaminants regarding various methods of energetic utilization of producer gas are listed in Table 1.8.

Table 1.8: Requirements for product gas in ICE and gas turbines (source: Nussbaumer et al., 1997; Bandi, 2003 and Steinbrecher and Walter, 2001)

| | Particle content ($mg/Nm^3$) | Particle size (µm) | Tar content ($mg/Nm^3$) | Alkali content ($mg/Nm^3$) |
|---|---|---|---|---|
| ICE | < 50 (25) | < 10 | < 50 (25) | n/v |
| Gas turbine | < 30 | < 5 | n/v | < 0.24 |

Discussing investment costs of the different engines, a clear tendency towards ICE can be found, followed by microturbines and EFGT. Stirling engines are still significantly more expensive (Alanne and Saari, 2004; McDonald and Rodgers, 2008). However, it should be taken into consideration that the latter three are still relatively new technologies which cannot provide the economies of scales of several decades of ICE manufacturing yet, and that, at least for microturbines, the market just recently started to become more mature and decreasing prices seem likely.

Concerning the size of the plant, Bridgwater (2002) considered that 35-40 $MW_e$ would be a reasonable size for an IGCC based plant, which could benefit from the efficiency advantages of increased scale, without suffering the economic disadvantages of increasing the biomass catchment area to supply fuel demands. It has to be taken into account that for a biomass gasification plant, the biomass fuel should come from the local area as a long distance transport cannot be justified economically due to its small heating value. According to Hislop and Hall (1996) because of the high transport costs and dispersed production of biomass, the maximum size of a generating plant is likely to be about 50-100 $MW_e$, far smaller than the typical fossil-fuelled plant. However, storage and handling equipment has inevitably to be proportionately larger and more expensive.

Baratieri et al (2009) considered that the ICE plant layout seem to be suitable for small size CHP plants (100-1000 $kW_e$), since the thermal power produced can be exploited at the local scale, avoiding the installation of an extended and expensive district heating network. Also according to these authors, the IGCC plant could be reasonably scaled up to medium sizes (10-20 $MW_e$), as it mainly generates electrical energy. According to Yong (2003) the most viable options for electricity generation from biomass gasification are steam turbine cycle for large-scale plants, gas turbine cycle for medium-scale plants and ICE for small-scale plants. The author also considers that today, commercially successful technologies for biomass gasification for electricity generation using gas engines get wide application because of their small system capacity, nimble arrangement, low investment, compact structure, reliable technique, low running cost, simple operation and maintenance and their low demand for gas quality. For power outputs below 200 kW he considers downdraft gasifiers as the best option and for higher power outputs the best option is fluidised bed gasifiers coupled with several ICE. Arena et al. (2010) reviewed the different devices that can be used to convert producer gas into electricity in a size range of 100-600 $kW_e$ and their electrical efficiency. They concluded that: steam turbines in that size range have a low net electrical efficiency (10-20%) and intensive capital costs, internal combustion gas turbines have an efficiency of 15-25% but present technical difficulties due to the producer gas contaminants, EFGT with an efficiency of 10-20% were considered a suitable option together with ICE (efficiency 13-28%) but among these two options they concluded that ICE is the solution that currently offers the higher reliability and provides the higher internal rate of return for the investigated range of electrical energy production.

The recommendations presented by Kurkela (2006), which are in good agreement with the ones cited above from other authors, can summarise the discussion of this section about the most suitable configuration depending on the size of the plant:

- Small-scale plants (<500 $kW_e$ + 1$MW_{th}$): downdraft gasifiers + ICE
- Medium-scale plants (0.5-15 $MW_e$ + 1-15 $MW_{th}$): fluidised bed / staged processes + several ICE, fuel cells or small gas turbines (future) and also fluidised bed + steam turbine cycle (> 3-5 $MW_e$)
- Large-scale plants (15-150 $MW_e$ + 15-150 $MW_{th}$): pressurised fluidised bed gasification + combined cycle / engine-steam turbine cycle and also possibly steam cycle.
- Co-firing in coal or natural gas power plants is also an option for plants bigger than 50 $MW_{th}$ of fuel input using fluidised bed gasification.

## 1.7 IMPLEMENTED BIOMASS GASIFICATION BASED PLANTS

Cogeneration or combine heat and power (CHP) is defined as the simultaneous generation of two different forms of useful energy using one single primary energy source. The most usual combination is the production of electricity and useful heat. Cogeneration technology provides greater conversion efficiencies than traditional generation methods as it harnesses heat that would otherwise be wasted. Also, $CO_2$ emissions can be substantially reduced. Furthermore, the heat by-product is available for use without the need for the further burning of a primary fuel. Figure 1.11 shows the efficiency advantage of CHP compared with conventional central station power generation and onsite boilers. When considering both thermal and electrical processes together, CHP typically requires only ¾ the primary energy separate heat and power systems require. CHP systems utilize less fuel than separate heat and power generation, resulting for same level of output, resulting in fewer emissions.

Cogeneration systems predominantly use natural gas, a fuel source which emits less than half the greenhouse gas, per unit of energy produced than the cleanest available conventional thermal power station using coal. The use of renewable primary energy sources like biomass avoids problems associate with traditional fossil fuels like price surge and volatility and brings many advantages including a greater reduction of

greenhouse gas/carbon dioxide emissions, local economic development, waste reduction and the security of a domestic fuel supply.

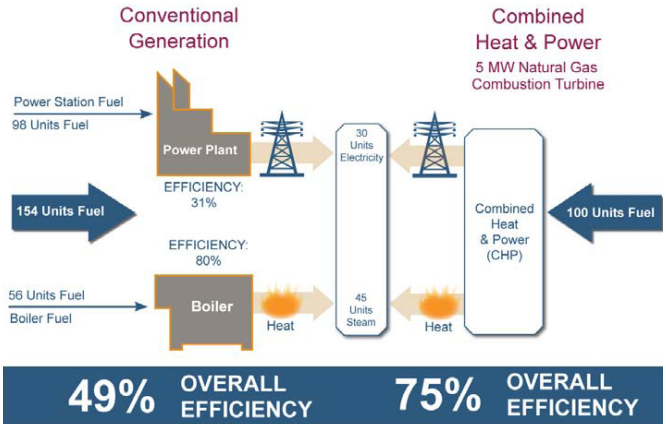


Figure 1.11: CHP versus separate heat and power production (source: EPA, 2008)

Compared with cogeneration, trigeneration is the generation of three energy services and/or manufactured products, seeking to take advantage of the maximum thermodynamic potential (maximum thermodynamic efficiency) of the consumed resources. However, in this thesis, a trigeneration plant is considered as a cogeneration plant integrated with a thermally driven technology, usually absorption chillers. In this way, the waste heat from the cogeneration plant is used to produce cooling.

Several biomass gasification cogeneration plants have been implemented in the past years (Section 1.7.1), mainly small scale cogeneration plants using downdraft gasifiers with internal combustion engines. However, little work has been done on trigeneration plants producing heat, cold and electricity and the literature on this field is very scarce (Section 1.7.2). Nevertheless, recent technological advancements and cost reductions of absorption chillers have made trigeneration more attractive.

### 1.7.1 Biomass gasification cogeneration plants

This section aims to present and review the most significant implemented biomass gasification facilities for heat and power generation. However, special emphasis will be put in those operating with ICE because are the ones to be modelled in the present

thesis. More information and examples on implemented and demonstration biomass cogeneration plants can be found in the studies of Knoef (2005), Maniatis (2001), Babu (2006) and Kwant and Knoef (2004).

IGCC plants are seen as the total final concept of a biomass to electricity system. The development and implementation, however, is complex, as it involves all components, from fuel to power, in the gasification system. Several projects have been initiated for IGCC applications over the last years, however few have been implemented. The best known are the Sydraft plant at Värnamo based on Foster Wheeler technology and the ARBRE plant based on TPS technology. The ARBRE plant project (Arable Biomass Renewable Energy), built near Eggborough (UK) in 2001, was among the first of its kind in the U.K. producing energy from gasified biomass. The plant cost £30 million ($48 million) but closed after only eight days of operation never to reopen.

The construction of Värnamo pressurized gasifier of Foster Wheeler (formerly Ahlström) started in September 1991. The integrated operation of the pressurised CFB gasifier with hot gas clean-up and power generation (6 $MW_e$) in a close-coupled Alstom's (now part of Siemens) Typhoon gas turbine was demonstrated for over 3,600 hours with an electric efficiency of 32% and heat power of 9 $MW_{th}$. When the test programme was concluded at the end of 1999 the plant was mothballed because the capacity was too small for commercial operation. Within the $6^{th}$ EU framework program, a new project was approved for clean hydrogen-rich synthesis gas production using the Värnamo gasifier (CHRISGAS Project).

Co-firing is an interesting application for an accelerated market penetration potential as the overall costs are relative low due to the existence of the power cycle in the coal or gas fired power plant. In co-combustion, biomass is mixed with coal before or during the combustion process so the biomass residual ash is also mixed with the coal ash. In co-firing, producer gas from biomass gasification is burned together with coal so no ash mixing occurs. Co-firing has the advantage to allow the use of coal ash as a construction material which has an existing market. Also the technical risks are low as the gas is utilised hot and therefore there is no tar problem. As with coal, fuel gas produced by biomass gasification can be co-fired with natural gas either directly in turbines, boilers or duct burners or as reburning fuel.

According to Kwant and Knoef (2004) the first gasifier for co-firing was installed in Zeltweg (Austria), followed by others in Lahti (Finland), Amer (the Netherlands), Vermont (USA) and Ruien (Belgium). The main characteristics of the Lahti and Vermont plants are summarised in Table 1.9

Table 1.9: Main characteristics of Lahti and Vermont Plants (Knoef, 2005; Maniatis. 2001; Kwant and Knoef, 2004)

| | | |
|---|---|---|
| **Customer** | Kymiarvi Power Station, Lahden lampovoyma Oy | Burlington Electric Department |
| **Planning company** | Foster Wheeler Energia OY | Future Energy Resources Corp. U.S. Department of Energy |
| **Technology** | CFB – Co-firing | 2 CFB gasifiers (indirect gasification) |
| **Fuel power** | 40 – 70 MW | 44 MW |
| **Heat power** | 40 – 70 $MW_{th}$ | n.a. |
| **Electrical power** | About 20 $MW_e$ of 167 $MW_e$ maximum capacity of the coal boiler plant | 8 – 9 $MW_e$ supplied to a boiler / steam cycle |
| **Fuel** | Recycled mixture (wood, board, paper, plastics, RDF) | Whole tree chips, residue wood, reconstituted wood pellets, forest thinnings |
| **Producer gas composition** | n.a. | $H_2$ ( 22%), CO (44.4%), $CO_2$ (12.2%), $CH_4$ (15.6%) (17-19 $MJ/Nm^3$) |

#### 1.7.1.1 Internal combustion engine plants

A great number of small-scale fixed bed gasifiers are either in operation or under development around the world. Most of the units are CHP plants where heat is used for district heating. In India and China alone, hundreds of gasifiers are in operation at farms and small industries to produce heat or electricity at a local level (Kwant and Knoef, 2004). This section aims just to mention the most well-known and relevant CHP plants integrating ICE.

- Güssing Plant (Austria)

A steam biomass gasification process has been demonstrated in Güssing (Austria). The combined heat and power (CHP) plant (Figure 1.12) has a fuel capacity of 8 MW, an electrical output of about 2$MW_e$ and heat output of 4.5$MW_{th}$ with an electrical efficiency of about 25%. Wood chips with a water content of 20 - 30% are used as fuel. The plant consists of a fast internal circulating fluidised bed (FICFB) steam gasifiers, a two stage gas cleaning system, a gas engine with an electricity generator, and a heat utilization system. The start-up of the plant was in January 2002. The calorific value of

the producer gas is 12–14 MJ/Nm$^3$ with the following composition: $H_2$ 35-45%, CO 20-30%, $CO_2$ 15-25%, $CH_4$ 8-12%, $N_2$ 3-5% and a tar content after gas cleaning of < 20 mg/Nm$^3$ (Knoef, 2005).

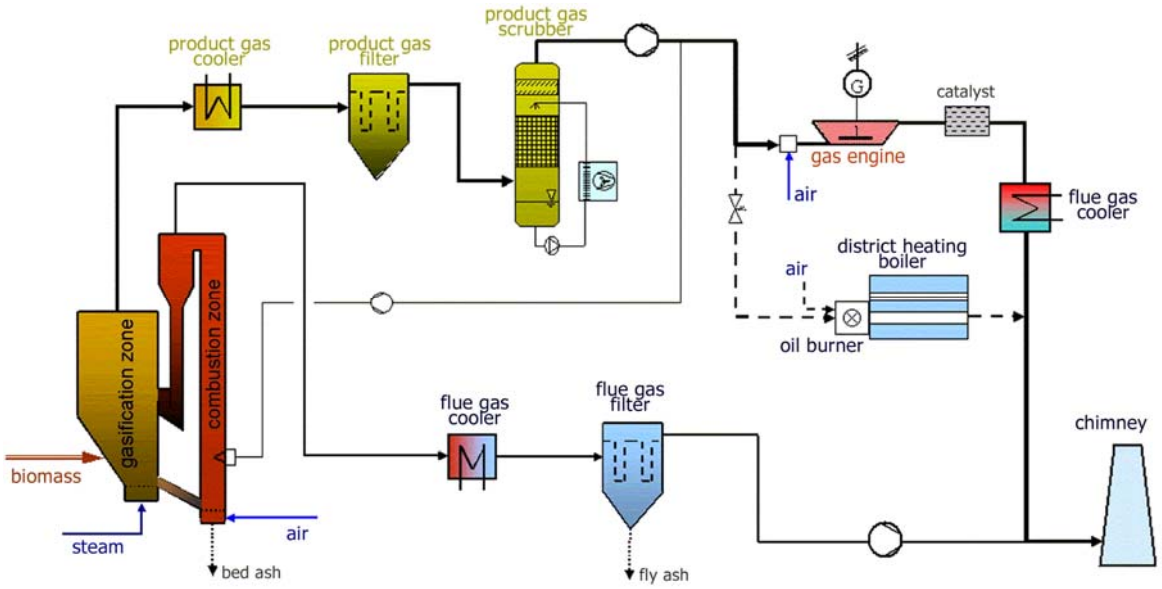


Figure 1.12: Process flow sheet of the Güssing Plant (Knoef, 2005)

- Harboøre Plant (Denmark)

Harboøre Plant was the first large scale biomass gasification (5 $MW_{th}$ Capacity) for CHP application that was built and commissioned in December 1993, by Babcock & Wilcox Vølund for the municipality of Harboøre, in Kyndby (Jutland, Denmark). The plant was originally intended solely to provide heat to the village heating grid and prove that a full-scale air blown updraft gasifier could be operated continuously. This was done successfully and some years later, in year 2000, the plant added gas engines for CHP. The Harboøre plant has a capacity up to 3.7 $MW_{th}$ fuel input and 1 $MW_e$ produced at the gas engine and 2 $MW_{th}$ supplied for district heating. In May 2010 the gasifier in Harboøre had a power production around 500 MWh per month, and a total supply of more than 32.000 MWh of electricity to the grid. Operational experience covers 110.000 hours of gasifier operation and 70.000 hours of engine operation (Heeb, 2010).

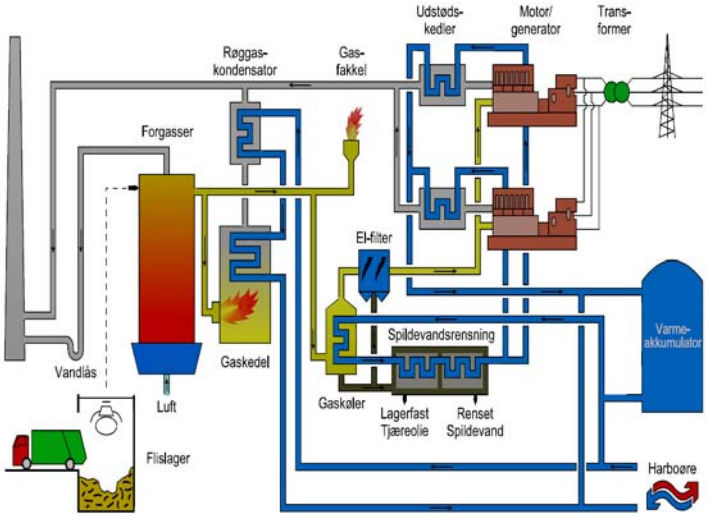


Figure 1.13: Process flow sheet of the Harboøre Plant (Denmark) (Babu, 2006)

- Movialsa Plant (Spain)

EQTEC Iberia is building a biomass gasification cogeneration plant at the alcohol distillery of the company Movialsa located at Campo de Criptana (Ciudad Real, Spain). The CHP plant has an electrical output of 5.9 $MW_e$ and produces 5600 kg/h of saturated steam at 6bar(g) and 159 $m^3$/h of hot water at 90ºC, which are used by the alcohol factory. The CHP plant will allow a total elimination of the bagasse and liquid effluent of the factory. Bagasse is used as fuel into the gasifier plant and liquid effluent, so called "vinazas" (mainly water with 1-2% of organic matter) is concentrated on a multistage evaporator using residual heat from producer gas engines. The plant is designed to be extended to a total power output of 13.8 $MW_e$. The main figures of the plant are summarised in Table 1.10.

Table 1.10: Main characteristics of Movialsa Plant (EQTEC Iberia, 2011)

| | |
|---|---|
| **Customer** | Movialsa |
| **Planning company** | EQTEC Iberia |
| **Technology** | Bubbling fluidised bed gasifier |
| **Fuel power** | 19600 (kW) (4000 kg/h) |
| **Heat power** | Steam (6 bar sat.): 5600 kg/h<br>Hot water (90ºC): 159$m^3$/h<br>(33.6% thermal efficiency) |
| **Electrical power** | 5.9 $MW_e$ (30.2% electrical efficiency) |
| **Fuel** | Bagasse |
| **Producer gas LHV** | 5.5 MJ/$Nm^3$ |

In addition to the plants referred in this section, other biomass gasification plants coupled with internal reciprocating engines have been constructed and operated in Europe:

- Moissanes (France) Updraft Gasifier (PRM Energy), 1 $MW_e$.
- Oberwart (Austria) Circulating fluidised bed (Repotech), 2.7 $MW_e$.
- Spiez (Switzerland) Dual-zone fixed bed downdraft (Pyroforce), 200 $kW_e$.
- Skive (Denmark) Renugas bubbling fluidised bed (Carbona), 5.5 $MW_e$, 11.5 $MW_{th}$.
- The Castor (Græsted, Denmark) Open core downdraft gasifier (BioSynergi Process), 90 $kW_e$
- Rossanno (Italy) Updraft gasifier, 4 $MW_e$.
- Gedinne (Belgium) Downdraft gasifier (Xylowatt S.A.), 0.3 $MW_e$ – 0.6 $MW_{th}$.
- Aqua-Tournai (Belgium) Downdraft gasifier (Xylowatt S.A.), 0.3 $MW_e$ – 0.6 $MW_{th}$.
- Wr. Neustadt (Austria) Twin-fire fixed bed gasifier (BMG), 0.5 $MW_e$, 0.7 $MW_{th}$.
- Viking (Denmark) Two-stage downdraft gasifier (DTU), 17.5 $kW_e$, 39 $kW_{th}$.
- Kokemäki Plant (Finland) Updraft gasifier (NOVEL process), 1.8 $MW_e$, 4.3 $MW_{th}$ (3.1 $MW_{th}$ without boiler).
- Enamora (Spain) BFB gasifier (EQTEC Iberia), 1.2 $MW_e$, 1.3 $MW_{th}$.

### 1.7.2 Biomass gasification trigeneration plants

Currently, biomass resources are mainly used in the production of heat and electricity (cogeneration) (REN21, 2007; Filho and Badr, 2004; Chinese and Meneghetti, 2005). Biomass cogeneration has been practiced by numerous industries for many years as a means of waste disposal and energy recovery. District heating combined with cogeneration has been used for several years in Northern Europe but it has not been considered a viable option for areas with warm climate up to now, as in these areas traditional cogeneration applications tend to prove financially unviable, due to the short operational time within the year (Chinese et al., 2004).

In this thesis, by trigeneration it is referred three products from the plant; chilled water provided by a chiller, hot water and electricity. Recent technological advancements and

cost reductions of absorption chillers have made trigeneration more attractive. Trigeneration combined with DHC (District heating and cooling) network is of great interest for relatively warm climates like Spain.

Very few works have been published concerning biomass fuelled trigeneration systems and even less focused on trigeneration integrating biomass gasification. In addition, it has not been possible to find, in the open literature, any existing demonstration trigeneration plant based on biomass gasification. However, few theoretical studies exist. Rentizelas et al. (2009) compared, in financial and technological terms, the ORC and gasification technology for trigeneration purposes aiming at serving a specific heating and cooling demand. ORC technology offered a solution of lower capital requirement and significantly lower operational and maintenance cost in comparison to gasification. Nonetheless, the notably higher power-to-heat ratio of the gasification technology allowed increased revenue from electricity generation and offset by far the higher technology-related cost. Therefore, gasification appeared to be a better solution in this comparison.

Huang et al (2011) studied a trigeneration system consisting of an ICE integrated with a downdraft biomass gasifier to supply electricity, hot water for space heating and cold to a commercial building. Hot water was generated using the waste heat recovered from the engine cooling and exhaust gases, excess heat was also used to drive and absorption cooling system. The system modelled had 250 $kW_e$ output at the full load. They concluded that the process efficiency of trigeneration (53.5-58.6%) was much higher than that of power only (20.5-22.9%), but it was lower than that of the cogeneration (61.4-66.5%). The authors considered that the trigeneration system with a biomass gasifier would be beneficial to the building system if the power/heat ratio is in the range of 0.5 to 0.75. They also found that the specific investment was very high for the small biomass trigeneration system ranging from 2520 £/kWe to 2579 £/kWe and that the system would perform much better economically in a building with a higher cooling load spread over a 12 month period instead of 5 month that they considered.

## 1.8 JUSTIFICATION AND OBJECTIVES

From the information presented in this chapter, it can be concluded the following. Biomass has been globally recognised, during several years, as the renewable resource that will make the most significant contribution for sustainable energy in the near to medium term. It is the only renewable that can directly replace fossil fuel based energy because allows continuous power generation and have a widespread availability. However, in nearly all of the EU-countries less than 50% of the available biomass resources are currently used and in most countries, the share is even significantly lower, which allows a high growth potential.

Biomass-to-electricity systems based on gasification have a number of potential advantages. Process efficiencies are much higher than the direct combustion systems in commercial use today and are comparable to high efficiency coal-based systems, but can be achieved at a smaller scale of operation. Thus, not only does biomass close the carbon cycle, but gasification based systems, due to their high efficiency, reduce $CO_2$ emissions and represents an attractive way of use of agricultural and forestry residues that could renovate rural economies and reduce energy dependency.

Considering that for a biomass gasification plant, the biomass fuel should come from the local area as a long distance transport cannot be justified economically; the size of a plant to be located in Catalonia should be that of small-medium scale.

After the literature review and according the opinion of different authors, for small and medium scale plants the recommended technologies are downdraft or fluidised bed gasifiers coupled with internal combustion engines. In addition, a great number of small-scale fixed bed gasifiers are either in operation or under development around the world. While ICEs are the solution that currently offers the higher reliability and provides the higher internal rate of return for the investigated range of electrical energy production.

Cogeneration has been used for many years for biomass gasification and several plants have been implemented. However, little work has been done on trigeneration plants producing heat, cold and electricity. Trigeneration plants are of great interest for warm climate and developing countries that usually have a high cooling demand but further research in this field is needed.

For these reasons, simple and reliable simulation tools are needed to give a better understanding of the whole process and as preliminary tools to evaluate the potential of trigeneration biomass gasification plants in a certain location. At a design stage, it is necessary to be able to quickly evaluate and calculate the outputs of the plant for different types of biomass, operating conditions and configurations. This accessible information is useful in order to achieve a better dissemination of this technology and encourage investors and local authorities to invest in this technology.

Taking into account the previously mentioned reasons, the main objective of this thesis is to develop a simplified but rigorous trigeneration plant model based on biomass gasification for the design, optimization and simulation of small-medium scale plants.

Considering the main objective of this thesis, the specific objectives are listed below:

- Revision and evaluation of different biomass gasification models followed by the selection of the most suitable biomass gasification model to be implemented for the simulation of these systems.
- Collection of published experimental data for different biomass and types of gasifiers (downdraft and fluidised bed).
- Development of a simple but rigorous model for downdraft and fluidised bed gasifiers.
- Development of a simple but reliable model for absorption chillers.
- Characterization and modelling of the different units implemented in a trigeneration plant (internal combustion engine, heat exchangers, clean-up section…)
- Development of a complete model for an air and air/steam biomass trigeneration plant considering different configurations for cold and hot water production.
- Application of the developed configurations to the ST-2 polygeneration plant that has to be implemented in the framework of Polycity Project in Cerdanyola del Vallès (Barcelona).

## 1.9 THESIS STRUCTURE

This thesis is divided into 6 chapters. The first chapter reviews the biomass general characteristics, actual use and potential of biomass resources both in Spain and EU. Different biomass conversion processes are also commented to focus later only on the biomass gasification process. Concerning biomass gasification, different steps, reactions and reactors are described followed by a summary of the most usual technologies for biomass to power generation as well as some examples of demonstration biomass gasification cogeneration plants. Finally, this chapter presents the justification and objectives of the thesis.

Chapter 2 reviews different approaches to model biomass gasification process: thermodynamic equilibrium models, kinetic models and ANN models. Then, these models are evaluated according their suitability to be applied to downdraft and fluidsed bed gasifiers. In addition, Chapter 2 also contains a review of experimental data for fluidised bed and downdraft gasifiers that has been gathered to be used in development and validation of different gasification models.

In Chapter 3, a modified thermodynamic equilibrium model is developed to determine the producer gas composition, LHV and cold gas efficiency based on ultimate analysis of biomass for downdraft and fluidised bed gasifiers. This model can be applied to systems that do not fully achieve equilibrium. Firstly, it is validated with published experimental data for downdraft and fluidised bed gasifiers. Then, the influence of several working parameters like ER, air-preheating, biomass moisture content, steam addition and oxygen enrichment in the producer gas composition is evaluated. The obtained predictions are also compared with those given by models developed by other authors.

In Chapter 4, two ANN models are developed, one for bubbling fluidised bed and the other for circulating fluidised bed gasifiers. Firstly, a brief summary of ANN definition, architecture, working principles and applications is given. Then, the ANN models are described. Both of them are based on experimental published data. The former one is for air, atmospheric pressure CFB gasifiers and the second one for atmospheric pressure air and air-steam BFB gasifiers. Finally, the results obtained with the ANN models are compared with those obtained by applying the modified equilibrium model for the same experimental data.

Chapter 5 deals with the modelling of the absorption chiller. Different approaches to the characteristic equation method are reviewed and a new one is presented. The new approach is based on a multiple regression fit using manufacturer's data to characterise part-load operation. The aim is to reduce the operating characteristics of absorption chillers into easier to handle simple algebraic equations that allow the model to be integrated in simulation and optimization programs.

Chapter 6 develops a whole small-medium size (250 $kW_e$ – 2 $MW_e$) biomass gasification trigeneration plant is model. Three different configurations of gasification based biomass to energy systems are investigated. All of them consist of a gasifier (downdraft or fluidised bed), an internal combustion engine, heat recovery section, gas clean-up and an absorption chiller. The differences between the three configurations are in how heat from exhaust gases and cooling water from the engine jacket is recovered and used. Later, these configurations are applied to a case study for the polygeneration plant ST-2 foreseen in Polycity project in Cerdanyola del Vallès (Barcelona).

Finally, chapter 6 presents the conclusions of the thesis and the possibilities of future work.

# Chapter 2

# Review of biomass gasification models

## 2.1 INTRODUCTION

One of the crucial processes in modelling a biomass gasification trigeneration plant is the biomass gasification step. The efficient operation of a biomass gasifier depends on a number of complex chemical reactions, including fast pyrolysis, partial oxidation of pyrolysis products, gasification of the resulting char, conversion of tar and lower hydrocarbons, and the water-gas shift reaction. These complicated processes require the development of mathematical models that can evaluate the influence of the main input variables, such as moisture content, air/fuel ratio on the producer-gas composition and the calorific value of the producer gas.

In this chapter, the main models developed for biomass gasification are reviewed. Then, they are compared to see which one suits better as a gasifier model, for downdraft and fluidised bed gasifiers, to be implemented in the trigeneration plant model. Furthermore, a literature search is done to gather published experimental data for downdraft and fluidised bed gasifiers using different biomasses and gasifying agents. This data will be then used to develop and validate the gasifier model.

## 2.2 KINETIC RATE MODELS

Kinetic models provide essential information on kinetic mechanisms to describe the conversion during biomass gasification, which is crucial in designing, evaluating and improving gasifiers. These rate models are accurate and detailed but computationally intensive (Sharma, 2008). Nevertheless, numerous researchers have focused extensively on kinetic models of biomass gasification: Wang and Kinoshita (1993), Di Blasi (2000), Fiaschi and Michelini (2001), Giltrap et al. (2003), Yang et al. (2003), Roshmi et al. (2004), Dennis et al. (2005), Babu and Seth (2006), Radmanesh et al. (2006), Gobel et al. (2007), Sharma et al. (2008), Fermoso et al. (2008), Zhong et al. (2009), Roy et al. (2009), Gerber et al. (2010) and Gordillo and Belghit (2011).

Kinetic models describe the char reduction process using kinetic rate expressions obtained from experiments and permit better simulation of the experimental data when the residence time of gas and biomass is relatively short.

The kinetic model proposed by Wang and Kinoshita (1993) is based on a mechanism of surface reactions in the reduction zone assuming a given residence time and reaction temperature. Giltrap et al. (2003) developed a model of the reduction zone of a downdraft biomass gasifier to predict the composition of the producer gas under steady-state operation, adopting the kinetic rate expressions of Wang and Kinoshita (1993). The accuracy of the model is limited by the availability of data on the initial conditions at the top of the reduction zone; pyrolysis and cracking reactions are not considered because the number of possible pyrolysis products, along with all the possible reactions and intermediate products, would make the model very complex. It assumes that all the oxygen from the air inlet is combusted to $CO_2$ and that the pyrolysis products are completely cracked. Solid carbon, in the form of char, is considered to be present throughout the reduction region. It is assumed that the char reactivity factor (CRF), which represents the reactivity of the char and is a key variable in the simulation, is taken as constant throughout the reduction zone. These authors tested the model with experimental data for two different downdraft gasifiers (Chee, 1987; Senelwa, 1997). Figure 2.1 compares the composition of the dry producer gas predicted by this model with those found experimentally. The model produced reasonable agreement with the experimental results for all components except $CH_4$. According to Giltrap et al. (2003), this over-prediction was the result of the assumption that $O_2$ in the air reacts only with char. The pyrolysis products are cracked in a region

of high temperature and in the presence of $O_2$, so it is probable that some of the $CH_4$ produced will undergo combustion with $O_2$. Figure 2.1 shows the results when the initial gas concentration is altered under the assumption that all of the $O_2$ in the air reacts with the $CH_4$ from the cracking of the pyrolysis gas. This assumption reduces the amount of $CH_4$ predicted, but the prediction is still higher than the concentrations found experimentally.

Jayah et al. (2003) developed a model based in the early work of Chen (1987) but with a few modifications. Chen's model was intended to estimate the length of the gasification zone and the diameter of the reactor, and to investigate the dependence of the reactor's performance on operating parameters such as feedstock moisture content, chip size, reactor insulation, input air temperature and gasifier load. Chen's model consists of three parts. The first part determines the amount of oxygen needed for a fixed input of fuel at a specific operating condition. The fuel-to-air ratio estimated from this first part of the model is then used as an input in the second part, where the drying, pyrolysis and combustion zones are all lumped together and considered as a single zone. The outputs from this "lumped" zone are the product concentrations and the temperatures of the gaseous and solid phases leaving the zone. These calculated concentrations and temperatures are then used as inputs in the third part of the model, which predicts the temperature profile along the axis of the gasification zone, the gas composition, the conversion efficiency and the length of the gasification zone at any given time interval. The main weakness of Chen's model is the over-prediction of the gas exit temperature from the "lumped" zone due to an unrealistically low estimate of heat loss and the omission of CO and $H_2$ in the pyrolysis gas. Jayah et al. (2003) therefore introduced modifications to overcome these deficiencies and also to suit a reactor with a variable rather than constant gasification zone diameter. For this reason, the authors incorporated Milligan's (1994) flaming pyrolysis sub-model instead of the algorithms used by Chen (1987). The aim of Milligan's Daming pyrolysis zone model is to calculate the composition of the product gas entering the gasification zone in terms of CO, $H_2$, $CO_2$, $H_2O$, $CH_4$ and $N_2$. As a result, the model used in the study by Jayah et al. (2003) consists of two sub-models, namely of the Daming pyrolysis and the gasification zones. The Daming pyrolysis zone sub-model is used to determine the maximum temperature and the product concentration of the gas leaving that zone. The gasification zone sub-model assumes that a single char particle moves vertically downwards along the vertical axis of the gasifier. This sub-model includes a description

of the physical and chemical processes, the flow equations, the transport phenomena and the conservation principles. The model is limited to considering the effect of packed char particles in the reduction zone.

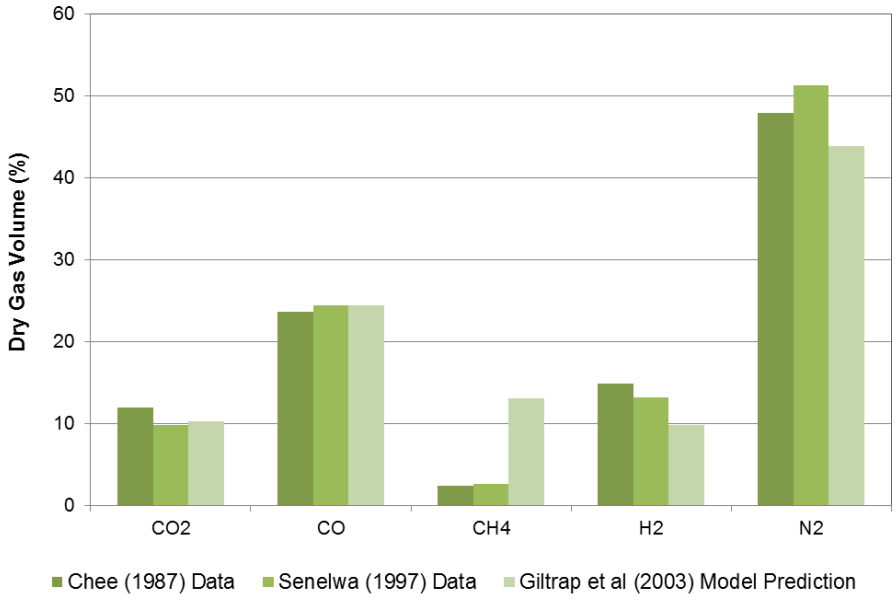


Figure 2.1: Predicted results from the model of Giltrap et al. (2003) compared with experimental data from Chee (1987) and Senelwa (1997).

Babu and Sheth (2006) modified Giltrap's model suggesting an exponentially varying CRF in order to predict better simulation of the temperature profile in the reduction reaction zone. The CRF value was increased both linearly and exponentially along the length of the reduction bed in the model. The model was simulated with a finite difference method to predict the temperature and composition profiles in the reduction zone. The model predictions were compared with the experimental data reported by Jayah et al. (2003) (Figure 2.2). Simulations were performed for varying CRFs ranging from 1 to 10,000, and linearly and exponentially as well. Simulations were also performed for different values of CRF (1, 10, 100 and 1000) held constant throughout the reduction zone. The authors of the study concluded that the CRF must be varied along the reduction zone of the downdraft gasifier and that their simulated results were in very good agreement with the experimental data of Jayah et al. (2003)—better, in fact, than the mathematical model of Jayah et al. (2003), which considered an exponentially varying CRF value.

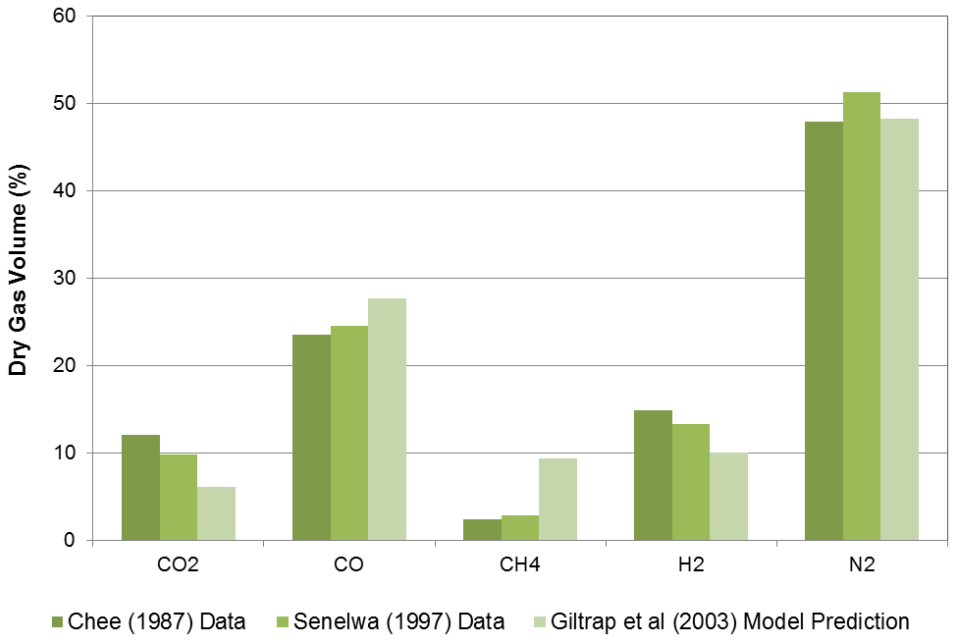


Figure 2.2: Predicted results from the model of Giltrap et al. (2003) compared with experimental data from Chee (1987) and Senelwa (1997) when the initial conditions of the model assumed that the $CH_4$ produced by the cracking of pyrolysis products reacts with $O_2$ entering the gasifier through the air inlet.

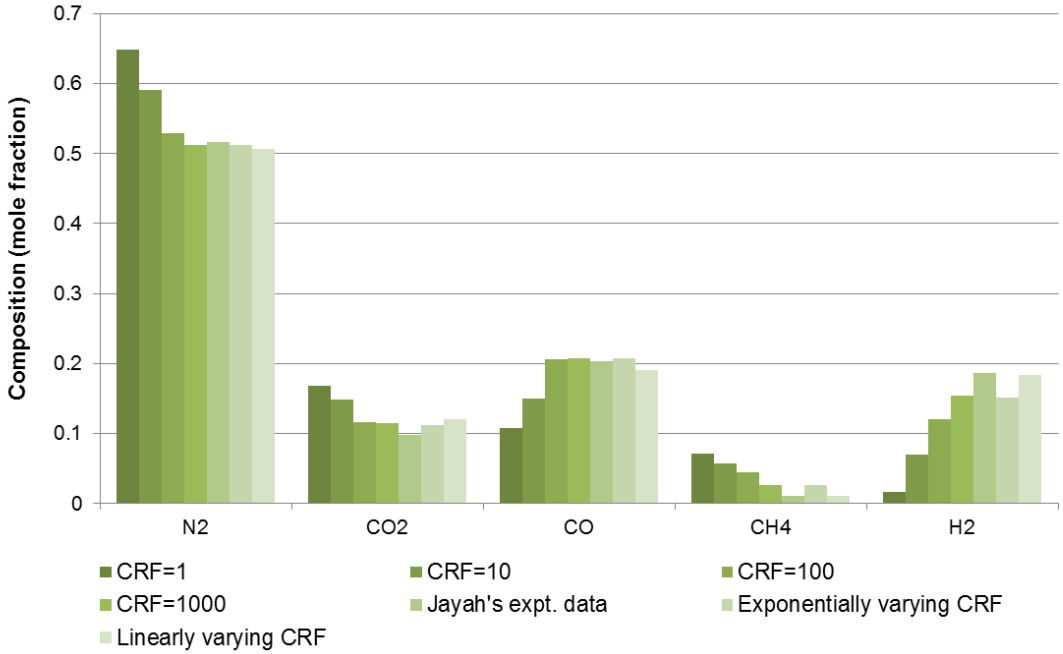


Figure 2.3: Comparison of various producer-gas compositions that have varying CRF values (Babu and Seth, 2006) with experimental data from Jayah et al. (2003).

Recently, Sharma (2008) presented a model for a downdraft gasifier in which the reduction zone was modelled using a finite rate of reaction following the chemical kinetics. The pyro-oxidation zone, prior to the reduction zone, was also modelled considering thermodynamic equilibrium. However, the author did not take into account any char combustion in the pyro-oxidation zone and also neglected the formation of methane there. The water-gas shift equilibrium was considered at the outlet of the pyro-oxidation zone. In the reduction zone, a linear variation of CRF was adopted. Following this previous work, Roy et al. (2009) developed a model for a downdraft gasifier based on chemical equilibrium in the pyro-oxidation zone and finite-rate kinetic-controlled chemical reactions in the reduction zone. The CRF was optimised by comparing the model's predictions against the experimental results from the literature.

## 2.3 THERMODYNAMIC EQUILIBRIUM MODELS

Kinetic rate models always contain parameters that limit their applicability to different plants. Thus, thermodynamic equilibrium calculations, which are independent of gasifier design, may be more suitable for process studies on the influence of the most important fuel process parameters. At chemical equilibrium, a reacting system is at its most stable composition, a condition achieved when the entropy of the system is maximised while its Gibbs free energy is minimised. However, thermodynamic equilibrium may not be achieved, mainly due to the relatively low operation temperatures (product gas outlet temperatures range from 750ºC to 1000ºC) (Bridgwater, 1995). Nevertheless, models based on thermodynamic equilibrium have been used widely. Some recent efforts include the work done by Bacon et al. (1982), Double et al. (1989), Ruggiero and Manfrida (1999), Zainal et al. (2001), Schuster et al. (2001), Altafini et al. (2003), Li et al. (2001, 2004), Melgar et al. (2007), Jarungthammachote and Dutta (2007 and 2008), Yoshida et al. (2008), Karamarkovic and Karamarkovic (2009), Huang and Ramaswamy (2009) and Haryanto et al. (2009) to predict the performance of commercial gasifiers. These authors have shown reasonable agreement between equilibrium predictions and experimental data.

Equilibrium models have two general approaches: stoichiometric and non-stoichiometric. The stoichiometric approach requires a clearly defined reaction mechanism that incorporates all chemical reactions and species involved. In the non-

stoichiometric approach, no particular reaction mechanisms or species are involved in the numerical simulation. The only input needed to specify the feed is its elemental composition, which can be readily obtained from ultimate analysis data (Li et al., 2004). The non-stoichiometric equilibrium model (Mathieu and Dubuisson, 2002) is based on minimising Gibbs free energy in the system without specifying the possible reactions taking place. The stoichiometric chemical equilibrium model is based on selecting those species that are present in the largest amounts, i.e. those which have the lowest value of free energy of formation. As noted by Prins et al. (2003), Desrosiers (1979) showed that under gasification conditions (with temperatures between 600 K and 1500 K) the only species present at concentrations higher than $10^{-4}$ mol% are CO, $CO_2$, $CH_4$, $H_2$, $N_2$, $H_2O$ and solid carbon (graphite). For this system of species, there are three independent chemical reactions (Reactions 3, 4, 6), according to Duhem's theory (Daubert, 1987). For the homogeneous system that consists of CO, $CO_2$, $CH_4$, $H_2$, $N_2$ and $H_2O$, there are two independent chemical reactions, resulting from the combination of Reaction 3 and Reaction 4 and also Reaction 3 and Reaction 6.

As shown by various authors (Smith and Missen, 1982; Jarungthammachote and Dutta, 2007), the two approaches (stoichiometric and non-stoichiometric) are essentially equivalent. A stoichiometric model may also use free energy data to determine the equilibrium constants of a proposed set of reactions.

Equilibrium models are based on some general assumptions that are in better agreement with some specific types of reactors for which equilibrium models have better predictive capabilities. Prins et al. (2007) presented these assumptions:

- The reactor is implicitly considered to be zero-dimensional.
- The gasifier is often regarded as a perfectly insulated apparatus, i.e. heat losses are neglected. In practice, gasifiers have heat losses to the environment, but this term can be incorporated in the enthalpy balance of the equilibrium model.
- Perfect mixing and uniform temperature are assumed for the gasifier although different hydrodynamics are observed in practice, depending on the design of the gasifier.
- The model assumes that gasification reaction rates are fast enough and residence time is long enough to reach the equilibrium state.

- No information about reaction pathways and the formation of intermediates is given in the model.
- Tars are not modelled.

Due to these assumptions, equilibrium models yield great disagreements under some circumstances. Typical pitfalls at relatively low gasification temperatures are the overestimation of $H_2$ and CO yields and the underestimation of $CO_2$, methane, tars and char (in fact, null values for these last three components above 800ºC) (Villanueva et al., 2008). For this reason, and as detailed below, several authors have modified and corrected the equilibrium model or used the quasi-equilibrium temperature (QET) approach.

Zainal et al. (2001) modelled the biomass gasification process on the basis of stoichiometric thermodynamic equilibrium. They predicted the composition of the producer gas for different biomass materials. Jarungthammachote and Dutta (2007) developed the thermodynamic equilibrium model based on the equilibrium constant for predicting the composition of a producer gas in a downdraft gasifier. They used coefficients for correcting the equilibrium constant of the water-gas shift reaction and the methane reaction in order to improve the model. Those coefficients were obtained from the comparison between the model and the results of other researchers' experiments. The predicted results from the modified model satisfactorily agree with experimental results reported by Jayah et al. (2003) (Table 2.1).

Jarungthammachote and Dutta (2008) applied the non-stoichiometric equilibrium model to three types of gasifiers: a central jet spouted bed, a circular split spouted bed and a spout-fluid bed. The simulation results from the model showed a significant deviation from the experimental data, especially for CO and $CO_2$. One important factor was carbon conversion. Thus, the model was modified to consider the effect of carbon conversion. The results improved and were closer to the experimental data (Table 2.2). However, this model could not give results with high accuracy for the spouted-bed gasification process. The heating value was also an important parameter because it is usually used to estimate the energy that could be gained from using that producer gas. The modified model predicted heating values that were generally higher than those from experiments because of the over-prediction of the CO content in the producer gas.

Table 2.1: Comparison of the results from the modified model (Jarunthammachote and Dutta, 2007) with the experimental data of Jayah et al. (2003) for biomass with different moisture content (MC).

| **Gas composition % mol d.b.** | **Model data** (Jarunthammachote and Dutta, 2007) MC (16%) | MC (14%) | **Experimental data** (Jayah et al., 2003) MC (16%) | MC (14%) |
|---|---|---|---|---|
| **$H_2$** | 16.81 | 16.80 | 17.00 | 12.50 |
| **CO** | 17.86 | 18.52 | 18.40 | 18.90 |
| **$CH_4$** | 1.05 | 1.06 | 1.30 | 1.20 |
| **$CO_2$** | 12.10 | 11.68 | 10.60 | 8.50 |
| **$N_2$** | 52.18 | 51.94 | 52.70 | 59.10 |
| ***m*** | 0.4472 | 0.4415 | 0.3361 | 0.3927 |

Table 2.2: Comparison between experimental results, original model and modified model of Jarunthammachote and Dutta (2008).

| | **$H_2$ (vol %)** | **$CO_2$ (vol %)** | **CO (vol %)** | **$CH_4$ (vol %)** | **$N_2$ (vol %)** | **$O_2$ (vol %)** | **HHV (MJ/Nm3)** |
|---|---|---|---|---|---|---|---|
| **Central jet spouted bed at 1323.3 K** | | | | | | | |
| Experiment | 12.56 | 14.56 | 14.97 | 0.7 | 54.96 | 2.27 | 3.906 |
| Original model | 11.08 | 2.6 | 30.36 | ~0 | 55.96 | - | 5.44 |
| Modified model | 13.55 | 8.73 | 19.18 | ~0 | 58.53 | - | 4.302 |
| **Circular split spouted bed at 1388.3 K** | | | | | | | |
| Experiment | 10.98 | 13.7 | 16.41 | 0.88 | 57.47 | 0.55 | 3.961 |
| Original model | 10.26 | 3.17 | 29.23 | ~0 | 57.34 | - | 5.183 |
| Modified model | 12.45 | 9.16 | 18.15 | ~0 | 60.22 | - | 4.022 |
| **Spout-fluid bed ER=0.35 at 1148.7 K** | | | | | | | |
| Experiment | 8.43 | 14.95 | 11.61 | 2.52 | 61.55 | - | 3.891 |
| Original model | 14.99 | 10.42 | 20.68 | ~0 | 53.9 | - | 4.688 |
| Modified model | 16.07 | 14.42 | 13.71 | ~0 | 55.8 | - | 3.917 |
| **Spout-fluid bed ER=0.30 at 1127.65 K** | | | | | | | |
| Experiment | 11.86 | 14.48 | 13.03 | 2.95 | 56.87 | - | 4.01 |
| Original model | 15.45 | 10.43 | 21.08 | ~0 | 53.3 | - | 4.801 |
| Modified model | 16.72 | 14.5 | 13.76 | ~0 | 55.02 | - | 4.01 |

A recent work on equilibrium modelling is the one presented by Deydier et al.(2011) for a gasifier composed of a travelling bed gasifier and of a high temperature chamber for the cracking of the tars produced. Two assumptions were used: the value of the vapour content in the gas leaving the gasifier was supposed to be equal to its equilibrium value if sufficient moisture enters the dryer. The second one stated that the gas and solid leaving the gasifier were in chemical equilibrium. They also used the model to observe

the influence of two operating parameters (mass flow rate of air and mass flow rate of biomass) concluding that the optimal value of the ratio of mass flow rate of air to the mass flow rate of biomass is associate with the exact and complete gasification of solid carbon, the so-called “carbon boundary”.

Li et al. (2001) used a non-stoichiometric equilibrium model (minimisation of Gibbs free energy) to predict the producer-gas composition from a circulating fluidised-bed coal gasifier. Li et al. (2004) employed the equilibrium model to predict the producer-gas compositions, product heating value and cold gas efficiency for circulating fluidised-bed gasification. They observed that real gasification processes deviate from chemical equilibrium. Therefore, in order to correct the deviations, they developed a phenomenological model to modify the equilibrium-based framework to account for key non-equilibrium factors. As they knew from a pilot-plant study the experimental carbon conversion and methane yield, it was possible to correct non-equilibrium effects by withdrawing the corresponding carbon and hydrogen from the equilibrium system. Figure 2.4 compares the experimental data and the predicted values from the modified model. This method was also applied successfully to coal gasifcation (Li et al., 2001) and to steam-methane reforming (Grace et al., 2001), where hydrogen was preferentially removed through perm-selective membranes.

Another approach is the use QET, whereby the equilibria of the reactions defined in the model are evaluated at a temperature that is lower than the actual process temperature. This approach was introduced by Gumz (1950). For fluidised-bed gasifiers, the average bed temperature can be used as the process temperature, whereas for downdraft gasifiers, the outlet temperature at the throat exit should be used. Li et al. (2001) found that the kinetic carbon conversion for pressurised gasification of sub-bituminous coal in the temperature range 747-877ºC is seen to be comparable to equilibrium predictions for a temperature about 250ºC lower. Bacon (1982) defined QETs for each independent chemical reaction. Based on 75 operational data points measured in circulating fluidised-bed (CFB) gasifiers operated on biomass, Kersten et al. (2002) showed that, for operating temperatures in the range 740-910ºC, the reaction equilibrium of Eqs. 1.3, 1.4 and 1.6 should be evaluated at much lower temperatures (respectively, 531 ± 25ºC, 583 ± 25ºC and 457 ± 29ºC). These QETs appear to be independent of process temperature in this range.

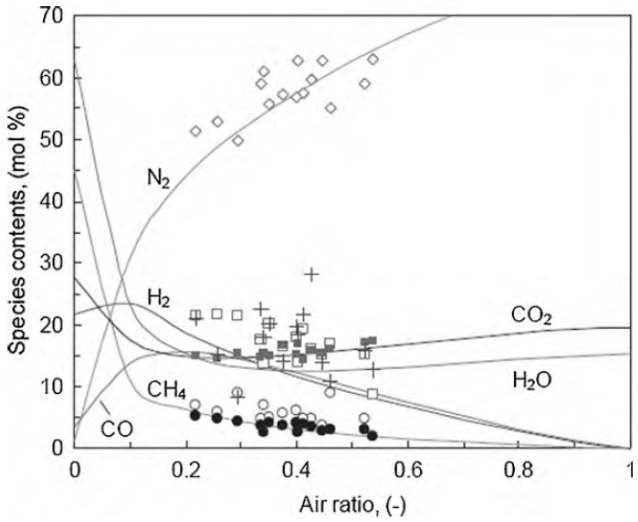


Figure 2.4: Comparison between the experimental gas composition and the gas composition predicted with the modified model. Data from the study of Li et al.(2004).

Most of the published works dealing with equilibrium models have been validated with air-blown downdraft gasifiers. However, the work of Schuster et al.(2001) was focused on steam gasification in a fluidised bed gasifier. The results of the equilibrium model for the gasifier (LHV x gas yield) were in the range of the measured results, though the $CH_4$ content in the product gas was overestimated. It was shown that the discrepancies in the prediction of the gas composition did not significantly influence the overall efficiency.

Detournay et al.(2011) developed a thermochemical equilibrium model for steam gasification in a fluidised bed. The thermodynamic equilibrium calculations were based on free Gibbs energy minimization. They considered the gas phase as a mixture of condensable and incondensable gases and the solid phase as a carbonate residue. The equilibrium results were compared with experimental data obtained by the same authors for a laboratory-scale fluidized bed using different catalysts: sand, alumina and Ni-alumina. They concluded that the thermodynamic equilibrium state calculated was far away from the experimental results obtained on sand particles. However, the use of catalyst allowed the system to get closer from the equilibrium, especially for the nickel based catalyst.

Loha et al. (2011) developed an equilibrium modeling approach to predict the gas composition of steam gasification in a fluidised bed gasifier. They observed that the

model under predicts the experimental values for $H_2$, CO and $CH_4$ and over predicts the value of $CO_2$. But the trend of changing the compositions with temperature and steam-to-biomass ratio was matching with the experimental results. Therefore, to introduce the kinetic effect on the process, the equilibrium constant $K_1$ and $K_2$ were corrected by multiplying a pre-factor each, 0.71 and 0.93, respectively. The modified model predicted the gas composition much closer to the experimental value and the average RMS value decreased from 3.34 to 2.62.

This literature review has shown that equilibrium models are useful tools for preliminary comparison, but that they cannot give highly accurate results for all cases. As mentioned above, thermodynamic equilibrium models do not require any knowledge of the mechanisms of transformation. Moreover, they are independent of the reactor and not limited to a specified range of operating conditions. They are valuable because they predict the thermodynamic limits of the gasification reaction system. Thus, in order to describe the behaviour of gasifiers more accurately, modifications have been made to equilibrium models.

## 2.4 ASPEN PLUS GASIFICATION MODELS

Some authors, trying to avoid complex processes and develop the simplest possible model that incorporates the principal gasification reactions and the gross physical characteristics of the reactor, have developed models using the process simulator Aspen Plus. Aspen Plus is a problem-oriented input program that is used to facilitate the calculation of physical, chemical and biological processes. It can be used to describe processes involving solids in addition to vapour and liquid streams. Aspen Plus makes model creation and updating easier, since small sections of complex and integrated systems can be created and tested as separate modules before they are integrated. This process simulator is equipped with a large property data bank containing the various stream properties required to model the material streams in a gasification plant, with an allowance for the addition of in-house property data. Where more sophisticated block abilities are required, they can be developed as FORTRAN subroutines.

Aspen Plus has been used to simulate coal conversion; examples include methanol synthesis (Kundsen et al., 1982 and Schwint, 1985), indirect coal liquefaction processes (Barker, 1983), integrated coal gasification combined cycle (IGCC) power plants (Phillips et al., 1986), atmospheric fluidised-bed combustor processes (Douglas and Young, 1990), compartment fluidised-bed coal gasifiers (Yan and Rudolph, 2000), coal hydrogasification processes (Backham et al., 2003) and coal gasification simulation (Lee et al., 1992). It has also been used to model and simulate a tyre pyrolysis unit within a gasification-based plant (Gómez et al., 2007).

However, the work that has been done on biomass gasification is less extensive. Mansaray et al. (2000a, 2000b, 2000c) used Aspen Plus to simulate a dual-distributor-type fluidised-bed rice husk gasifier. Two thermodynamic models were developed: a one-compartment model, where the hydrodynamic complexity of the fluidised-bed gasifier was neglected and an overall equilibrium approach was used; and a two-compartment model, where the complex hydrodynamic conditions presented within the gasification chamber were taken into account. The models were capable of predicting the reactor temperature, gas composition, gas higher heating value, and overall carbon conversion under various operating conditions, including bed height, fluidisation velocity, equivalence ratio, oxygen concentration in the fluidising gas, and rice husk moisture content. Because of the large amount of volatile material in biomass and the complexity of biomass reaction rate kinetics in fluidised-beds, the authors ignored char gasification and simulated the gasification process by assuming that biomass gasification follows the Gibbs equilibrium. The reactions considered in the development of the model were pyrolysis, partial combustion and gasification. Predictions of the core, annulus and exit temperatures, as well as the mole fractions of the combustible gas components and product-gas higher heating value, agreed reasonably well with experimental data. Correlations of the overall carbon conversion were not very good. The discrepancies between experimental and predicted overall carbon conversions were attributed to uncertainties in the sampling procedure.

Mathieu and Dubuisson (2002) modelled wood gasification in a fluidised bed using Aspen Plus. The model was based on the minimisation of the Gibbs free energy and the process was uncoupled in pyrolysis, combustion, Boudouard reaction and gasification. The authors performed a sensitivity analysis and concluded that there is a critical air temperature above which preheating is no longer efficient, that there is an

optimum oxygen factor, that the oxygen enrichment of air plays an efficient role under a certain value, and that the operating pressure has only a slight positive effect on process efficiency.

Mitta et al. (2006) modelled a fluidised-bed tyre gasification plant with air and steam using Aspen Plus and validated their results with the gasification pilot plant located at the Chemical Engineering Department of the Technical University of Catalonia. Their gasification model was divided into three different stages: drying, devolatilisation-pyrolysis and gasification-combustion. Figure 2.5 shows the Aspen Plus flowsheet of the model. When the raw material is fed, the first step is the heating and drying of the particles. A “RSTOIC” module was used to model this instantaneous drying. Due to the high content of volatiles in the tyre, the authors considered the devolatilisation step of its conversion. This devolatilisation process, namely the fast pyrolysis mechanism, produces volatile gases, tars and char. The “RYIELD” block was used to model the pyrolysis/devolatilisation part of the model. It was assumed that the total yield of volatiles equals the volatile content of the parent fuel determined by the proximate analysis. The “RGIBBS” reactor module was used to model the gasification and combustion reaction. The stream from the “RYIELD” block and the preheated oxygen and steam were directed into the “RGIBBS” module, which can predict the equilibrium composition of the produced gas from “RYIELD” at a specified temperature and pressure. The ash from the gasification process was removed from the “RGIBBS” module. In the model, an overall equilibrium approach was employed by neglecting the hydrodynamic complexity of the gasifier. Although higher hydrocarbons, tars and oils were produced in the gasifier, they were considered non-equilibrium products in order to decrease the complexity of the model. Therefore, $CH_4$ was the only hydrocarbon taken into consideration in the calculation. All of the results of the model were normalised to make them free from tars. The sulphur in the tyre was assumed to be converted mainly into $H_2S$. Steady-state conditions were assumed. The model was able to predict the composition of the produced gas under various working conditions, including the flow rate, composition and temperature of the feed materials, as well as the operating pressure and temperature.

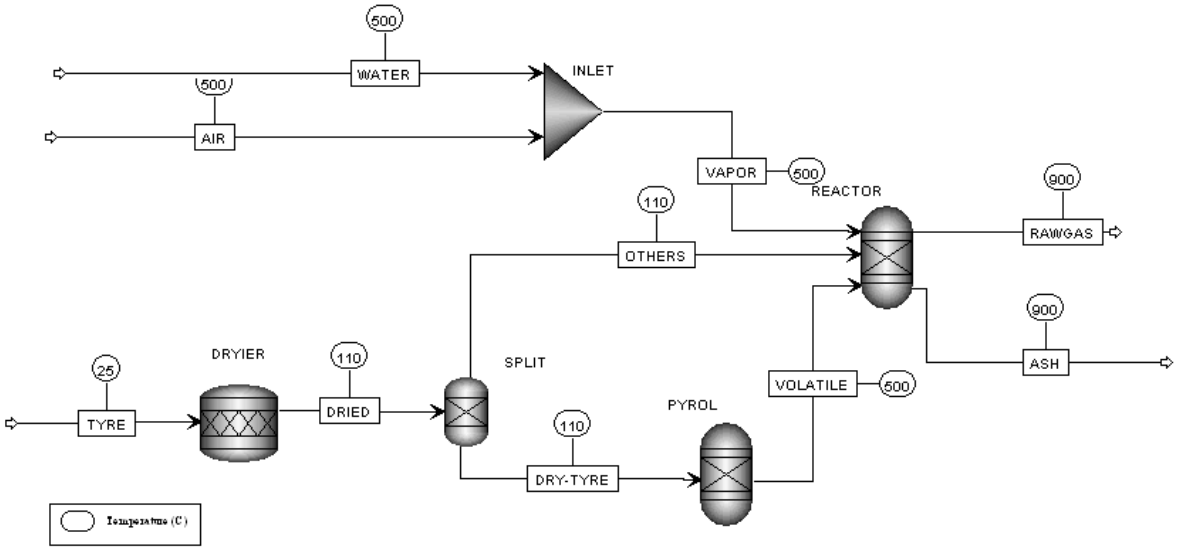


Figure 2.5: Simulation diagram in Aspen Plus for a fluidised-bed tyre gasification process (source: Mitta et al., 2006).

Nikoo and Mahinpey (2008) developed a model capable of predicting the steady-state performance of an atmospheric fluidised-bed gasifier by considering the hydrodynamic and reaction kinetics simultaneously. They used four Aspen Plus reactor models and external FORTRAN subroutines for hydrodynamics and kinetics nested to simulate the gasification process (Figure 2.6). The Aspen Plus yield reactor, “RYIELD”, was used to simulate the decomposition of the feed. In this step, biomass was converted into its constituting components, including carbon, hydrogen, oxygen, sulphur, nitrogen and ash, by specifying the yield distribution according to the biomass ultimate analysis. A separation column model was used to separate the volatile materials and solids in order to perform the volatile reactions. The Aspen Plus Gibbs reactor, “RGIBBS”, was used for volatile combustion, in conformity with the assumption that volatile reactions follow the Gibbs equilibrium. The Aspen Plus CSTR reactor, “RCSTR”, performed char gasification using reaction kinetics, written as an external FORTRAN code. The hydrodynamic parameters divided the reactor into two regions, bed and freeboard, and each region was simulated by one ”RCSTR”. The authors validated their model using different sets of operating conditions for a lab-scale pine gasifier with air and steam. They found good qualitative agreement between the model’s prediction and the experimental data, but they considered further improvements to the model, such as implementing tar production by defining non-equilibrium products in the “RGIBBS” reactor, as well as parameters considering mass transfer inside solid particles and heat

transfer inside the particles, between phases, and between the material and the wall. However, the authors observed that the production of hydrogen increases with temperature, thereby enhancing carbon conversion efficiency. The equivalence ratio is directly proportional to $CO_2$ production and carbon conversion efficiency. Increasing the steam-to-biomass ratio increases hydrogen and carbon monoxide production and decreases $CO_2$ and carbon conversion efficiency. The average particle size, ranging from 0.25 to 0.75 mm, does not seem to contribute significantly to the composition of the product gases.

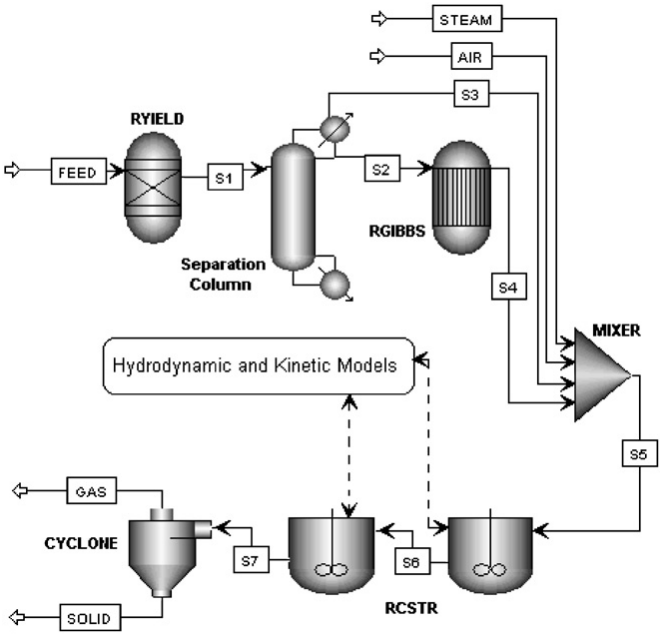


Figure 2.6: Simulation diagram in Aspen Plus for an atmospheric fluidised-bed gasification process (source: Nikoo and Mahinpey, 2008).

Hannula and Kurkela (2010) developed a process model for pressurised fluidised-bed gasification of biomass using Aspen Plus. Eight main blocks were used to model the fluidised-bed gasifier, complemented with FORTRAN subroutines nested in the programme to simulate hydrocarbon and $NH_3$ formation as well as carbon conversion. The model was validated with experimental data derived from a PDU-scale test rig operated with various types of biomass. The model was shown to be suitable for simulating the gasification of pine sawdust, pine and eucalyptus chips as well as forest residues, but not for pine bark or wheat straw.

Other authors have worked with Aspen Plus to model the gasification process for coal and biomass. Faaij et al.(1997) modelled a biomass and wastes IGCC for electricity production. Yan and Rudolph (2000) developed a model for a compartmented fluidised-bed coal gasifier process, Sudiro et al. (2009) modelled the gasification process to obtain synthetic natural gas from petcoke. Paviet et al. (2009) describe a very simple two-step model of chemical equilibrium in the wood biomass gasification process. Robinson and Luyben (2008) presented an approximate gasifier model that can be used for dynamic analysis using Aspen Dynamics. They used a high-molecular-weight hydrocarbon that is present in the Aspen library as a pseudofuel and the proposed approximate model captured the essential macroscale thermal, flow, composition and pressure dynamics. Doherty et al. (2008, 2009) developed a model for a circulating fluidised bed and studied the effect of varying the equivalence ratio, temperature, level of air preheating, biomass moisture and steam injection on the product gas composition, the gas heating value and the cold gas efficiency. The same authors (Doherty et al., 2010) developed a model for a biomass gasification-oxide fuel cell power system using Aspen Plus. The SOFC stack model, equilibrium type based on Gibbs free energy minimisation, performed heat and mass balances and considered ohmic, activation and concentration losses for the voltage calculation. Van der Meijden et al. (2010) also used Aspen Plus as a modelling tool to quantify the differences in overall process efficiency for producing synthetic natural gas in three different gasifiers (entrained-flow, allothermal and circulating fluidised-bed gasifier).

## 2.5 ARTIFICIAL NEURAL NETWORK GASIFICATION MODELS

Non-mechanistic, non-equilibrium modelling using neural networks for biomass gasification has also been reported (Guo et al., 2001; Brown et al., 2006). Artificial neural networks (ANN) have been extensively used in the fields of pattern recognition, signal processing, function approximation and process simulation. Sometimes a hybrid neural network (HNN) model is synthesised for process modelling (Psichogios and Ungar, 1992). This modelling approach usually combines a partial first-principles model, which describes certain characteristics of the process being simulated and involves a multilayer feedforward neural network (MFNN) that serves as an estimator of unmeasured process parameters that are difficult to model from first principles. MFNN is a universal function approximator, which has the ability to approximate any

continuous function to an arbitrary precision even without a priori knowledge of the structure of the function to be approximated (Hornik, 1991).

Guo et al. (2001) developed a hybrid neural network model to predict the product yield and gas composition of biomass gasification in an atmospheric pressure steam fluidised bed gasifier. They conducted a series of gasification runs on a bench scale facility, with four types of biomass as feed stock. These results were used to train the neural network. They developed four identical, in topological structure, neural networks to determine the gas production rate as function of the bed temperature ($T$) and gasification time ($t_g$) for the four major gas species. Topology of the neural networks developed is schematically illustrated in Figure 2.7.

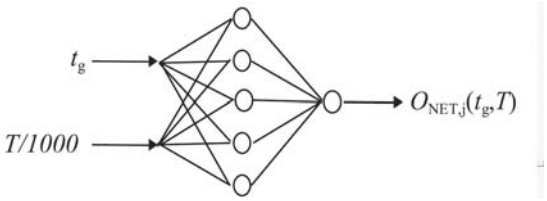


Figure 2.7: Schematic diagram of one neural network developed by Guo et al. (2001).

The four neural networks developed were typical two layer feedforward ANN. First they had the input layer, which had two nodes for the two input parameters. In order to equalize the magnitude of the inputs, temperature was divided by 1000 before it came to the input layer. The intermediate layer was the hidden layer, which had five neurons. Sigmoid transfer function was used as the activation function of the hidden layer and also in the output layer. For this reason, the outputs of the neural network were in the range of [0, 1] that were then properly scaled to obtain the desired value of kmol/h of the different gas species. Since different biomass has different gasification behaviour, the model was trained with experimental data of one biomass at a time. The chemotaxis algorithm (Willys et al., 1991) was used in the training. Postulating that adjustments of the weights occur in a random manner and follow a multivariate Gaussian distribution with zero mean, this algorithm adjusted weights by adding Gaussian distributed values to old weights. They concluded that the gasification profiles generated by the neural networks reflected the real gasification process of biomass.

Brown et al. (2006) developed a reaction model for computation of products compositions of biomass gasification in an atmospheric air gasification fluidised bed reactor. A non-stoichiometric equilibrium model based on total tar measurements was first applied to estimate the distribution of tar species. The product distribution was then formulated as a stoichiometric equilibrium model with reaction equilibrium temperature differences. Although certain temperature differences appeared to be uncorrelated to independent variables such as temperature and ER, other temperature differences were strongly correlated to these variables. Since there was no clear evidence of any single or characteristic relationship between operational variables and temperature differences, they used an ANN to parameterise the reaction temperature differences, even with a data sample of limited size.

The ANN was structured having one hidden layer and one output layer using sigmoid function as the activation function and linear function in the output layer. The problem was solved with standard backpropagation of errors to the hidden layer.

This combination of equilibrium model and ANN was further investigated and improved by the same authors (Brown et al., 2007).

## 2.6 EVALUATION AND SELECTION OF THE MOST SUITABLE BIOMASS GASIFICATION MODEL

One of the specific objectives of this thesis is to develop a simple but rigorous model to predict the behaviour of downdraft and fluidised bed gasifiers that could be implemented in a biomass gasification trigeneration plant. For this reason, in the present section, the previously presented models are compared and the most suitable one, according to the available data, will be chosen.

In their work, Gómez-Barea and Leckner (2010) did an extensive review on modelling of biomass gasification in bubbling and circulating fluidized bed gasifiers. Models were classified in three groups according to the simplification adopted to solve the fluid-dynamics: computational fluid-dynamics models (CFDM), fluidization models (FM) and black-box models (BBM). They considered FM the best developed model up to date for fluidised bed gasifiers, consisting of a comprehensive theoretical treatment, linked with experimental observations made during the last five decades. A selection of FM for

simulation of bubbling and circulating fluidised bed biomass gasification is listed in their work. According to these authors, CFD models for fluidised bed gasifiers are relative new, and in spite of offering promising expectation, much has to be added. In their work, several CFD models for BFB biomass gasification are also listed but they could not find any for CFB biomass gasification. Finally, BBM were considered to be quite useful in some cases, but the treatment is limited and the prediction capability is lower than that of FM and CFDM. The set of models called BBM, because the processes inside the reactors are not resolved, consist of overall mass (species) and heat balances over the entire gasification reactor supported by the assumptions to acquire the knowledge of the material distribution in the gasifier. The complexity of these BBM varies widely from one to another depending of the aim: from simple heat and mass balances to predict the overall performance to the prediction of the main gas and solids composition. Equilibrium models and modified equilibrium models are included in this group of BBM.

In addition, Gómez-Barea and Leckner (2010) consider that for the proper application of equilibrium models, the temperature has to be high enough and the residence time larger than the time needed to complete the reactions. This does not usually occur in fluidised bed biomass gasifiers because of the low temperature, between 750 and 900ºC. As a result, equilibrium models overestimate the yields of $H_2$ and CO, underestimate that of $CO_2$ and predict an outlet stream free from $CH_4$, tars and char. Therefore, a priori, equilibrium models do not seem to be accurate enough for design of fluidised bed biomass gasifiers. Despite this, they are considered simple and useful for first estimations. To improve these kinds of models, pseudo-equilibrium models (or more advanced models) have to be applied. Pseudo-equilibrium models aim at making the equilibrium calculations more realistic by supporting the equilibrium models with empirical relations. These considerations are in agreement with the ones reported by Villanueva et al. (2008), where chemical equilibrium is considered a good approach when simulating entrained-flow gasifiers in chemical process simulators or for downdraft fixed-bed gasifiers as long as high temperature and gas residence time are achieved in the throat. In contrast, and according to these authors, updraft fixed-bed, dual fluidised-bed and stand-alone fluidised-bed gasifiers should be modelled by revised equilibrium models or, in some extreme cases, by detailed rate-flow models.

For downdraft gasifiers, many researchers have reported models based on thermodynamic equilibrium model, considering very high residence time and fast reaction rates, within the gasifier (Altafini et al., 2003; Melgar et al., 2007; Sharma, 2008; Jarungthammachote and Dutta, 2007; Ruggiero and Manfrida, 1999; Zainal et al., 2001; Huang and Ramaswamy, 2009). These model predictions have been compared with experimental data and authors agree that the predicted trends for variations in the operating parameters are in good agreement with the experimental data and that the performance of a biomass downdraft gasifier can be approximated reasonably well by the equilibrium model.

After analysing the different models developed it can be concluded that equilibrium models are rigorous, computationally simple, a useful tool for preliminary comparison and a design aid in evaluating the behaviour of biomass gasification. Therefore, they are suitable to be easily integrated in a more complex model of a whole biomass gasification trigeneration plant without problems. Even though they cannot adjust equally well in all types of gasifiers. Considering the lack of our own experimental data and taking into account that only published experimental data is available, an equilibrium model has been selected as the best option to model this process in the trigeneration plant. For this reason, the aim is to develop a new modified equilibrium model based on pure equilibrium models previously developed by other authors. This new modified equilibrium model should be able to be adapted to different gasifiers and real processes that do not fully achieve equilibrium and as a result, it should predict reasonable good values for downdraft and fluidised bed gasifiers.

## 2.7 DATA SELECTION FOR DEVELOPMENT AND VALIDATION OF GASIFICATION MODELS

Due to the lack of our own experimental data, it has been necessary to search, in the open available literature, reported experimental data from other authors for downdraft and fluidised bed gasifiers. The aim was to create a database with published data that could be then use to develop and validate the gasifier model to be implemented in the trigeneration plant model. So, the experimental published data obtained can be classified in two groups depending on the type of reactor (downdraft and fluidised bed).

The initial intention was to look for published experimental data for downdraft and fluidised bed gasifiers operating with different gasifying agents rather than air. However, it has not been possible in all cases because, for instance, most of the available experimental data for downdraft gasifiers is for air gasification.

Data selection was a difficult task mainly due to the fact that usually not all information is given in the literature. Besides the selected and listed studies, more of them were reviewed but not selected because they presented some lack of data concerning biomass primary composition and analysis and/or operating gasification conditions. Special emphasis was put in that data previously used to validate other models.

- Selected experimental data from downdraft gasifiers

  Published data from Jayah et al. (2003), Drogu et al. (2002), Erlich and Fransson (2011) and Lv et al. (2007) was selected for air biomass gasification. Concerning other gasifying agents, the published data that can be found is very scarce. It was only possible to find data from Hanaoka et al. (2005) for air/steam gasification and from Lv et al. (2007) for oxygen/steam gasification.

  Different authors have previously used data from Jayah et al. (2003) to validate their models (Babu and Sheth, 2005; Jarungthammachote and Dutta, 2007; Melgar et al., 2007). The experimental test rig used by the authors to collect data was an 80 $kW_{th}$ downdraft test gasifier with an inner reactor diameter of 0.92 m and 1.15 m long. Rubber wood was selected as the feed material for the study. Drogu et al. (2002) gasified hazelnut shells in a pilot scale (5 $kW_e$) downdraft gasifier while Erlich and Fransson (2011) gasified wood, sugar cane bagasse from sugar/alcohol production and empty fruit bunch (EFB) from palm-oil production in a simple constructed pelled-fired downdraft gasifier of about 20$kW_{th}$. Lv et al. (2007) studied the hydrogen-rich gas production from biomass air and oxygen-steam gasification in a downdraft gasifier of a total height of 1.3 m and an inner diameter of 35 cm. The biomass used in their experiment was pine wood blocks with a moisture content of 8%.

- Selected experimental data from fluidised bed gasifiers

  Data from fluidised bed gasifiers was selected for atmospheric pressure gasifiers because are the most suitable ones for a small-medium scale gasification plant like the one modelled in the present thesis (see Chapter 1). In addition, and due to the large variability of bed materials that can be used (catalytic or inert), it was decided just to select data from gasifiers operating with inert beds.

  As a result, data from circulating fluidised bed gasifiers was obtained from Li et al. (2004) and van der Drift et al. (2001) for air gasification. Li et al. (2004) tested six sawdust species in a pilot-scale circulating fluidised bed of 6.5 m tall and 0.1 m diameter while van der Drift et al. (2001) gasified 10 different biomass residues in a 500 $kW_{th}$ circulating fluidised bed gasification facility.

  Concerning bubbling fluidised bed gasifiers, it was easier to obtain experimental data for different gasifying agents. Data for air biomass gasification was obtained from Narvaez et al. (1996), Campoy (2009) and Kaewluan and Pipatmanomai (2011). Results from air/steam gasification were obtained from Campoy (2009) and Lv et al. (2004). Campoy (2009) also reported results for enriched air/steam gasification and Gil et al. (1997) for oxygen gasification.

  Narvaez et al. (1996) gasified pine sawdust in a small pilot plant BFB gasifier of 6 cm of internal diameter. Campoy (2009) developed his experiments for different biomasses in a 150 $kW_{th}$ pilot plant. Kaewluan and Pipatmanomai (2011) gasified rubber wood chips in a 100 $kW_{th}$ while Lv et al. (2004) gasified pine sawdust in a BFB with a total height of 1.4 m, a fluidised bed diameter of 40 mm and a freeboard diameter of 60 mm. Gil et al (1997) used a BFB of 3.2 m high and 15 cm of internal diameter for pine wood chips gasification.

## 2.8 CONCLUSIONS

Models of several different types have been developed for gasification systems - kinetic, equilibrium and artificial neural networks. Unlike kinetic models that predict the progress and product composition at different positions along a reactor, an equilibrium model predicts the maximum achievable yield of a desired product from a reacting system. It also provides a useful design aid in evaluating the possible limiting behaviour of a complex reacting system that is difficult or unsafe to reproduce experimentally or in commercial operation. Equilibrium models are less computationally intensive than kinetic models and they are a useful tool for preliminary comparison. However, they cannot give highly accurate results for all cases. They are considered a good approach when simulating entrained-flow gasifiers in chemical process simulators or for downdraft fixed-bed gasifiers as long as high temperature and gas residence time are achieved in the throat. In contrast, updraft fixed-bed, dual fluidised-bed and stand-alone fluidised-bed gasifiers should be modelled by revised equilibrium models or, in some extreme cases, by detailed rate-flow models.

After analysing and comparing different developed models for biomass gasification and considering that only published experimental data is available to develop the present model, an equilibrium model was selected as the best option to model this process in the trigeneration plant model. However, it will not be a pure equilibrium model, it will be a new modified equilibrium model that will be able to be adapted to different gasifiers and real processes that do not fully achieve equilibrium with the aim to predict reasonable good values for downdraft and fluidised bed gasifiers.

In order to develop and validate the model for the gasifier, a literature search was done to gather published experimental data for downdraft and fluidised bed gasifiers. Studies that did not contain all information about biomass characteristics and operating conditions were discarded. As a result, it was possible to get some data from different authors, biomasses, gasifiers and gasifying agents. However for some cases, only data for air gasification was available.

# Chapter 3

# Development and validation of a biomass gasification modified equilibrium model

## 3.1 INTRODUCTION

In Chapter 2, the importance of a mathematical model predicting producer gas composition, from biomass gasification, using elemental analysis of biomass was stated. Among the existing models, equilibrium models were selected because they are simple, rigorous and a useful tool for preliminary calculations. The objective of the present chapter is to develop a modified equilibrium model able to determine the producer gas composition, LHV and cold gas efficiency based on ultimate analysis of biomass and that can be applicable to different types of biomass. To achieve this objective, a pure equilibrium model based on the previous work of other authors is firstly developed and then modified in order to apply the model to systems that do not fully achieve equilibrium. Finally, this model is validated with published experimental data and used to evaluate the influence of several working parameters like ER, air-preheating, biomass moisture content, steam addition and oxygen enrichment in the producer gas composition.

## 3.2 PURE EQUILIBRIUM MODEL

In order to modify an equilibrium model is then necessary to build first a pure equilibrium model. For this reason, a pure stoichiometric thermodynamic equilibrium model based on the equilibrium equations was firstly implemented based on the previous ones developed by Zainal et al. (2001), Melgar et al. (2007) and Jarunthammachote and Dutta (2007). Because of the procedure to develop a pure equilibrium model is already described somewhere else (Zainal et al., 2001; Melgar et al., 2007; Jarunthammachote and Dutta, 2007), in this section, only few considerations that differ from the other authors or are important for the understanding of the model are mentioned.

The pure equilibrium model and then the modified equilibrium model are built in the equation solver program ”Engineering Equation Solver” (EES, 2010). EES has been found very suitable for modelling this kind of system, since it contains all necessary thermodynamic functions. The gasification model is made up of a series of modules each containing one process. In EES it is possible for the model builder to make a user interface, which can make the model user-friendly. In this gasification model, the user interface consists of windows, which contains drawings and tables with input and output values, diagrams and hot areas with links to other windows. This way of presenting the input and output variables makes easier to the user getting an overview of the operating conditions in a certain computation.

The gasifier is considered as a continuous flowing and reacting system intended for steady-state operation at constant pressure (atmospheric pressure). The reactor is seen as zero-dimensional, which means that no spatial distribution of parameters is considered, nor there is any change effected with time because all forward and reverse reactions have reached chemical equilibrium. Figure 3.1 shows all feed and product streams and the different units considered in the pure thermodynamic equilibrium model. Steam generation and air preheating units are optional. Steam generation unit is only used if steam is added to the gasifier.

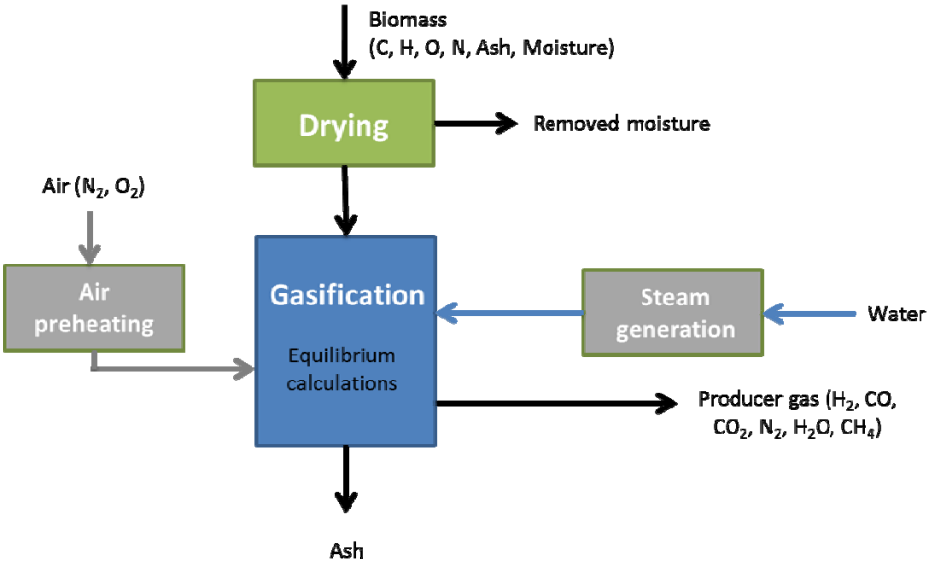


Figure 3.1: Feed and product streams entering and leaving the gasifier for pure equilibrium model.

For the pure equilibrium model of this section, the assumptions made by other authors when developing equilibrium models (Ramanan et al., 2008; Zainal et al., 2001; Sharma, 2008; Gøbel et al., 2007) are also applicable:

- All carbon content in biomass is converted into gaseous form and reaction temperature and residence time for reactants are sufficiently high to reach chemical equilibrium.
- Ash and nitrogen (from fuel and air) are inert and are not involved in any of the reactions.
- The ideal gas law is applicable.
- The reaction is auto-thermal and no external source of heat is applied. The process is completely adiabatic so no heat losses occur from the gasifier.
- The amount of tar in producer gas is assumed to be negligible.
- The pressure in the char bed is atmospheric and constant.
- No radial temperature gradients/concentrations exist.
- No gas is accumulated in the char bed.
- There is no resistance to conduction of heat and diffusion of mass inside the char particles.
- No oxygen is present in the producer gas.
- Producer gas comprises only $CO_2$, CO, $H_2$, $CH_4$, $N_2$ and $H_2O$.

The formula considered to describe the biomass composition in the present model is $CH_xO_yN_z$. Different correlations from the literature (Sheng and Azevedo, 2005) are available for calculating the higher heating value of biomass ($HHV_b$). Because the formulae based on the ultimate analysis are generally more accurate, the HHV in the present model is calculated using the correlation proposed by Channiwala and Parikh (2002):

$$HHV_b \text{ (MJ/kg)} = 0.3491 \cdot C + 1.1783 \cdot H + 0.1005 \cdot S - 0.1034 \cdot O - 0.0151 \cdot N - 0.0211 \cdot Ash \quad \text{Eq. 3.1}$$

The standard enthalpy of formation of biomass is computed using the stoichiometric combustion equation as follows (Baratieri et al., 2008):

$$h_{f,b} = LHV_b + 1 \cdot h_{f,CO_2} + \frac{x}{2} \cdot h_{f,H_2O,g} + \frac{z}{2} \cdot h_{f,N_2} - \left(1 + r + \frac{x}{4} - \frac{y}{2}\right) \cdot h_{f,O_2} \quad \text{Eq. 3.2}$$

where $h_{f,CO_2}, h_{f,H_2O,g}, h_{f,N_2}, h_{f,O_2}$ are the enthalpies of formation of combustion products and $O_2$ under complete combustion of the solid fuel.

The specific enthalpies for different substances have the same reference point (25ºC and 1 atm) and are calculated using the EES database. Air is assumed to be dry air and consists of 21% $O_2$ and 79% $N_2$ on volume basis. If enriched air is used as a gasification agent, then the oxygen percentage of the mixture is increased.

The enthalpy of water and steam used in this model is the one provided by EES for "H2O". If the water temperature is below 100ºC, and considering that the whole process takes place at atmospheric pressure, the water enthalpy is calculated using the one provided for "H2O" and adding the specific evaporation enthalpy (-2442 kJ/kg).

The specific enthalpy of biomass ($h_b$) at a given temperature is computed by means of the following expression obtained from the correlation reported by TenWolde et al. (1988) for the heat capacity of dry wood:

$$h_b(kJ/kg) = h_{f,b} + \frac{0.003867 \cdot (T^2 - 298^2)}{2} + 0.1031 \cdot (T - 298) \quad \text{Eq. 3.3}$$

where T is temperature expressed in K.

Ash specific enthalpy is assumed to be zero (Fock and Thomsen, 1999).

The specific enthalpy of producer gas leaving the gasifier is calculated using the specific enthalpy of the individual gaseous components.

Mass and energy balances of the drying, air preheating and steam generation unit are established. The wet biomass flow entering the drying unit is split in three flows (dry biomass, ash and water). The mass flows leaving the drying unit are dry biomass, ash and steam. Mass conservation equations for the four components (C, H, O and N) are set and the total enthalpy of the mass flows in and out is determined by summation of the product of mass flows and their specific enthalpy. The added heat to the drying unit is determined from the energy balance, since all other quantities are known.

The biomass moisture content leaving the drying unit is set by the user as well as the drying, air preheated and steam temperature.

The expressions used to calculate the equilibrium constants for the water-gas shift reaction and the methane reaction are the ones proposed by Jarungthammachote and Dutta (2007). However, several different expressions from other authors were reviewed: 5 for water-gas shift reaction (Jarungthammachote and Dutta, 2007; Zainal et al., 2001; Bentzen and Gøbel, 1995; Gómez-Barea and Leckner, 2010; de Souza-Santos, 1989) and two for the methane reaction (Jarungthammachote and Dutta, 2007; Zainal et al., 2001) (Appendix I).

The gasification efficiency is defined as the ratio of the usable heat content of the producer gas to the heat content of the feed biomass:

$$\eta_{CG}(\%) = \frac{LHV_g \cdot m_g}{LHV_b \cdot m_b} \cdot 100 \qquad \text{Eq. 3.4}$$

The equivalence ratio (ER) is defined as the moles of oxygen actually supplied to the gasifier to that required for stoichiometric combustion:

$$ER = \frac{AF\ ratio_{measured}}{AF\ ratio_{stoichiometric}} \qquad \text{Eq. 3.5}$$

where *AF ratio* stands for the air to fuel ratio ($Nm^3$ air/kg fuel).

## 3.3 MODIFIED EQUILIBRIUM MODEL

A real gasification system differs from an ideal reactor at chemical equilibrium. Usually, pure equilibrium model typical pitfalls at relative low gasification temperature are overestimation of $H_2$ and CO yields and underestimation of $CO_2$, $CH_4$, tars and char. These results may have a major impact on gasifiers performance (overprediction of carbon conversion) and, in some cases, it leads to serious disagreements in the prediction of light-gas composition.

For this reason, the pure equilibrium model has been modified to increase the results' accuracy and to adapt it to different types of gasifiers. Previously, other authors also developed modified or pseudo equilibrium models (Jayah et al., 2003; Jarungthammachote and Dutta, 2007; Li et al. 2004) (see Section 2.3).

The modifications introduced to the present pure equilibrium model essentially consist in:

- Adding a pyrolysis unit that, using correlations, predicts the formation of gas, char and volatiles in this step of the gasification process.
- Considering heat losses in pyrolysis and gasification units. These heat losses can be estimated by the user fixing a percentage of the product of dry biomass mass flow entering the system (kg/h) and its LHV (kJ/kg).
- Adding tar and char leaving the gasifier as a percentage of tar and char produced in the pyrolysis unit added.
- Particles leaving the gasifier and set by the user as mg/$Nm^3$ in the producer gas. These particles are considered to consist only of carbon.
- Setting the amount of $CH_4$ produced. For this reason, the equilibrium constant for methane reaction is not taken in to account.

Figure 3.2 shows a screenshot of the user interface modified equilibrium model developed in EES and including all feed, product streams as well as different units considered. Pyrolysis unit is a hot area linked with another window where user can select the pyrolysis correlations depending on the gasifier design (downdraft of fluidised bed).

Char leaving pyrolysis and gasifier units is considered to be composed primarily of carbon and therefore it is assumed in the model solely to consist of carbon. Char specific enthalpy is determined by a regression (Gøbel and Bentzen, 1995) created from a dataset based on the enthalpy of graphite (Knack et al., 1973). The expression used is:

$$h_{char}(kJ/kg) = 0.0004 \cdot T^2 + 0.8679 \cdot T - 381.61 \qquad \text{Eq. 3.6}$$

where T is temperature measured in Kelvin.

The specific enthalpy of particles leaving the gasifier is calculated using the same expression than for char because, in their experiments, Bentzen et al. (1998) found out that the particles leaving the gasifier were mostly soot.

Since now, not all carbon contained in biomass is converted into gas species, it is necessary to define the concept of carbon conversion efficiency ($\eta_C$) as:

$$\eta_C(\%) = \frac{Total\ amount\ of\ carbon\ in\ the\ gas\ outlet\ stream}{Total\ amount\ of\ carbon\ in\ the\ biomass\ inlet\ stream} \cdot 100 \qquad \text{Eq. 3.7}$$

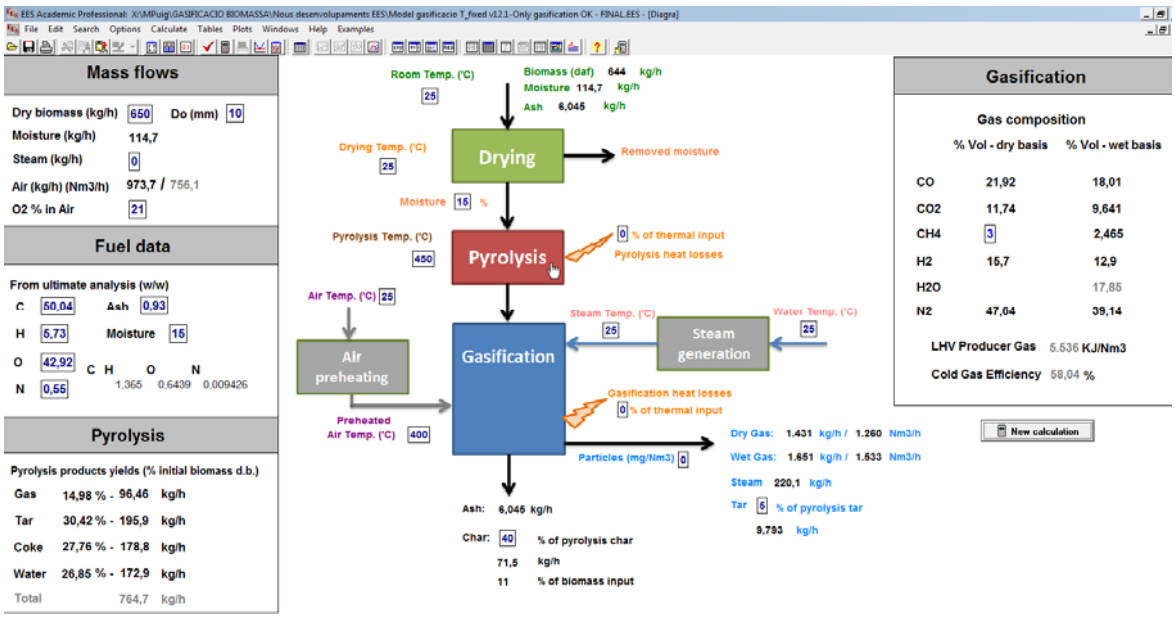


Figure 3.2: Screenshot of modified equilibrium model including feed and product streams entering and leaving the gasifier. Variables in blue color are inputs for the model.

Tar specific enthalpy is calculated using a correlation obtained by applying Jobaks method. The procedure followed to obtain this correlation is explained in Appendix II.

$$h_{tar} = -4.659 \cdot 10^{-7} \cdot (T - 273.15)^3 + 0.00193 \cdot (T - 273.15)^2 + 0.131 \cdot (T - 273.15) - 1796.4 \quad \text{Eq. 3.8}$$

where T is temperature expressed in K.

Model parameters include pyrolysis temperature, % of pyrolysis char and tar leaving the gasifier and heat losses in the gasifier. They can be directly introduced by the user using the user's interface, if the information is known, or adjusted automatically. The automatic adjustment of these parameters is done by means of using the experimental and modelled output gas composition for each data set. The least-squares technique is used as described in the equation below:

$$Min \sum_{i=1}^{n} \sum_{j=1}^{m} \left( x_{i,j} - y_{i,j} \right)^2 \quad \text{Eq. 3.9}$$

where *x* is the yield of the gas specie *m* (CO, $CO_2$, $H_2$, $N_2$) calculated by the model and *y* is the corresponding experimental value. *n* is the number of data points. The minimisation was carried out by the Variable Metric Method available in EES.

### 3.3.1 Pyrolysis unit

The main objective of this modelling subunit is determining the yields of char, tar and volatiles produced during the pyrolysis and also to determine the composition of the light gas. For this reason, experimental data from several authors has been studied to obtain correlations for predicting these parameters as a function of the pyrolysis temperature (see Appendix III).

After reviewing different experimental data for biomass gasification, and due to different yields on pyrolysis products obtained depending on the type of reactor and pyrolysis, two different correlations have to be considered when modelling the pyrolysis unit. For this reason, the correlations calculated from the experimental data of Fagbemi et al. (2001) are used to model the pyrolysis stage in a fixed bed reactor (downdraft,

updraft…). If pyrolysis stage takes place in a fluidised bed, the correlations obtained by Gomez-Barea et al. (2010) will then be used. The model also gives the possibility not to use any of these correlations and to introduce the desired yields manually. It has also to be taken into account that only correlations for wood pyrolysis are considered. However, it is also possible to extend the model including pyrolysis correlations for other kinds of biomass and agricultural residues.

The correlations used in the present unit are as follows:

- Wood pyrolysis in a fluidised bed, correlations given by Gomez-Barea et al. (2010):

$$Gas\ yield(\text{mass\% d.b.}) = 311.10 - 351.45 \cdot \left(\frac{T_p}{T_{ref}}\right) + 121.43 \cdot \left(\frac{T_p}{T_{ref}}\right)^2$$

$$Char\ yield(\text{mass\% d.b.}) = \text{-}15.03 + 50.58 \cdot \left(\frac{T_p}{T_{ref}}\right) - 18.09 \cdot \left(\frac{T_p}{T_{ref}}\right)^2$$

$$Liquid\ yield(\text{mass\% d.b.}) = \text{-}196.07 + 300.86 \cdot \left(\frac{T_p}{T_{ref}}\right) - 103.34 \cdot \left(\frac{T_p}{T_{ref}}\right)^2 \qquad \text{Eq. 3.10}$$

$$CO\ (\text{vol\%}) = 240.53 - 225.12 \cdot \left(\frac{T_p}{T_{ref}}\right) + 67.50 \cdot \left(\frac{T_p}{T_{ref}}\right)^2$$

$$CO_2(\text{vol\%}) = -206.86 + 267.66 \cdot \left(\frac{T_p}{T_{ref}}\right) - 77.50 \cdot \left(\frac{T_p}{T_{ref}}\right)^2$$

$$CH_4(\text{vol\%}) = -168.64 + 214.47 \cdot \left(\frac{T_p}{T_{ref}}\right) - 62.51 \cdot \left(\frac{T_p}{T_{ref}}\right)^2$$

$$H_2(\text{vol\%}) = 234.97 - 257.01 \cdot \left(\frac{T_p}{T_{ref}}\right) + 72.50 \cdot \left(\frac{T_p}{T_{ref}}\right)^2$$

Where $T_p$ is the pyrolysis temperature (ºC) and $T_{ref}$=500ºC

- Correlations for conventional pyrolysis of wood in a fixed bed reactor obtained from experimental data of Fagbemi et al. (2001):

$$Gas\ yield(\text{mass\% d.b.}) = -1.09 \cdot 10^{-6} \cdot T_p^{\,3} + 0.0022 \cdot T_p^{\,2} - 1.392 \cdot T_p + 288.534$$

$$Tar\ yield(\text{mass\% d.b.}) = 1.33 \cdot 10^{-6} \cdot T_p^{\,3} - 0{,}0028 \cdot T_p^{\,2} + 1{,}797 \cdot T_p - 339{,}139$$

$$Char\ yield(\text{mass\% d.b.}) = -6.6 \cdot 10^{-7} \cdot T_p^{\,3} + 0.00137 \cdot T_p^{\,2} - 0.93579 \cdot T_p + 230.5279$$

$$Water\ yield(\text{mass\% d.b.}) = 2.54 \cdot 10^{-7} \cdot T_p^{\,3} - 5.24 \cdot 10^{-4} \cdot T_p^{\,2} + 0{,}335 \cdot T_p - 40{,}883 \quad \text{Eq. 3.11}$$

$$CO(\text{vol\%}) = 0.0371 \cdot T_p + 19.961$$

$$CO_2(\text{vol\%}) = 0.000143 \cdot T_p^{\,2} - 0.27808 \cdot T_p + 139.948$$

$$CH_4(\text{vol\%}) = -9 \cdot 10^{-5} \cdot T_p^{\,2} + 0.1221 \cdot T_p - 25.206$$

$$H_2(\text{vol\%}) = 0.0469 \cdot T_p - 16.963$$

In addition to these correlations, energy, mass and molar balances for each element (C, H, O and N) are set and used to calculate pyrolysis products. The energy balance has been formulated to include an overall heat loss of the pyrolysis unit. This estimation of the heat losses can be fixed by the user as a percentage of the product of dry biomass mass flow entering the system (kg/h) and its LHV (kJ/kg).

## 3.4 VALIDATION OF THE MODEL WITH EXPERIMENTAL DATA

In this section, the modified equilibrium model is used to reproduce experimental data of different authors. According to the literature review (Chapter 2), comparison of theoretical results of equilibrium models with experimental data has been done, mainly, for air-blown downdraft gasifiers. However, in the present work, experimental data for downdraft and also fluidised bed gasifiers operating with different gasifying agents has been selected (see Section 2.3).

The literature search has been intense (Section 2.3). However, unfortunately, in some cases like for CFB gasifiers, it has not been possible to find more published papers were gasification was done with another gasification agent rather than air.

The differences between experimental and predicted values are estimated by the root-mean-square (RMS) values for each set of data:

$$RMS = \sqrt{\frac{\sum_{i}^{N} (Experiment_i - Model_i)^2}{N}} \qquad \text{Eq. 3.12}$$

where N is the number of data point.

### 3.4.1 Downdraft biomass gasifiers

The results obtained with the modified equilibrium model are validated with those obtained experimentally by different authors for different kinds of biomass. In order to predict the results and due to the lack of some information in the authors' paper, the model parameters are adjusted by minimising the sum of the differences between experimental and modelled results for producer gas composition.

This validation for air gasification is done for the following experimental data:

- Jayah et al. (2003) (Table 3.1): In this case, the model accounts for no biomass drying, air preheating and heat losses. Pyrolysis unit temperature has been adjusted to 440.5ºC and a percentage of char leaving the pyrolysis unit has been set to match the amount of char leaving the gasifier and measured by the authors (38%).
- Drogu et al. (2002) (Figure 3.3 and Table 3.2): In this case, only the values for the optimum operating air/fuel ratio have been selected. No biomass drying and air preheating are considered. Heat losses account for 2.3% of energy input (biomass) and pyrolysis unit temperature has been set at 490ºC. A percentage of the amount of char leaving the pyrolysis unit (33%) has been set to match the amount of char reported to be leaving the gasifier. The RMS values calculated for CO, $CO_2$, $H_2$ and $N_2$ gas species are 2.38, 2.15, 1.49 and 1.97 respectively.
- Erlich and Fransson (2011) (Table 3.3): No biomass drying and air preheating have been considered. Pyrolysis unit temperature is set at 500ºC and no tar and char production. Heat losses of 5% of the energy input have been taken into account.

The validation of the modified equilibrium model for air/steam gasification has been done for the experimental data of Hanaoka et al. (2005). The model parameters have

been adjusted at 600ºC of pyrolysis temperature, 5.5% of heat losses and 41.5% of pyrolysis tar leaving the gasifier. The moisture content of the samples is unknown. In the author's paper it is only said that it was reduced below 10%, for this reason it has been assumed to be 10% for all biomasses. Results are presented in Table 3.4.

In the case of $O_2$/steam gasification, the validation has been done for the experimental data of Lv et al. (2007) (Table 3.6). The same study also reported experimental data for air gasification (Table 3.5). In both cases, the model is adjusted considering a pyrolysis temperature of 422ºC, heat losses of 9.5% of energy input, and 26% and 49% of pyrolysis char and tar, respectively, leaving the gasifier.

Table 3.1: Comparison of predicted results from the present modified equilibrium model with experimental data from Jayah et al. (2003) for air biomass gasification in a downdraft gasifier.

| | | Jayah et al. (2003) | Model | Jayah et al. (2003) | Model | Jayah et al. (2003) | Model | Jayah et al. (2003) | Model | Jayah et al. (2003) |
|---|---|---|---|---|---|---|---|---|---|---|
| **A/F ratio** | **Moist (%)** | **% $CH_4$ (by mole d.b.)** | **% CO (by mole d.b.)** | | **% $CO_2$ (by mole d.b.)** | | **% $H_2$ (by mole d.b.)** | | **% $N_2$ (by mole d.b.)** | |
| 2.03 | 18.50 | 1.4 | 19.6 | 19.6 | 10.8 | 9.9 | 16.4 | 17.2 | 51.8 | 51.9 |
| 2.20 | 16.00 | 1.1 | 19.3 | 20.2 | 10.5 | 9.7 | 14.5 | 18.3 | 54.6 | 50.7 |
| 2.37 | 14.70 | 1.1 | 18.5 | 19.4 | 10.6 | 9.7 | 12.3 | 17.2 | 57.5 | 52.6 |
| 1.96 | 16.00 | 1.3 | 20.5 | 18.4 | 10.3 | 10.6 | 17.3 | 17.0 | 50.6 | 52.7 |
| 2.12 | 15.20 | 1.3 | 19.8 | 19.7 | 10.4 | 10.8 | 15.0 | 13.2 | 53.6 | 55.0 |
| 2.29 | 14.00 | 1.2 | 19.0 | 18.9 | 10.5 | 8.5 | 12.9 | 12.5 | 56.4 | 59.1 |
| 1.86 | 14.70 | 1.1 | 21.5 | 19.1 | 9.9 | 11.4 | 19.0 | 15.5 | 48.6 | 52.9 |
| 2.04 | 13.80 | 1.3 | 20.5 | 22.1 | 10.1 | 10.5 | 15.9 | 12.7 | 52.3 | 53.4 |
| 2.36 | 12.50 | 1.2 | 18.8 | 19.1 | 10.4 | 10.7 | 12.0 | 13.0 | 57.6 | 56.0 |
| RMS | | - | 1.26 | | 0.99 | | 2.71 | | 2.91 | |

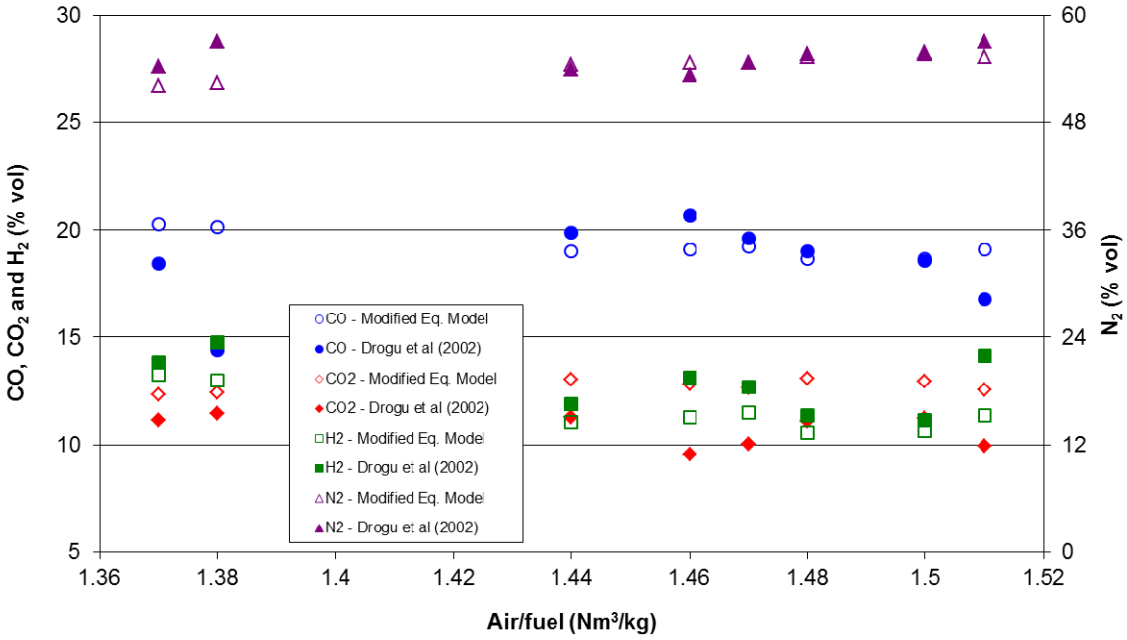


Figure 3.3: Comparison of producer gas composition (CO, $CO_2$, $H_2$ and $N_2$) measured experimentally by Drogu et al. (2002) and predicted by the present modified equilibrium model for air biomass gasification in a downdraft gasifier.

Table 3.2: Comparison of predicted results from the present modified equilibrium model with experimental data from Drogu et al. (2002) for air biomass gasification in a downdraft gasifier.

| A/F ratio | Model | Drogu et al. (2002) | Model | Drogu et al. (2002) | Model | Drogu et al. (2002) |
|---|---|---|---|---|---|---|
| | Char (kg/h) | | Ash (kg/h) | | Dry gas ($Nm^3/h$) | |
| 1.38 | 0.271 | 0.161 | 0.028 | 0.030 | 6.70 | 6.22 |
| 1.51 | 0.313 | 0.183 | 0.033 | 0.035 | 8.04 | 7.26 |
| 1.46 | 0.341 | 0.201 | 0.036 | 0.038 | 8.57 | 8.15 |
| 1.47 | 0.345 | 0.209 | 0.036 | 0.040 | 8.71 | 8.15 |
| 1.44 | 0.380 | 0.228 | 0.040 | 0.044 | 9.45 | 9.18 |
| 1.37 | 0.399 | 0.243 | 0.042 | 0.050 | 9.86 | 9.48 |
| 1.48 | 0.419 | 0.267 | 0.044 | 0.055 | 10.52 | 10.07 |
| 1.5 | 0.458 | 0.305 | 0.048 | 0.059 | 11.62 | 10.96 |
| RMS | 0.142 | | 0.007 | | 0.52 | |

Table 3.3: Comparison of predicted results from the present modified equilibrium model with experimental data from Erlich and Fransson (2011) for air biomass gasification in a downdraft gasifier.

| | Model | Erlich & Fransson (2011) | Model | Erlich & Fransson (2011) | Model | Erlich & Fransson (2011) | Model | Erlich & Fransson (2011) |
|---|---|---|---|---|---|---|---|---|
| **Biomass** | **% CO (by mole d.b.)** | | **% $CO_2$ (by mole d.b.)** | | **% $H_2$ (by mole d.b.)** | | **% $N_2$ (by mole d.b.)** | |
| Wood | 23.6 | 25.7 ± 1.7 | 10.0 | 9.9 ± 1.0 | 13.6 | 11.9 ± 1.1 | 50.2 | 50.4 ± 1.7 |
| Bagasse | 22.0 | 23.3 ± 1.2 | 10.7 | 11.4 ± 0.9 | 12.8 | 9.9 ± 0.6 | 51.8 | 52.6 ± 0.9 |
| EFB | 19.0 | 17.4 ± 1.5 | 10.9 | 13.7 ± 0.6 | 13.0 | 12.9 ± 0.3 | 55.7 | 55.0 ± 1.0 |
| RMS | 1.1 | | 1.0 | | 1.4 | | 0.2 | |

Table 3.4: Comparison of predicted results from the present modified equilibrium model with experimental data from Hanaoka et al. (2005) for air-steam gasification in a downdraft gasifier.

| | Hanaoka et al. (2005) | Model | Hanaoka et al. (2005) | Model | Hanaoka et al. (2005) | Model | Hanaoka et al. (2005) |
|---|---|---|---|---|---|---|---|
| **Biomass feedstock** | **% $CH_4$ (by mole d.b. $N_2$ free)** | **% CO (by mole d.b. $N_2$ free)** | | **% $CO_2$ (by mole d.b. $N_2$ free)** | | **% $H_2$ (by mole d.b. $N_2$ free)** | |
| Larch | 7.00 | 27.09 | 27.20 | 34.50 | 31.40 | 31.41 | 31.40 |
| Eucalyptus | 7.60 | 25.31 | 27.60 | 35.67 | 33.80 | 31.41 | 27.70 |
| Bamboo | 7.70 | 24.18 | 28.70 | 36.64 | 35.60 | 31.48 | 25.00 |
| Palm tree bark | 6.20 | 28.96 | 23.70 | 33.97 | 34.40 | 30.87 | 33.60 |
| Used ground coffee beans | 8.90 | 21.42 | 22.90 | 37.61 | 31.70 | 32.07 | 28.90 |
| Residue of squeezed Satsuma | 6.60 | 20.55 | 19.20 | 37.53 | 34.90 | 35.31 | 36.20 |
| Tea waste | 6.10 | 28.96 | 17.90 | 32.09 | 35.20 | 32.85 | 36.50 |
| Residue of squeezed soybeans | 7.40 | 23.69 | 16.30 | 35.78 | 33.50 | 33.12 | 36.90 |
| Shiitake mushroom fungus-bed | 6.80 | 19.29 | 25.30 | 41.07 | 31.10 | 32.84 | 33.50 |
| RMS | - | 5.48 | | 4.35 | | 3.37 | |

Table 3.5: Comparison of predicted results from the present modified equilibrium model with experimental data from Lv et al. (2007) for air gasification in a downdraft gasifier.

| Dry biomass (kg/h) | Air ($Nm^3/h$) | Lv et al. (2007) | Model | Lv et al. (2007) | Model | Lv et al. (2007) | Model | Lv et al. (2007) | Model | Lv et al. (2007) |
|---|---|---|---|---|---|---|---|---|---|---|
| | | % $CH_4$ (by mole d.b. $N_2$ free) | % CO (by mole d.b. $N_2$ free) | | % $CO_2$ (by mole d.b. $N_2$ free) | | % $H_2$ (by mole d.b. $N_2$ free) | | LHV ($MJ/Nm^3$) | |
| 7.26 | 9.11 | 6.23 | 26.58 | 29.56 | 33.46 | 30.02 | 33.73 | 31.40 | 4.63 | 5.44 |
| 10.45 | 13.27 | 6.58 | 27.03 | 24.59 | 33.75 | 36.41 | 32.64 | 28.49 | 4.60 | 5.05 |
| 10.30 | 14.32 | 6.82 | 29.40 | 25.53 | 34.99 | 34.88 | 28.79 | 28.93 | 4.25 | 4.76 |
| 9.90 | 13.55 | 8.21 | 28.68 | 25.20 | 36.07 | 34.36 | 27.05 | 29.16 | 4.33 | 5.05 |
| 6.62 | 7.98 | 4.36 | 24.09 | 27.92 | 32.62 | 30.11 | 38.92 | 35.39 | 4.69 | 5.17 |
| 8.50 | 11.52 | 5.45 | 29.00 | 28.77 | 33.40 | 31.76 | 32.15 | 31.88 | 4.33 | 4.78 |
| 9.00 | 12.20 | 5.70 | 28.99 | 27.52 | 33.61 | 33.39 | 31.70 | 31.47 | 4.34 | 4.60 |
| 9.50 | 12.90 | 6.01 | 29.01 | 25.81 | 33.90 | 33.32 | 31.08 | 31.17 | 4.34 | 4.82 |
| 9.90 | 13.55 | 8.21 | 28.68 | 25.20 | 36.07 | 34.36 | 27.05 | 29.16 | 4.33 | 5.05 |
| 10.55 | 14.55 | 9.02 | 28.50 | 25.07 | 37.04 | 35.62 | 25.44 | 27.12 | 4.30 | 5.26 |
| RMS | | - | 3.05 | | 1.90 | | 2.17 | | 0.62 | |

Table 3.6: Comparison of predicted results from the present modified equilibrium model with experimental data from Lv et al. (2007) for oxygen/steam gasification in a downdraft gasifier.

| Dry biomass (kg/h) | $O_2$ (95%) ($Nm^3/h$) | Steam (kg/h) | Lv et al. (2007) | Model | Lv et al. (2007) | Model | Lv et al. (2007) | Model | Lv et al. (2007) |
|---|---|---|---|---|---|---|---|---|---|
| | | | % $CH_4$ (by mole d.b. $N_2$ free) | % CO (by mole d.b. $N_2$ free) | | % $CO_2$ (by mole d.b. $N_2$ free) | | % $H_2$ (by mole d.b. $N_2$ free) | |
| 6.03 | 1.70 | 4.50 | 3.29 | 27.66 | 39.21 | 30.73 | 25.75 | 38.32 | 30.51 |
| 6.64 | 1.80 | 4.40 | 6.01 | 28.21 | 38.66 | 31.63 | 24.45 | 34.16 | 28.58 |
| 3.50 | 1.00 | 1.20 | 3.58 | 39.41 | 42.65 | 24.65 | 22.29 | 32.36 | 29.91 |
| 7.29 | 2.00 | 3.20 | 4.78 | 35.12 | 37.65 | 27.06 | 28.89 | 33.04 | 27.17 |
| 4.51 | 1.50 | 3.04 | 3.02 | 32.42 | 35.73 | 31.90 | 30.86 | 32.67 | 29.20 |
| 4.97 | 1.50 | 3.35 | 3.16 | 30.74 | 36.25 | 30.42 | 27.68 | 35.68 | 31.29 |
| 5.35 | 1.50 | 3.61 | 4.09 | 29.09 | 35.00 | 30.42 | 27.74 | 36.41 | 31.61 |
| RMS | | | - | 6.93 | | 3.80 | | 5.17 | |

Comparing the predicted values with the experimental reported values from different authors, it can be said that the modified equilibrium model predicts with good accuracy the behaviour of downdraft gasifiers, especially for air biomass gasification conditions. In the case of air/steam gasification (Hanaoka et al., 2005) larger differences are observed between the experimental and calculated values. However, this can be due to the fact that very different biomasses are being used and only one adjustment has

been done for all the data set. Maybe it would be necessary to adjust the model for each kind of biomass but, unfortunately, no more data for each biomass is available. In addition, the moisture content of biomass is unknown and has been estimated to be 10% which can also lead to some differences in the predicted values. It has also to be taken into account that experimental measurements are also associated to a measurement error that most times is not reported. Only in the work of Erlich and Fransson (2011) the standard deviation is given. This error in the experimental data could lead to values closer to the predicted ones.

Considering $O_2$/steam gasification, bigger differences than those found for air gasification, between experimental and predicted data are observed. However, it can be seen how the process of oxygen-steam gasification in a downdraft gasifier improves the hydrogen yield by volume compared with air gasification. Further, gas heating value is nearly doubled.

From these results it can be concluded that predicted values are in good agreement with the experimental reported values for air biomass gasification in downdraft gasifiers. However, the accuracy is not so good in the predictions for air/steam or $O_2$/steam gasification. Because of the available data for these last two cases is limited, it would be necessary to get more experimental data to verify if the differences are due to the model, the gasifier or also measurement errors. Even though the modified equilibrium model provides a good tool for preliminary calculations.

### 3.4.2 Fluidised bed biomass gasifiers

In this section, the results obtained with the modified equilibrium model are compared with those found experimentally in fluidised bed gasifiers by different authors. This comparison has been done for air (Campoy, 2009; Li et al., 2004), air/steam (Campoy, 2009), oxygen/steam (Gil et al., 1997) and enriched air/steam (Campoy, 2009) biomass gasification.

In the case of experimental data from Campoy (2009), only the data for wood pellets is considered. Experimental data has been separated in air or air/steam gasification data (Table 3.7) and enriched air/steam gasification data (Table 3.8). For this reason, two

adjustments have been made. In the first case, the model is adjusted considering a pyrolysis temperature of 680ºC, heat losses of 7% of energy input, and 42% and 26% of pyrolysis char and tar, respectively, leaving the gasifier. In the second case (enriched air-steam gasification), the model is adjusted considering a pyrolysis temperature of 750ºC and heat losses of 10% of energy input.

Comparing the RMS values of both tables it can be seen how the adjustment and prediction is better for air or air-steam biomass gasification (Table 3.7) than for enriched air biomass gasification (Table 3.8) for all gas species yields. In this second case, the $H_2$ yield is clearly underestimated while in most cases $CO_2$ yield is overestimated. In both cases, the model usually predicts higher values of producer gas flowrate ($Nm^3/h$) than the experimental ones obtained.

Table 3.7: Comparison of predicted results from the modified equilibrium model with experimental data from Campoy (2009) for air or air-steam gasification in a bubbling fluidised bed gasifier.

| | | | Model | Campoy (2009) | Model | Campoy (2009) | Model | Campoy (2009) |
|---|---|---|---|---|---|---|---|---|
| Dry biomass (kg/h) | Air ($Nm^3/h$) | Steam (kg/h) | % CO (by mole d.b.) | | % $CO_2$ (by mole d.b.) | | % $H_2$ (by mole d.b.) | |
| 20.5 | 17 | 0 | 20.6 | 18.2 | 14.4 | 14.2 | 18.1 | 13.2 |
| 17.5 | 17 | 3 | 16.5 | 13.8 | 16.4 | 16.9 | 17.6 | 14.6 |
| 19.1 | 15.5 | 5 | 14.2 | 11.5 | 19.1 | 18.6 | 22.6 | 16.2 |
| 15 | 17 | 0 | 18.8 | 17.6 | 13.9 | 14.9 | 11.1 | 12.6 |
| 15 | 17 | 3.2 | 15.4 | 15.0 | 16.3 | 16.2 | 14.5 | 14.0 |
| 15 | 17 | 6 | 12.4 | 11.9 | 18.5 | 18.6 | 14.9 | 16.2 |
| 11.5 | 17 | 0 | 13.5 | 15.8 | 15.9 | 15.1 | 4.9 | 8.7 |
| 12.2 | 17 | 2.5 | 12.9 | 15.4 | 16.8 | 15.9 | 8.5 | 11.9 |
| 12.2 | 17 | 5.1 | 11.1 | 13.8 | 18.1 | 17.0 | 10.3 | 13.3 |
| RMS | | | 2.1 | | 0.7 | | 3.5 | |
| **Dry biomass (kg/h)** | **Air ($Nm^3/h$)** | **Steam (kg/h)** | **Producer gas ($Nm^3$d.b./h)** | | **LHV (MJ/$Nm^3$ d.b.)** | | | |
| 20.5 | 17 | 0 | 33.7 | 22.3 | 6.7 | 5.9 | | |
| 17.5 | 17 | 3 | 31.0 | 23.2 | 5.8 | 5.2 | | |
| 19.1 | 15.5 | 5 | 32.9 | 26.1 | 6.3 | 5.3 | | |
| 15 | 17 | 0 | 26.8 | 21.4 | 5.4 | 5.4 | | |
| 15 | 17 | 3.2 | 27.8 | 25.9 | 5.2 | 5.1 | | |
| 15 | 17 | 6 | 28.0 | 26.5 | 5.1 | 5.1 | | |
| 11.5 | 17 | 0 | 22.5 | 23.3 | 4.1 | 4.8 | | |
| 12.2 | 17 | 2.5 | 23.9 | 27.3 | 4.3 | 4.9 | | |
| 12.2 | 17 | 5.1 | 24.4 | 28.4 | 4.2 | 4.8 | | |
| RMS | | | 5.8 | | 0.6 | | | |

Table 3.8: Comparison of predicted results from the present modified equilibrium model with experimental data from Campoy (2009) for enriched air-steam gasification in a bubbling fluidised bed gasifier.

| Dry biomass (kg/h) | Air+$O_2$ ($Nm^3$/h) ($\%O_2$ vol) | Steam (kg/h) | Model | Campoy (2009) | Model | Campoy (2009) | Model | Campoy (2009) | Campoy (2009) |
|---|---|---|---|---|---|---|---|---|---|
| | | | % CO (by mole d.b.) | | % $CO_2$ (by mole d.b.) | | % $H_2$ (by mole d.b.) | | % $CH_4$ (by mole d.b.) |
| 12.4 | 13.4 (30) | 3.7 | 22.8 | 18.9 | 17.1 | 17.6 | 19.3 | 16.4 | 5.5 |
| 10.0 | 10.3 (30) | 5.6 | 18.4 | 15.7 | 20.2 | 18.8 | 21.3 | 18.3 | 5.7 |
| 16.2 | 12.0 (30) | 4.7 | 22.3 | 20.8 | 17.8 | 15.8 | 16.9 | 20.0 | 6.7 |
| 12.0 | 8.7 (30) | 6.5 | 17.9 | 15.3 | 20.9 | 20.3 | 18.5 | 22.3 | 7.1 |
| 14.0 | 13.9 (35) | 4.3 | 24.8 | 20.0 | 18.3 | 16.8 | 16.2 | 17.5 | 5.6 |
| 11.8 | 10.1 (35) | 6.2 | 21.6 | 17.5 | 20.3 | 18.0 | 19.2 | 21.8 | 5.1 |
| 16.8 | 11.5 (35) | 4.9 | 23.5 | 23.9 | 19.7 | 12.6 | 13.1 | 22.4 | 7.3 |
| 12.6 | 8.5 (35) | 7.4 | 18.9 | 19.3 | 22.8 | 16.2 | 15.5 | 25.1 | 7.4 |
| 21.6 | 15.2 (40) | 2.1 | 27.8 | 27.4 | 19.7 | 16.2 | 8.5 | 18.3 | 7.3 |
| 16.2 | 12.2 (40) | 4.4 | 25.7 | 25.1 | 20.8 | 13.7 | 11.6 | 23.1 | 6.5 |
| 14.8 | 11.7 (40) | 4.9 | 24.5 | 23.9 | 21.7 | 14.6 | 11.9 | 22.3 | 6.7 |
| 13.2 | 9.6 (40) | 6.6 | 21.7 | 20.2 | 23.6 | 16.7 | 13.0 | 24.5 | 6.9 |
| 12.0 | 8.9 (40) | 6.4 | 21.5 | 19.3 | 23.6 | 17.0 | 13.6 | 25.7 | 6.7 |
| 18.8 | 10.7 (40) | 5.3 | 23.3 | 28.5 | 23.0 | 9.2 | 9.3 | 25.7 | 8.1 |
| 14.0 | 7.4 (40) | 7.3 | 20.4 | 23.5 | 24.7 | 14.6 | 11.9 | 27.5 | 7.7 |
| RMS | | | 2.8 | | 6.3 | | 9.5 | | - |

| Dry biomass (kg/h) | Air+$O_2$ ($Nm^3$/h) ($\%O_2$ vol) | Steam (kg/h) | Model | Campoy (2009) | Model | Campoy (2009) |
|---|---|---|---|---|---|---|
| | | | Producer gas ($Nm^3$ d.b./h) | | LHV (MJ/$Nm^3$ d.b.) | |
| 12.4 | 13.4 (30) | 3.7 | 25.2 | 22.3 | 6.9 | 6.1 |
| 10.0 | 10.3 (30) | 5.6 | 20.8 | 17.2 | 6.7 | 6.0 |
| 16.2 | 12.0 (30) | 4.7 | 32.0 | 23.5 | 7.0 | 7.2 |
| 12.0 | 8.7 (30) | 6.5 | 24.1 | 17.9 | 6.8 | 6.9 |
| 14.0 | 13.9 (35) | 4.3 | 26.6 | 24.8 | 6.9 | 6.4 |
| 11.8 | 10.1 (35) | 6.2 | 23.2 | 18.4 | 6.6 | 6.8 |
| 16.8 | 11.5 (35) | 4.9 | 30.7 | 22.9 | 7.0 | 8.1 |
| 12.6 | 8.5 (35) | 7.4 | 23.7 | 17.9 | 6.7 | 7.8 |
| 21.6 | 15.2 (40) | 2.1 | 36.3 | 30.5 | 7.0 | 8.1 |
| 16.2 | 12.2 (40) | 4.4 | 28.2 | 24.0 | 6.8 | 8.0 |
| 14.8 | 11.7 (40) | 4.9 | 25.9 | 22.3 | 6.8 | 7.8 |
| 13.2 | 9.6 (40) | 6.6 | 23.4 | 18.8 | 6.6 | 7.7 |
| 12.0 | 8.9 (40) | 6.4 | 21.4 | 17.8 | 6.6 | 7.6 |
| 18.8 | 10.7 (40) | 5.3 | 31.9 | 23.4 | 6.8 | 9.3 |
| 14.0 | 7.4 (40) | 7.3 | 24.5 | 17.3 | 6.6 | 8.7 |
| RMS | | | 5.6 | | 1.2 | |

A comparison between predicted and experimental values reported by Gil et al. (1997) is shown in Table 3.9. Pyrolysis temperature has been adjusted at 560ºC and heat losses of 0.5% of energy input, and 46% of pyrolysis tar leaving the gasifier are considered.

From this table (Table 3.9) it can be seen that the predicted results are not in very good agreement with experimental data. There is always an underestimation of CO yield and overestimation of $CO_2$ and $H_2$ yields. These deviations lead to disagreements with LHV of producer gas. Predicted values give a LHV 30% lower than experimental values.

Table 3.9: Comparison of predicted results from the present modified equilibrium model with experimental data from Gil et al. (1997) for oxygen-steam gasification of wood chips in a fluidised bed.

| ER | Steam/Biomass Ratio | Gil et al. (1997) | Model | Gil et al. (1997) | Model | Gil et al. (1997) | Model | Gil et al. (1997) |
|---|---|---|---|---|---|---|---|---|
| | | % $CH_4$ (by mole d.b.) | % CO (by mole d.b.) | | % $CO_2$ (by mole d.b.) | | % $H_2$ (by mole d.b.) | |
| 0.23 | 0.52 | 7.4 | 33.5 | 48.0 | 25.0 | 27.5 | 29.9 | 14.7 |
| 0.29 | 0.66 | 7.0 | 32.8 | 47.5 | 28.2 | 30.0 | 26.6 | 14.9 |
| 0.30 | 0.70 | 6.6 | 32.6 | 44.4 | 28.9 | 35.2 | 26.2 | 13.9 |
| 0.32 | 0.72 | 7.2 | 32.1 | 47.5 | 30.5 | 27.7 | 24.1 | 13.8 |
| 0.33 | 0.75 | 7.2 | 31.8 | 49.4 | 32.2 | 24.9 | 21.9 | 14.8 |
| 0.36 | 0.83 | 6.5 | 31.0 | 45.3 | 33.1 | 30.9 | 22.4 | 14.1 |
| 0.22 | 0.49 | 7.1 | 33.4 | 46.9 | 24.1 | 14.4 | 31.5 | 28.2 |
| 0.22 | 0.50 | 6.8 | 33.7 | 45.4 | 24.1 | 18.5 | 31.4 | 24.9 |
| 0.24 | 0.54 | 6.9 | 33.5 | 46.5 | 25.0 | 18.8 | 30.3 | 25.7 |
| 0.24 | 0.54 | 6.4 | 33.6 | 45.2 | 24.6 | 16.4 | 31.1 | 27.7 |
| 0.26 | 0.58 | 6.3 | 33.8 | 43.5 | 25.6 | 17.9 | 29.6 | 29.3 |
| 0.27 | 0.60 | 6.6 | 33.6 | 44.3 | 26.3 | 21.0 | 28.6 | 28.1 |
| 0.27 | 0.60 | 6.3 | 33.7 | 44.7 | 26.1 | 18.2 | 29.1 | 24.8 |
| 0.30 | 0.68 | 6.1 | 32.0 | 43.6 | 26.9 | 20.2 | 30.2 | 26.8 |
| 0.43 | 0.99 | 5.3 | 29.2 | 31.6 | 37.2 | 36.8 | 19.9 | 23.9 |
| 0.46 | 1.05 | 6.0 | 26.9 | 39.6 | 40.9 | 36.3 | 16.9 | 17.0 |
| 0.23 | 0.35 | 6.6 | 38.4 | 47.5 | 21.6 | 16.2 | 29.2 | 22.7 |
| 0.25 | 0.39 | 7.0 | 38.2 | 46.7 | 23.1 | 22.0 | 26.9 | 19.3 |
| 0.34 | 0.52 | 7.4 | 36.5 | 37.0 | 29.4 | 29.0 | 19.8 | 18.6 |
| 0.38 | 0.58 | 7.2 | 35.1 | 42.3 | 32.3 | 26.6 | 17.6 | 17.2 |
| RMS | | - | 11.6 | | 5.6 | | 6.8 | |

The experimental values from Li et al. (2004) have been compared with the predicted ones in Table 3.10. The model is adjusted considering a pyrolysis temperature of 780ºC, heat losses of 7.5% of energy input, and 20% and 65% of pyrolysis char and tar leaving the gasifier.

Table 3.10: Comparison of predicted results from the present modified equilibrium model with experimental data from Li et al. (2004) for air and air-steam gasification in a circulating fluidised bed.

| Dry biomass (kg) | ER | Steam/Biomass Ratio | Model | Li et al. (2004) | Model | Li et al. (2004) | Model | Li et al. (2004) |
|---|---|---|---|---|---|---|---|---|
| | | | % CO (by mole d.b.) | | % $CO_2$ (by mole d.b.) | | % $H_2$ (by mole d.b.) | |
| 103.8 | 0.46 | 0 | 8.5 | 11.0 | 19.3 | 15.9 | 1.5 | 3.1 |
| 110.6 | 0.47 | 0 | 7.8 | 9.6 | 19.7 | 17.1 | 1.3 | 3.0 |
| 118.6 | 0.36 | 0.024 | 14.2 | 14.7 | 17.2 | 16.5 | 3.8 | 4.0 |
| 108.2 | 0.39 | 0.223 | 10.7 | 12.6 | 19.1 | 15.7 | 3.9 | 3.8 |
| 88.1 | 0.30 | 0 | 17.9 | 16.6 | 15.9 | 15.0 | 6.6 | 5.5 |
| 112.3 | 0.34 | 0 | 15.5 | 13.4 | 16.7 | 15.6 | 5.4 | 3.5 |
| 120.8 | 0.29 | 0 | 18.7 | 14.6 | 15.6 | 15.7 | 8.4 | 4.2 |
| 140.0 | 0.25 | 0 | 20.1 | 19.9 | 14.2 | 14.5 | 8.6 | 5.1 |
| 164.8 | 0.28 | 0 | 19.1 | 17.9 | 14.0 | 16.3 | 7.6 | 7.3 |
| 55.2 | 0.45 | 0 | 9.9 | 10.0 | 17.1 | 18.3 | 1.9 | 5.9 |
| RMS | | | 1.9 | | 2.0 | | 2.4 | |

| Dry biomass (kg) | ER | Steam/Biomass Ratio | Model | Li et al. (2004) | Model | Li et al. (2004) |
|---|---|---|---|---|---|---|
| | | | Producer gas ($Nm^3$) | | LHV ($MJ/Nm^3$ d.b.) | |
| 103.8 | 0.46 | 0 | 271.2 | 303.1 | 1.9 | 3.0 |
| 110.6 | 0.47 | 0 | 292.8 | 342.9 | 1.8 | 2.8 |
| 118.6 | 0.36 | 0.024 | 269.2 | 307.2 | 3.2 | 4.1 |
| 108.2 | 0.39 | 0.223 | 259.1 | 297.6 | 2.7 | 3.7 |
| 88.1 | 0.30 | 0 | 183.9 | 206.2 | 4.2 | 4.8 |
| 112.3 | 0.34 | 0 | 249.9 | 276.3 | 3.5 | 3.9 |
| 120.8 | 0.29 | 0 | 252.1 | 257.3 | 4.3 | 4.2 |
| 140.0 | 0.25 | 0 | 273.1 | 288.4 | 4.9 | 5.6 |
| 164.8 | 0.28 | 0 | 339.9 | 387.3 | 4.4 | 4.6 |
| 55.2 | 0.45 | 0 | 146.7 | 178.8 | 1.9 | 2.5 |
| RMS | | | 33 | | 0.7 | |

In Table 3.10 it can be observed how producer gas composition is predicted with reasonably good accuracy by the modified equilibrium model developed. However, the amount of producer gas generated and its LHV are underestimated.

Comparing the results for downdraft gasifiers and fluidised bed gasifiers, it is clear that, in both cases, the best predicted values are for gasification using air or air-steam as gasification agent. The largest RMS values are found for oxygen and enriched air-steam gasification. However, in this worst case, the results obtained for downdraft gasifiers are better than for fluidized bed. Anyway, it would be necessary to have more experimental data of downdraft gasifiers operating with enriched air-steam or air-steam to validate the model and see whether or not the model does not fit properly or the observed differences are due to these gasifiers in particular.

Focusing in air or air-steam gasification, the most feasible option for a small-medium scale biomass gasification plant, adjustments obtained for both kinds of gasifiers are similar, but in some cases better for downdraft gasifiers than for fluidised bed.

Due to the fact that usually it is more difficult to predict the behaviour of biomass gasification in fluidised bed gasifiers than in downdraft gasifiers and because some experimental data is available, it was decided to develop an ANN model for this kind of gasifiers. The aim of developing an ANN is to evaluate the potential of these models for biomass gasification that almost has not been studied before. Developing this model serves to study the possibility to apply ANN to biomass gasification real processes when experimental data is available.

## 3.5 EFFECT OF FEEDSTOCK PROPERTIES AND OPERATING PARAMETERS

Because biomass is very variable in its composition and properties and also the gasifier conditions can be change; it is of great interest to have a model sensitive enough to predict the effect of the operational variables on the quality of producer gas. For this reason, the present developed model has been use to study the influence of moisture content in biomass, ER, air-preheating, steam injection and oxygen enrichment on producer gas. At the same time, the influence of these variables is compared with that reported by other authors. Due to the fact that the predictions of the model want to be compared with those from other authors, the adjustment of operating parameters like heat losses, % char leaving the gasifier… are set according the considerations of those other authors.

### 3.5.1 Effect of moisture content on producer gas composition

The effect of initial moisture content of wood chips on the producer gas composition at 800ºC has been studied and compared with that reported by Zainal et al. (2001) (Figure 3.4). This figure shows that the values obtained with both models are very similar. In both cases it can be observed that the composition of the inert nitrogen is almost constant with moisture content. The composition of the methane produced is almost constant and at a very low percentage (0.7-1.6%). The percentage of hydrogen

in the fuel gas increases continuously with the moisture content from about 20% to 25% for an increase in moisture content from 0% to 40%. A similar trend is also observed for the carbon dioxide; however the increase is from about 5% to 15%. The percentage of carbon monoxide reduces from about 28% to 15% for the same variation of moisture content. The same tendencies were observed by Altafini et al. (2003) for sawdust gasification, Jarungthammachote and Dutta (2007) for municipal solid waste gasification and Gautam (2010) and Plis and Wilk (2011) for wood chips gasification.

If the process is considered completely adiabatic thus additional air flow is required when increasing the moisture content in order to generate the heat required to keep the desired temperature. This is reflected by an increase of the equivalence ratio (Figure 3.5), if this air flow is not supplemented, a decrease in gasifier temperature is observed. The small increase in $H_2$ concentration is overshadowed by the rapid decrease of CO when increasing the moisture content. The overall effect is a decrease of the LHV of producer gas when the moisture is increased, which can also be seen in Figure 3.5.

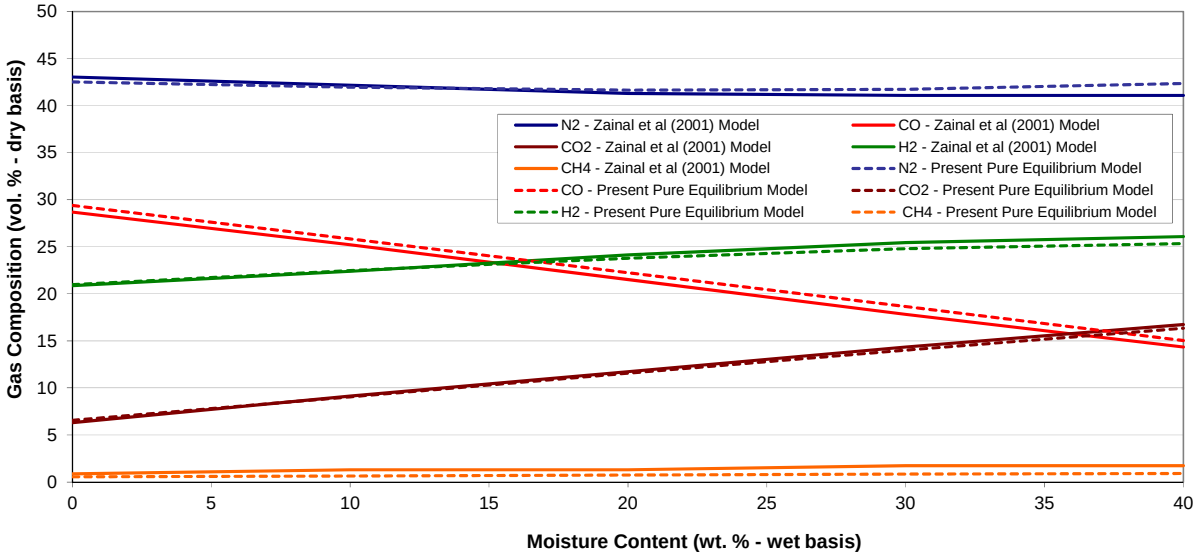


Figure 3.4: Comparison of the effect of moisture content in wood chips on gas composition at 800ºC using Zainal et al. (2001) model and the pure adiabatic equilibrium model developed in the present study.

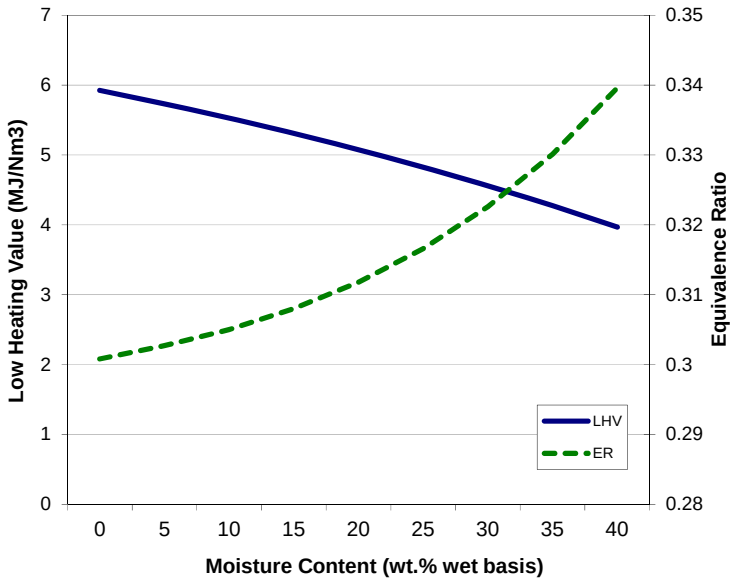


Figure 3.5: Effect of moisture content in wood chips on LHV of producer gas and ER at 800ºC using the pure adiabatic equilibrium model developed in the present study.

### 3.5.2 Effect of equivalence ratio (ER) on producer gas composition

The variation of producer gas composition as function of the equivalence ratio (ER) in an adiabatic gasifier of woodchips with a moisture content of 10% is shown in Figure 3.6. Considering an autothermal gasifier, the gasification temperature depends on the amount of air fed to the gasifier (Figure 3.7), i.e. it is controlled by the ER. As a result, varying ER or gasification temperature will have the same effect on producer gas composition, heating value, and gasification efficiency. For this reason, only ER is plotted against producer gas composition and LHV.

These results were compared with the ones published by, Plis and Wilk (2011), Mathieu and Dubuisson (2002) and Baratieri et al. (2008). The three models and our model present the same qualitative and quantitative tendencies. The percentage of $CH_4$ remains very low and decreases when ER increases. $H_2$ percentage decreases from 22.5 to 6.5% when ER increases from 0.3 to 0.6, the same behaviour was observed by Plis and Wilk (2011) where the decrease for the same range of ER values was from 20 to 6.5%. While $H_2$ decreases, $CO_2$ slightly increases from 8.6 to 11.6%

(8.5 to 11.3% for Plis and Wilk (2011)) and the CO percentage decreases from 26.2 to 16.5% in this model and from 25.9 to 16.6% for Plis and Wilk (2011).

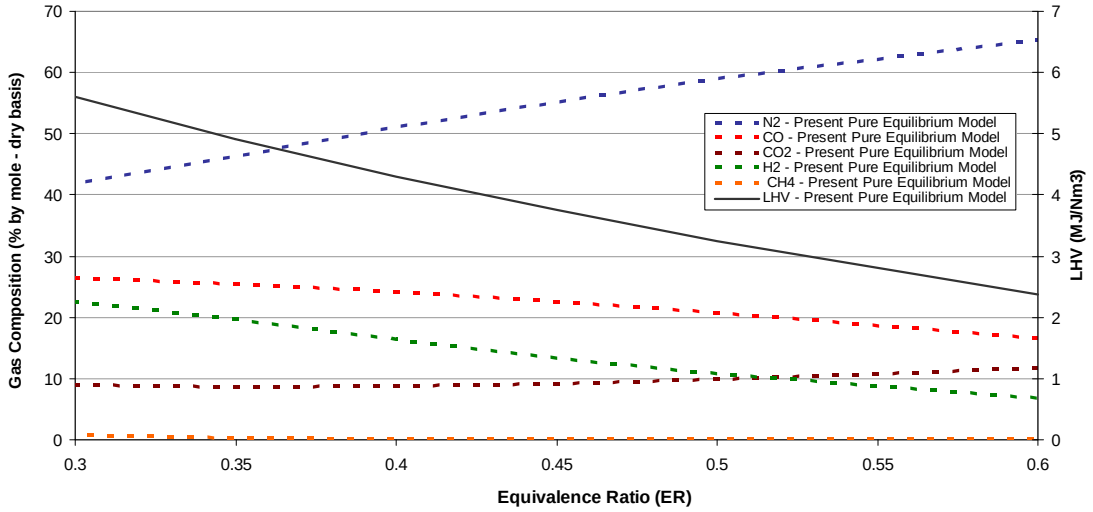


Figure 3.6: Variation of the composition of producer gas for the present pure equilibrium model when increasing the ER for adiabatic wood chips gasification with a moisture content of 10%.

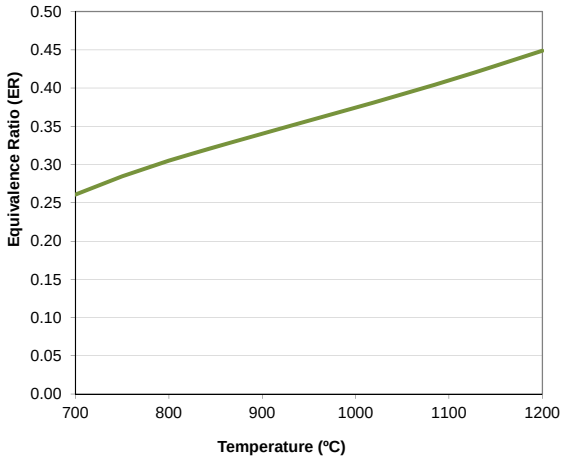


Figure 3.7: Effect of the temperature on the equivalence ratio in adiabatic conditions for the present pure equilibrium model when increasing the temperature for wood chips gasification with a 10% of moisture content.

### 3.5.3 Effect of air preheating on producer gas composition

Air preheating is a means of increasing the conversion efficiency of the gasification process. The sensible heat in the air causes a rise in the gasification temperature, which in turn influences the product gas composition, causing an increase in the production of combustible gases, $H_2$ and CO. This change in producer gas composition affects the gas HHV and hence the gasifier cold gas efficiency. Air preheating offers an alternative and more economical approach than oxygen blown systems. The overall efficiency of the process on a thermal basis would be increased if the heat required for air preheating is recovered from the gas cooling section of the plant. The use of high temperature air as an oxidant achieves downsizing of the plant (Sugiyama et al., 2005) because a smaller volume of air is needed to bring the gasifier to the required operating temperature; which in turn reduces the size of the reactor and gas clean-up system needed.

The influence of air preheating on the gasification or reactor temperature was investigated (Figure 3.8). It was found that the gasification temperature increased almost linearly with air temperature for all ERs (Doherty et al., 2009; Babu and Sheth, 2005). As Doherty et al. (2009) stated, there is a limit on the level of air preheating for each ER. This level is limited by the effectiveness of the heat exchange equipment used but also limited by the operating temperature constrain of the reactor. Fluidised bed gasifiers should not operate over 1000ºC to ensure that the ash melting temperature is not reached, which would cause agglomeration and de-fluidisation. Air preheating at high ERs is limited to a low level e.g. for a CFB at an ER=0.37, and according to the present model, an air temperature of not more than 170ºC would be recommended because the corresponding gasification temperature is 978ºC whereas for an ER=0.29 the air could, in theory, be heated to 850ºC because the gasification temperature stays below 967ºC.

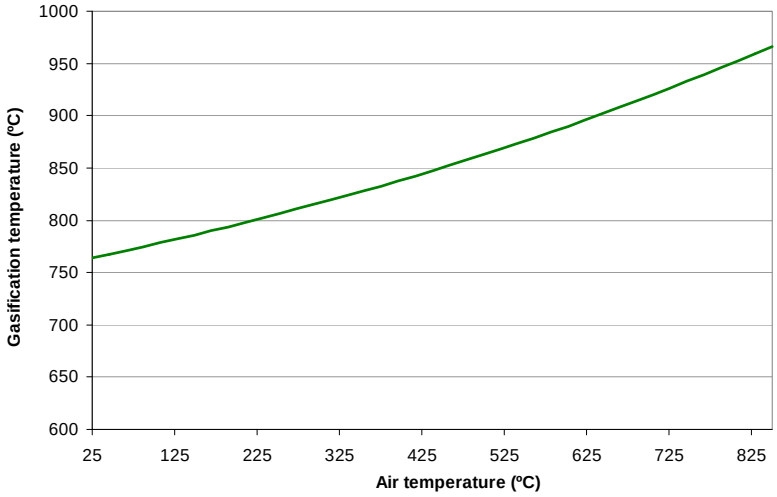


Figure 3.8: Effect of air preheating on gasification temperature using the present modified equilibrium for hemlock wood chips gasification with a moisture content of 11.7% and ER=0.29.

The influence of air inlet temperature for hemlock wood chips (11.7% moisture) gasification using the present modified equilibrium model is shown in Figure 3.9. The product gas composition for an ER=0.29 and considering heat losses of 3% and carbon loss of 2% is plotted against air temperature. The rising temperature promotes the products of endothermic reactions and simultaneously the reactants of exothermic reactions. Another important consideration is that the air temperature has a greater influence on the product gas composition for low ERs. For an ER of 0.29 CO and $H_2$ content increased 5.5 and 5.4 percentage points, respectively, over the air temperature range whereas for an ER of 0.35 CO and $H_2$ content increases only 4 and 0.1 points, respectively, for the same temperature range. It was also found that air temperature has a significant influence on composition only up to a certain level, after which additional preheating has little effect. For both commented ER this level is reached at about 700ºC which agrees with Lucas et al. (2004) that reported an increase of $H_2$ content with increasing air preheat temperature but no rise between 700ºC and 830ºC. Also Yang et al. (2006) refers to a critical air temperature which air preheating is no longer efficient if the purpose is to maximise the yield of gaseous products. As expected, it is also observed that LHV and cold gas efficiency increase when increasing air inlet temperature (Mathieu and Dubuisson, 2002; Doherty et al., 2009).

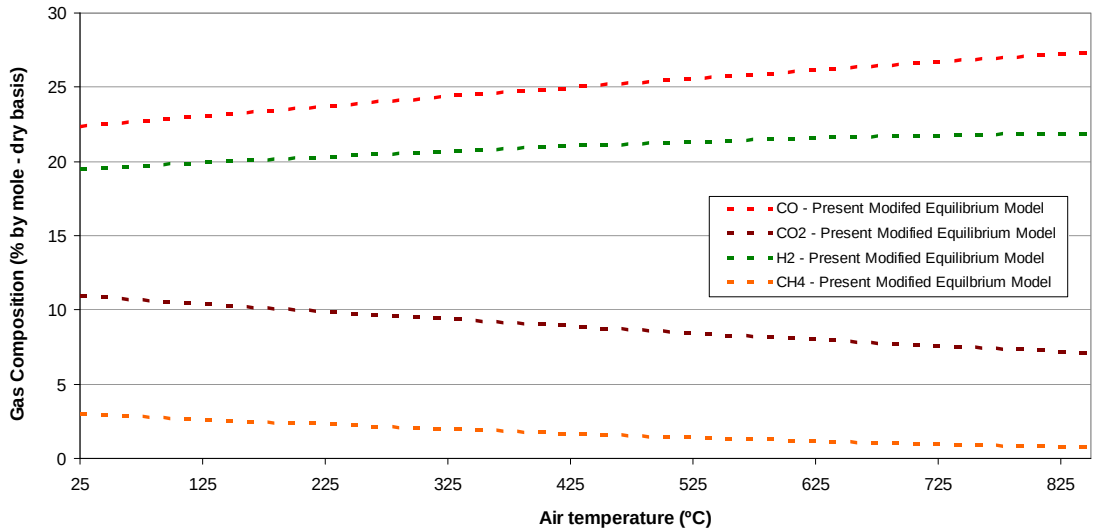


Figure 3.9: Variation of the composition of producer gas for the present modified equilibrium model when increasing the air inlet temperature for hemlock wood chips gasification with a moisture content of 11.7% and ER=0.29.

### 3.5.4 Effect of steam injection on producer gas composition

The influence of steam injection on gasifier performance for an ER of 0.34 was studied (Figure 3.10) and compared with the results presented by Doherty et al. (2009). Like these authors did, the steam injection rate was varied from 0 to 10.5 kg/h. The producer gas LHV decreased only slightly from 5.25 to 5.14 MJ/kg. Steam injection causes a rise in H2O content, which results in a lower LHV. CO and $CH_4$ are shifted and reformed respectively with the additional $H_2O$, decreasing their contents and producing more $CO_2$. The most important effect of steam injection is the rise in $H_2$ content, in this case increases by 1% over the range of steam injection. Doherty et al. (2009) observed a slight increase in cold gas efficiency, from 66.1% to 66.5% while here a slight decrease of 1% for the same whole range is observed. Mathieu and Dubuisson (2002) also observed that water injection produced a decrease of cold gas efficiency from 80.1% down to 78.6% when the amount of steam increased up to 0.3 kg/kg air and when the temperatures of air and steam were 800ºC and oxygen factor 25%. They found this tendency true whatever the air temperature, preheated or not, and whatever the enrichment of air in $O_2$.

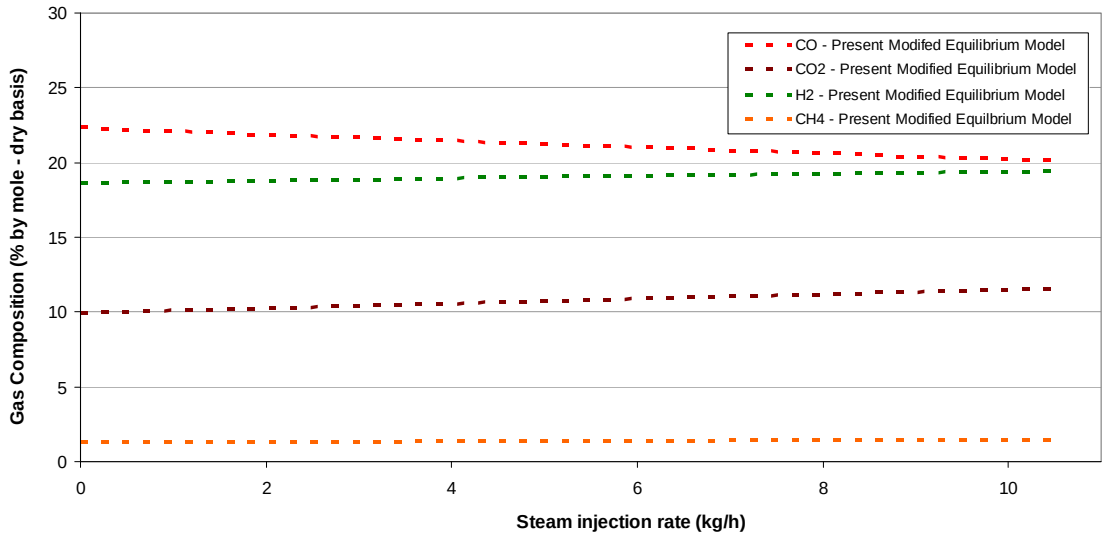


Figure 3.10: Variation of the composition of producer gas for the present modified equilibrium model when increasing the steam injection rate for an ER=0.34 for hemlock wood chips gasification with a moisture content of 11.7%.

Increasing steam injection causes a decrease in the gasifier temperature due to highly endothermic reforming and water-gas reactions unless heat is supplied from an external source. As stated by Doherty et al. (2009), a decrease in temperature is undesirable as this would degrade the gasifier performance and could lead to high tar yield. For this reason, air preheating should be considered when using high moisture fuels and steam injection.

### 3.5.5 Effect of oxygen enrichment on producer gas composition

The effect of oxygen enrichment in the air on producer gas composition and LHV is studied and compared with that reported by Babu and Sheth (2005). Figure 3.11 shows how the composition of producer gas changes with oxygen fraction in the air for wood chips gasification, ER of 0.3 and initial moisture content of 10% with no air preheating.

As it can be observed in Figure 3.11 the $N_2$ yield decreases with increasing oxygen fraction as expected. The methane content is very low and in a percentage of less than 1%. The percentage of hydrogen in the producer gas increases continuously with oxygen fraction, from about 25% to 32% for an increase of oxygen fraction from 25% to

50%. A similar trend is also observed for carbon monoxide however the increase is from 30% to 42%. $CO_2$ reminds more or less constant and at around 10%.

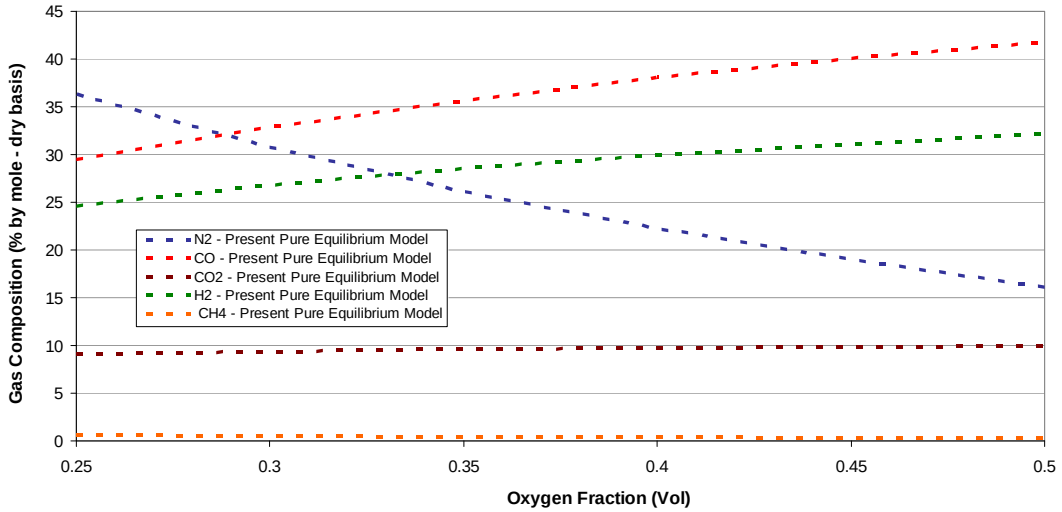


Figure 3.11: Effect of the oxygen enrichment on the composition of producer gas for wood chips gasification with 10% of moisture content and ER of 0.3 using the present pure equilibrium model.

In Figure 3.12 it can be observed how the reaction temperature increases from 1100 K to 1200 K when oxygen fraction increases from 25% to 50%. For the same increase of oxygen fraction the LHV of producer gas increases from 6 MJ/Nm$^3$ to 7.8 MJ/Nm$^3$. The increment of LHV is due to increase in the amount of CO and $H_2$. The same results were obtained by Babu and Sheth (2005) and concluded that using air with enriched oxygen gives higher calorific values of producer gas.

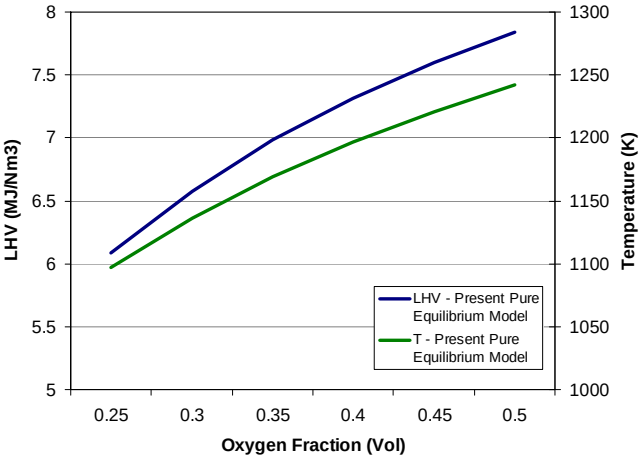


Figure 3.12: Effect of the oxygen enrichment on the gasification temperature and producer gas LHV for wood chips gasification with 10% of moisture and ER=0.3.

## 3.6 CONCLUSIONS

In this chapter, a new modified equilibrium model, built in the equation solver program EES, is presented. A user interface has been implemented to make the model user-friendly. Firstly, a pure equilibrium model was developed based on the previous work of other authors and then modified in order to apply the model to systems that do not fully achieve equilibrium.

The modifications introduced to the pure equilibrium model essentially consist in:

- Adding a pyrolysis unit that predicts the formation of gas, char and volatiles.
- Considering heat losses in pyrolysis and gasification units.
- Adding tar and char leaving the gasifier.
- Considering particles leaving the gasifier.
- Setting the amount of $CH_4$ produced.

If no information is available, these model parameters, which can be introduced by the user, are automatically adjusted by means of minimising the difference between experimental and predicted results for producer gas composition.

The modified equilibrium model has been validated with published experimental data. For downdraft gasifiers, the predicted values for air gasification are in very good agreement with the experimental ones for all cases and different gasifiers with RMS values between 0.2 and 3.05 for the different producer gas species (CO, $CO_2$, $N_2$, $H_2$). However larger differences between predicted and experimental data are observed for air-steam (RMS= 3.37 – 5.48) and $O_2$-steam gasification (RMS= 3.80 – 6.93). In these last two cases, it has not been possible to find more published papers containing experimental data. For this reason, the obtained results and deviations cannot be compared with those that could be obtained for other downdraft gasifiers.

Concerning fluidised bed gasifiers, model predictions are in good agreement with experimental published data for air and air-steam gasification (RMS=0.7 – 3.5) but significant deviations are observed for oxygen (RMS=5.6 – 11.6) and enriched-air (RMS= 2.8 - 9.5) biomass gasification. These deviations are larger than for downdraft gasifiers.

From these results it can be concluded that the model is accurate enough to predict the behaviour of downdraft and fluidised bed gasifiers for air gasification. However, more experimental data is needed to evaluate the prediction capability of the model for air/steam biomass gasification in downdraft gasifiers. Even though the predictions are worse for $O_2$/steam gasification, this is of minor importance due to the gasifier model will be integrated in a biomass trigeneration model for a small-medium scale plant that will operate mainly with air as gasifying agents due to economic considerations.

In addition, the model is sensitive enough to evaluate the influence of ER, air preheating, steam injection, oxygen enrichment and biomass moisture content in the quality of producer gas. The results predicted by the model are in good agreement with those predicted by other authors' models and can be summarised as follows:

- Increasing the moisture content of biomass reduces the LHV of the producer gas because the small increase in $H_2$ concentration is overshadowed by the rapid decrease of CO.
- For an adiabatic process, increasing the ER also means increasing the gasification temperature and decreasing the LHV of producer gas.
- The use of high temperature air has a significant influence on composition only up to a certain level and it is limited by the operating temperature constrain of the reactor.
- Steam injection in biomass gasification raises the $H_2$ content of producer gas.
- The LHV, CO and $H_2$ yields of producer gas increase when the oxygen fraction of air increases.

Even the predictions are also good for fluidised bed gasifiers, it was decided to develop an ANN model that could reproduce the behaviour of these gasifiers using the same input data than the modified equilibrium model. The aim of developing an ANN is to evaluate the great potential of these models for biomass gasification, that have only been applied before in very few occasions and that can be easily extended and improved when more data is available.

# Chapter 4

# Development and validation of artificial neural network models for biomass gasification in fluidised bed reactors

## 4.1 INTRODUCTION

In the previous chapter, a modified equilibrium model was developed and considered a good approach to model biomass gasification in a downdraft and even in a fluidised bed gasifier. However, due to the fact that usually it is more difficult to predict the behaviour of biomass gasification in fluidised bed gasifiers using equilibrium models, it was decided to develop an ANN model for this kind of gasifiers that could be easily extended and improved when more data was available.

This chapter presents a brief summary on ANN main concepts followed by the development of two ANN: one for CFB and the other for BFB gasifiers. Both models are based on experimental published data. At the end of the chapter, the results obtained with the ANN models are compared with those obtained by applying the modified equilibrium model for the same experimental data.

## 4.2 ARTIFICIAL NEURAL NETWORKS

An artificial neural network (ANN) is a system based on the operation of biological neural networks (Figure 4.1), a computational model inspired in the natural neurons. Natural neurons receive signals through synapses located on the dendrites or membrane of the neuron. When the signals received are strong enough (surpass a certain threshold), the neuron is activated and emits a signal through the axon. This signal might be sent to another synapse, and might activate other neurons.

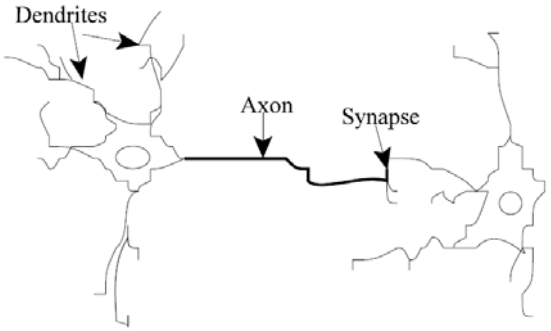


Figure 4.1: Natural neurons

An ANN is composed of a large number of highly interconnected processing elements (neurones or nodes) working in unison to solve specific problems. ANNs, like people, learn by example. An ANN is configured for a specific application, such as pattern recognition or data classification, through a learning process. Learning, in biological systems, involves adjustments to the synaptic connections that exist between the neurones. This is true for ANNs as well. Neural networks have been trained to perform complex functions in various fields of application including pattern recognition, identification, classification, speech, vision and control systems.

### 4.2.1 Network architectures

The expressions “structure”, “architecture” or “topology” of an ANN are used to talk about the way in which computational neurons are organized in the network. Particularly, these terms are focused in the description of how the nodes are connected and in how the information is transmitted through the network.

A neuron with a single *i* elements input vector is shown below (Figure 4.2). Here the individual element inputs ($p_1$, $p_2$, $p_3$ … $p_i$) are multiplied by weights ($IW_{1,1}$, $IW_{1,2}$ ….$IW_{1,i}$) and the weighted values are fed to the summing junction. Their sum is simply *IWp*, the dot product of the (single row) matrix ***IW*** and the vector *p*.

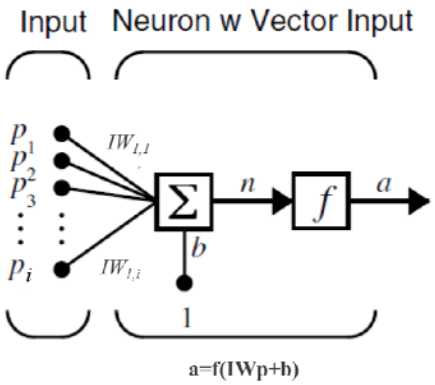


Figure 4.2: Artificial neuron structure with a single *i* elements input vector.

The neuron has a bias *b*, which is summed with the weighted inputs to form the net input *n*. This sum, *n* (Eq 4.1), is the argument of the transfer function *f*.

$$n = IW_{1,1}\,p_1 + IW_{1,2}\,p_2 + \ldots + IW_{1,i}\,p_i + b \qquad \text{Eq. 4.1}$$

A one-layer network with *i* elements input and *j* neurons is presented in Figure 4.3.

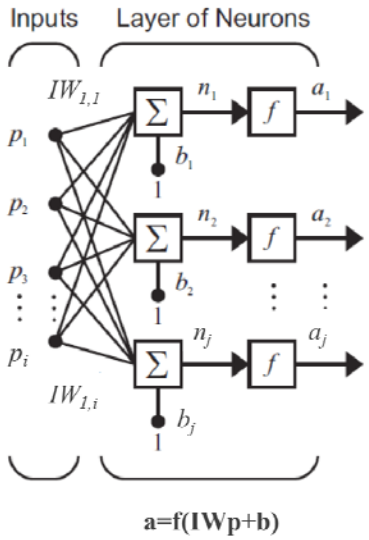


Figure 4.3: One layer network with *i* elements input vector and *j* neurons.

In this network, each element of the input vector *p* is connected to each neuron input through the weight matrix *IW*. The $j^{th}$ neuron has a summer that gathers its weighted inputs and bias to form its own scalar output *n(j)*. The various *n(j)* taken together form an *j*-element net input vector *n*. Finally, the neuron layer outputs form a column vector *a*. The expression for *a* is shown at the bottom of the figure. It is common for the number of inputs to a layer to be different from the number of neurons. A layer is not constrained to have the number of its inputs equal to the number of its neurons.

A network can have several layers. Each layer has a weight matrix, a bias vector and an output vector. It is common for different layers to have different numbers of neurons. A constant input 1 is fed to the biases for each neuron. The outputs of each intermediate layer are the inputs to the following layer.

The layers of a multilayer network play different roles. A layer that produces the network output is called an output layer. All other layers are called hidden layers.

A classification of the ANNs is obtained considering the direction of the flow of the information through the layers, the connectivity among the neurones of a neural network is related with the way in which the exit of neurons are directed to become into entrances for other neurons:

- Feedforward networks (Figure 4.4) allow signals to travel one way only; from input to output. There is no feedback (loops) i.e. the output of any layer does not affect that same layer. This kind of network architecture is most commonly used with the backpropagation algorithm.
- Feedback networks (Figure 4.4) can have signals travelling in both directions by introducing loops in the network. They are very powerful and can get extremely complicated.

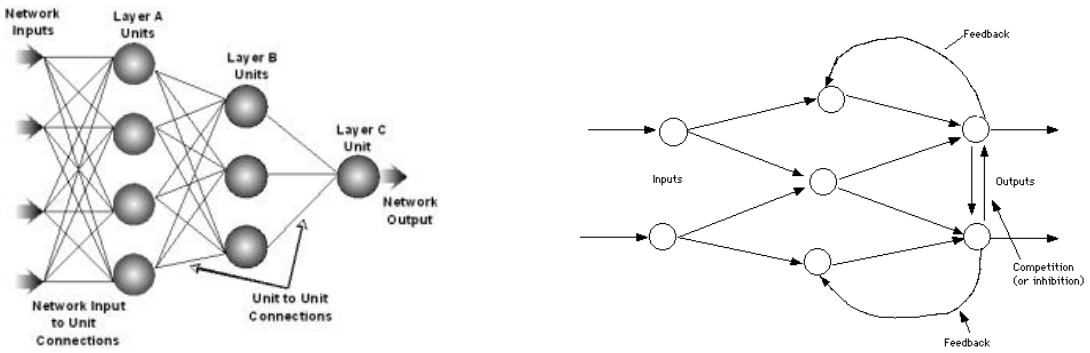


Figure 4.4: Feedforward ANN (left) and ANN with feedback and competition (right).

### 4.2.2 Training an artificial neural network

A neural network has to be configured such that the application of a set of inputs produces the desired set of outputs. The main property in all ANNs is the ability to learn from its surroundings, which is shown with the improvement of their performance through learning. Following the way learning is performed, we can distinguish two major categories of neural networks:

- Fixed networks, in which the weights cannot be changed. In such networks, the weights are fixed a priori according to the problem to solve.
- Adaptive networks, which are able to change their weights. In this case the neural network is “trained” by feeding it teaching patterns and letting it change its weights according to some learning rule.

A learning rule or algorithm is a prewritten group of rules to solve a learning process. In other words, learning or training an ANN basically consists in the modification of its weight through the application of a learning algorithm when a group of patterns is presented. There is not a unique learning algorithm for the design of the neural networks. In a general way, all learning methods used for adaptive neural networks can be classified into two major categories: supervised learning and unsupervised learning:

- ANN with supervised learning: in this case the learning rule is provided with a set of examples (the training set) of proper network behaviour where there is an input to the network and its corresponding correct (target) output. As the inputs

are applied to the network, the network outputs are compared to the targets. The learning rule is then used to adjust the weights and biases of the network in order to move the network outputs closer to the targets.

- ANN with unsupervised or self-organised learning: it does not require any external element to adjust the weight of the communication links to their neurons. In this case the weights and biases are modified in response to network inputs only. There are no target outputs available.

The training must be stopped at the right time. If training continues for too long, it results in overlearning. Overlearning means that the neural network extracts too much information from the individual cases forgetting the relevant information of the general case. It occurs whenever a network is trained for too long on the same input, thus losing its ability to generalise. There are two schools of thought for avoiding this problem: the first is to use cross-validation and similar techniques to check for the presence of overtraining and optimally select hyperparameters such as to minimize the generalization error. The second is to use some form of regularization.

#### 4.2.2.1 Least mean square error supervised training

The Least Mean Square error (LMS) algorithm is an example of supervised training, in which the learning rule is provided with a set of examples of desired network behaviour: $\{p_1,t_1\}$, $\{p_2, t_2\}$, … , $\{p_i, t_i\}$

Here $p_i$ is an input to the network, and $t_i$ is the corresponding target output. As each input is applied to the network, the network output is compared to the target. The error is calculated as the difference between the target output and the network output. The average of the sum of these errors wants to be minimized.

$$MSE = \frac{1}{i} \cdot \sum_{i=1}^{i} (t(i) - a(i))^2 \qquad \text{Eq. 4.2}$$

The LMS algorithm environment adjusts the weights and biases of the linear network so as to minimize this Mean Square Error (MSE).

#### 4.2.2.2 Transfer function

The activation function defines the output of the neuron in terms of the activity level at its input. Different expressions can be used for the neuron's activation function, like a step, sigmoid, tangent sigmoid or linear function, presented in Figure 4.5.

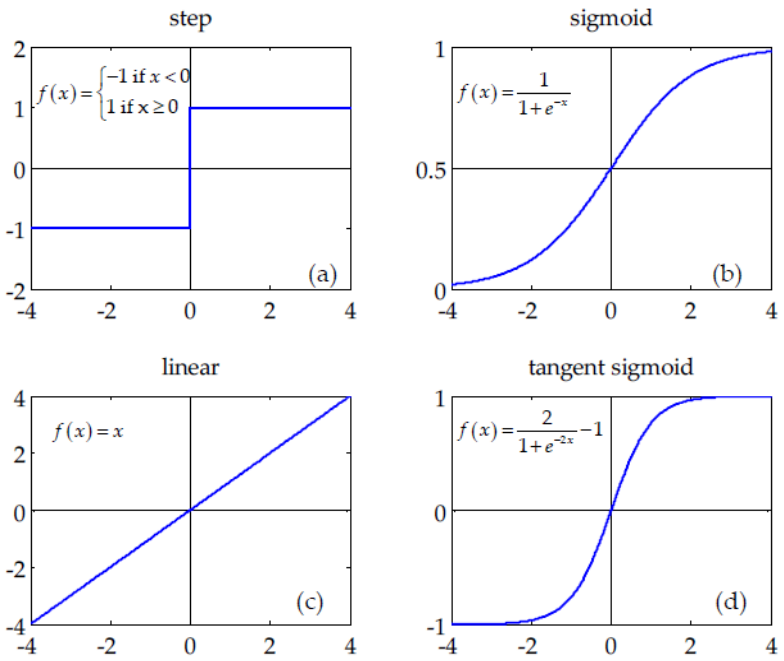


Figure 4.5: Different neuron activation functions: (a) step; (b) sigmoid; (c) linear; (d) tangent sigmoid

#### 4.2.2.3 The backpropagation algorithm

Backpropagation was created by generalizing the Widrow-Hoff learning rule to multiple-layer networks and nonlinear differentiable transfer functions. Input vectors and the corresponding target vectors are used to train a network until it can approximate a function, associate input vectors with specific output vectors, or classify input vectors in an appropriate way as defined by the user.

The backpropagation algorithm uses supervised learning, which means that the algorithm is provided with examples of the inputs and outputs we want the network to compute, and then the error (difference between actual and expected results) is calculated. The idea of the backpropagation algorithm is to reduce this error, until the

ANN learns the training data. The training begins with random weights, and the goal is to adjust them so that the error will be minimal.

Standard backpropagation is a gradient descent algorithm, as is the Widrow-Hoff learning rule, in which the network weights are moved along the negative of the gradient of the performance function. The term backpropagation refers to the manner in which the gradient is computed for nonlinear multilayer networks.

Properly trained backpropagation networks tend to give reasonable answers when presented with inputs that they have never seen. The three transfer functions most commonly used for backpropagation are tan-sigmoid, log-sigmoid and linear. Feedforward networks often have one or more hidden layers of sigmoid neurons followed by an output layer of linear neurons. Multiple layers of neurons with nonlinear transfer functions allow the network to learn nonlinear and linear relationships between input and output vectors. The linear output layer lets the network produce values outside the range –1 to +1. Networks with biases, a sigmoid layer, and a linear output layer are capable of approximating any function with a finite number of discontinuities.

There are many variations of the backpropagation algorithm. For instance, Matlab environment neural network toolbox includes different backpropagation training algorithms. Among the several backpropagation training algorithms, gradient descent, and gradient descent with momentum are often too slow for practical problems. There are other algorithms that operate in the batch mode and can converge from ten to one hundred times faster than the previously mentioned ones. These faster algorithms fall into two main categories depending if they use heuristic techniques or standard numerical optimization techniques.

For the learning phase, the data must be divided in two sets: the training data set, which is used to calculate the error gradients and to update the weights, and the validation data set, which allows to select the optimum number of iterations in which the networks learns general information from the training set. As the number of iterations increases, the training error drops whereas the validation data set error begins to drop, then reaches a minimum and finally increases. Continuing the learning process after the point when the validation error arrives to a minimum leads to a process called overfitting, when the network became specific to the pattern vectors that

form the training data set. After finishing the learning process, another data set (test set) is used to validate and confirm the prediction accuracy.

Usually, in the ANNs approaches, data normalization is necessary before starting the training process, to ensure that the influence of the input variable in the course of model building is not biased by the magnitude of their native values, or their range of variation. The normalization technique used consist in a linear transformation of the input/output variables to the range [0,1].

#### 4.2.2.4 Levenberg-Marquardt algorithm

An efficient method used for weights adaptation is the Levenberg-Marquardt algorithm (Levenberg, 1944; Marquardt, 1963), which is a combination between the gradient descendent rule and the Gauss-newton method. The algorithm uses a parameter to decide the step size, which takes large values in the first iterations (equivalent with the gradient descent algorithm), and small values in the later stages (equivalent with the Gauss-Newton method). It combines the ability of both methods (i.e. convergence from any initial state in the case of gradient descent, and rapid convergence when reach the vicinity of the minimum error in the case of Gauss-Newton method) while avoiding their drawbacks (Bishop, 2002; Hagan and Menhaj, 1994).

## 4.3 ARTIFICIAL NEURAL NETWORK MODELS DEVELOPED

Little research has been done in the field of ANN models for biomass gasification (see Chapter 2) considering the great potential of these models and their wide application.

Having in mind that the modified equilibrium model developed in the previous chapter (Chapter 3) does not adjust for fluidised bed gasifiers as good as for downdraft gasifiers, the aim of this chapter is to develop a simple model that could reproduce the performance of fluidised bed gasifiers without requiring very detailed information and ANN models are considered a good approach. The ANN models developed in the present chapter use the same available input data than the equilibrium model.

Since different kinds of biomass and different gasifiers have different gasification behaviour, two ANN models are presented. The first one models circulating fluidized bed gasifiers and the second one bubbling fluidized bed gasifiers. In addition, and in order to get more reliable results and use more homogeneous data, only data for wood gasification was considered. To develop the ANN models, published experimental data from different authors and different gasifiers was used. Although it would have been desirable to have a large database of experimental data for the same gasifier at different operating conditions.

### 4.3.1 Data selection

The selection of an appropriate set of variables for inclusion as inputs to the model is a vital step in model development, as the performance of the final model is heavily dependent on the input variables used. Selection of the best set of input variables is essential to be able to model the system under consideration reliably. When the available data set is highly dimensional, it is necessary to select a subset of the potential input variables to reduce the number of free parameters in the model in order to obtain good generalization with finite data. The correct choice of model inputs is also important for improving computational efficiency. However, the topic of input selection is a difficult one. Real systems are generally complex and mostly associated with nonlinear processes. Consequently, the dependencies between output and input variables, as well as conditional dependencies between variables, are difficult to measure.

In this thesis an extensive literature review was done in order to obtain published experimental data that could be used to develop the ANN models (see Chapter 2). This was an arduous and difficult task because in most of published papers not all information needed (such as biomass proximate and ultimate analysis and producer gas yield and composition) was given.

Data for atmospheric pressure circulating fluidised bed ANN model was obtained for air gasification in an inert bed from Li et al. (2004) and van der Drift et al. (2001). The operational variables of the database were feedstock composition (VM, FC, Ash, Moisture, C, H, O, N and S) equivalence ratio (ER) and gasification temperature ($T_g$).

Published experimental data for atmospheric bubbling fluidised bed, which could be used for the ANN model, was available for air, air-steam, enriched air-steam and oxygen-steam gasification in inert bed. However, after evaluating and performing preliminary tests with all this experimental data, the ANN model for BFB was developed only for air and air-steam gasification. Enriched air-steam and oxygen-steam data could not be included in the previous model and was not sufficient for developing another ANN model. For this reason, only the data from Narvaez et al. (1996), Campoy (2009), Kaewluan and Pipatmanomai (2011) and Lv et al. (2004) was used.

The operational variables of the database were the same than those for CFB gasifiers but another variable, which accounted for the amount of steam injected, was also considered (VB). VB stands for the ratio between amount of steam injected and biomass flowrate.

In both ANN models, the data sets were divided into training (80%) and validation-test subsets (20%), randomly selected from the available database. Due to the small size of the database, validation and test sets were the same.

Since the transfer function used in the hidden layer was tangent sigmoid ("tansig"), all samples were normalized in the range 0.2 – 0.8. So, any samples from the training and validation-test sets ($p_i$) were scaled to a new value ($\bar{p}_i$) as follows (Khataee and Mirzajani, 2010):

$$\bar{p}_i = 0.2 + \frac{0.6 \cdot (p_i - \min(p_i))}{\max(p_i) - \min(p_i)} \qquad \text{Eq. 4.3}$$

### 4.3.2 Proposed ANN model for circulating fluidised bed gasifiers

Since it was previously mentioned, the available input variables for the ANNs were feedstock composition (VM, FC, Ash, Moisture, C, H, O, N and S), equivalence ratio (ER) and gasification temperature ($T_g$). However, the small size of the database (18 sets) together with preliminary validation tests and results from the literature (Brown et al., 2006; Brown et al., 2007) suggested reducing the number of input variables. Fixed carbon (FC) and volatile matter (VM) as stated by Brow et al. (2006) based on the

previous works of van Krevelen (1950) and Jenkins et al. (1998) were considered as dependent variables because the FC ratio is proportional to both the H/C and O/C ratios. Considering that the gas species to be determined are CO, $CO_2$, $H_2$ and $CH_4$, Nitrogen (N) and sulphur (S) were not considered either as input variables. In addition, their amount in wood is very low and, in some cases, almost negligible compared with the content of carbon (C), hydrogen (H) and oxygen (O). The characteristics of the seven input and five output variables are shown in Table 4.1.

Table 4.1: Characteristics of input and output variables to the ANN models for circulating fluidised bed gasifiers.

| **Input variables for the ANNs** | **Range** |
|---|---|
| Ash content of biomass (% d.b.) | 0.4 – 3.34 |
| Moisture content of biomass (% w.b.) | 3.5 – 22.0 |
| Carbon content of biomass (C) (% d.b.) | 47.66 – 52.99 |
| Oxygen content of biomass (O) (% d.b.) | 38.38 – 43.55 |
| Hydrogen content of biomass (H) (% d.b.) | 5.43 – 7.86 |
| Equivalence ratio (ER) (-) | 0.19 – 0.64 |
| Gasification temperature ($T_g$ ) (ºC) | 701 – 861 |
| **Output variables for the different ANNs** | **Range** |
| $H_2$ in producer gas (% vol. d.b.) | 3.00 – 7.30 |
| $CH_4$ in producer gas (% vol. d.b.) | 1.20 – 4.60 |
| $CO_2$ in producer gas (% vol. d.b.) | 13.94 – 18.30 |
| CO in producer gas (% vol. d.b.) | 6.90 – 21.40 |
| Producer gas yield ($Nm^3$ d.b. / kg biomass d.b.) | 1.72 – 3.30 |

Five artificial neural networks were employed. One ANN for each of the four major gas species of producer gas (CO, $CO_2$, $H_2$, $CH_4$) and another ANN to determine producer gas yield. Topology of the ANNs was determined through a procedure of trial and error and all five networks are identical in topological structure (Figure 4.6).

After evaluating several differently structured neural networks, an ANN with a single hidden layer with 2 neurons and an output layer with one neuron was selected for each case. The ANNs were carried out in two steps; the former was to train the network whereas the later was to test the network with data, which were not used for training. The ANNs were trained using the Lavenberg-Marquadt backpropagation algorithm, implemented in the Matlab neural network toolbox (Matlab, 2010). The “tansig” (hyperbolic tangent sigmoid) transfer function was used as the activation function for the hidden layer and the “purelin” (linear) transfer function was used for the output

layer. The system adjusted the weights of the internal connections to minimize errors between the network output and target output.

The performance of the different ANNs was statistically measured by the root mean square error (RMSE) and regression coefficient ($R^2$), which were calculated with the experimental values and networks predictions. In Figure 4.7 the different experimental and predicted data are compared through linear regression models. The values of $R^2$ and RMSE for each output are presented in the different graphs. As it can be seen, all correlations have a $R^2$ value higher than 0.99 except $H_2$ which is a little bit lower (0.977).

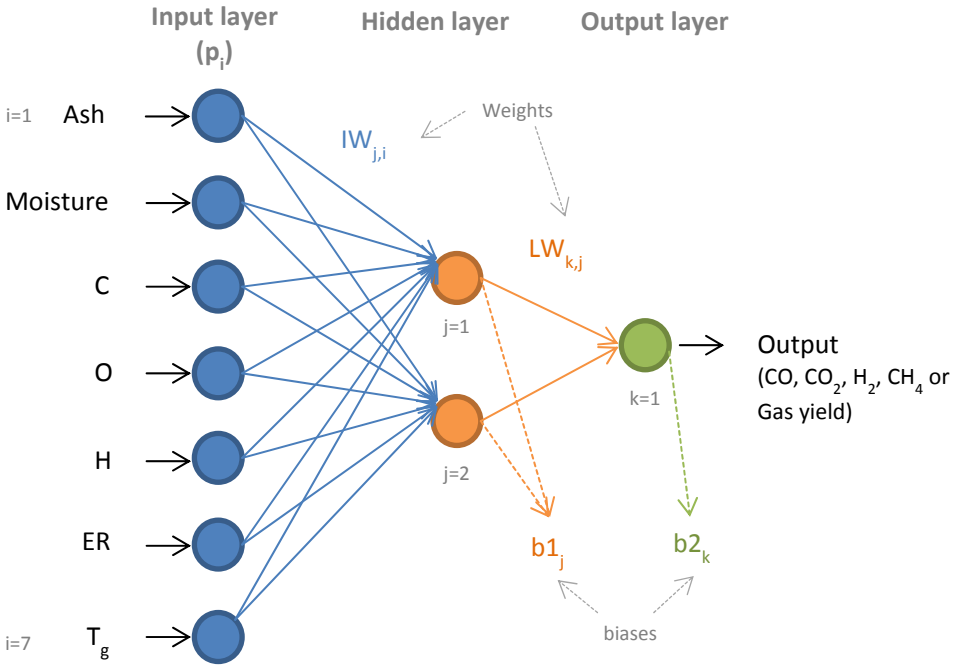


Figure 4.6: Schematic diagram of one ANN for a circulating fluidised bed gasifier.

According to Verma et al. (2006) and Hamzaoui et al. (2011) to satisfy the statistical test of intercept and slope; the interval between the highest and lowest values of the intercept must contain zero and the interval between the highest and lowest values of the slope must contain one. The limits for test indicators are shown in Table 4.2, with slope containing one and with the intercept containing zero. Consequently, the

proposed ANNs passed the test with 99.8% of confidence level. This test with information above guarantees that whole ANN model, containing five ANNs, has a satisfactory level of confidence. Table 4.3 gives the obtained parameters ($IW_{j,i}$, $LW_{1,j}$, $b1_j$, b2 ) of the best fit for 2 neurons in the hidden layer for each of the five ANN developed in the CFB model. These parameters were used in the proposed model to simulate the output values. Consequently, the proposed ANNs models follow:

$$a_{output} = \sum_{j=1}^{j=2}\left[ LW_{1,j} \cdot \left( \frac{2}{1+\exp\left(-2\cdot\left(\sum_{i=1}^{i=7}\left(IW_{j,i}\cdot \bar{p}_i\right)+b1_j\right)\right)} - 1 \right)\right] + b2 \qquad \text{Eq. 4.4}$$

Table 4.2: Intercept and slope statistical test for CFB gasifiers ANN model.

| **Intercept and slope statistical test** | |
|---|---|
| **CO** | |
| $Intercept_{lower}$= -0.4245 | $Intercept_{upper}$= 0.2926 |
| $Slope_{lower}$ = 0.9766 | $Slope_{upper}$ = 1.0299 |
| **$CO_2$** | |
| $Intercept_{lower}$= -1.0523 | $Intercept_{upper}$= 0.4079 |
| $Slope_{lower}$ = 0.9766 | $Slope_{upper}$ = 1.0676 |
| **$CH_4$** | |
| $Intercept_{lower}$= -0.0639 | $Intercept_{upper}$= 0.2193 |
| $Slope_{lower}$ = 0.9299 | $Slope_{upper}$ = 1.0272 |
| **$H_2$** | |
| $Intercept_{lower}$= -1.2595 | $Intercept_{upper}$= 0.9760 |
| $Slope_{lower}$ = 0.8289 | $Slope_{upper}$ = 1.2454 |
| **Producer gas yield** | |
| $Intercept_{lower}$= -0.1878 | $Intercept_{upper}$= 0.1991 |
| $Slope_{lower}$ = 0.9272 | $Slope_{upper}$ = 1.0766 |

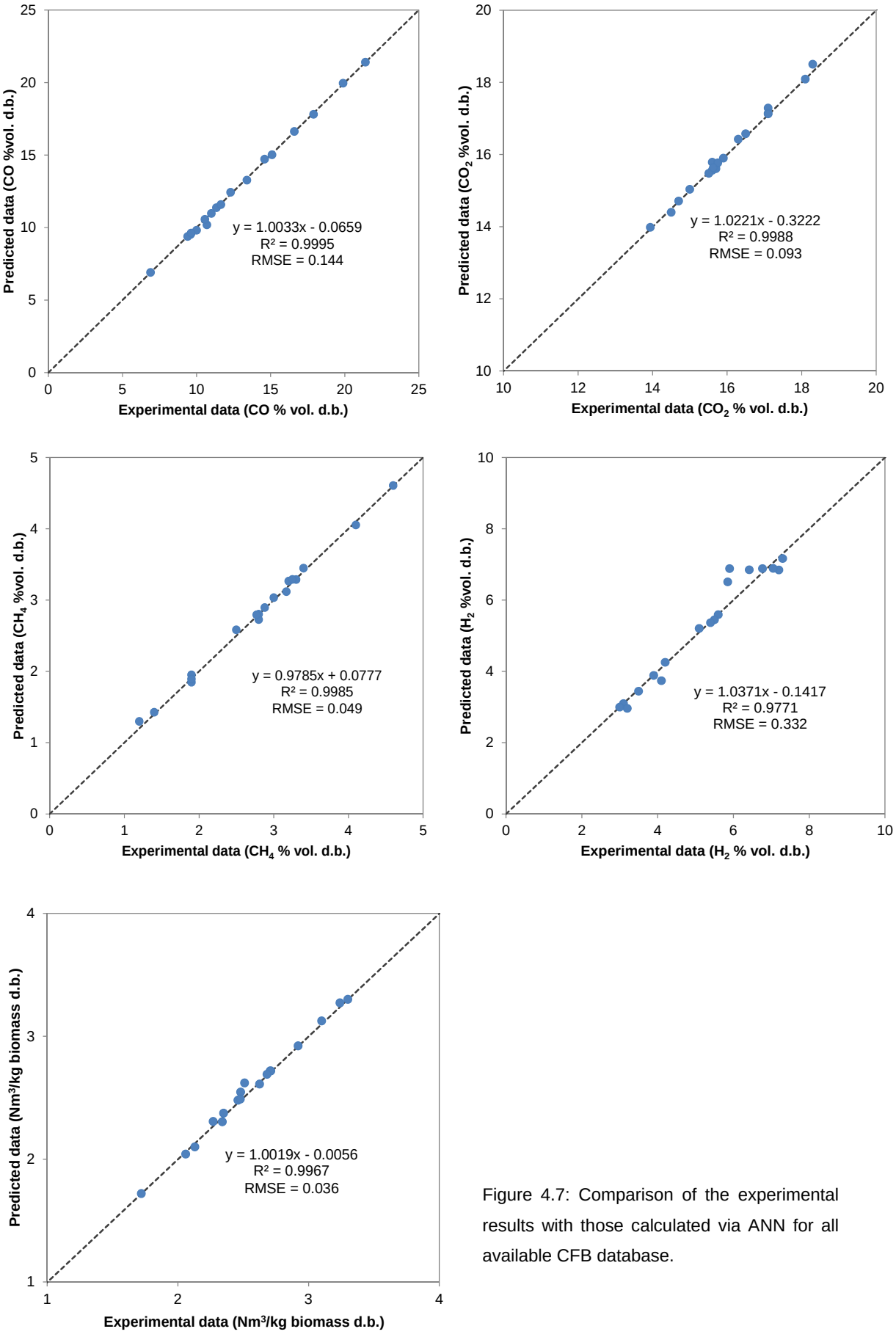


Figure 4.7: Comparison of the experimental results with those calculated via ANN for all available CFB database.

Table 4.3: Weights and biases of the designed ANNs for the four major gas species of producer gas (CO, $CO_2$, $H_2$, $CH_4$) and producer gas yield for CFB gasifiers ANN model.

| | | | | | | |
|---|---|---|---|---|---|---|
| **CO** | | | | | | |
| **$IW_{i,j}$** | | | | | | |
| -3.2006 | 0.0722 | -0.5638 | 5.3061 | -3.7749 | -0.9014 | -0.9632 |
| -1.1408 | -1.8333 | -0.3493 | -0.1148 | 0.4085 | 3.8072 | 0.8495 |
| **$LW_{1,j}$** | | | **$b1_j$** | | **b2** | |
| 5.4159 | -10.0337 | | 3.6063 | | 12.9445 | |
| | | | 0.0732 | | | |
| **$CO_2$** | | | | | | |
| **$IW_{i,j}$** | | | | | | |
| 1.7859 | 3.1087 | 4.0413 | 5.0279 | 1.9819 | 1.5078 | 0.6350 |
| 9.8078 | 9.1839 | -12.4537 | -2.3948 | -15.3984 | 9.5719 | 4.0890 |
| **$LW_{1,j}$** | | | **$b1_j$** | | **b2** | |
| 4.6685 | 3.9112 | | -7.6506 | | 10.2800 | |
| | | | 2.1235 | | | |
| **$CH_4$** | | | | | | |
| **$IW_{i,j}$** | | | | | | |
| 1.1889 | 2.4613 | -1.7017 | 4.4029 | 0.2984 | -2.6040 | 2.7315 |
| 1.4276 | 3.9629 | 2.6406 | 3.0161 | 0.8706 | -1.9226 | -2.5402 |
| **$LW_{1,j}$** | | | **$b1_j$** | | **b2** | |
| 1.2490 | 6.3563 | | -3.8959 | | 8.5215 | |
| | | | -5.2290 | | | |
| **$H_2$** | | | | | | |
| **$IW_{i,j}$** | | | | | | |
| -1.7403 | 3.4878 | 0.8185 | -3.3632 | -4.0765 | -7.8066 | -0.7735 |
| -16.8436 | 24.2709 | 1.2959 | -3.6059 | -6.6673 | -20.5250 | -18.7020 |
| **$LW_{1,j}$** | | | **$b1_j$** | | **b2** | |
| 3.0137 | -1.9792 | | 3.9094 | | 7.8781 | |
| | | | 17.6810 | | | |
| **Producer gas yield** | | | | | | |
| **$IW_{i,j}$** | | | | | | |
| -6.8841 | -6.4443 | -2.3434 | -1.3813 | -3.7339 | -9.9848 | -1.4279 |
| -5.7169 | -1.6951 | 1.5775 | 3.2875 | -3.6455 | 19.7080 | -6.0075 |
| **$LW_{1,j}$** | | | **$b1_j$** | | **b2** | |
| -0.5083 | 0.3425 | | 14.6688 | | 2.4497 | |
| | | | -0.8342 | | | |

#### 4.3.2.1 Sensitivity analysis

In order to assess the relative importance of the input variables, the evaluation process based on the neural net weight matrix and Garson equation (Garson, 1991) was used (Khataee and Mirzajani, 2010; Hamzaoui et al., 2011). Garson proposed an equation based on the partitioning of connection weights. The numerator describes the sums of absolute products of weights for each input while the denominator represents the sum of all weights feeding into hidden unit, taking the absolute values. The proposed equation, adapted to the present ANN topology, is as follows:

$$I_i = \frac{\sum_{j=1}^{j=2}\left(\left(\frac{\left|IW_{j,i}\right|}{\sum_{i=1}^{i=7}\left|IW_{j,i}\right|}\right)\cdot\left|LW_{1,j}\right|\right)}{\sum_{i=1}^{i=7}\left\{\sum_{j=1}^{j=2}\left(\left(\frac{\left|IW_{j,i}\right|}{\sum_{i=1}^{i=7}\left|IW_{j,i}\right|}\right)\cdot\left|LW_{1,j}\right|\right)\right\}} \quad \text{Eq. 4.5}$$

Where $I_i$ is the relative influence of the $i^{th}$ input variable on the output variable. The relative importance of the different input variables, for each ANN, calculated using Eq. 4.5 is shown in Figure 4.8. As can be observed, all of the variables have a strong effect on the different outputs (CO, $CO_2$, $H_2$, $CH_4$ and producer gas yield).

It can be seen how variables that account for biomass composition (C, H, O) represent between 31.7% and 54.1% of the importance on CO, $CO_2$, $H_2$ and $CH_4$ prediction. However, this importance is reduced to 25% for producer gas yield. On the other hand ER is the most important variable for producer gas yield prediction (37.6%) while it is also important for CO and $H_2$ (31.2 and 30.2%) and less important for $CO_2$ (11.5%) and $CH_4$ (12.6%). Gasification temperature has a relative constant importance in all cases (around 10%) except for $CO_2$ where it is lower (4.9%).

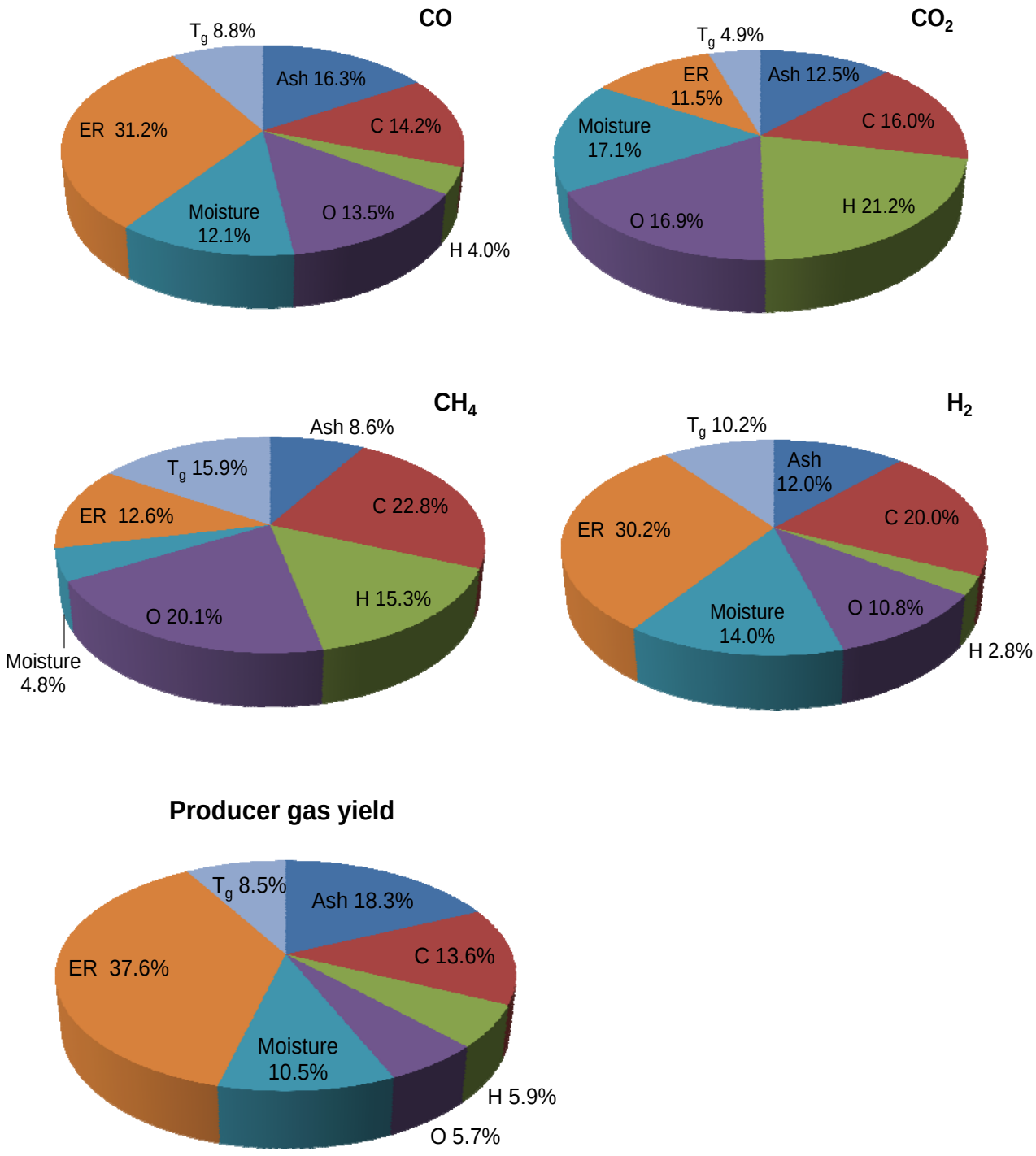


Figure 4.8: Relative importance (%) of input variables on the value of the different outputs for the four main producer gas components and producer gas yield.

### 4.3.3 Proposed ANN model for bubbling fluidised bed gasifiers

In this model, the same procedure as in the previous one for CFB gasifiers was applied. The model also aims to predict producer gas composition (CO, $CO_2$, $H_2$, $CH_4$) and producer gas yield for BFB gasifiers operating at atmospheric pressure and using air or air-steam as gasifying agents.

The input variables for the ANNs used in the present model were the same as those of the previous model (Ash, Moisture, C, H, O, ER and $T_g$) with the addition of "VB" that accounted for the ratio between injected steam and biomass flowrate. The characteristics of the eight input and five output variables are shown in Table 4.4.

Table 4.4: Characteristics of input and output variables to the ANN models for bubbling fluidised bed gasifiers.

| **Input variables for the ANNs** | **Range** |
|---|---|
| Ash content of biomass (% d.b.) | 0.55 – 1.10 |
| Moisture content of biomass (% w.b.) | 6.28 – 25 |
| Carbon content of biomass (C) (% d.b.) | 45.89 – 50.54 |
| Oxygen content of biomass (O) (% d.b.) | 41.11 – 47.18 |
| Hydrogen content of biomass (H) (% d.b.) | 5.64 – 7.08 |
| Equivalence ratio (ER) (-) | 0.19 – 0.47 |
| Gasification temperature ($T_g$ ) (ºC) | 700 – 900 |
| Injected steam ratio (VB) (kg steam/kg biomass d.b.) | 0 – 0.04 |
| **Output variables for the different ANNs** | **Range** |
| $H_2$ in producer gas (% vol. d.b.) | 4.97 – 26.17 |
| $CH_4$ in producer gas (% vol. d.b.) | 2.40 – 6.07 |
| $CO_2$ in producer gas (% vol. d.b.) | 9.82 – 18.60 |
| CO in producer gas (% vol. d.b.) | 10 – 29.47 |
| Producer gas yield ($Nm^3$ d.b. / kg biomass d.b.) | 1.17 – 3.42 |

The data set available included 36 data patterns. From these, 80% were used for training the network and the remaining 20% were randomly selected and used as validation-test data set. Like in the previous model, five ANNs were employed for the four major gas species of producer gas (CO, $CO_2$, $H_2$, $CH_4$) and producer gas yield. Topology of the ANNs was also determined through a procedure of trial and error and after evaluating several differently structured neural networks, ANNs with a single hidden layer with 2 neurons and an output layer with one neuron were also selected. The ANNs were trained using the Lavenberg-Marquadt backpropagation algorithm,

implemented in the Matlab neural network toolbox. The “tansig” (hyperbolic tangent sigmoid) transfer function was used as the activation function for the hidden layer and the “purelin” (linear) transfer function was used for the output layer.

The performance of the ANNs were also statistically measured by the root mean square error (RMSE) and regression coefficient ($R^2$). In Figure 4.9 the different experimental and predicted data were compared through a linear regression model and the values of $R^2$ and RMSE for each output are presented. All correlations have a $R^2$ value higher than 0.99 except $CO_2$ which is a little bit lower (0.98).

The limits for intercept and slope test indicators are shown in Table 4.5, with slope containing the one and with the intercept containing zero. Consequently, the proposed ANN model, composed by five ANNs, passed the test with 99.8% of confidence level in all cases.

Table 4.5: Intercept and slope statistical test for BFB gasifier ANN model.

| **Intercept and slope statistical test** | |
|---|---|
| **CO** | |
| $Intercept_{lower}$= -0.7537 | $Intercept_{upper}$= 1.9362 |
| $Slope_{lower}$ = 0.9002 | $Slope_{upper}$ = 1.0310 |
| **$CO_2$** | |
| $Intercept_{lower}$= -0.5586 | $Intercept_{upper}$= 2.6116 |
| $Slope_{lower}$ = 0.8172 | $Slope_{upper}$ = 1.0347 |
| **$CH_4$** | |
| $Intercept_{lower}$= -0.1133 | $Intercept_{upper}$= 0.5884 |
| $Slope_{lower}$ = 0.8684 | $Slope_{upper}$ = 1.0167 |
| **$H_2$** | |
| $Intercept_{lower}$= -0.8968 | $Intercept_{upper}$= 0.8896 |
| $Slope_{lower}$ = 0.9378 | $Slope_{upper}$ = 1.0445 |
| **Producer gas yield** | |
| $Intercept_{lower}$= -0.1344 | $Intercept_{upper}$= 0.2362 |
| $Slope_{lower}$ = 0.9045 | $Slope_{upper}$ = 1.0504 |

Table 4.6 gives the obtained parameters ($IW_{j,i}$, $LW_{1,j}$, $b1_j$, b2 ) of the best fit for 2 neurons in the hidden layer for each ANN developed. This model, like the previous one, follows Eq. 4.4.

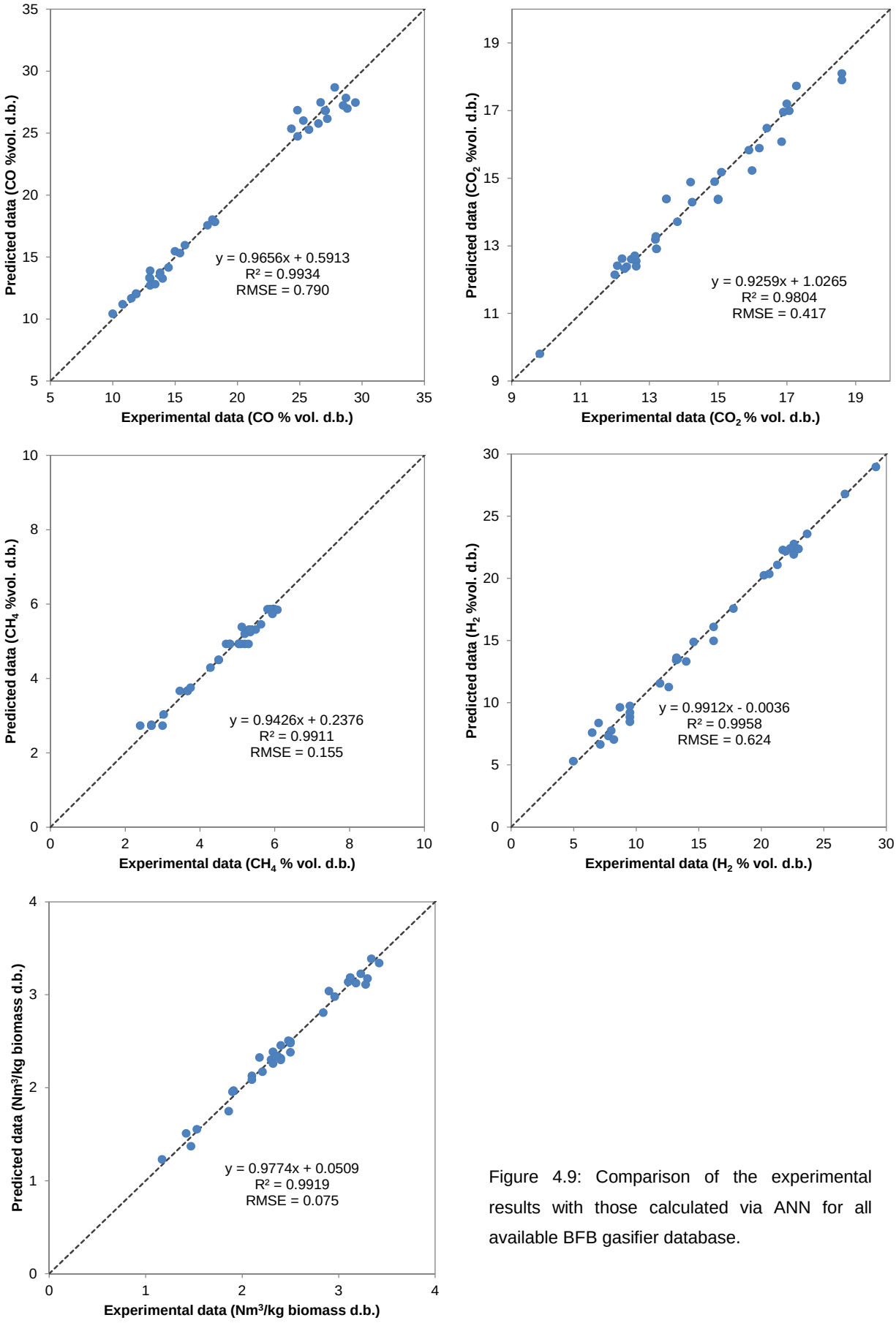


Figure 4.9: Comparison of the experimental results with those calculated via ANN for all available BFB gasifier database.

Table 4.6: Weights and biases of the designed ANNs for the four major gas species of producer gas (CO, $CO_2$, $H_2$, $CH_4$) and producer gas yield for BFB gasifier ANN model.

| | | | | | | | |
|---|---|---|---|---|---|---|---|
| **CO** | | | | | | | |
| **$IW_{i,j}$** | | | | | | | |
| -0.9005 | -22.8979 | 0.3383 | -10.2693 | 13.9051 | -0.5125 | 1.2177 | -1.6145 |
| -4.0218 | -2.0805 | -0.6249 | -1.9391 | -1.0988 | 0.6812 | -0.1740 | 0.5222 |
| **$LW_{1,j}$** | | | **$b1_j$** | | **b2** | | |
| -33.7782 | -39.6833 | | 15.6788 | | 12.3524 | | |
| | | | 3.6788 | | | | |
| **$CO_2$** | | | | | | | |
| **$IW_{i,j}$** | | | | | | | |
| 8.6144 | -1.1591 | -9.1504 | 4.1321 | -0.7413 | -12.6004 | 1.6067 | 4.8547 |
| -0.4782 | 3.9688 | -5.2829 | 1.2131 | 18.4774 | -3.4298 | -6.4298 | 7.5909 |
| **$LW_{1,j}$** | | | **$b1_j$** | | **b2** | | |
| 3.5726 | -2.6414 | | 4.4389 | | 13.4535 | | |
| | | | -5.3372 | | | | |
| **$CH_4$** | | | | | | | |
| **$IW_{i,j}$** | | | | | | | |
| -27.6038 | 30.0594 | -31.5068 | -31.9344 | 49.1297 | 85.5683 | 10.8387 | 1.0029 |
| -56.8348 | -245.3845 | 194.6359 | -29.1672 | 243.0979 | 158.8235 | -82.2433 | 103.3151 |
| **$LW_{1,j}$** | | | **$b1_j$** | | **b2** | | |
| -0.4665 | -1.0988 | | -28.9205 | | 4.2972 | | |
| | | | -79.8145 | | | | |
| **$H_2$** | | | | | | | |
| **$IW_{i,j}$** | | | | | | | |
| -2.6766 | 3.3581 | -1.7070 | 0.7123 | -1.0042 | -1.4738 | -0.0854 | 2.3963 |
| 1.0173 | 0.0697 | 3.1264 | 1.8738 | 0.1026 | 1.6956 | 5.1339 | -6.0746 |
| **$LW_{1,j}$** | | | **$b1_j$** | | **b2** | | |
| 13.8413 | 8.0323 | | -1.3738 | | 13.6191 | | |
| | | | -0.7616 | | | | |
| **Producer gas yield** | | | | | | | |
| **$IW_{i,j}$** | | | | | | | |
| -5.3707 | -31.8927 | 4.4783 | -23.2472 | 19.3959 | 10.3177 | 4.3555 | -12.2481 |
| -4.1585 | -10.9772 | 2.1819 | -5.8447 | 6.7403 | 4.6368 | 4.3425 | -1.4914 |
| **$LW_{1,j}$** | | | **$b1_j$** | | b**2** | | |
| -0.5422 | 1.2019 | | 22.8709 | | 1.7517 | | |
| | | | 6.0126 | | | | |

#### 4.3.3.1 Sensitivity analysis

The relative influence of the input variables was evaluated using Eq. 4.5 like for CFB gasifiers model. The relative importance of the different input variables for each ANN is shown in Figure 4.10. As can be seen, all of the variables have a strong effect on the different outputs (CO, CO2, H2, CH4 and producer gas yield). Variables that account for biomass composition (C, H, O) always represent, like in CFB model, more than 25% of the importance of all studied outputs. The importance of ER is reduced in all cases. However, ER and VB together represent around 20% of importance in all cases except for CO.

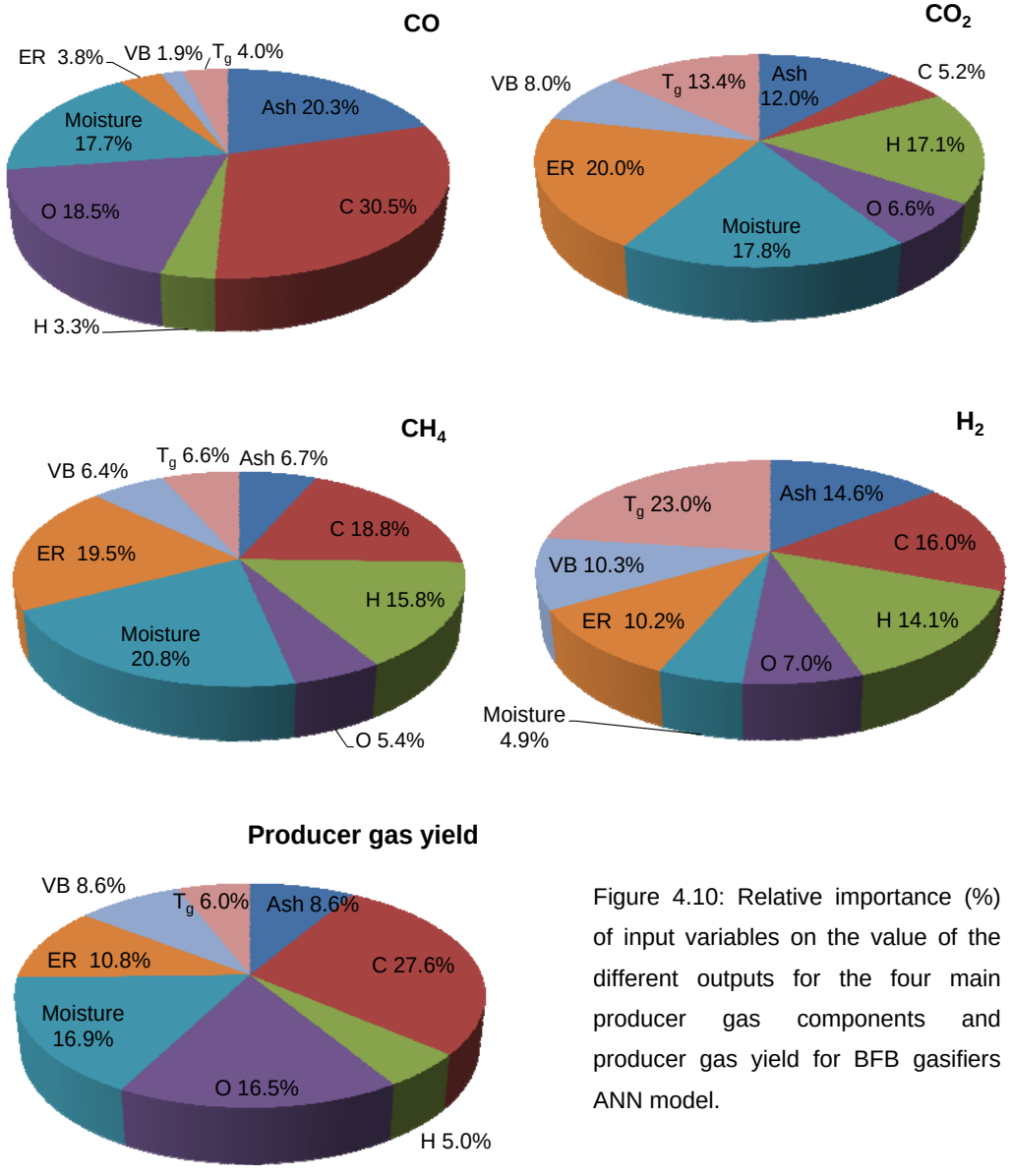


Figure 4.10: Relative importance (%) of input variables on the value of the different outputs for the four main producer gas components and producer gas yield for BFB gasifiers ANN model.

### 4.3.4 Comparison of obtained with ANN models and modified equilibrium model

Results presented in Section 4.3.2 show how the percentage composition of the main four gas species in producer gas and producer gas yield for a biomass CFB gasifier can be successfully predicted by applying a neural network with two hidden neurons in the hidden layer and using backpropagation algorithm. The results obtained by these ANNs show high agreement with published experimental data used: very good correlations ($R^2$>0.99) in all cases, except for $H_2$ ($R^2$>0.97), and small RMSEs.

These results obtained with applying ANNs for CFB gasifiers were compared with those found using the modified equilibrium model approach for the experimental data of Li et al. (2004) (Section 3.4.2). Table 4.7 shows the comparison of RMSE values obtained with both approaches. Clearly, the ANN model has a better adjustment with a reduction between 86 to 92.5% of the RMSE values.

Table 4.7: Comparison on RMSE values obtained by applying the modified equilibrium model developed vs. the ANN model for experimental data of a CFB gasifier from Li et al. (2004).

| **RMSE** | **CO** (%vol. d.b.) | **$CO_2$** (%vol. d.b.) | **$H_2$** (%vol. d.b.) | **$CH_4$** (%vol. d.b.) | **Producer gas yield** ($Nm^3$/kg biomass d.b.) |
|---|---|---|---|---|---|
| **Modified Equilibrium model** | 1.9 | 2.0 | 2.4 | - | 0.4 |
| **ANN Model** | 0.144 | 0.093 | 0.332 | 0.049 | 0.036 |

The ANN model developed for BFB gasifiers with the same topology than the one developed for CFB gasifiers also predicts with good agreement the percentage composition of the main four gas species in producer gas and producer gas yield. The results obtained by these ANNs also show high agreement with experimental published data used: very good correlations ($R^2$>0.99) in all cases, except for $CO_2$ ($R^2$ =0.98), and small RMSE values. If these results are compared with those found using the modified equilibrium model approach for Campoy (2009) experimental data (Section 3.4.2). Table 4.8 shows the comparison of RMSE values obtained with both approaches. The ANN model also presents a reduction between 62 to 82% of the RMSE.

Table 4.8: Comparison on RMSE values obtained by applying the modified equilibrium model developed vs. the ANN model for experimental data of a BFB gasifier from Campoy (2009).

| RMSE | CO (%vol. d.b.) | $CO_2$ (%vol. d.b.) | $H_2$ (%vol. d.b.) | $CH_4$ (%vol. d.b.) | Producer gas yield ($Nm^3$/kg biomass d.b.) |
|---|---|---|---|---|---|
| **Modified Equilibrium model** | 2.1 | 0.7 | 3.5 | - | 0.3 |
| **ANN Model** | 0.790 | 0.417 | 0.624 | 0.155 | 0.075 |

From the results presented in the present chapter, it can be concluded that ANN models clearly predict with better accuracy the producer gas composition and yield for fluidized bed gasifiers than equilibrium models. ANNs are useful when the primary goal is outcome prediction and important interactions of complex nonlinearities exist in a data set like in this case because they can approximate arbitrary nonlinear functions. However, model building in ANN refers to selecting the “optimal” network architecture, network topology, data representation, training algorithm, training parameters and terminating criteria, such that some desired level of performance is achieved. In addition, a large set of appropriate and representative experimental data that accounts for the variability that wants to be studied is also necessary.

## 4.4 CONCLUSIONS

This chapter has presented the fundamentals of ANN models and has proposed two ANN models, the former one for CFB gasifiers and the second one for BFB gasifiers. These models can be further integrated in complex polygeneration energy plants models.

ANNs are useful when the primary goal is outcome prediction and important interactions of complex nonlinearities exist in a data set like in this case, because they can approximate arbitrary nonlinear functions. However, model building in ANN refers to selecting the “optimal” network architecture, network topology, data representation, training algorithm, training parameters and terminating criteria, such that some desired level of performance is achieved. In addition, a large set of appropriate and representative experimental data that accounts for the variability that wants to be studied is also necessary.

Both ANN models developed present the same topology that was determined through a procedure of trial and error. Each model is composed by five ANNs to determine the four major gas species of producer gas (CO, $CO_2$, $H_2$, $CH_4$) and producer gas yield. Each ANN has a single hidden layer with 2 neurons and an output layer with one neuron. Each ANN was trained using the Lavenberg-Marquadt backpropagation algorithm, implemented in the Matlab neural network toolbox. The “tansig” transfer function was used as the activation function for the hidden layer and the “purelin” transfer function was used for the output layer. The performance of each ANNs was statistically measured by the root mean square error (RMSE) and regression coefficient ($R^2$), which were calculated with the experimental values and network predictions.

The values of $R^2$ for all cases, in both models, are higher than 0.99 except $H_2$ for CFB model (0.977) and $CO_2$ for BFB (0.98). RMSE values are very low and were compared with those obtained by applying the modified equilibrium model developed in Chapter 3. For ANN BFB model RMSE values are between 62 and 82% lower than the ones obtained with the other approach. However, for ANN CFB model, this reduction increases up to 86 to 92.5 %. In addition, both models have passed the intercept and slope statistical test with 99.8% of confidence level.

Considering that it is very scarce the literature that can be found on ANN models for biomass gasifiers, this chapter provides a good approach of the great potential of this kind of models in this field. Especially considering the complexity of biomass gasification that includes many interdependent chemical reactions. However, ANN models need a large experimental database to be trained and they are not independent of the reactor design like thermodynamic equilibrium models. ANN models are limited to a specified range of operating conditions for which they were trained.

# Chapter 5

# Development and validation of a simplified model for absorption chillers

## 5.1 INTRODUCTION

Absorption chillers are a key element in trigeneration plants. For this reason, to model the whole biomass gasification trigeneration plant, it is necessary to have a model for the absorption chiller. However, complete thermodynamic models of thermal chillers have many equations with a non-linear structure that has hindered their use in detailed energy simulation and optimisation programmes.

In this chapter, different approaches to model absorption chillers are reviewed and special attention is paid to two approaches of the characteristic equation method. They are studied and compared to see which one best fits the catalogue and experimental data of thermal chillers. In addition, a modified second approach of the characteristic equation is proposed and evaluated. Finally, a model that allows reducing the operating characteristics of absorption chillers into easier to handle simple algebraic equations is given.

## 5.2 ABSORPTION CHILLERS CONCEPTS

Absorption chillers can be activated with recovered heat in several forms (hot water, steam, thermal oil, exhausts gases, etc.). The available capacities range from few kW up to 6 MW. The working principle of an absorption system is similar to that of a mechanical compression system with respect to the refrigerant path through the evaporator and condenser. The compression of the vapour is carried out by means of a "heat driven" compression cycle consisting of two main components, absorber and generator (see Figure 5.1).

Absorption cooling systems always work with a mixture, i.e. a working pair, consisting of a volatile component (refrigerant) and an absorbent. The most common working pairs are Water (refrigerant) / Lithium Bromide (absorbent) and Ammonia (refrigerant) / Water (absorbent). These two main types of mixtures are applied mainly according to the required chilled temperature, the available waste heat or the cooling media for the absorber-condenser (using a cooling tower or an air cooler):

- Chilled temperature > 5 °C: Water / Lithium Bromide (LiBr) absorption chiller.
- Chilled temperature < 5 °C: Ammonia / Water absorption chiller.

The simplest design of an absorption chiller (single-effect, Figure 5.1) consists of an evaporator, a condenser, an absorber, a generator, a solution heat exchanger and a solution pump. The basic cooling cycle is the same for the absorption and electric chillers. Both systems use a low-temperature liquid refrigerant that absorbs heat from the water to be cooled and converts to a vapour phase (in the evaporator section). The refrigerant vapours are then compressed to a higher pressure (by a compressor or a generator), converted back into a liquid by rejecting heat to the external surroundings (in the condenser section), and then expanded to a low- pressure mixture of liquid and vapour (in the expander section) that goes back to the evaporator section and the cycle is repeated.

The basic difference between the electric chillers and absorption chillers is that an electric chiller uses an electric motor for operating a compressor used for raising the pressure of refrigerant vapours and an absorption chiller uses heat for compressing refrigerant vapours to a high-pressure. The rejected heat from the power-generation

equipment (e.g. turbines, micro turbines, and engines) may be used with an absorption chiller to provide the cooling in a CHP system.

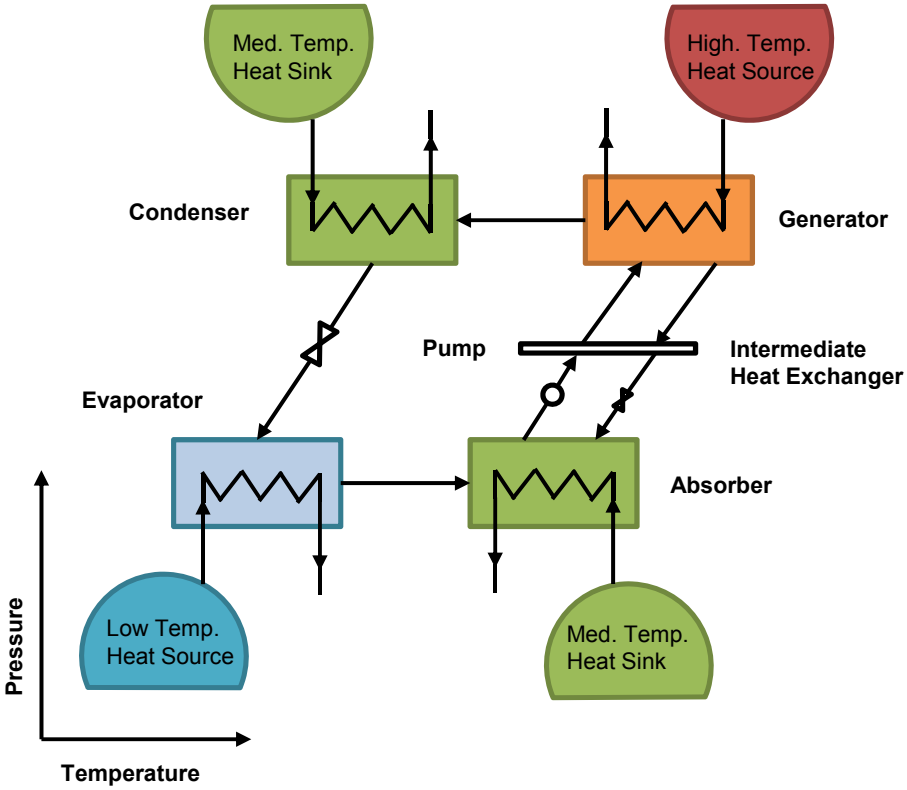


Figure 5.1: Schematic diagram of a single-effect absorption chiller

A more efficient configuration is the double-effect absorption chiller (Figure 5.2). The easiest way to describe this cycle is to consider two single-effect cycles staged on top of each other. The cycle on top is driven either directly by a natural gas or oil burner, or indirectly by steam or exhaust gases. Heat is added to the generator of the topping cycle (primary generator), which generates refrigerant vapour at a relatively higher temperature and pressure. The vapour is then condensed at this higher temperature and pressure and the heat of condensation is used to drive the generator of the bottoming cycle (secondary generator), which is at a lower temperature.

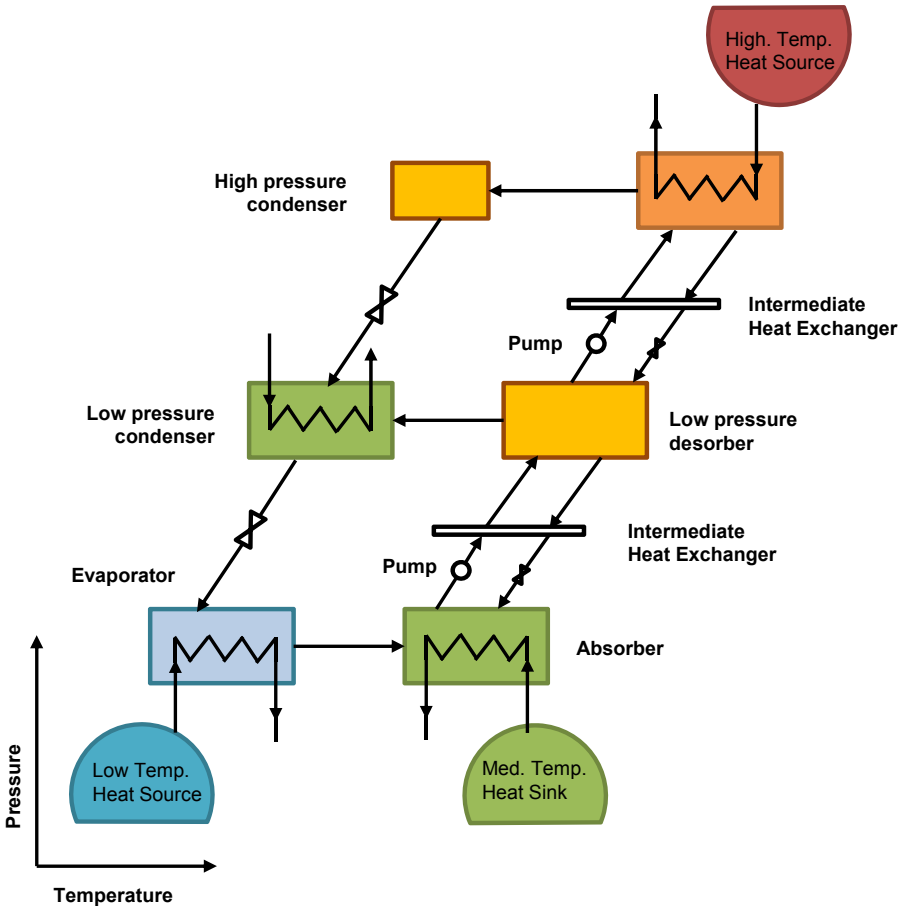


Figure 5.2: Schematic diagram of a double-effect absorption chiller.

## 5.3 ABSORPTION CHILLERS MODELLING

Several complete thermodynamic models of thermal chillers are available (Ng et al., 1997 and 1999; Chua et al., 2000; Gordon and Ng, 2005; Sathyabhama and Babu, 2008). However, they have many equations with a non-linear structure that make them not suitable for integration in energy simulation and optimisation programmes. For this reason, several authors have worked in reducing the operating characteristics of absorption chillers into easier to handle simple algebraic equations.

In this sense, Kim and Infante Ferreira (2008) presented a model capable of describing the behaviour of absorption cycles with a convenient number of characteristic constants for quick simulation of absorption systems. Though this model has been applied to several examples of single-effect absorption chillers using various aqueous

working fluids, it may not adapt well enough to reproduce the performance of commercial or experimental chillers. With current artificial neural network models it is possible to calculate the performance of several types of absorption chillers in order to avoid the complexity of rigorous thermal chiller models (Sencan et al., 2006; Manohar et al., 2006). This approach does not require prior thermodynamic modelling to estimate chiller performance. However, it calls for a large number of experimental data at different operating conditions to train the ANN that it is not easy to obtain.

Several authors have proposed other approaches based on the characteristic equation model to describe the performance characteristics of absorption chillers. This model uses a characteristic equation approach (Hellman et al., 1999) that has been used to fit catalogue data (Hellman and Ziegler, 1999) or experimental data (Kühn and Ziegler 2005) and to calculate the optimal operating temperature for solar cooling systems (Lecuona et al., 2008). With this approach, both the cooling capacity and the COP of the chiller are expressed as functions of the external heat exchanger fluid temperatures combined in the so-called characteristic temperature difference ($\Delta\Delta t$). The characteristic equation predicts the part load behaviour of absorption chillers and avoids the need for extensive numerical simulations of the internal thermodynamic cycle.

Two approaches to the characteristic equation method are analysed in the following section: the one proposed by Hellmann et al. (1999), which is a simple model using energy balances, relations describing heat and mass transfer characteristics, and the thermophysical properties of the working fluids. This approach is also applied and extended in the Solac Computer Design Tool (Albers, 2002), where the characteristic equation method was applied to each component of the chiller rather than to just one characteristic equation for the whole absorption chiller; and the one presented by Kühn and Ziegler (2005), which is an adaptation of the characteristic equation method in which the authors define an arbitrary characteristic temperature function and a linear characteristic equation to carry out a numerical fit of the experimental data.

### 5.3.1 Basics of the characteristic equation method

Here, the basics of the characteristic equation method are presented for describing the performance of absorption chillers and the approaches used so far to implement this method.

A simple model to describe the performance characteristics of absorption chillers, based on the earlier works of other authors, was proposed in Hellmann et al. (1999). The heat transfer equations (which implicitly also include the internal mass transfer) in the four major components relate the transferred heat loads to the driving temperature differences encountered in the heat exchangers:

$$\begin{aligned}\dot{Q}_E &= UA_E \cdot \omega_E \cdot (T_E - \tau_E)\\ \dot{Q}_C &= UA_C \cdot \omega_C \cdot (\tau_C - T_C)\\ \dot{Q}_A &= UA_A \cdot \omega_A \cdot (\tau_A - T_A)\\ \dot{Q}_G &= UA_G \cdot \omega_G \cdot (T_G - \tau_G)\end{aligned} \qquad \text{Eq. 5.1}$$

The internal temperatures of the four heat exchangers can be combined using Dühring's rule for the dissolution field of aqueous lithium bromide:

$$\tau_G - \tau_A = B \cdot (\tau_C - \tau_E) \qquad \text{Eq. 5.2}$$

Where *B* is an average solution concentration in the generator and the absorber, with a value of roughly 1.1 for single-effect $H_2O$/LiBr absorption chillers. By combining Eq. 5.1 and Eq. 5.2, it is possible to determine the relation between the external temperatures:

$$\frac{\dot{Q}_G}{UA_G \cdot \omega_G} + \frac{\dot{Q}_A}{UA_A \cdot \omega_A} + B \cdot \left( \frac{\dot{Q}_C}{UA_C \cdot \omega_C} + \frac{\dot{Q}_E}{UA_E \cdot \omega_E} \right) = T_G - T_A - B \cdot (T_C - T_E) = \Delta\Delta t \qquad \text{Eq. 5.3}$$

This equation indicates the total of the heat flows exchanged between an absorption chiller and the ambient scale with a characteristic temperature difference $\Delta\Delta t$. When a serial flow from the absorber to the condenser with a constant mass flow rate is assumed, Eq. 5.3 is not appropriate for specifying the actual operating conditions

because the absorber outlet temperature is not commonly specified in the manufacturers' data. Therefore, the characteristic temperature difference is reduced to:

$$\Delta\Delta t = T_G - T_{AC} - B \cdot (T_{AC} - T_E) \quad \text{Eq. 5.4}$$

$$T_{AC} = \frac{1}{2} \cdot (T_{cw,in} + T_{cw,o}) \quad \text{Eq. 5.5}$$

To eliminate the heat loads of the generator, absorber and condenser from Eq. 5.3, the energy balances of the four major components are introduced Eq. 5.6:

$$\dot{Q}_E = \dot{m}_{refr} \cdot (h_{vaporE} - h_{liquidC})$$

$$\dot{Q}_C = \dot{m}_{refr} \cdot (h_{vaporG} - h_{liquidC}) \quad \text{Eq. 5.6}$$

$$\dot{Q}_A = \dot{m}_{refr} \cdot h_{vaporE} + \dot{m}_{strong} \cdot h_{strongG} - \dot{m}_{weak} \cdot h_{weakA} - Q_{hex}$$

$$\dot{Q}_G = \dot{m}_{refr} \cdot h_{vaporG} + \dot{m}_{strong} \cdot h_{strongG} - \dot{m}_{weak} \cdot h_{weakA} - Q_{hex}$$

where $Q_{hex}$ stands for the heat exchanged in the solution heat exchanger between the strong and the weak solution streams. The heat loads of the condenser, absorber and generator can be expressed as function of the evaporator load as follows (Eq. 5.7):

$$\dot{Q}_C = \frac{h_{vaporG} - h_{liquidC}}{h_{vaporE} - h_{liquidC}} \cdot \dot{Q}_E = C' \cdot \dot{Q}_E$$

$$\dot{Q}_A = \frac{h_{vaporE} - h_{strongG}}{h_{vaporE} - h_{liquidC}} \cdot \dot{Q}_E + m_{weak} \cdot (h_{strongG} - h_{weakA}) - Q_{hex} = A' \cdot \dot{Q}_E + \dot{Q}_{loss} \quad \text{Eq. 5.7}$$

$$\dot{Q}_G = \frac{h_{vapor\,G} - h_{strongG}}{h_{vaporE} - h_{liquidC}} \cdot \dot{Q}_E + m_{weak} \cdot (h_{strongG} - h_{weakA}) - Q_{hex} = G' \cdot \dot{Q}_E + \dot{Q}_{loss}$$

Where $Q_{loss}$ is an equivalent for the solution heat exchanger loss, that is, the heat that is required in the generator for heating and that is rejected in the absorber for cooling the solution streams to the appropriate internal equilibrium temperatures. After

substituting these heat loads in Eq. 5.3, simple expressions to calculate the cooling capacity and the COP are obtained (Eq. 5.8-5.12):

$$\dot{Q}_E = s \cdot \Delta\Delta t - \alpha \cdot \dot{Q}_{loss} = s \cdot (\Delta\Delta t - \Delta\Delta t_{\min}) \quad \text{Eq. 5.8}$$

$$COP = \frac{\dot{Q}_E}{\dot{Q}_G} = \frac{\dot{Q}_E}{G' \cdot \dot{Q}_E + \dot{Q}_{loss}} = \frac{\Delta\Delta t - \Delta\Delta t_{\min}}{G' \cdot \Delta\Delta t + \left(\frac{1}{\alpha} - G'\right) \cdot \Delta\Delta t_{\min}} \quad \text{Eq. 5.9}$$

with:

$$s = \frac{1}{\frac{G'}{UA_G \cdot \omega_G} + \frac{A'}{UA_A \cdot \omega_A} + B \cdot \left(\frac{C'}{UA_C \cdot \omega_C} + \frac{1}{UA_E \cdot \omega_E}\right)} \quad \text{Eq. 5.10}$$

$$\alpha = \frac{\frac{1}{UA_G \cdot \omega_G} + \frac{1}{UA_A \cdot \omega_A}}{\frac{G'}{UA_G \cdot \omega_G} + \frac{A'}{UA_A \cdot \omega_A} + B \cdot \left(\frac{C'}{UA_C \cdot \omega_C} + \frac{1}{UA_E \cdot \omega_E}\right)} \quad \text{Eq. 5.11}$$

$$\Delta\Delta t_{\min} = \frac{\alpha}{s} \cdot \dot{Q}_{loss} = \left(\frac{1}{UA_G \cdot \omega_G} + \frac{1}{UA_E \cdot \omega_E}\right) \cdot \dot{Q}_{loss} \quad \text{Eq. 5.12}$$

The parameter $\Delta\Delta t_{min}$ may be interpreted as the minimum driving temperature difference required to overcome the solution heat exchanger loss before the chiller can start to produce cold.

Hellmann et al. (1999) concluded that *B, s, α* and *G'* can be regarded as constant and independent of $\Delta\Delta t$, but not $\Delta\Delta t_{min}$ because it varies significantly, between 1.7 and 7.2, with $\Delta\Delta t$. They attributed this variation to the fact that $Q_{loss}$ varies considerably with the load, in their case, between 6 kW and 26 kW approximately, for a chiller with a maximum capacity of 70kW. The introduction of a linear correlation between $\Delta\Delta t_{min}$ and $\Delta\Delta t$ improved the accuracy of the model. In another study, Hellmann and Ziegler (1999) kept parameters *α* and *G'* constant and found that the results were much better and the deviations were below 5% if they correlated both the slope *s* and $\Delta\Delta t_{min}$ linearly

to the difference of the arithmetic mean temperatures of the cooling and chilled water (Eq. 5.13-5.14).

$$s = s_I + s_{II}.(T_{AC} - T_E)$$ Eq. 5.13

$$\Delta\Delta t_{\min} = r_I + r_{II}.(T_{AC} - T_E)$$ Eq. 5.14

#### 5.3.1.1 First approach to the characteristic equation method

In this first approach to the characteristic equation method two different ways of solving the set of equations, depending on the available information, were used:

- Hellman et al. (1999) determined the average values of the characteristic parameters *B, s, α, $\Delta\Delta t_{min}$* and *G'* required in the model using the following known design data: UA-values, weak solution flow rate and the external heat carrier flow rates for a $H_2O$/LiBr absorption chiller.
- The Solac Computer Design Tool (Albers, 2002) uses the same definition for *$\Delta\Delta t$* (Eq. 5.4) but proposes an equation for each main heat exchanger:

$$Q_u = s_u \cdot \Delta\Delta t - s_u \cdot \Delta\Delta t_{\min_u}$$ Eq. 5.15

where the subindex *u* corresponds to the different heat exchanger units (Evaporator, Generator, Absorber and Condenser). The external outlet temperatures of the heat exchangers can be calculated using the following equation:

$$T_{u,o} = 2 \cdot T_u - T_{u,in}$$ Eq. 5.16

Indexes *in* and *o* stand for input and output, respectively. Eq. 5.17 also needs to be used for external energy balances:

$$Q_u = 2 \cdot m_u \cdot Cp_u \cdot (T_{u,in} - T_u)$$ Eq. 5.17

A four-dimensional, linear equation system must be solved (Eq. 18):

$$\begin{aligned}
&\Delta\Delta t - T_G - B\cdot T_E + (1+B)\cdot T_{AC} = 0\\
&s_E\cdot\Delta\Delta t + 2\cdot m_E\cdot Cp_E\cdot T_E = 2\cdot m_E\cdot Cp_E\cdot T_{E\,in} + s_E\cdot\Delta\Delta t_{\min E}\\
&s_G\cdot\Delta\Delta t + 2\cdot m_G\cdot Cp_G\cdot T_G = 2\cdot m_G\cdot Cp_G\cdot T_{G\,in} + s_G\cdot\Delta\Delta t_{\min G}\\
&s_{AC}\cdot\Delta\Delta t - 2\cdot m_{AC}\cdot Cp_{AC}\cdot T_{AC} = -2\cdot m_{AC}\cdot Cp_{AC}\cdot T_{AC\,in} + s_{AC}\cdot\Delta\Delta t_{\min AC}
\end{aligned}$$ Eq. 5.18

The values for the slope ($s_u$) and the axis interval ($\Delta\Delta t_{minu}$) can be determined from only two reference operation data points under steady state conditions that can be taken from the manufacturers' specifications. To reduce the non-compliance of simulated data with the manufacturers' data and because the linearity assumptions required are not exactly true for real processes, the characteristic parameters are not taken as constant but as linear functions of $\Delta t_{ACE} = T_{AC} - T_E$.

$$\begin{aligned}
&Q_E = s_E(\Delta t_{ACE})\cdot\Delta\Delta t - s_E(\Delta t_{ACE})\cdot\Delta\Delta t_{\min E}(\Delta t_{ACE})\\
&Q_G = s_G(\Delta t_{ACE})\cdot\Delta\Delta t - s_G(\Delta t_{ACE})\cdot\Delta\Delta t_{\min G}(\Delta t_{ACE})\\
&Q_{AC} = s_{AC}(\Delta t_{ACE})\cdot\Delta\Delta t - s_{AC}(\Delta t_{ACE})\cdot\Delta\Delta t_{\min AC}(\Delta t_{ACE})\\
&s_u(\Delta t_{ACE}) = s_{uI}\cdot\Delta t_{ACE} + s_{uII}\\
&\Delta\Delta t_{\min u}(\Delta t_{ACE}) = r_{uI}\cdot\Delta t_{ACE} + r_{uII}
\end{aligned}$$ Eq. 5.19

To find values $s_{ul}$, $s_{ull}$, $r_{ul}$, $r_{ull}$ to determine the characteristic parameters ($s_u$ and $\Delta\Delta t_{minu}$), four reference operation points must be evaluated from the manufacturers' data instead of two.

#### 5.3.1.2 Second approach to the characteristic equation method

In this approach, described by Kühn and Ziegler (2005), a numerical fit was carried out to improve the results of the characteristic equation method. These authors used the following arbitrary characteristic temperature function (Eq. 5.20):

$$\Delta\Delta t' = T_G - a'\cdot T_{AC} + e'\cdot T_E$$ Eq. 5.20

They also defined a linear characteristic equation (Eq. 5.21):

$$\dot{Q}_E = s'\cdot\Delta\Delta t' + r'$$ Eq. 5.21

Insertion of *ΔΔt'* in the characteristic equation yields Eq. (5.22):

$$\dot{Q}_E = s' \cdot T_G - s' \cdot a' \cdot T_{AC} + s' \cdot e' \cdot T_E + r' \qquad \text{Eq. 5.22}$$

### 5.3.2 Comparison of the two approaches

The approaches considered above have been compared using the data for a solar-powered water/LiBr absorption chiller reported by Gommed and Grossman (1990) in order to evaluate which one is the best.

#### 5.3.2.1 First approach

In the first approach to the characteristic equation method, as has been mentioned above, there are two different ways of solving the set of equations, depending on the available information:

The first method of solving the set of equations, developed by Hellman et al. (1999), was evaluated by the same authors using data published by Gommed and Grossman (1990) of a solar-powered water/lithium bromide absorption chiller based on a physical-mathematical model and design data ($U_{AE}$=11.9 kW/K, $U_{AC}$=17.9 kW/K, $U_{AA}$=6.1 kW/K, $U_{AG}$=8.5 kW/K, $U_{Ahex}$=2.0 kW/K, $m_{weak}$=0.45 kg/s, $m_{hw}$=3.2 kg/s, $m_{cwC}$=4.0 kg/s, $m_{cwA}$=3.7 kg/s, $m_{ch}$=2.3 kg/s). The authors used the results to predict the part load behaviour of the absorption chiller studied while considering some parameters as constants: *B*=1.15, *s*=2.14 kW/K, *α*=0.61, *G'*=1.04, $\Delta\Delta t_{min}$=3K. Thus, they concluded that *B, s, α* and *G'* can be regarded as constant and independent of *ΔΔt*, but not of $\Delta\Delta t_{min}$. They introduced a linear correlation between $\Delta\Delta t_{min}$ and *ΔΔt* ($\Delta\Delta t_{min} \approx$ 1.9 K + 0.1• *ΔΔt*) that improved the accuracy of the model. These two parameters (1.9K and 0.1) are fit parameters and cannot be related to any physical quantity involved. Figure 5.3 represents the cooling capacity published by Gommed and Grossman (1990) versus the fitted cooling capacity calculated using this first approach with $\Delta\Delta t_{min}$ = 3K as well as with the linear correlation between $\Delta\Delta t_{min}$ and *ΔΔt* . The authors reported that introducing the linear correlation improves the accuracy of the model because

when $\Delta\Delta t_{min}$ was constant, the deviations were mostly below 20% and with the linear correlation between $\Delta\Delta t_{min}$ and $\Delta\Delta t$, deviations are always below 15%.

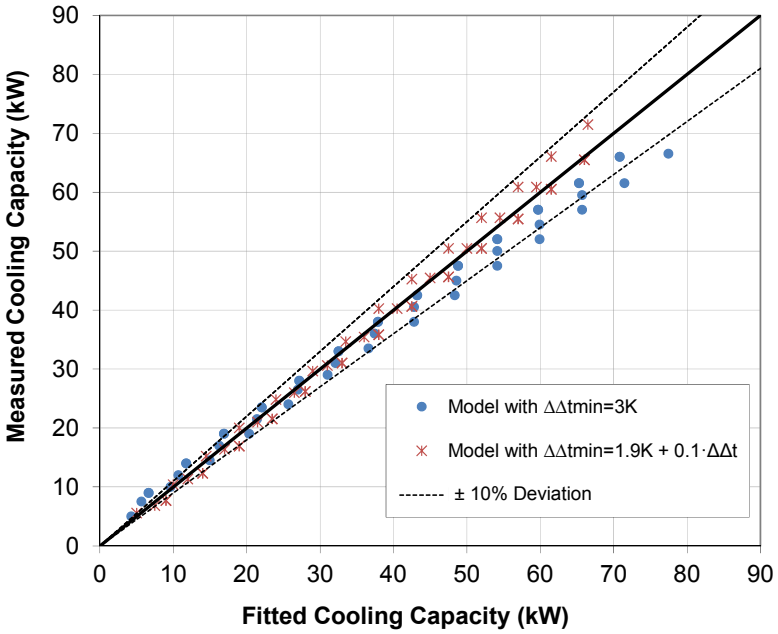


Figure 5.3: Cooling capacity published by Gommed and Grossman (1990) versus fitted cooling capacity calculated with $\Delta\Delta t_{min} = 3K$ and with a linear correlation between $\Delta\Delta t_{min}$ and $\Delta\Delta t$ using the first approach for the characteristic equation method.

When the design data is not available from the manufacturer it is possible to use the solving method proposed in the Solac Computer Design Tool (Albers, 2002) which uses the same definition for $\Delta\Delta t$ and proposes an equation for each main heat exchanger. As described previously, when the slope ($s_u$) and the axis interval ($\Delta\Delta t_{minu}$) are considered constant they can be determined from Eq. 5.18 with only two reference operation data points under steady state conditions. However when the characteristic parameters are not taken as constant but as linear functions of $\Delta t_{ACE}$ to determine the characteristic parameters ($s_u$ and $\Delta\Delta t_{minu}$) from Eq. 5.19 four reference operation points must be evaluated from the manufacturers' data instead of two.

Considering $s_u$ and $\Delta\Delta t_{minu}$ as constants, Eq. 5.18 was solved using two points from the data published by Gommed and Grossman (1990). In addition to this, two groups of points were arbitrarily chosen to study how selection of the experimental points influences the results (Table 5.1). The results obtained after solving the system of equations with EES (EES, 2010) are shown in Table 5.1 where it can be observed that

the values for parameters $s_E$, $\Delta\Delta t_{minE}$, $s_G$ and $\Delta\Delta t_{minG}$ depended strongly on the set of selected points. With these parameters, the values of $Q_E$ were calculated for different values of $\Delta\Delta t$ using published data. Then, the calculated values of $Q_E$ were compared with the real values of $Q_E$ published by Gommed and Grossman (1990) (Figure 5.4). As Figure 5.4 shows, the results obtained depend on the arbitrary group of data points selected. Similar results were obtained after solving the system of equations Eq. 5.19 using four points. To study the effect of the selection of these points, eight points, distributed in two groups, were selected (Table 5.2). The system of equations was not easy to solve because more than one solution is possible. Figure 5.5 shows the best solution found for each group of points using the data from Gommed and Grossman (1990).

Table 5.1: Chosen points from data published by Gommed and Grossman (1990) to solve equation system in Eq. 5.18 and results obtained for $s_E$ and $\Delta\Delta t_{minE}$.

| | 1st Group of points | | 2nd Group of points | |
|---|---|---|---|---|
| | 1' | 2' | 3' | 4' |
| $Q_E$ (kW) | 26.50 | 40.50 | 66.00 | 38.00 |
| $Q_G$ (kW) | 38.97 | 56.64 | 86.28 | 57.14 |
| $\Delta\Delta t$ | 15.60 | 23.00 | 36.10 | 23.00 |
| **Results** | | | | |
| $s_E$ | 1.892 | | 2.137 | |
| $\Delta\Delta t_{minE}$ | 1.593 | | 5.221 | |
| $s_G$ | 2.388 | | 2.224 | |
| $\Delta\Delta t_{minG}$ | -0.7202 | | -2.696 | |

Table 5.2: Chosen points from data published by Gommed and Grossman (1990) to solve equation system in Eq. 5.19 and results obtained for $r_{EI}$, $r_{EII}$, $s_{EI}$ and $s_{EII}$.

| | 1st Group of points | | | | 2nd Group of points | | | |
|---|---|---|---|---|---|---|---|---|
| | 1' | 2' | 3' | 4' | 5' | 6' | 7' | 8' |
| $Q_E$ (kW) | 61.50 | 52.00 | 19.00 | 19.00 | 66.00 | 38.00 | 66.50 | 47.50 |
| $Q_G$ (kW) | 80.39 | 75.91 | 28.15 | 33.04 | 86.28 | 57.14 | 95.00 | 62.50 |
| $\Delta\Delta t$ | 33.50 | 31.00 | 10.90 | 12.50 | 36.10 | 23.00 | 39.20 | 25.80 |
| $\Delta t_{ACE}$ | 18.21 | 31.27 | 17.48 | 30.63 | 18.30 | 30.98 | 31.56 | 17.95 |
| **Results** | | | | | | | | |
| $r_{EI}$ | 0.08045 | | | | 0.1552 | | | |
| $r_{EII}$ | -0.5421 | | | | -3.241 | | | |
| $s_{EI}$ | -0.007378 | | | | -0.002783 | | | |
| $s_{minEII}$ | 2.022 | | | | 1.859 | | | |

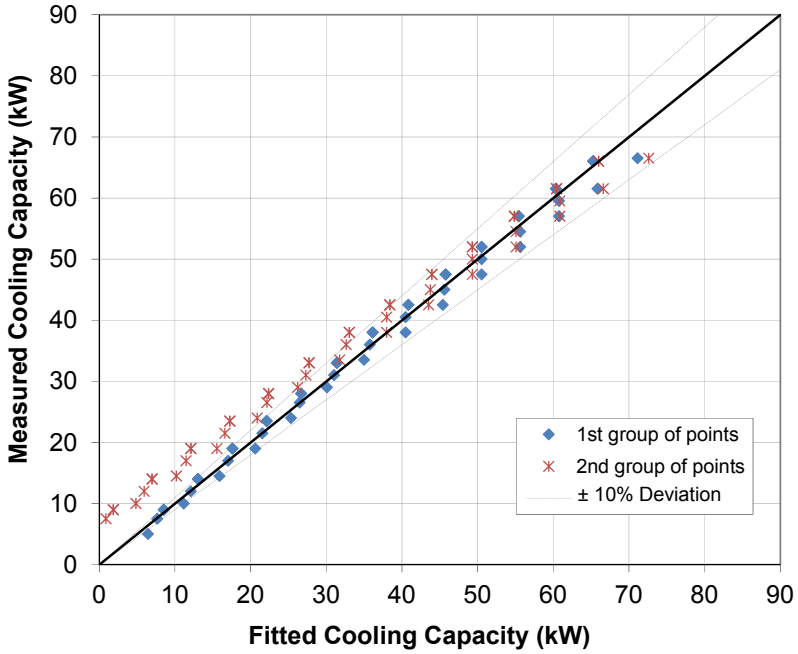


Figure 5.4: Cooling capacity published by Gommed and Grossman (1990) versus fitted cooling capacity for both values of $s_E$ and $\Delta\Delta t_{minE}$ using the first approach for the characteristic equation method.

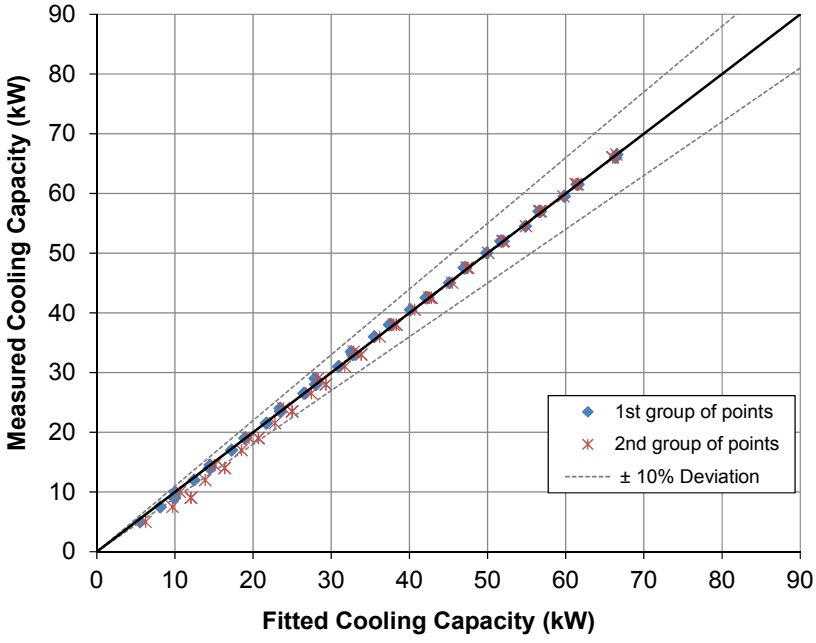


Figure 5.5: Cooling capacity (Gommed and Grossman, 1990) versus calculated cooling capacity for both values of $r_{EI}$ ,$r_{EII}$ ,$s_{EI}$ and $s_{EII}$. using the first approach for the characteristic equation method.

The present obtained results confirm that this approach performs better with four points (non-constant values of $s_u$ and $\Delta\Delta t_{minu}$; non-linear model) than with only two (linear model). However, in both cases, the value of the characteristic parameters depended too much on the selected points. Another problem with this approach is how to solve the system of equations because, as more than one solution for each parameter is obtained, it is necessary to check which one fits best.

#### 5.3.2.2 Second approach

With this second approach no point selection is needed. The authors' procedure (Kühn and Ziegler, 2005) is followed, all measured points are used and an arbitrary characteristic temperature function ($\Delta\Delta t'$) as defined in Eq. 5.20. A multiregression fit was carried out with Microsoft Excel (2003) to calculate the value of the four parameters: *s', a', e'* and *r'* in Eq. 5.22. The multiple linear regression algorithm chooses regression coefficients to minimise the residual sum of squares. The numerical fit of the four parameters resulted in the following equations (Eq. 5.23) for the data published by Gommed and Grossman (1990):

$$\dot{Q}_E = 1.864 \cdot T_G - 4.2929 \cdot T_{AC} + 2.4295 \cdot T_E + 3.917 \qquad \text{Eq. 5.23}$$

$$\Delta\Delta t' = T_G - 2.3031 \cdot T_{AC} + 1.3034 \cdot T_E$$

The cooling capacity versus fitted cooling capacity, calculated using the previous expressions (Eq. 23), is given in Figure 5.6. In Figure 5.7, cooling capacity and driving heat are plotted as a function of $\Delta\Delta t'$.

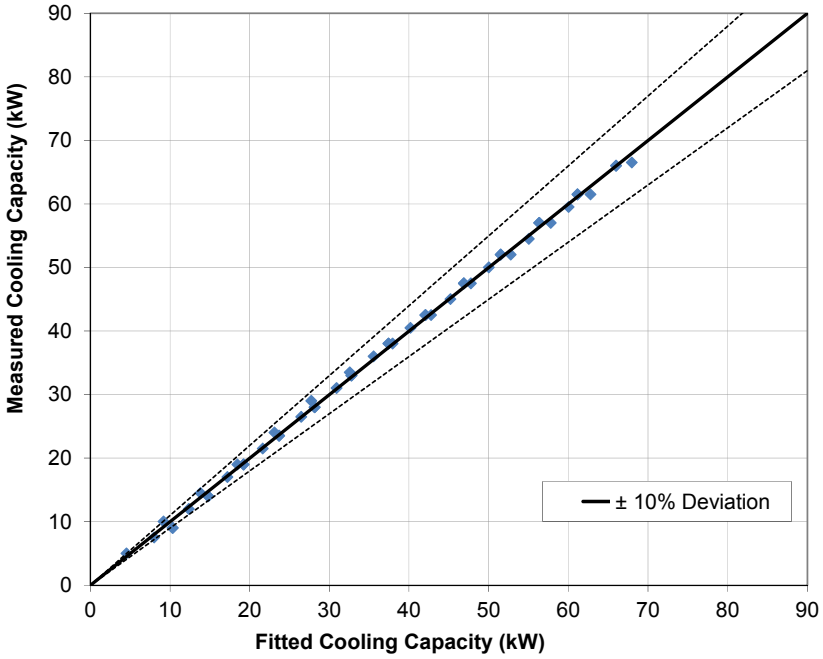


Figure 5.6: Cooling capacity (Gommed and Grossman, 1990) versus fitted cooling capacity calculated with the second approach for the characteristic equation method.

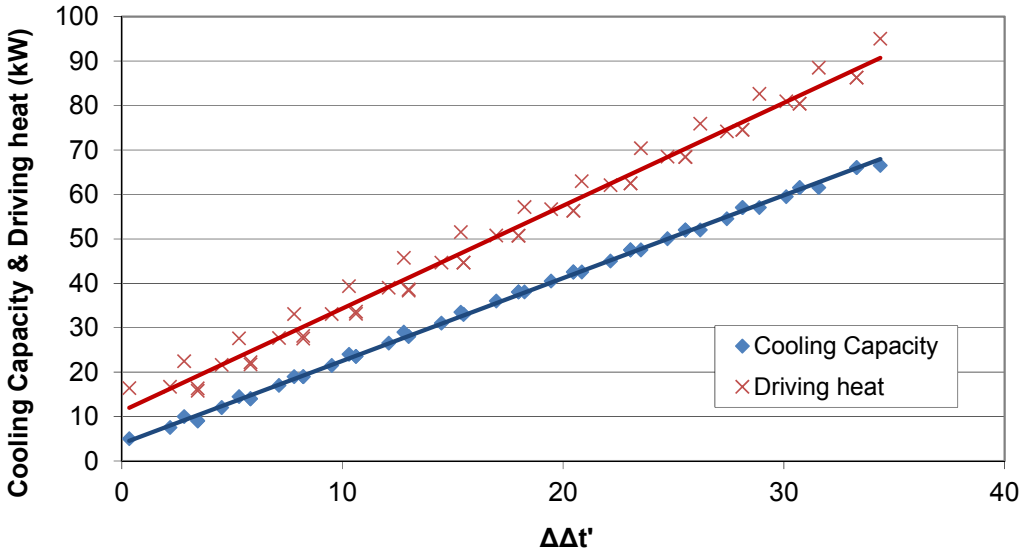


Figure 5.7: Cooling capacity and driving heat as function of *ΔΔt'* for the data from Gommed and Grossman (1990).

With this approach, almost all the data points were within the 10% deviation range (Figure 5.6) whereas with the first approach several points were out of this range (Figure 5.4). It was also observed that the cooling capacity versus $\Delta\Delta t$ had a greater deviation from the linear behaviour than when it was plotted against $\Delta\Delta t'$ (Figure 5.7). In Figure 5.7, the scatter is slightly larger for driving heat than for cooling capacity because the fit was not done for driving heat but for cooling capacity as already stated in Kühn and Ziegler (2005).

After studying these two approaches with the same data, it can be concluded that the second approach, the adaptation of the characteristic equation, is the simplest way to obtain an equation that is exact enough to be used for modelling the thermal chiller performance. This approach can be used to describe the behaviour of a chiller at design flow rates and different external temperatures with a simple linear equation.

In Puig-Arnavat et al. (2010) several cases where this second approach is applied to experimental and catalogue data of single-effect and double-effect absorption chillers of different capacities and manufacturers can be found.

### 5.3.3 Modifications of the second approach to the characteristic equation method

In the second approach, Kühn and Ziegler (2005) carried out a numerical fit to improve the results of the characteristic equation method. However, they use the external arithmetic mean temperature of the external flows of the absorption chiller ($T_G$, $T_{AC}$, $T_E$). When manufacturer's data is used, usually, the temperatures given by the manufacturer to characterise the part-load behaviour are $T_{inG}$, $T_{oE}$ and $T_{inAC}$. Albers and Ziegler (2008) suggested that if a linear part load behaviour is found for $\Delta\Delta t$, a linear behaviour should also be expected for modified characteristic temperature difference ($\Delta\Delta t^*$) when more often inlet and outlet temperatures are used:

$$\Delta\Delta t^* = T_{inG} - (1+B)\cdot T_{inAC} + B\cdot T_{oE} \qquad \text{Eq. 5.24}$$

Based on this study, and in order to get simpler and easier to obtain expressions, another characteristic equation function is proposed ($\Delta\Delta t''$) for the procedure of Kühn

and Ziegler (2005). This new funcion accounts for a combination of the temperatures usually given by the manufacturers in their catalogues:

$$\Delta\Delta t'' = T_{inG} - a''\cdot T_{inAC} + e''\cdot T_{oE} \qquad \text{Eq. 5.25}$$

Like Kühn and Ziegler (2005) did, a linear characteristic equation is also defined:

$$\dot{Q}_E = s''\cdot\Delta\Delta t'' + r'' \qquad \text{Eq. 5.26}$$

Insertion of *ΔΔt''* in the characteristic equation yields Eq. 5.26:

$$\dot{Q}_E = s''\cdot T_{inG} - s''\cdot a''\cdot T_{inAC} + s''\cdot e''\cdot T_{oE} + r'' \qquad \text{Eq. 5.27}$$

In order to check if this approach gives similar results than the one proposed by Khün and Ziegler (2005), both approaches (*ΔΔt'* and *ΔΔt''*) have been used to fit catalogue data from a commercial equipment. The commercial absorption chiller used is a single-effect hot-water-fired $H_2O$/LiBr 4.5 kW absorption chiller (Rotartica, 2006). Figure 5.8 presents the adjustment and obtained equations for *ΔΔt'* and Figure 5.9 presents the adjustment and obtained equations for *ΔΔt''*. From both figures it can be seen that both approaches give similar results. However, with *ΔΔt''* slightly better values for $R^2$ are obtained. For this reason, the present proposed approach will be used to characterise the absorption chiller in the biomass gasification trigeneration plant model.

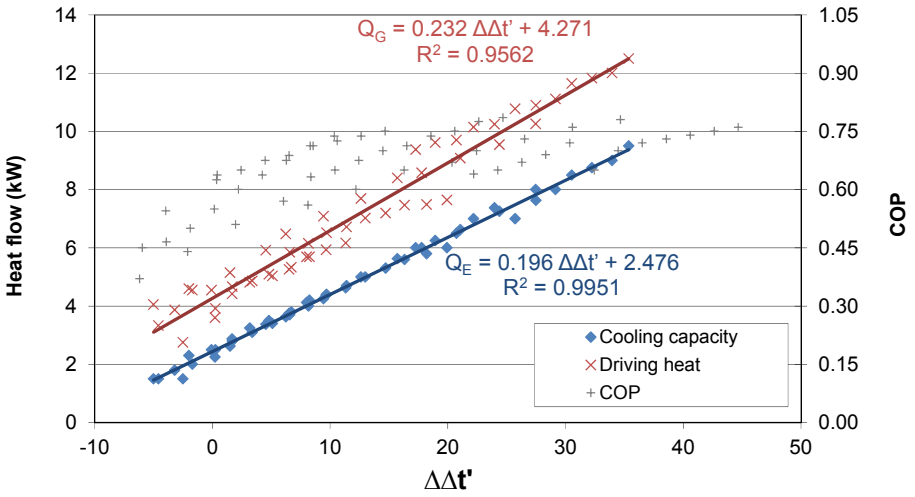


Figure 5.8: Catalogue cooling and driving heat capacity as function of *ΔΔt'* for a single effect $H_2O$/LiBr 4.5 kW absorption chiller.

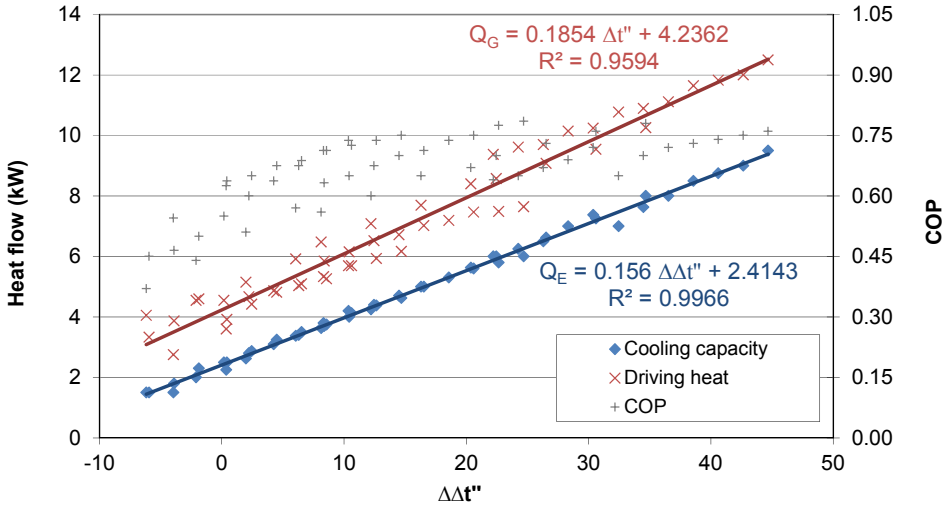


Figure 5.9: Catalogue cooling and driving heat capacity as function of *ΔΔt''* for a single effect $H_2O$/LiBr 4.5 kW absorption chiller.

## 5.4 CONCLUSIONS

Two approaches based on the characteristic equation method for describing the performance of absorption chillers have been studied. After comparing the results obtained using experimental data corresponding to the performance of a single-effect absorption chiller, it was concluded that the second approach—the adaptation of the characteristic equation method developed by Kühn and Ziegler (2005)—is the simplest and that it provides similar or better accuracy than the other approach, which has been implemented in some simulation programmes. The proposed characteristic equation method is an arbitrary characteristic temperature function where parameters are fitted according to a multiple regression fit. A variation of the characteristic equation method developed by Kühn and Zigler (2005) is also proposed. In this proposal instead of using the external arithmetic mean temperature of the external flows of the absorption chiller ($T_G$, $T_{AC}$, $T_E$), the temperatures usually given by the manufacturers to characterise the part-load behaviour are used ($T_{inG}$, $T_{oE}$ and $T_{inAC}$). This new approach permits to get simpler and easier to obtain expressions to characterise the part load behaviour of absorption chillers. The comparison of these two last approaches using catalogue data for a single-effect absorption chiller shows that they give very similar results in both cases.

As a result, it can be said that a new approach to the characteristic equation method, based on the previous work of Kühn and Zigler (2005), has been developed and can be used to model absorption chillers. This approach can be easily implemented using manufacturer's data of absorption chillers. It avoids both the use of unrealistic, overly simple models based on constant COP for different operating conditions and the use of highly complicated models that require a thorough knowledge of the chiller design parameters.

# Chapter 6

# Model of a biomass gasification trigeneration plant

## 6.1 INTRODUCTION

In Chapter 1 it was seen how little work has been done in the field of biomass gasification trigeneration plants neither in modelling nor in implementation. In Chapter 2 biomass gasification models were reviewed and in Chapter 3 and 4 a modified equilibrium model and an ANN model were developed for downdraft and fluidised bed gasifiers. Chapter 5 dealt with modelling of absorption chillers. In this chapter, all previously developed models are integrated in the model of a small-medium scale biomass gasification trigeneration plant (250 $kW_e$ - 2 $MW_e$).

The proposed trigeneration plant contains five main units: a gasifier, an internal combustion engine, heat exchangers for heat recovery, a clean-up section for producer gas and an absorption chiller. The modelling of the implemented units is presented. In addition, three different configurations which differ in how heat from exhaust gases and cooling water from the engine jacket is recovered and used are considered. Finally, these configurations are applied to a case study for the polygeneration plant ST-2 foreseen in Polycity project in Cerdanyola del Vallès (Barcelona).

## 6.2 MODEL OF A BIOMASS GASIFICATION TRIGENERATION PLANT

The objective of this section is to develop the model for a biomass gasification trigeneration plant that produces simultaneously heat, cold and electricity. The size of the plant is that of a small-medium scale trigereneration plant (250 $kW_e$ - 2 $MW_e$) that could be installed in a new urban development area to which it could supply its production. Considering that for a biomass gasification plant, the biomass fuel should come from the local area, as a long distance transport cannot be justified economically, bigger sizes are not recommended. The plant is designed to be fed with natural biomass (wood chips, almond shells…).

Heat and cold are assumed to be delivered to the district heating and cooling (DHC) that could supply different companies to be located in the surroundings of the plant. Electricity is assumed to be sold to the grid.

The whole plant consists of four sections: producer gas production, heat recovery, producer gas clean-up and producer gas utilisation. For this reason, the proposed trigeneration system contains the following main units: a gasifier, an internal combustion engine, which is the basic primary mover of the system; heat exchangers for heat recovery; a clean-up section and an absorption chiller.

The gasifier should be a downdraft or a fluidised bed atmospheric pressure gasifier operating with air as gasifying agent. Air is selected as the gasifying agent because it is the most economic option and gasifiers that use oxygen require an air separation unit to provide the gaseous/liquid oxygen and this is not cost-effective at small scales. Air gasification in downdraft and fluidised bed gasifiers has been previously modelled in Chapter 3 and 4. These models will define the producer gas that can be produced and then, for a fixed biomass fuel and gasification technology, the quantity and quality of this producer gas.

An internal combustion engine (ICE) has been selected as de producer gas utilisation unit because according to different authors (Kurkela, 2006; Baratieri et al., 2009; Yong, 2003) this is the recommended technology for this plant size. In addition, ICE is a mature technology that currently offers the higher reliability and has been successfully proven in several implemented biomass gasification plants.

Different types of absorption chillers are actually available in the market. For this reason, three different configurations of the trigeneration plant are proposed. Each configuration integrates a different type of absorption chiller: single-effect hot water, double-effect steam or double-effect exhaust gases driven absorption chiller.

Figure 6.1, Figure 6.2 and Figure 6.3 show three generalized diagrams of the different modelled configurations for the trigeneration plant. Whilst heat and power are provided by the engine and producer gas and exhaust gases, refrigeration is obtained by using an absorption system. The system is operated in the following way: the biomass gasifier generates producer gas as a fuel. This producer gas needs to be cooled down before the cleaning system. For this reason, this rejected heat can be used to pre-heat air and/or generate steam for the gasification or to produce hot water. Afterwards, cooled producer gas passes through the cleaning section that functions as an interface between the characteristics of the producer gas and those required by the specific generator set system. Clean producer gas is fed to the ICE that produces electricity and exhaust gases. An absorption system, which is run by waste heat from the engine exhaust gases (directly or indirectly), is used to supply the cooling.

As it can be seen in the figures, the main differences among the configurations are located in the producer gas utilization section. The gas is always used in an ICE and the differences are mainly in how heat from exhaust gases and cooling water from the engine jacket is recovered and used.

In the first configuration (Figure 6.1), exhaust gases directly feed a double-effect exhaust gases absorption chiller. Hot water from the cooling circuit of the engine and hot water from producer gas cooling are directly used for the DHC network that usually operates at 85/70ºC.

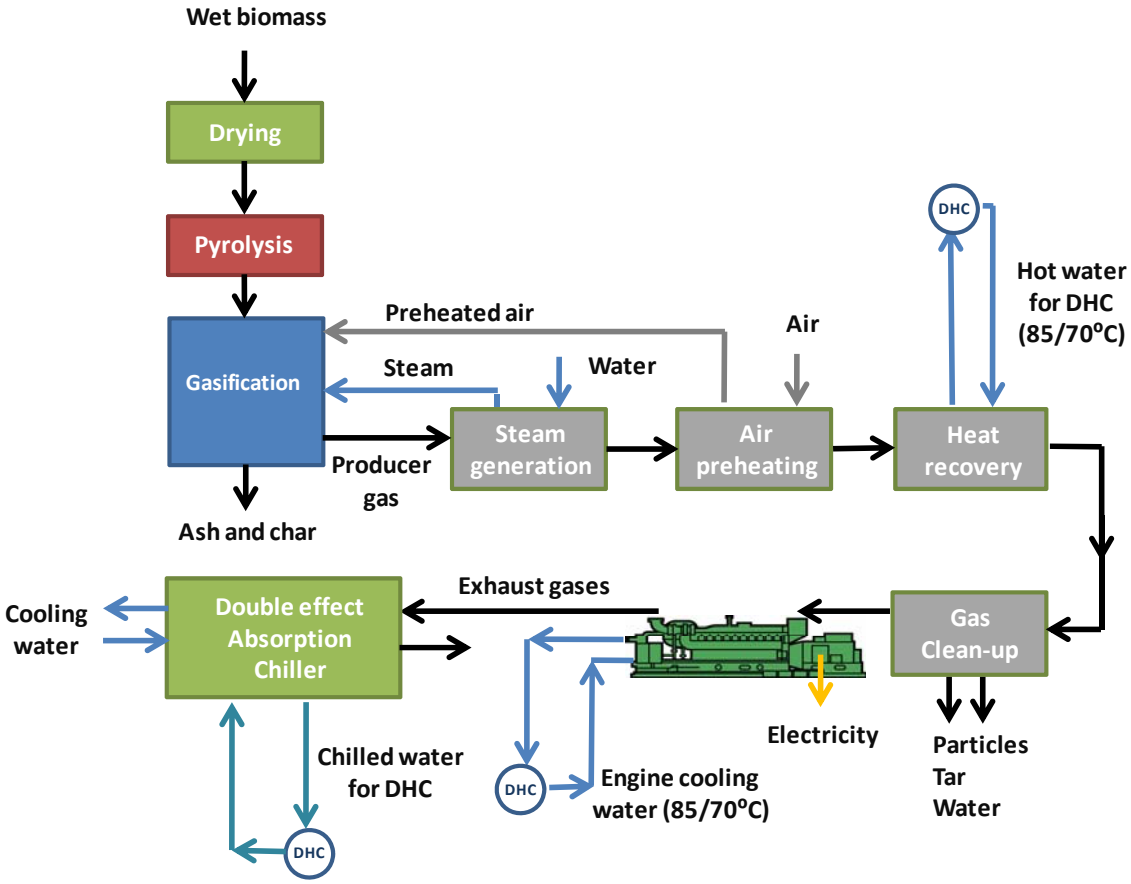


Figure 6.1: First configuration of the biomass gasification trigeneration plant. In this case the exhaust gases are used directly in a double-effect absorption chiller.

In the second configuration (Figure 6.2), exhaust gases are used to increase the temperature of the cooling water from engine jackets up to 98ºC and also to heat the water that returns from the DHC at 70ºC. This water at 98ºC is then mixed with that produced at the same temperature, in the heat recovery unit, and feed to a single-effect hot water absorption chiller. The water flow rate leaves the generator unit of the chiller at approximately 88ºC ant it is then sent to the DHC network.

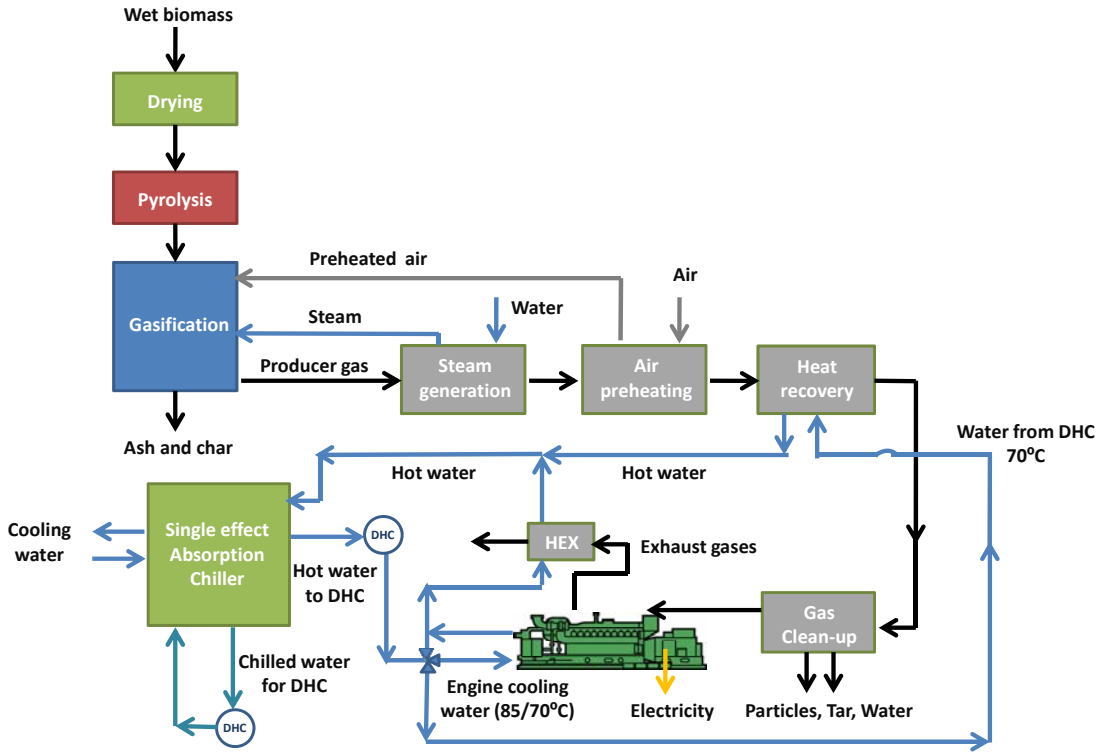


Figure 6.2: Second configuration of the biomass gasification trigeneration plant. In this case the exhaust gases are used to generate hot water to feed a single-effect absorption chiller.

The third configuration (Figure 6.3) consists of a double-effect steam absorption chiller that is fed with steam generated using the heat from exhaust gases. Hot water from the heat recovery unit and from the cooling circuit of the engine is used for the DHC network that operates at 85/70ºC.

In the following sections, the different units integrated in the trigeneration plant are described and their modelling is presented.

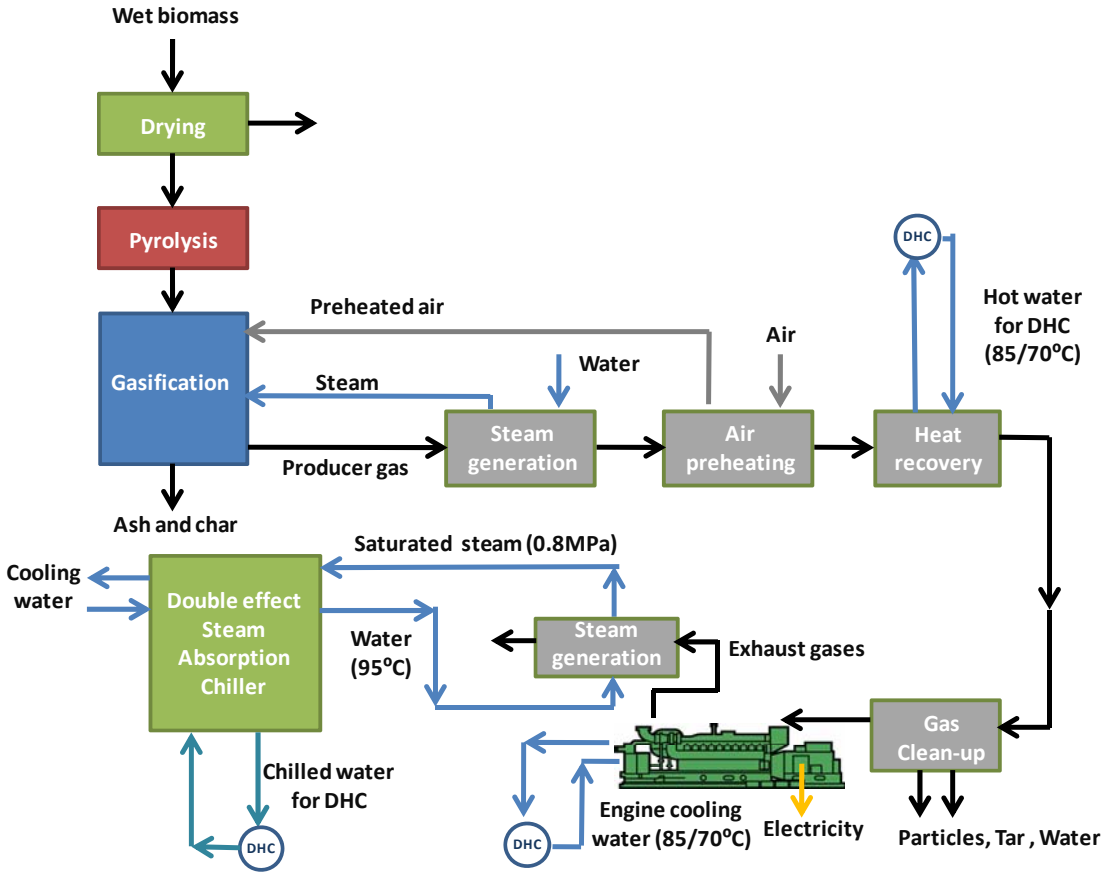


Figure 6.3: Third configuration of the biomass gasification trigeneration plant. In this case the exhaust gases are used to generate steam to feed a double-effect absorption chiller.

### 6.2.1 Producer gas production section

The producer gas production section is the same for the three proposed configurations. It is represented by a downdraft or a fluidised bed gasifier, modelled using the modified equilibrium approach (Chapter 3) or the artificial neural network approach (Chapter 4), respectively.

Both models give the producer gas composition (% vol. of CO, $CO_2$, $CH_4$, $H_2$, $N_2$ and $H_2O$), LHV and ash and producer gas flow rate. In addition, if the production of char, tar and particles is considered the flow rates are also given.

The model parameters can be directly introduced by the user through the user's friendly interface or can be adjusted automatically if some experimental data from the gasifier to be modelled is available.

### 6.2.2 Heat recovery section

The aim of this section is to cool down the producer gas to 150ºC while the rejected heat is used to generate steam and/or preheat air for the gasification. In addition, and in order to reach the desired 150ºC, hot water at 85ºC is produced for the DHC network (first and third configurations) or at 98ºC for the single-effect absorption chiller (second configuration). The return temperature of the hot water from the DHC network is always considered to be at 70ºC. This section is modelled through mass and energy balances.

### 6.2.3 Producer gas clean-up section

The presence of by-products in the producer gas makes it necessary to clean the gaseous flow before its use by the power generation section.

A conventional gas purification arrangement for a biomass plant could be adopted for the producer gas clean-up, including the following stages: cyclone, bag filter, scrubber and a chiller-demister (Baratieri et al, 2009; Arena et al, 2010). For the considered configurations, all the clean-up treatment stages should be characterised by a pressure of 1 bar as the thermal conversion process is conducted at atmospheric pressure.

After the cooling stages, the gas should pass through the cyclone, capable of removing particulate matter of a diameter greater than approximately 5 μm, and through the bag filter, which has high removal efficiency for a wide range of granulometries. The gas would be then treated with a scrubber, which would reduce its temperature to less than 100ºC. This purification process would favour steam condensation and the removal of the sulphur and halogenous compounds, so increasing the reliability of the power generator. Finally, the chiller-demister would further cool the producer gas below its dew point to reach the values of 25ºC and 60% of relative humidity, typically required by the engine inlet specification systems (Arena et al., 2010).

It would be reasonable to use this conventional wet cleaning system for the syngas treatment because gas engines are generally fuelled with cold gas and the dew point of the producer gas is generally higher than the gas inlet temperature and hence a condensate will be generated in all gas cleaning systems (Baratieri et al, 2009).

In the present configurations, gas cleaning is modelled considering and overall efficiency (%) of the different clean-up stages in removing particles and tars. Condensed water from producer gas when it is cooled to 25ºC and 60% of relativity humidity is calculated assuming the same properties than air and using the psychometric diagram for air.

### 6.2.4 Internal combustion engine

Internal combustion engines (ICE) are one of the most mature cogeneration technologies. Cogeneration units are able to produce simultaneously heat and power (or electricity) using the same fuel. The most extended cogeneration units are internal combustion engines together with turbines, microturbines and fuel cells. In a cogeneration unit, the heat is recovered from the exhausts gas and/or from the cooling circuits.

Internal combustion engines are available for a wide range of capacities (3 kW – 20 MW) and high electrical efficiency (35 - 45 %). The useful heat is recovered from two different circuits, the exhausts gases with typical temperatures between 300 - 400 ºC and the refrigeration circuit of the engine producing hot water up to 90 ºC.

Because the biggest application of producer gas has been in driving ICE, several manufacturers are specialised in ICE for producer gas from gasification, among all of them, the most well-known are: General Motors, Caterpillar, Wartsila, Guascor, Tessari Energia, Deutz and the mostly common used General Electric Jenbacher engine.

In their work, Baratieri et al. (2009) assumed constant thermal and electric efficiencies of 35% and 40%, respectively, for the internal combustion gas engine. However, the power and thermal production of the engines can be approximated using linear relations respect to the fuel consumption (Cho et al., 2009; Ortiga, 2010). A linear correlation can be made for each output using experimental data or manufacturer data

of the engine at several partial loads. This relation (fuel consumption-output power) trend to be linear and avoids the use of non-linear efficiencies that depends of the unit's load.

In this thesis, the ICE is modelled based on correlations obtained from manufacturer's data for part load operation of conventional ICE. Data has been obtained from GE Jenbacher modules especially adapted to work with producer gas. However, data from any other manufacturer could also have been used. The correlations were obtained for different sizes of ICEs (J316 GS, J320 GS, J616 GS and J620 GS) that cover the whole range of power output of the trigeneration plant. In Figure 6.4 the electrical power output versus the fuel power input is represented. Figure 6.5 shows the thermal power output versus the fuel power input and Figure 6.6 represents the thermal power from exhaust gases (cooled down to 120ºC) versus the fuel power input. Table 6.1 gives the correlations obtained for these ICEs that have been integrated in the model and used to calculate the outputs from the ICE.

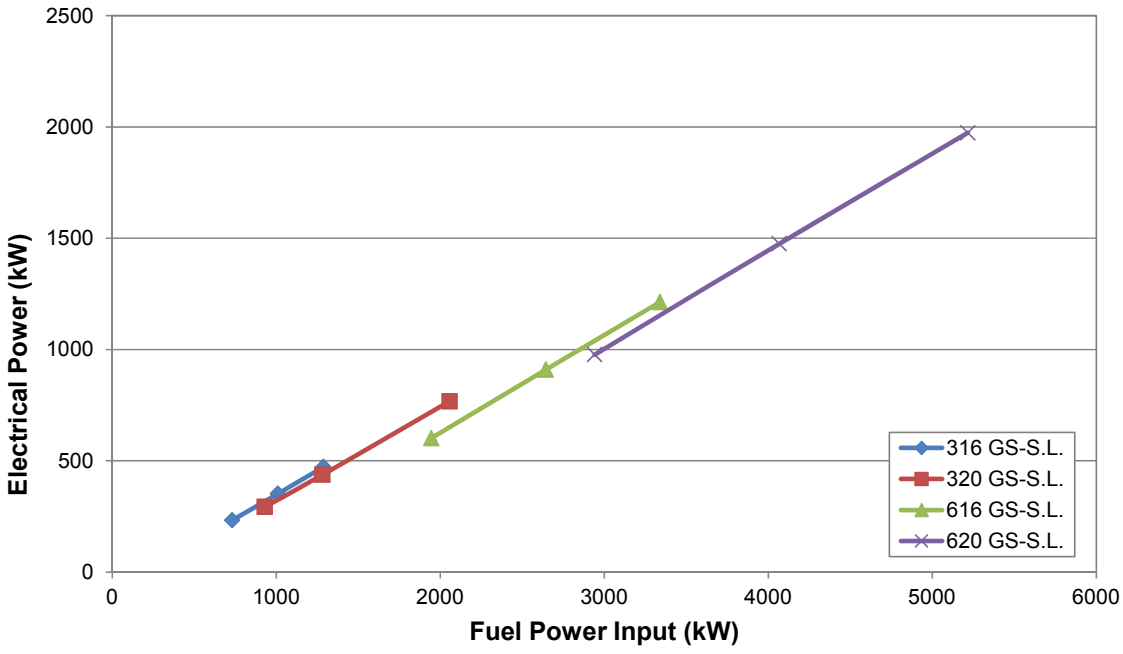


Figure 6.4: Generated electrical power (kW) versus fuel power input (kW) for the different ICE modelled and integrated in the biomass gasification trigeneration plant model.

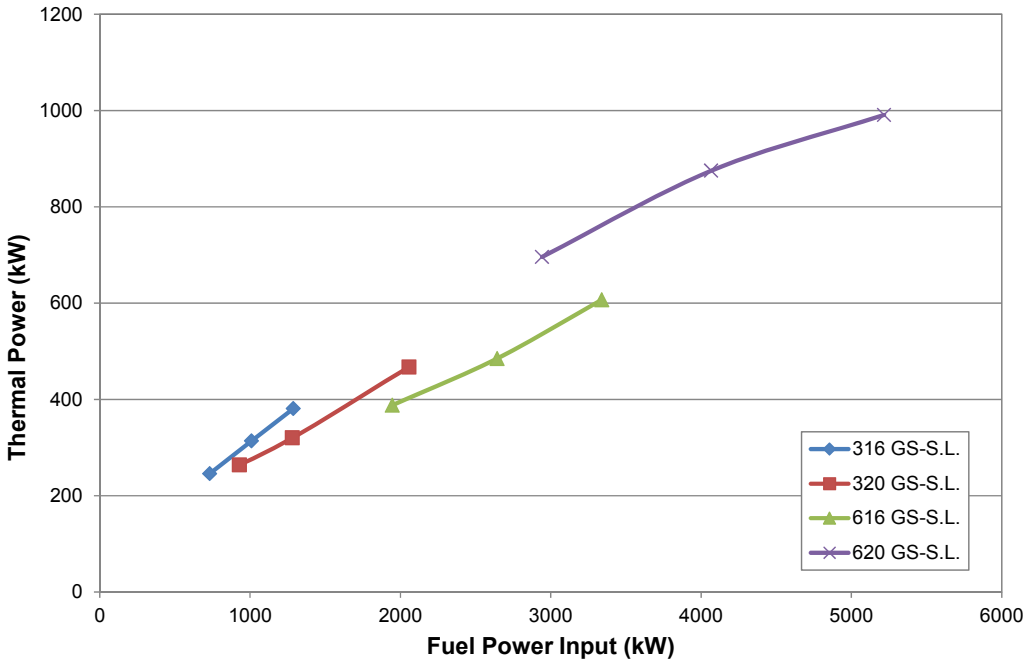


Figure 6.5: Generated thermal power (kW) versus fuel power input (kW) for the different ICE modelled and integrated in the biomass gasification trigeneration plant model.

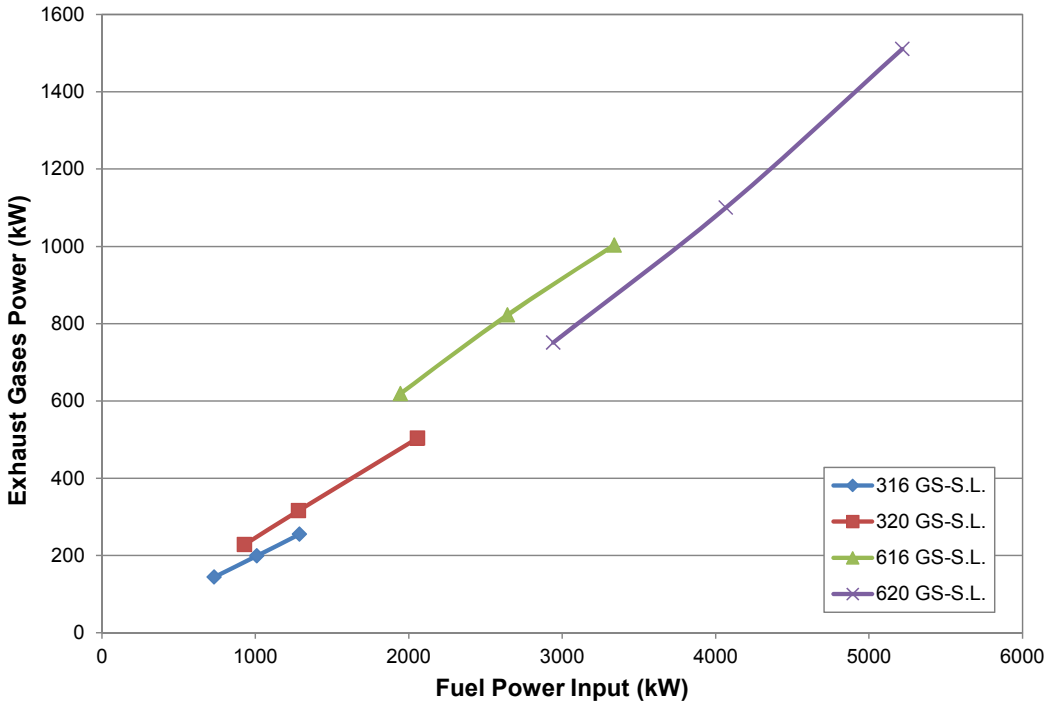


Figure 6.6: Generated thermal power from exhaust gases cooled down to 120ºC (kW) versus fuel power input (kW) for the different ICE modelled and integrated in the biomass gasification trigeneration plant model.

Table 6.1: Calculated correlations for ICEs part load operation outputs.

| ICE Types | Electrical output (kW) | Thermal output (kW) | Exhaust gases output (kW) |
|---|---|---|---|
| **J316 GS** | $W_e = 0.430 \cdot Q_{in} - 81.821$ | $Q_{th} = 0.243 \cdot Q_{in} + 68.433$ | $Q_{exhaust} = 0.200 \cdot Q_{in} - 2.303$ |
| **J320 GS** | $W_e = 0.421 \cdot Q_{in} - 100.71$ | $Q_{th} = 0.182 \cdot Q_{in} + 91.782$ | $Q_{exhaust} = 0.244 \cdot Q_{in} + 1.897$ |
| **J616 GS** | $W_e = 0.439 \cdot Q_{in} - 251.13$ | $Q_{th} = 0.157 \cdot Q_{in} + 77.879$ | $Q_{exhaust} = 0.276 \cdot Q_{in} + 85.908$ |
| **J620 GS** | $W_e = 0.438 \cdot Q_{in} - 310.58$ | $Q_{th} = 0.130 \cdot Q_{in} + 325.98$ | $Q_{exhaust} = 0.334 \cdot Q_{in} - 240.750$ |

### 6.2.5 Absorption chiller

In Chapter 5 a modified adaptation of the characteristic equation method, developed by Kühn and Ziegler (2005), has been proposed as the simplest way to model absorption chillers. In this proposed characteristic temperature function, the parameters are fitted according to a multiple regression fit and $T_{inG}$, $T_{inAC}$ and $T_{oE}$ can be directly used to model the part-load operation of the chiller. These temperatures are the ones with the highest influence on the chiller's performance. If any of these temperatures is changed, then the model can predict the part load behaviour of the chiller under different operating conditions and gives a more realistic prediction than just using a constant COP.

The developed multiregression fits were carried out with Microsoft Excel (2003) using Broad manufacturer's data (Broad, 2004) of different types: double-effect direct exhaust gas driven absorption chillers (BE models), single-effect hot water absorption chiller (BDH models) and double-effect steam absorption chillers (BS models). Data from this manufacturer was used because it is that of typical absorption chillers and allowed to create a general model for each type of absorption chiller. However, data from other manufacturers (Thermax, Trane, Hitachi...) could also have been used.

For Broad absorption chillers, manufacturer's part load curves, for different external flows temperatures combination, are the same for all absorption chillers of the same type, even though they have different capacities. For this reason, only correlations for the smallest absorption chiller of each type that could be implemented in the trigeneration plant, are calculated. These correlations are calculated for $Q_E$, $Q_G$, $Q_{AC}$ and $m_{AC}$. $Q_E$, $Q_G$ and $Q_{AC}$ stand for the heat fluxes (kW) in the evaporator, generator and absorber-condenser and $m_{AC}$ for cooling water flow-rate.

Then, in order to calculate the cooling capacity and flow rates for bigger capacity absorption chillers of the same type, a factor ($f_{abs}$) that depends on the exhaust gases, hot water or steam flow-rate has to be calculated. This factor is then multiplied by the values of $Q_E$, $Q_G$, $Q_{AC}$, $m_{AC}$ and $m_E$ calculated for the smallest capacity chiller.

- Model for a double-effect direct exhaust gases fired absorption chiller

The numerical fit for BE-50, the smallest that could be implemented in the trigeneration plant model, resulted in the following equations:

$$Q_E = 43.796 \cdot T_{oE} - 20.302 \cdot T_{inAC} + 1.415 \cdot T_{inG} + 168.885$$

$$Q_G = 30.231 \cdot T_{oE} - 14.563 \cdot T_{inAC} + 0.939 \cdot T_{inG} + 171.257 \qquad \text{Eq. 6.1}$$

$$Q_{AC} = 74.027 \cdot T_{oE} - 34.865 \cdot T_{inAC} + 2.354 \cdot T_{inG} + 340.142$$

Where $Q_E$, $Q_G$ and $Q_{AC}$ stand for the heat fluxes (kW) in the evaporator, generator and absorber-condenser, respectively. Chilled water outlet ($T_{oE}$), generator inlet ($T_{inG}$) and cooling water inlet ($T_{inAC}$) temperatures are in the range of 5-10ºC, 400-500ºC and 24-32ºC, respectively. The nominal values of this BE-50 absorption chiller are detailed in Table 6.2.

Table 6.2: Nominal values of the Broad absorption chillers used to model the absorption chiller of the biomass gasification trigeneration plant (Broad, 2004).

| **Nominal values of absorption chiller** | **BE-50** | **BDH-40** | **BS-20** |
|---|---|---|---|
| Cooling capacity ($Q_{E,nominal}$) | 582 kW | 407 kW | 233 kW |
| Heating capacity ($Q_{G,nominal}$) | 449 kW | 543 kW | 168 kW |
| Chilled water flowrate (7ºC/12ºC) ($m_E$) | 100 $m^3$/h | 70 $m^3$/h | 40 $m^3$/h |
| Cooling water flowrate (37ºC/30ºC) ($m_{AC,\ nominal}$) | 123 $m^3$/h | 117 $m^3$/h | 49 $m^3$/h |
| Exhaust gas consumption (500ºC/170ºC) ($m_G$) | 3681 kg/h | - | - |
| Hot water flowrate (98ºC/88ºC) ($m_G$) | - | 48.6 $m^3$/h | - |
| Saturated steam 0.8MPa ($m_G$) | - | - | 252 kg/h |

According to the manufacturer's data, chilled water flow rate remains constant while cooling water flowrate ($m_{AC}$) doesn't. It is a function of the absorption chiller's capacity:

$$m_{AC} = m_{AC,no\,min\,al} \cdot 7.9632 \cdot \exp(0.0253 \cdot Capacity) \qquad \text{Eq. 6.2}$$

$$Capacity(\%) = \frac{Q_E}{Q_{E,no\,min\,al}} \cdot 100 \qquad \text{Eq. 6.3}$$

The factor ($f_{abs}$) to calculate the production ($Q_E$, $Q_G$, $Q_{AC}$, $m_{AC}$ and $m_E$) of bigger absorption chillers of the same type is defined by Eq. 5.4.

$$f_{abs} = 0.00027035 \cdot m_G + 0.00563511 \qquad \text{Eq. 6.4}$$

- Model for a single-effect hot water fired absorption chiller

The procedure followed to model this type of absorption chiller is the same than the previous one. The obtained equations for the numerical fit of BDH-40 model are as follows:

$$Q_E = 30.519 \cdot T_{oE} - 28.545 \cdot T_{inAC} + 17.321 \cdot T_{inG} - 668.432$$

$$Q_G = 38.502 \cdot T_{oE} - 37.993 \cdot T_{inAC} + 22.776 \cdot T_{inG} - 844.396 \qquad \text{Eq. 6.5}$$

$$Q_{AC} = 69.021 \cdot T_{oE} - 66.538 \cdot T_{inAC} + 40.097 \cdot T_{inG} - 1512.828$$

The temperature ranges are 5-12ºC for $T_{oE}$, 85-110ºC for $T_{inG}$ and 24-32ºC for $T_{inAC}$ and the nominal values of this BDH-40 absorption chiller are detailed in Table 6.2.

According to the manufacturer's data, like in the previous case, cooling water flowrate ($m_{AC}$) is a function of the absorption chiller's capacity (Eq. 5.2). A factor ($f_{abs}$, Eq. 5.6) is calculated and then multiplied by the values of $Q_E$, $Q_G$, $Q_{AC}$, $m_{AC}$ and $m_E$ found using the previous expressions for BDH-40 model.

$$f_{abs} = 0.00002058677 \cdot m_G - 0.00203361 \qquad \text{Eq. 6.6}$$

- Model for double-effect steam fired absorption chiller

In this case, the obtained equations for the numerical fit of BS-20 model only include $t_{oE}$ and $t_{inAC}$ because steam is always considered to be saturated steam at 0.8MPa.

$$Q_E = 14.956 \cdot T_{oE} - 7.458 \cdot T_{inAC} + 344.269$$

$$Q_G = 10.250 \cdot T_{oE} - 5.183 \cdot T_{inAC} + 244.946 \qquad \text{Eq. 6.7}$$

$$Q_{AC} = 25.206 \cdot T_{oE} - 12.641 \cdot T_{inAC} + 589.215$$

The temperature ranges are 5-10ºC for $T_{oE}$ and 24-32ºC for $T_{inAC}$.

The nominal values of this BS-20 absorption chiller are detailed in Table 6.2. Cooling water flowrate ($m_{AC}$) is also a function of the absorption chiller's capacity (Eq. 5.2). Like in the previous cases, a factor ($f_{abs}$, Eq. 5.8) is calculated in order to determine the cooling capacity and flowrates for bigger capacity absorption chillers of the same type.

$$f_{abs} = 0.00395876 \cdot m_G + 0.00601168 \qquad \text{Eq. 6.8}$$

### 6.2.6 Efficiency and primary energy savings of trigeneration plants

In recent years, the operators of the energy sector have put an increasingly focus on issues concerning energy saving and implementation of high-efficiency energy systems, both from the technical and from the regulatory point of view. Energy efficiency of trigeneration systems can be measured using different parameters. In this section, the mostly used parameters for evaluating the efficiency of co- and trigeneration systems are presented and employed for the proposed trigeneration configurations:

- Overall efficiency of trigeneration system ($\eta_t$).
- Primary energy savings (PES) of the trigeneration system compared with a conventional system:
    - Using the Directive 2004/8/CE of the European Comission on the promotion of cogeneration based on a useful heat demand.
    - Using the methodology proposed by Chicco and Mancarella (2007) consisting of an adaptation to trigeneration systems of the primary

energy savings of cogeneration systems presented by Cardona and Piacentino (2005).

- Electrical Equivalence Performance (REE), a method to evaluate the efficiency of co- and trigeneration systems that is being applied in Spain for the recognition of the electricity producer in the special production regime according to Spanish regulation.

#### 6.2.6.1 Trigeneration system overall efficiency

The overall trigeneration efficiency is defined as the ratio of total useful energy output (electrical ($W_e$), heat ($Q_{heat}$) and cold ($Q_{cold}$)) to the total fuel energy input ($Q_{fuel}$) and can be expressed as:

$$\eta_t(\%) = \frac{W_e + Q_{cold} + Q_{heat}}{Q_{fuel}} \cdot 100 \qquad \text{Eq. 6.9}$$

It has to be taken into account that this metric does not differentiate between the value of the power output and the thermal output; instead, it treats power output and thermal output as additive properties with the same relative value. In reality and in practice, thermal output and power output are not interchangeable because they cannot be converted easily from one to another. For this reason and as stated by Roqueta and Márquez (2004) it cannot be considered a method to measure the efficiency but a comparative parameter for systems with the same ratio between useful heat and electricity.

#### 6.2.6.2 Trigeneration system primary energy savings

One of the most adequate indicators to evaluate energy viability of a trigeneration system is the analysis of the Primary Energy Savings (PES). This ratio compares the trigeneration system with an equivalent conventional system.

Two different methodologies are used to compute the primary energy savings, the first one according the high-efficiency criteria of the Directive 2004/8/EC and the second one following the methodology of Chicco and Mancarella (2007).

- Primary energy savings according to the Directive 2004/8/EC

  Directive 2004/8/EC indicates that high efficiency cogeneration shall fulfil the following criteria: cogeneration production from cogeneration units shall provide primary energy savings of at least 10% compared with the references for separate production of heat and electricity. In addition, it remarks that production from small (<1MW$_e$) and micro scale (<50 kW$_e$) units providing primary energy savings may qualify as high-efficiency cogeneration.

  The amount of primary energy saving provided by cogeneration production defined in accordance with Annex II of the mentioned directive shall be calculated on the basis of the following formula:

$$PES(\%) = \left( 1 - \frac{1}{\frac{\eta_{CHP,heat}}{\eta_{ref,heat}} + \frac{\eta_{CHP,e}}{\eta_{ref,e}}} \right) \cdot 100 \qquad \text{Eq. 6.10}$$

  Where:

  $\eta_{CPH,heat}$ is the heat efficiency of the cogeneration production defined as annual useful heat output divided by the fuel input used to produce the sum of useful heat output and electricity from cogeneration.

  $\eta_{ref,heat}$ is the efficiency reference value for separate heat production.

  $\eta_{CPH,e}$ is the electrical efficiency of the cogeneration production defined as annual electricity from cogeneration divided by the fuel input used to produce the sum of useful heat output and electricity from cogeneration.

  $\eta_{ref,e}$ is the efficiency reference value for separate electricity production.

According to this Directive, useful heat demand corresponds to heat produced in a cogeneration process to satisfy an economically justifiable demand for heat or cooling.

In this case, the useful heat output computes the heat for heating purposes and also the heat to feed the absorption chiller.

- Primary energy savings for trigeneration according to Chicco and Mancarella (2007)

Chicco and Mancarella (2007) introduced a new generalized performance indicator named trigeneration primary energy savings (TPES) with the aim of effectively evaluating the primary savings from different combined heat, cold and power alternatives. They considered the trigeneration plant as a black box with only the relevant input-output energy flows and defined the TPES indicator as:

$$TPES = 1 - \frac{Q_{fuel}}{\frac{W_e}{\eta_{ref,e*}} + \frac{Q_{heat}}{\eta_{ref,heat*}} + \frac{Q_{cold}}{\eta_{ref,e*} \cdot COP_{ref}}} \quad \text{Eq.6.11}$$

Where:

$W_e$ is the net trigeneration electricity output (including electricity sold to the grid, and excluding the possible energy needed to feed electric equipment).

$Q_{heat}$ is the net useful trigenerated heat output (excluding the possible thermal energy needed to feed absorption chillers).

$Q_{cold}$ is the net trigenerated cooling energy output (excluding the possible cooling used within the plant).

The efficiencies $\eta_{ref,e*}$ and $\eta_{ref,heat*}$ are the separate production reference efficiencies, referred to the primary energy (fuel thermal energy content) as input, for electrical and thermal power, respectively.

$COP_{ref}$ is the equivalent COP of the compression electric chiller chosen as reference for the cooling production.

There are no official guidelines to assign numerical values to the reference efficiencies. It would be possible to assume average efficiency values, clearly dependent on the type of production units operating in a specific country or to compare the combined energy system with the best available technologies for separate production. In order to highlight the impact of the selection of the numerical values for the separate production references the procedure used by Chicco and Mancarella (2007) of considering different reference efficiency scenarios is followed. Three different reference efficiency scenarios were used (Table 6.3). The low-efficiency reference values could be used for a typical comparison with equipment used in non-centralized systems for residential or tertiary applications. The average references were calculated using the average efficiencies of conventional equipment and the average electrical efficiency of the Spanish electric grid (Moya, 2010). Finally, the state of the art reference corresponds to the best technologies available today.

Table 6.3: Reference efficiency scenarios to calculate TPES.

| Efficiency scenario | $\eta_{ref,heat*}$ | $\eta_{ref,e*}$ | $COP_{ref}$ |
|---|---|---|---|
| Low efficiency | 0.75 | 0.30 | 2.0 |
| Average | 0.80 | 0.44 | 2.5 |
| State-of-the-art | 0.92 | 0.55 | 3.0 |

#### 6.2.6.3 Electrical Equivalence Performance (Rendimiento Eléctrico Equivalente, REE)

REE is a parameter that measures the efficiency of a cogeneration system and it has been used by the Spanish legislation since 1994 for the licences of co- and trigeneration for electricity production in special regime. In this section, REE is calculated according the expression given in Annex I of the Royal Decree 661/2007, 25$^{th}$ of May:

$$REE = \frac{W_e}{\left[ Q_{fuel} - \frac{Q_{heat} + Q_{cold}}{\eta_{ref,heat}} \right]} \cdot 100 \qquad \text{Eq.6.12}$$

According to this Royal Decree 661/2007 there are minimum values for the REE depending on the type of fuel used. For solid biomass included in groups b.6 and b.8 this $REE_{min}$ is equal to 30% and if the plant size is less than 1MW this percentage may be reduced by 10%, that means a $REE_{min}$ equal to 27%.

## 6.3 CASE STUDY

The developed configurations for trigeneration plants enable a parametric study of different types of biomass and operating conditions, supporting the design and optimization of the integral gasifying plant, including the flows of biomass, producer gas and residual water, and the scaling of the ICE engines and absorption chillers corresponding to a certain energy input.

The purpose of this section is to apply the developed configurations to the polygeneration plant ST-2 foreseen in the European Project Polycity in Cerdanyola del Vallès. The assessment analysis performed is also presented.

### 6.3.1 Overview of the Spanish site of Polycity project in Cerdanyola del Vallès

Polycity project (TREN/05FP6EN/S07.43964/51381) was financed by the European Commission's initiative Concerto (VI Framework Programme). The Polycity project dealt with different aspects of urban development in three European sites: new constructions in Cerdanyola del Vallès (Barcelona, Spain) with tri-generation, innovative energy distribution and thermal cooling; the conversion of an old city quarter in Turin (Italy), with heating network based energy supply, and new building constructions on a large former military ground in the town of Ostfildern (Stuttgart, Germany).

Polycity Spanish site has been developed in a new area of 340 hectares in growth located in Cerdanyola del Vallès near Barcelona. At the end will comprise a roof area of 1,890,000 $m^2$, with a residential area for 15,000 inhabitants and an activity area that will create 40,000 jobs. A high efficiency energy system was planned to be implemented in the new urban development called “Parc de l’Alba”, in order to produce electricity, heating and cooling. This polygeneration system comprises high-efficiency natural gas cogeneration plants with an electrical output of about 16 $MW_e$, in a first stage, with thermal cooling facilities and a district heating and cooling network to connect the plant with the Science and Technology Park, which represents the core of the “Parc de l’Alba”.

As mentioned above, the area includes a Science and Technology Park with the Synchrotron Light Facility (ALBA) as well as residential buildings. The ST-4 plant, the first one implemented, provides electricity, hot and chilled water to the Synchrotron and the technological park buildings through a district heating and cooling network of four tubes.

The development of the “Parc de l’Alba” in Cerdanyola del Vallès was divided in two phases:

- Phase I: construction of an energy production plant ST-4 located in the technological park, to supply energy to the Synchrotron Laboratory (ALBA) and other users of the park (442,700 $m^2$ of offices and 62,000 $m^2$ of equipment). This phase is already implemented and started its operation in July 2010. The ST-4 uses a district heating and cooling network to provide hot and cold water simultaneously. A detailed description of this plant can be found elsewhere (Ortiga, 2011).
- Phase II: construction of three new energy supply plants (ST-2, ST-3 and ST-5). This phase is still in a development stage and the first plant to be implemented in this second phase is ST-2.

The foreseen energy supply plants and DHC network can be seen in Figure 6.7.

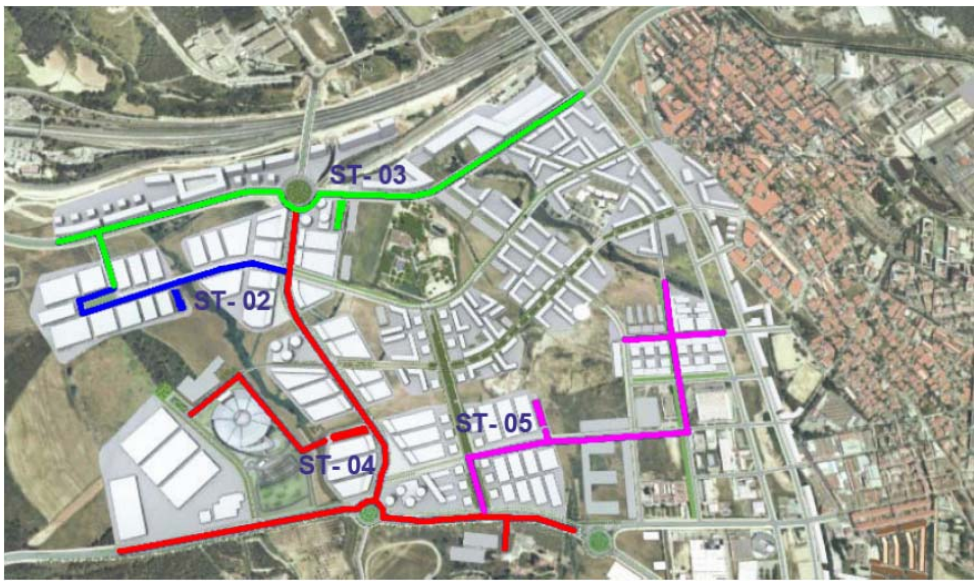


Figure 6.7: Foreseen energy supply plants and DHC network in Alba park in Cerdanyola del Vallès.

### 6.3.2 ST-2 Plant

After the already built ST-4 polygeneration plant, the next one to be implemented is ST-2 polygeneration plant. This plant will use both natural gas and renewable energy sources to produce electricity, hot and chilled water and will integrate a solar cooling plant and a biomass gasification plant.

The ST-2 plant was supposed to be finished before the end of Polycity project (May 2011) however it is currently at the engineering stage. The delays in the start-up of ST-4 plant due to bureaucratic and economic conflicts between third parties, together with a dramatic reduction in thermal energy demand have delayed the construction of ST-2 Plant. Synchrotron light laboratory has reduced its operating hours around 70% which means a reduction in its heat, cold and electricity demand. In addition and due to economic downturn other real estate promoters have abandoned or postponed their investments in the area. However, there is a strong commitment by the joint venture formed by Tecnocontrol and Lonjas Tecnología, the winners of the call or tenders, to build and start operation of ST-2 plant.

The solar cooling plant will have up to 2,000 $m^2$ of solar collectors. It will use flat plate collectors with adsorption chillers or evacuated tube collectors with absorption chillers.

The gasification plant will work with forestry residues or sub products from the local industry. The producer gas will be used in a dedicated cogeneration engine of around 1$MW_e$ to produce electricity. Chilled water will be produced via an absorption chiller. The electricity will be sold to the grid and chilled and hot water produced will be used for the DHC network. Because the biomass gasification plant has a small size compared with the other polygeneration plants it will always work at its maximum capacity.

In order to study different possible configurations for the ST-2 plant, the three configurations developed in the present chapter are applied.

### 6.3.3 Input data for the model

The gasification plant that the company Taim-Weser S.A. has in its facilities located in Cartuja Baja, Zaragoza, is taken as a reference to get the necessary input data for the configurations. This plant was selected because it is in the electrical size range considered for the ST-2 plant project.

The plant is based on a downdraft gasifier with a nominal electric power of 765 $kW_e$ and recoverable thermal power of 1200-1400 $kW_{th}$. The biomass is unloaded in a covered reception area where it is conditioned by means of crushing and drying processes. In this respect, the characteristics of the gasifier permit a great deal of flexibility with respect to the composition of the biomass, as well as a wide selection of grain sizes, ranging from approximately 0.2 to 10 cm. Once in the gasifier, the biomass is subjected to a thermochemical combustion process under oxygen deficit conditions, leading to the production of gas and the degradation of the biomass, which is converted to ash. The resulting producer gas, after a cleaning and conditioning process, is then oxidized in a cogeneration unit (internal combustion motor) and, in this manner, electrical energy is produced. Then waste heat is used to heat the warehouse of the company.

The technical specifications of the gasification plant used in this thesis are provided by the company Taim-Weser and presented in Table 6.4.

Table 6.4: Technical specifications of Taim-Weser gasification plant in Zaragoza.

| Technical specifications | |
|---|---|
| **Fuel characteristics** | |
| Type of fuel | Wood chips |
| Moisture content | 10-15% |
| Size | 0.2-10 cm |
| **System characteristics** | |
| Biomass consumption | 650 kg/h |
| LHV producer gas | 4.75-5.58 MJ/Nm$^3$ |
| Volume of producer gas | 1170-1470 Nm$^3$/h |
| Operating temperature | 1200ºC |
| Ash-char | 10% of biomass input |
| Tars | <3% of condensate volume |
| **Outputs** | |
| Electrical power | 765 $kW_e$ |
| Recoverable thermal power | 1200 – 1400 $kW_{th}$ |
| Operating hours | 7000 h/year |

In all cases, an input of 650 kg/h of wood chips with a 15% of moisture is considered. The proximate and ultimate analysis of biomass, given by the company, is presented in Table 6.5. Pyrolysis unit temperature has been adjusted to 450ºC and a percentage of char and tar leaving the pyrolysis unit has been set to match the amount of char-ash and tar leaving the gasifier and reported by the company (40% and 5% respectively). The air is preheated up to 400ºC and the $CH_4$ percentage leaving the gasifier is given to the model. The temperature of producer gas when leaving the gasifier is considered to be 700ºC as stated by the company. The three different configurations have been studied and are presented in the following sections.

Table 6.5: Proximate and ultimate analysis of the wood chips used in Taim-Weser gasification plant.

| Wood chips | |
|---|---|
| **Proximate analysis (% wt. d.b.)** | |
| Fixed carbon | 18.57 |
| Volatile matter | 80.50 |
| Ash | 0.76 |
| **Ultimate analysis (% wt. d.b.)** | |
| C | 50.04 |
| H | 5.73 |
| O | 42.92 |
| N | 0.55 |
| S | 0.00 |
| HHV | 20.19 MJ/kg |

### 6.3.4 Different studied configurations and methodology

As previously mentioned, three different configurations for biomass gasification trigeneration plants that could be implemented in ST-2 plant in Cerdanyola del Vallès were studied:

- Configuration 1

  This configuration is composed by the drying, pyrolysis and gasification units followed by the steam generation and air preheating units. Once producer gas leaves the air preheating unit, it passes through the heat recovery unit where heats the water from 70ºC up to 85ºC for the DHC network. After this unit, producer gas goes to the clean-up section which includes a cyclone, bag filter, scrubber and a chiller-demister. Then, producer gas is fed into the ICE. Hot water at 85ºC, from the engine jacket cooling circuit, is sent together with the hot water generated in the heat recovery unit to the DHC network. Exhaust gases from the engine are fed into a double-effect exhaust absorption chiller that produces chilled water for the DHC network.

- Configuration 2

  This configuration is integrated by the same units than the previous one. However, in this case, the absorption chiller is a single-effect hot water driven absorption chiller. For this reason, the heat recovery unit heats water from 70 to 98ºC. This water stream at 98ºC is then mixed with the water from the cooling jacket of the engine and the return water of the DHC which are also heated up to 98ºC using the exhaust gases of the engine. Then, this water stream is fed to the absorption chiller. Once it leaves the absorption chiller, the water at 88ºC approximately goes to the DHC network.

- Configuration 3

  In this configuration, the absorption chiller is a double-effect steam absorption chiller. The steam to drive the absorption chiller is generated using the exhaust gases from the engine. Heat recovery unit produces water at 85ºC that is then mixed with the water at 85ºC from the cooling jacket of the engine and used in the DHC network.

Complete diagrams of the three configurations implemented in EES software with the simulated results are shown in Figure 6.8, Figure 6.9 and Figure 6.10.

In order to calculate *PES* and *REE*, the values of $\eta_{ref,heat}$ and $\eta_{ref,e}$ were taken from the Commission decision of 21st of December 2006 establishing harmonised efficiency reference values for separate production of electricity and heat in application of Directive 2004/8/EC of the European Parliament and of the Council.

According to Annex I of this Decision, the harmonized efficiency reference value of 2006-11 for separate electricity production from wood fuels is 33%. No climatic correction is necessary for Barcelona area and after the grid loss correction of 0.945 (because all the electricity generated, at 22.5 kV, is exported to the grid) the resulting efficiency reference value for the separate production of electricity in this cogeneration unit is:

$$\eta_{ref,e}=33 \cdot 0.945= 31.2\% \qquad \text{Eq.6.13}$$

According to Annex II of the same Decision, the harmonized efficiency reference value for separate production of heat for wood fuels ($\eta_{ref,heat}$) is 86%.

Table 6.6 shows the simulated results for producer gas and electricity generation. The results are the same for the three configurations because the same model for the gasifier is used. It can be seen how the model is able to produce results that are in good agreement with those reported by Taim-Weser S.A. for producer gas composition, LHV, electrical output and efficiency of the engine.

Table 6.6: Comparison between results from the biomass gasification model and those reported by Taim-Weser S.A. for wood chips gasification in a downdraft gasifier.

| | **Present model** (% vol. d.b.) | **Manufacturer** (% vol. d.b.) |
|---|---|---|
| **$N_2$** | 47.64 | 45 – 55 |
| **$H_2$** | 15.7 | 15 – 20 |
| **CO** | 21.92 | 13 – 20 |
| **$CO_2$** | 11.74 | 8 – 15 |
| **$CH_4$** | 3 | 2 – 4 |
| **LHV (MJ/Nm$^3$)** | 5.54 | 4.75-5.58 |
| **Producer gas (Nm$^3$/h d.b.)** | 1260 | 1170-1470 |
| **Electrical output ($kW_e$)** | 717.8 | 765 |
| **Electrical efficiency of the engine (%)** | 37.04 | 36.1 – 37.3 |

Table 6.7 shows the different calculated results for annual electricity, heat and cold production for each configuration considering 7000 h of operation per year. In addition, the values of overall efficiency, *PES, TPES* and *REE* are given and can be compared.

Table 6.7: Results from the different configurations for the biomass gasification trigeneration plant.

| | **Configuration 1** | **Configuration 2** | **Configuration 3** |
|---|---|---|---|
| **Electricity production (MWh)** | 5024.6 | 5024.6 | 5024.6 |
| **Heat production for DHC (MWh)** | 4950.4 | 5481.98 | 4950.4 |
| **Cold production for DHC (MWh)** | 4459.7 | 2025.1 | 4551.4 |
| **COP Absorption chiller** | 1.37 | 0.75 | 1.40 |
| **Overall efficiency ($\eta_t$) (%)** | 61.8 | 53.6 | 62.1 |
| **REE** | 0.40 | 0.34 | 0.41 |
| **PES (Directive 2004/8/EC)** | 8.90 | 9.27 | 8.89 |

It can be seen how the electricity production is the same for the three different configurations because the amount of producer gas and its composition is the same for all of them. Heat production for DHC is slightly higher in Configuration 2 while cold production in configuration 3 is the highest. Cold production in configuration 3 is almost double than in configuration 2 and only a little bit higher than in configuration 1. This is because configurations 1 and 3 use double-effect absorption chillers with a COP that is almost twice the COP of configuration 2. Considering the overall efficiency, it is higher in configuration 3 than in the other cases, but little difference exist between configurations 1 and 3. This small difference is because the COP of the double-effect steam absorption chiller is slightly higher than the one of the double-effect exhaust absorption chiller.

The *REE* value is also higher in the third configuration but closely followed by configuration 1. The $REE_{min}$ (Royal Decree 661/2007) for this plant size (<1MW) is 27%. All configurations exceed the minimum value to be considered in the Spanish special regimen of production.

Concerning PES (Directive 2004/8/EC), all studied configurations have positive primary energy savings. For this reason and because they are small scale they can be considered “high efficiency” systems. In addition, these savings are close to 10%.

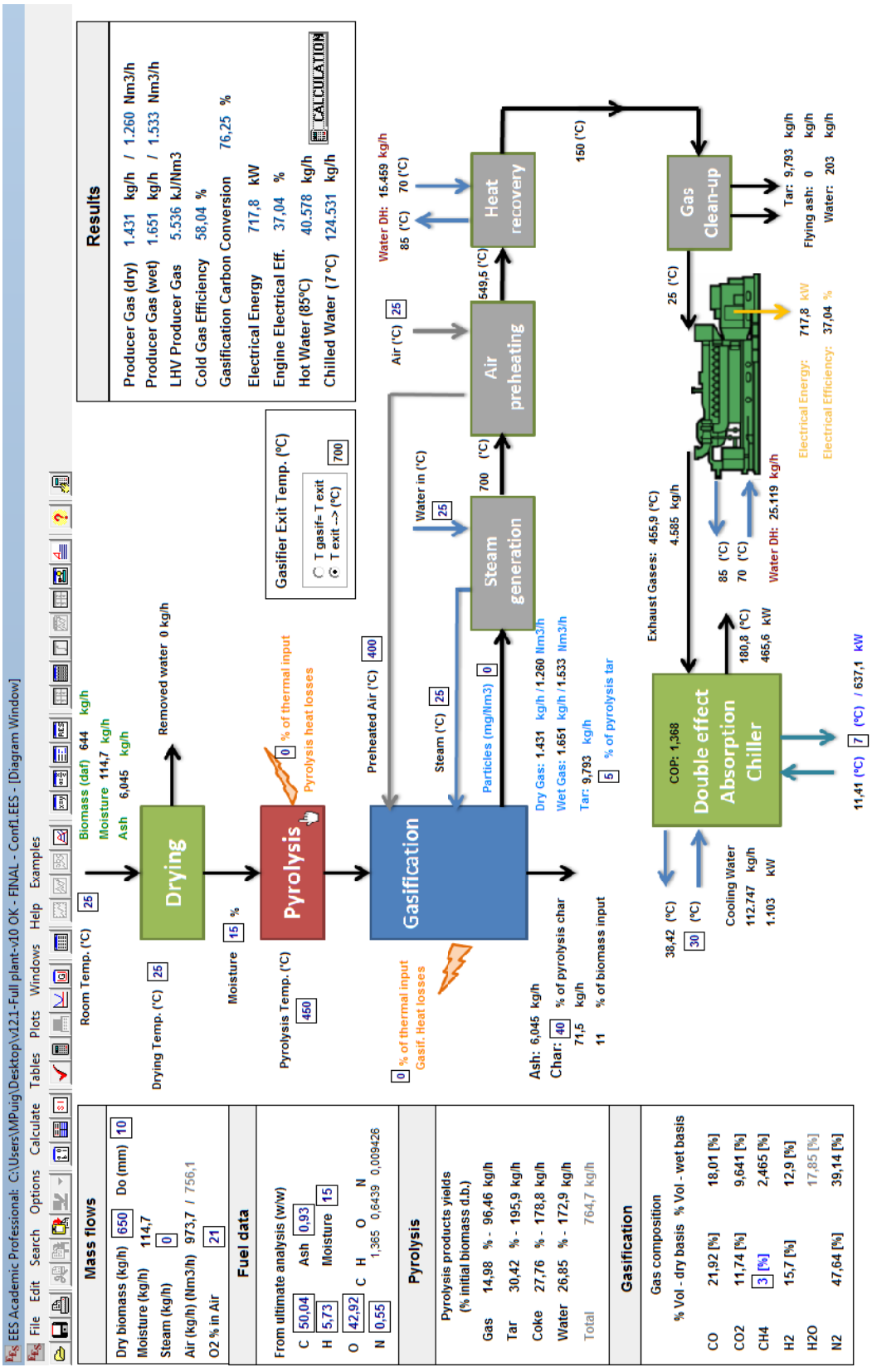


Figure 6.8: First configuration of the biomass gasification trigeneration plant implemented in EES software.

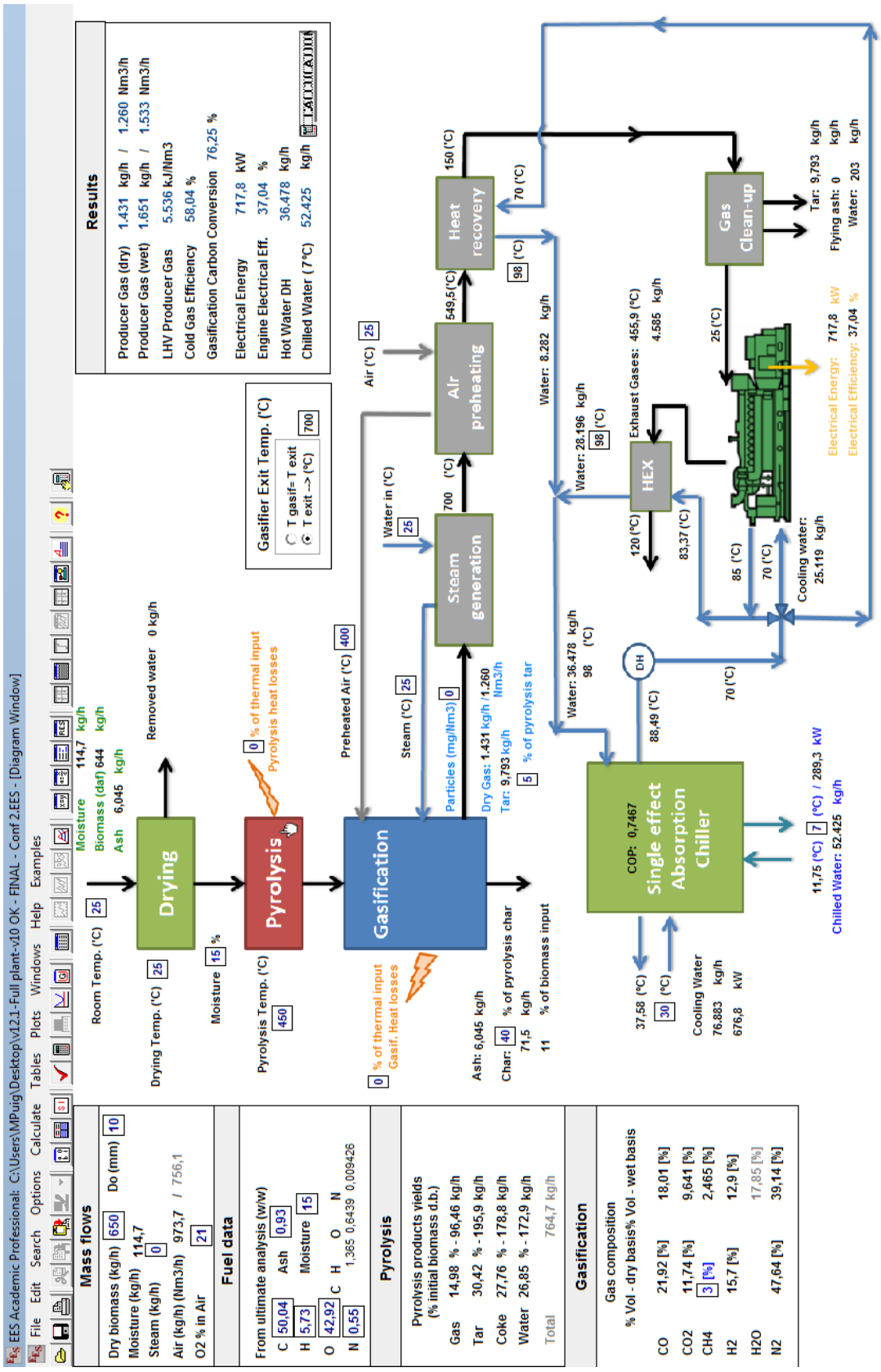


Figure 6.9: Configuration 2 of the biomass gasification trigeneration plant implemented in EES software.

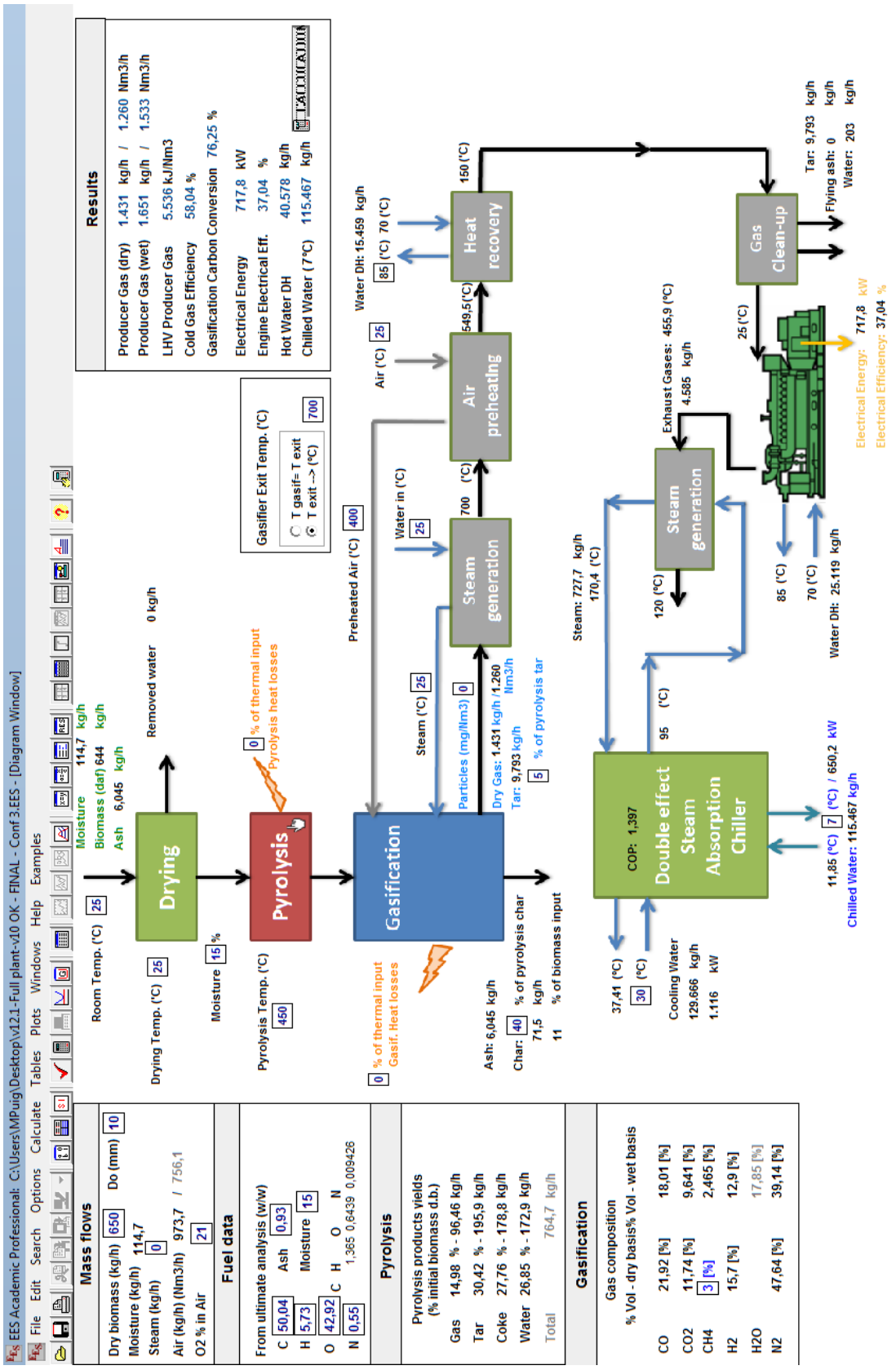


Figure 6.10: Configuration 3 of the biomass gasification trigeneration plant implemented in EES software.

Trigeneration primary energy savings (TPES) calculated according the procedure of Chicco and Mancarella (2007), considering different reference efficiency scenarios (Section 6.2.6.2), are presented in Figure 6.11. In the low efficiency scenario, trigeneration energy savings represent more than 15% in all cases, however for average and state of the art energy scenarios the values of TPES are negative.

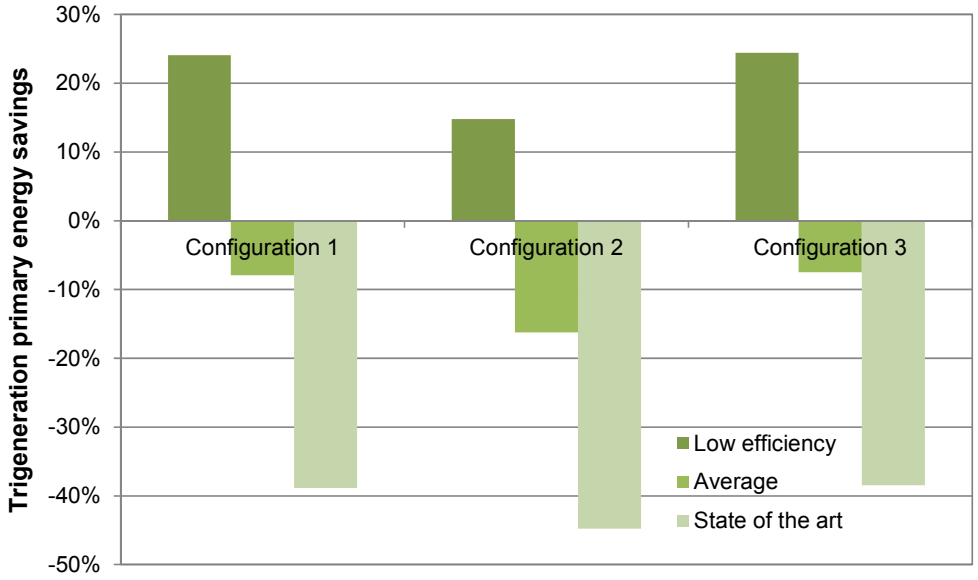


Figure 6.11: Trigeneration primary energy savings (TPES) for different energy efficiency scenarios and calculated according to Chicco and Mancarella (2007) procedure.

## 6.4 CONCLUSIONS

Little work has been done in the field of biomass gasification trigeneration plants neither in modelling nor in implementation. In this chapter, a whole small-medium size (250 $kW_e$ – 2 $MW_e$) biomass gasification trigeneration plant is modelled. The proposed trigeneration system contains four main units: a gasifier, an internal combustion engine, heat exchangers for heat recovery and an absorption chiller. In addition, three different configurations which differ in how heat from exhaust gases and cooling water from the engine jacket is recovered and used are considered. Due to the electrical size of interest all configurations considered include an internal combustion engine (ICE) coupled with an absorption chiller to produce heat and cold.

The three different configurations account for three different absorption chillers types: a single-effect hot water absorption chiller and two double-effect absorption chillers, one feed with exhaust gases and the other one with steam.

These configurations have been applied in a case study of the ST-2 plant to be implemented in Cerdanyola del Vallès in the framework of Polycity Project. The model has proved effective to simulate electricity generation and both the composition and gas production compared with the results given by Taim-Weser S.A. All three configurations have the same electricity generation while differ in heat and cold production. Configuration 2 with a single-effect absorption chiller has the highest production of heat for the district heating network but cold production is half of that obtained with the other two configurations. Considering REE all configurations have a REE higher than 27% which is the minimum required by law to be included in the Spanish special regimen production. Primary energy savings calculated according the Directive 2004/8/EC are, close to 10%, which means that all this configurations can be considered “high efficiency systems”. When calculating the trigeneration primary energy savings (TPES) following the procedure of Chicco and Mancarella (2007), TPES higher than 15% are obtained in all cases for a low efficiency scenario while for an average or state-of-the-art efficiency scenario the TPES are negative.

# Chapter 7

# Conclusions and further work

## 7.1 CONCLUSIONS

A reliable, affordable and clean energy supply is of major importance for society, economy and the environment. In this context, modern use of biomass (as opposed to traditional use) is considered a very promising clean energy option for reduction of greenhouse gas emissions. The promise includes a widely available, renewable and $CO_2$-neutral resource, suited for modern applications for power generation, fuels and chemicals. Biomass has a distinct advantage over the use of other renewables, like solar cells and wind power, which are restricted because of the intermittent power generation.

Gasification is a clean and highly efficient conversion process that offers the possibility to convert various feed stock to a wide variety of applications. It has the advantage over combustion of more efficient and better controlled heating, higher efficiencies in power production and the possibility to be applied for chemicals and fuel production. Gasification has been considered both in advanced applications in developed countries, as well as for rural electrification in developing countries. As such it has been considered the enabling technology for modern biomass use.

The recommended technologies for cogeneration plants depend on the size of the plant. For small scale plants (< 1$MW_e$) the best option are downdraft gasifiers combined with internal combustion engines while for medium scale plants (1-15 $MW_e$) fluidised bed gasifiers in combination with internal combustion engines or fuel cells and gas turbines (in a near future) are also a good option. Among the biomass gasification plants implemented in the last years, they are mainly small cogeneration plants using downdraft gasifiers with internal combustion engines.

While biomass gasification based cogeneration plants have been studied for years and several implemented plants exists; very few works have been published concerning biomass fuelled trigeneration systems and even less focused on trigeneration integrating biomass gasification. However, recent technological advancements and cost reductions of absorption chillers have made trigeneration more attractive. Trigeneration combined with DHC (District heating and cooling) network is of great interest for relatively warm climates.

The efficient operation of a biomass gasifier depends on a number of complex chemical reactions, including fast pyrolysis, partial oxidation of pyrolysis products, gasification of the resulting char, conversion of tar and lower hydrocarbons, and the water-gas shift reaction. These complicated processes, coupled with the sensitivity of the product distribution to the rate of heating and residence time in the reactor, required the development of mathematical models. Models of several different types have been developed for gasification systems, basically: kinetic, equilibrium and artificial neural networks. Equilibrium models are not computationally intensive, predict the maximum achievable yield of a desired product from a reacting system and thus are a useful tool for preliminary comparison. However, pure equilibrium models cannot give highly accurate results for all cases. Usually, they overestimate the yields of $H_2$ and CO, underestimate that of $CO_2$ and predict an outlet stream free from $CH_4$, tars and char.

In the present study, a new approach for a modified equilibrium model is implemented based on the previous pure equilibrium models developed by other authors. The aim of the model is to simulate the biomass gasification real process, in which only a partial approach to chemical equilibrium is achieved. The modifications introduced consist in:

- Adding a pyrolysis unit that, using correlations, predicts the formation of gas, char and volatiles in this step of the gasification process.

- Considering heat losses in pyrolysis and gasification units.
- Adding tar and char leaving the gasifier as a percentage of tar and char produced in the pyrolysis unit added.
- Particles leaving the gasifier and set by the user.
- Setting the amount of $CH_4$ produced.

The modified equilibrium model has been validated with published experimental data and also compared with the predictions of other authors' models. The model has proven to be accurate enough to predict the behaviour of downdraft and fluidised bed gasifiers for air gasification. In addition, it is also sensitive enough to evaluate the influence of ER, air preheating, steam injection, oxygen enrichment and biomass moisture content in the quality of producer gas. However, more experimental data is needed to evaluate the prediction capability of the model for air/steam biomass gasification in downdraft gasifiers.

Besides this modified equilibrium model, two artificial neural network (ANN) models have been developed for fluidised bed gasifiers based on experimental published data: one for air, atmospheric pressure CFB gasifiers and the second one for atmospheric pressure air and air-steam BFB gasifiers. The adjustments of ANN models with experimental data are better than for the modified equilibrium model. The root mean square error is reduced between 62 and 92.5% compared with the modified equilibrium model. In addition, the values of $R^2$ for all cases, in both models, are higher than 0.99 except $H_2$ for CFB model (0.977) and $CO_2$ for BFB (0.98).

The aim of developing these ANN models was to evaluate the suitability of these kind of models for biomass gasification because they have only been applied before in very few occasions. Considering that it is very scarce the literature that can be found on ANN models for biomass gasifiers, the results obtained with these ANN models are promising and show the great potential that they have in this field; especially considering the complexity of biomass gasification that includes many interdependent chemical reactions. In addition, they can be easily extended and improved when more data is available.

Because absorption chillers are a key element in trigeneration plants it is necessary to have reliable and simple models that can be implemented in detailed energy simulation and optimisation programmes. In this thesis, a new approach to the characteristic

equation method, based on the previous work of Kühn and Zigler (2005), has been developed. This approach provides similar results than the proposed by Kühn and Zigler (2005) and the parameters are also fitted according to a multiple regression fit. Data, usually given by manufacturer's for part-load operation ($T_{inG}$, $T_{oE}$, $T_{inAC}$), is directly used. The developed model avoids both the use of unrealistic, overly simple models based on constant COP for different operating conditions and the use of highly complicated models that require a thorough knowledge of the chiller design parameters.

The previously developed gasification and absorption chillers models have been integrated in a small-medium size trigeneration plant model. This trigeneration plant accounts for three different configurations. All configurations include a gasifier, a heat recovery section that uses the heat from producer gas for air preheating, steam and hot water generation, a gas clean-up section and an internal combustion engine (ICE) coupled with an absorption chiller to produce electricity, heat and cold. The main differences between the three configurations are in how heat from exhaust gases and cooling water from the engine jacket is recovered and used in the absorption chiller. Three different absorption chillers, one for each configuration, have been considered: a single-effect hot water driven absorption chiller and two double-effect absorption chillers, one driven by exhaust gases and the other one by steam. The ICE is modelled by means of correlations from part load manufacturer's data. These correlations allowed a better prediction than considering only fixed efficiency values.

These three biomass gasification trigeneration configurations have been applied in a case study of the ST-2 plant to be implemented in Cerdanyola del Vallès. The model has proven effective to simulate electricity generation and both the composition and gas production compared with the results given by a manufacturer of biomass gasification CHP plant (Taim-Weser S.A.). All three configurations have the same electricity generation while differ in heat and cold production. Configuration 2 with a single-effect absorption chiller has the highest production of heat for the district heating network but cold production is half of that obtained with the other two configurations. Considering REE all configurations have a REE higher than 27% which is the minimum required by law to be included in the Spanish special regimen of production. Primary energy savings calculated according the Directive 2004/8/EC are positive and close to 10%, which means that all this configurations can be considered "high efficiency

systems". When calculating the trigeneration primary energy savings (TPES), values higher than 15% are obtained in all cases for a low efficiency scenario while for an average or state-of-the-art efficiency scenario the TPES were negative.

In conclusion, it can be said that in this thesis, simple and reliable simulation tools have been developed in order to predict the behaviour of a biomass gasification trigeneration plant. The model allows the evaluation of the potential of trigeneration biomass gasification plants in a certain location and at a design stage, this model can easily evaluate and calculate the outputs of the trigeneration plant for different types of biomass, operating conditions and configurations. In addition, the developed model can be further integrated into bigger optimization models that accounts for different technologies and energy production configurations.

## 7.2 FURTHER WORK

Several aspects in the present thesis still require attention and they are worth mentioning in this section so as to encourage future research:

- The validation of the thermodynamic equilibrium model has been carried out using only published experimental data. It would be interesting to validate it with experimental data that could be obtained from the polygeneration plant ST2 to be implemented in Cerdanyola del Vallès or from another existing plant. In the same sense, it would be interesting to use this monitored data also to validate the trigeneration plant configurations and to improve the models and correlations already implemented.
- This thesis provides a good approach of the potential of ANN models for biomass gasification modelling. Considering that it is very scarce the literature that can be found on ANN models for biomass gasifiers, further research in this field can be done. In addition, to have a more robust ANN model for BFB and CFB gasifiers, it is necessary to enlarge the experimental database used for training. The new data should account for different operating conditions and biomasses in order to have enough points to cover the whole range and variability that wants to be modelled.

- Another aspect that could be further developed in the future is the integration of the biomass gasification model or the developed trigeneration configurations into optimization models. These optimization models can be used to select the optimal configuration and operation of an energy supply system considering the energy demand profile of the users as well as economical and environmental indicators. A modular environment was developed for this purpose in Ortiga (2010). This environment uses a user friendly interface where each unit of the energy supply system is defined as an independent block that can be connected with other blocks in order to define the energy supply system to be analyzed. The environment uses GAMS to solve the model and can be used to optimize the configuration, the operation or any other variable of the energy supply system (e.g. payback period, emissions, energy production) considering operational or legal constraints.

# Appendix I: Calculation of water-gas shift equilibrium constant

As stated in Chapter 1, the main reactions occurring in the gasification zone are:

- Methane reaction → $C + 2H_2 \leftrightarrow CH_4$
- Boudouard reaction → $C + CO_2 \leftrightarrow 2CO$ Eq. I.1
- Water-gas reaction → $C + H_2O \leftrightarrow CO + H_2$

Zainal et al. (2001), Jarungthammachote and Dutta (2007) and Higman and van der Burgt (2008) have stated that the Boudouard reaction and the water-gas reaction can be combined to give the water-gas shift reaction:

Water-gas shift reaction → $CO + H_2O \leftrightarrow CO_2 + H_2$ Eq. I.2

According to Jarungthammachote and Dutta (2007) and due to the requirements of equilibrium constant values for water-gas shift reaction, the following equations are used for the equilibrium state of ideal gas mixture:

$$\ln K = -\frac{\Delta G_T^o}{R \cdot T} \quad \text{Eq. I.3}$$

$$\Delta G_T^o = \sum_i \nu_i \Delta g_{f,T,i}^o \quad \text{Eq. I.4}$$

where the $R$ is the universal gas constant (8.314 kJ/(kmol·K)), $\Delta G^o_T$ is the standard Gibbs function of reaction, and $\Delta g^o_{f,T,i}$ represents the standard Gibbs function of formation at given temperature T of the gas species *i* which can be expressed by the empirical equation below:

$$\Delta g_{f,T,i}^o(kJ/kmol) = h_f^o - a' \cdot T \cdot \ln(T) - b' \cdot T^2 - \left(\frac{c'}{2}\right) \cdot T^3 - \left(\frac{d'}{3}\right) \cdot T^4 + \left(\frac{e'}{2 \cdot T}\right) + f' + g' \cdot T$$

Eq. I.5

The values of coefficients *a'-g'* and the enthalpy of formation of the gases are presented in Table I.1.

Table I.1: Values of $h_f^o$ (kJ/kmol) and coefficients of the empirical equation for $\Delta g_{f,T}^o$ (kJ/kmol) (Jarungthammachote and Dutta, 2007).

| | $h_f^o$ | a' | b' | c' | d' | e' | f' | g' |
|---|---|---|---|---|---|---|---|---|
| **CO** | -110.5 | $5.619 \cdot 10^{-3}$ | $-1.190 \cdot 10^{-5}$ | $6.383 \cdot 10^{-9}$ | $-1.846 \cdot 10^{-12}$ | -489.1 | 0.8684 | -0.06131 |
| **$CO_2$** | -393.5 | $-1.949 \cdot 10^{-2}$ | $3.122 \cdot 10^{-5}$ | $-2.448 \cdot 10^{-8}$ | $6.946 \cdot 10^{-12}$ | -489.1 | 5.270 | -0.1207 |
| **$H_2O$** | -241.8 | $-8.950 \cdot 10^{-3}$ | $-3.672 \cdot 10^{-6}$ | $5.209 \cdot 10^{-9}$ | $-1.478 \cdot 10^{-12}$ | 0.0 | 2.868 | -0.01722 |
| **$CH_4$** | -74.8 | $-4.620 \cdot 10^{-2}$ | $1.130 \cdot 10^{-5}$ | $1.319 \cdot 10^{-8}$ | $-6.647 \cdot 10^{-12}$ | -489.1 | 14.11 | -0.2234 |

In their work, Zainal et al. (2001) also give an equation for calculating $K_1$ equilibrium constant:

$$\ln K_1 = \frac{5870.53}{T} + 1.86 \cdot \ln T - 2.7 \cdot 10^{-4} \cdot T - \frac{58200}{T^2} - 18.007 \qquad \text{Eq. I.6}$$

Another expression to calculate $K_1$ is given in Bentzen and Gøbel (1995):

$$1/K_1 = (0.000001303 \cdot T + 0.000717) \cdot T - 1.3006 \qquad \text{Eq. I.7}$$

And by Gómez-Barea and Leckner (2010):

$$K_1 = 0.029 \exp(4094/T) \qquad \text{Eq. I.8}$$

This last one is similar to the one given by de Souza-Santos (1989):

$$K_1 = 0.0265 \exp(3958/T) \qquad \text{Eq. I.9}$$

The $K_1$ values for different gasification temperatures were calculated and checked for these five approaches and compared with the ones that appear in Basu (2005), Knoef (2005) and Callaghan (2006) in Figure I.1 and Figure I.2. The five approaches gave

almost the same results and they are in agreement with the values found in the literature cited (Figure I.3).

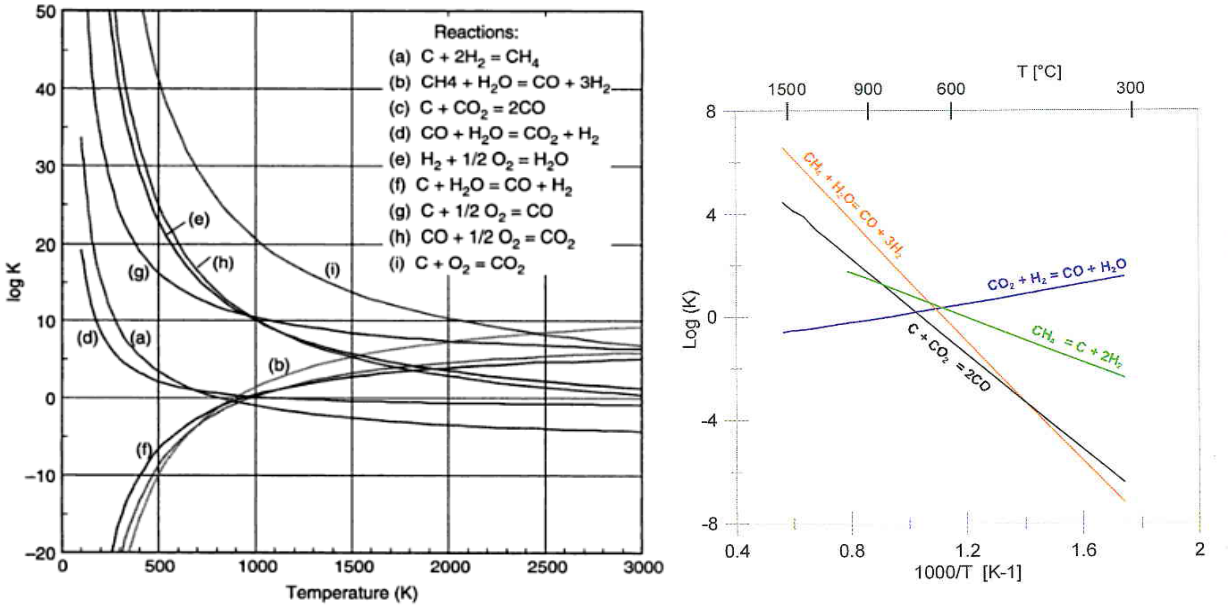


Figure I.1: Calculated equilibrium constants for a number of gasification reactions versus temperature (source: Basu, 2006) (left). Equilibrium constants of various reactions versus temperature (source: Knoef, 2005) (right)

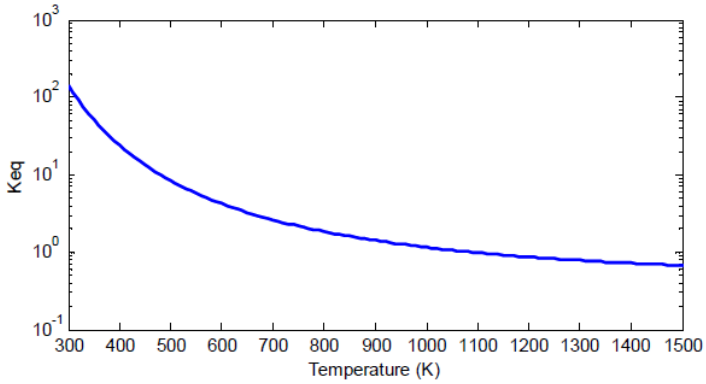


Figure I.2: Equilibrium constant of water-gas shift reaction as function of temperature (source: Callaghan, 2006)

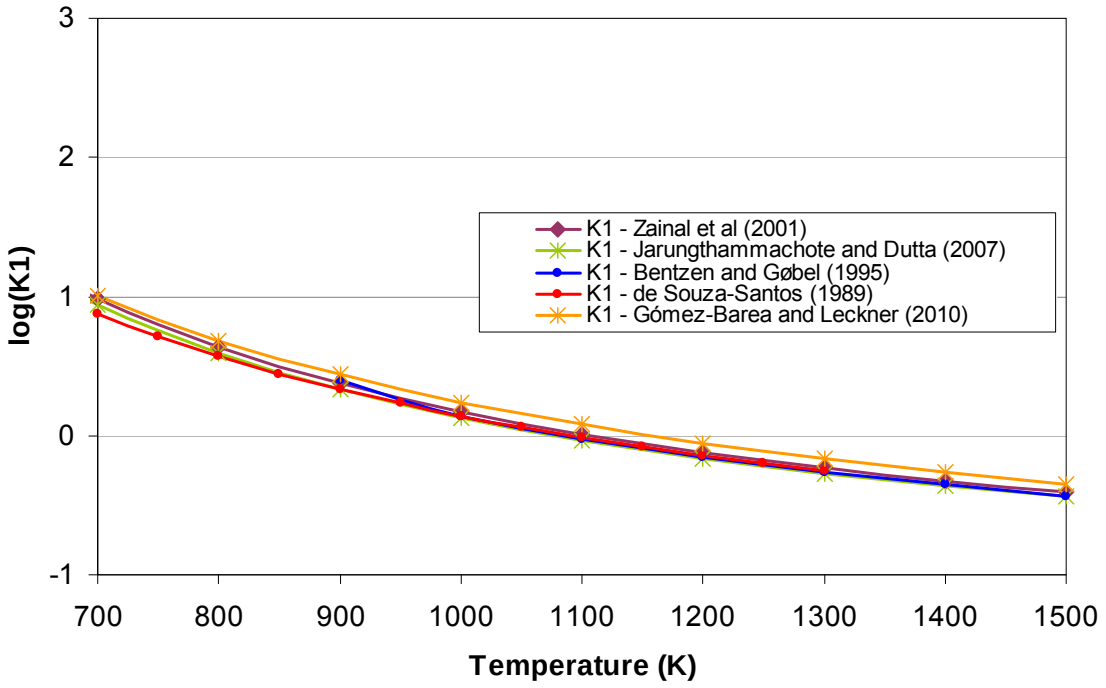


Figure I.3: Equilibrium constant $K_1$ calculated for several gasification temperatures using the approaches of Zainal et al. (2001), Jarungthammachote and Dutta (2007), Bentzen and Gøbel (1995), Gómez-Barea and Leckner (2010) and de Souza-Santos (1989).

In order to calculate the equilibrium constant for methane reaction Jarungthammachote and Dutta (2007) procedure, described previously, can be used; and also the expression given by Zainal et al. (2001):

$$\ln K_2 = \frac{7082.848}{T} - 6.567 \cdot \ln T - \frac{7.466 \cdot 10^{-3}}{2} \cdot T + \frac{-2.164 \cdot 10^{-6}}{6} \cdot T^2 + \frac{0.701 \cdot 10^{-5}}{2 \cdot T^2} + 32.541$$

Eq. I.10

The results given by both approaches give very similar values (Figure I.4) and are also in good agreement with the published data of Basu (2006) and Knoef (2005) (Figure I.1).

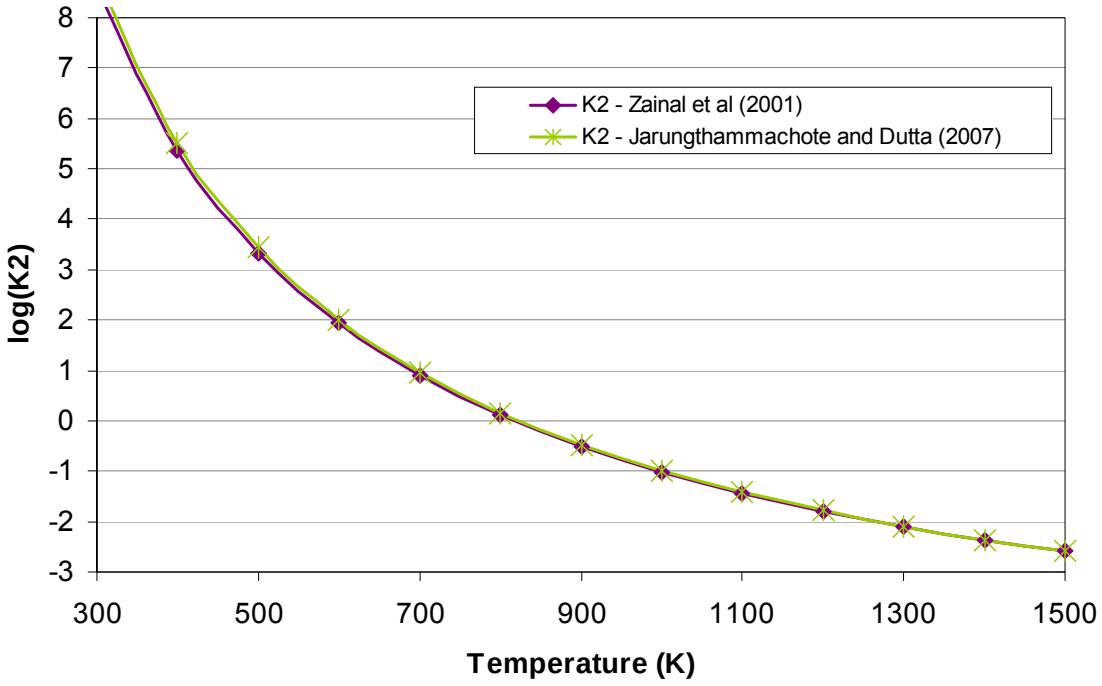


Figure I.4: Equilibrium constant $K_2$ calculated for several gasification temperatures using the approaches of Zainal et al. (2001) and Jarungthammachote and Dutta (2007).

# Appendix II: Tar specific enthalpy calculation

This annex describes how the pyrolysis tar enthalpy is determined using Jobaks method. It is assumed that pyrolysis tar only consists of seven organic compounds: benzene, toluene, phenol, guaiacol, methylguaiacol, ethylguaiacol and isoeugenol (Fock and Thomsen, 1999).

In Jobaks method, they split the organic compounds in individual groups. The individual groups used are:

- Individual groups that don't have a ring structure: -OH, -O-, $-CH_3$, $>CH_2$, =CH and $=CH_2$
- Single groups that have a ring structure: =CH- and =C<.

The specific heat capacity of an organic compound can be found using the following expression (Reid et al., 1987):

$$Cp = \left(\sum_j [(n_j \cdot \Delta_a]) - 37.93\right) + \left(\sum_j [(n_j \cdot \Delta_b]) + 0.210\right) \cdot T + \left(\sum_j [(n_j \cdot \Delta_c]) - 3.91 \cdot 10^{-4}\right) \cdot T^2 + \left(\sum_j [(n_j \cdot \Delta_d]) - 2.06 \cdot 10^{-7}\right) \cdot T^3$$

Eq. II.1

T is temperature in Kelvin, $n_j$ is the number of individual groups of type j, and $\Delta_a$, $\Delta_b$, $\Delta_c$ and $\Delta_d$ are constants for the respective single groups. The constants can be found as tabulated values in Reid et al. (1987) and these values are presented in the table below (Table II.1), together with the constant $\Delta_H$ and the molar mass of the utilized single groups:

Table II.1: Constants and molar mass for individual groups (Reid et al., 1987)

| | | $\Delta_a$ | $\Delta_b$ | $\Delta_c$ | $\Delta_d$ | $\Delta_H$ | Molar mass |
|---|---|---|---|---|---|---|---|
| **Groups with ring structure** | **=CH-** | -2,14 | 0,0574 | -0,00000164 | -1,59E-08 | 2090 | 13 |
| | **=C<** | -8,25 | 0,101 | -0,000142 | 6,78E-08 | 46430 | 12 |
| **Groups without ring** | **-OH** | -2,8 | 0,111 | -0,000116 | 4,94E-08 | -221650 | 17 |
| | **-O-** | 25,5 | -0,0632 | 0,000111 | -5,48E-08 | -132220 | 16 |
| | **$-CH_3$** | 19,5 | -0,00808 | 0,000153 | -9,67E-08 | -76450 | 15 |

| | | | | | | | |
|---|---|---|---|---|---|---|---|
| **structure** | **>CH$_2$** | -0,909 | 0,0095 | -5,44E-05 | 1,19E-08 | -20640 | 14 |
| | **=CH-** | -8 | 0,105 | -9,63E-05 | 3,56E-08 | 37970 | 13 |
| | **=CH$_2$** | 23,6 | -0,0381 | 0,000172 | -1,03E-07 | -9630 | 14 |

The following table (Table II.2) shows the number of individual groups included in each of the seven components considered in tar.

Table II.2: Number of individual groups in each of the seven tar components considered

| **$n_j$** | **=CH-** | **=C<** | **-OH** | **-O-** | **-CH3** | **>CH2** | **=CH-** | **=CH2** |
|---|---|---|---|---|---|---|---|---|
| **Benzen** | 6 | | | | | | | |
| **Toluen** | 5 | 1 | | | 1 | | | |
| **Phenol** | 5 | 1 | 1 | | | | | |
| **Guaiacol** | 4 | 2 | 1 | 1 | 1 | | | |
| **Methylguaiacol** | 3 | 3 | 1 | 1 | 2 | | | |
| **Ethylguaiacol** | 3 | 3 | 1 | 1 | 2 | 1 | | |
| **Isoeugenol** | 3 | 3 | 1 | 1 | 1 | 1 | 1 | 1 |

Accordingly, the specific heat capacity (J/mol·K) calculated for the seven substances at any temperature can be seen in the following table (Table II.3).

Table II.3: Calculated specific heat capacity (J/mol·K) for the seven substances included in tar.

| **T (K)** | **Benzen** | **Toluen** | **Phenol** | **Guaiacol** | **Methylguaiacol** | **Ethylguaiacol** | **Isoeugenol** |
|---|---|---|---|---|---|---|---|
| **100** | 0.77 | 17.83 | 4.89 | 42.18 | 59.24 | 67.30 | 70.15 |
| **200** | 44.96 | 65.86 | 57.78 | 95.54 | 116.43 | 132.44 | 140.68 |
| **300** | 82.46 | 107.29 | 100.45 | 140.33 | 165.17 | 188.18 | 200.61 |
| **400** | 113.93 | 142.72 | 134.36 | 177.63 | 206.41 | 235.56 | 251.16 |
| **500** | 140.05 | 172.73 | 160.98 | 208.47 | 241.15 | 275.63 | 293.56 |
| **600** | 161.46 | 197.90 | 181.77 | 233.91 | 270.36 | 309.44 | 329.03 |
| **700** | 178.83 | 218.82 | 198.18 | 255.02 | 295.01 | 338.03 | 358.79 |
| **800** | 192.84 | 236.08 | 211.69 | 272.85 | 316.09 | 362.46 | 384.07 |
| **900** | 204.14 | 250.26 | 223.75 | 288.45 | 334.56 | 383.77 | 406.10 |
| **1000** | 213.39 | 261.94 | 235.82 | 302.87 | 351.42 | 403.01 | 426.09 |
| **1100** | 221.26 | 271.72 | 249.37 | 317.18 | 367.63 | 421.24 | 445.28 |
| **1200** | 228.42 | 280.17 | 265.87 | 332.42 | 384.17 | 439.49 | 464.89 |
| **1300** | 235.52 | 287.89 | 286.76 | 349.66 | 402.03 | 458.83 | 486.14 |

Enthalpy of formation can be calculated using the following expression (Reid et al., 1987)

$$\Delta h^{o}_{298K} = 68290 + \sum_{j} n_j \cdot \Delta_H \qquad \text{Eq. II.2}$$

Specific enthalpy at any temperature in (J/mol) can then be found from enthalpy of formation and the specific heat capacities:

$$dh = C_p \cdot dT \qquad \text{Eq. II.3}$$

$$\int_{h_o}^{h} dh = \int_{298}^{T} C_p \cdot dT \qquad \text{Eq.II.4}$$

$$h = h^o + \left(\sum_j [(n_j \cdot \Delta_a]) - 37.93\right) \cdot (T - 298) + \frac{1}{2} \cdot \left(\sum_j [(n_j \cdot \Delta_b]) + 0.210\right) \cdot (T^2 - 298^2) + \frac{1}{3} \cdot \left(\sum_j [(n_j \cdot \Delta_c]) - 3.91 \cdot 10^{-4}\right) \cdot (T^3 - 298^3) +$$
$$+ \frac{1}{4} \cdot \left(\sum_j [(n_j \cdot \Delta_d]) - 2.06 \cdot 10^{-7}\right) \cdot (T^4 - 298^4) \qquad \text{Eq. II.5}$$

Table II.4: Specific Enthalpy of the seven tar components at different temperatures in J/mol

| | Specific enthalpies | | | | | | |
|---|---|---|---|---|---|---|---|
| **T (K)** | **Benzen** | **Toluen** | **Phenol** | **Guaiacol** | **Methylguaiacol** | **Ethylguaiacol** | **Isoeugenol** |
| **100** | 72225 | 35982 | -107496 | -279353 | -315595 | -339360 | -236153 |
| **200** | 74570 | 40224 | -104271 | -272391 | -306737 | -329290 | -225518 |
| **300** | 80994 | 48934 | -96280 | -260530 | -292591 | -313185 | -208370 |
| **400** | 90861 | 61482 | -84472 | -244574 | -273953 | -291932 | -185708 |
| **500** | 103602 | 77298 | -69650 | -225220 | -251525 | -266316 | -158409 |
| **600** | 118714 | 95867 | -52470 | -203060 | -225907 | -237015 | -127227 |
| **700** | 135759 | 116736 | -33442 | -178582 | -197605 | -204602 | -92794 |
| **800** | 154368 | 139509 | -12931 | -152165 | -167024 | -169548 | -55619 |
| **900** | 174237 | 163849 | 8847 | -124086 | -134474 | -132215 | -16089 |
| **1000** | 195127 | 189478 | 31819 | -94515 | -100165 | -92863 | 25532 |
| **1100** | 216869 | 216174 | 56060 | -63516 | -64211 | -51647 | 69102 |
| **1200** | 239356 | 243777 | 81791 | -31048 | -26628 | -8615 | 114602 |
| **1300** | 262550 | 272183 | 109380 | 3035 | 12667 | 36288 | 162135 |

An average tar enthalpy can be found (Table II.5) out from the enthalpy for the seven compounds (Table II.4) considering the mol distribution determined by Larsen (1999) for pyrolysis. The experiments of Larsen (1999), cited by Fock and Thomsen (2000) indicate that benzene and toluene each represent around 4% while the five phenols

constituting approx. 55% of light tar. The seven compounds are in most cases combined minimum one quarter of the total quantity of tar.

Table II.5: Specific enthalpy of tar in J/mol and J/g

| T (ºC) | J/mol | J/g |
|---|---|---|
| **100** | -229348 | -1758 |
| **200** | -221816 | -1701 |
| **300** | -208914 | -1602 |
| **400** | -191501 | -1468 |
| **500** | -170330 | -1306 |
| **600** | -146042 | -1120 |
| **700** | -119166 | -914 |
| **800** | -90123 | -691 |
| **900** | -59222 | -454 |
| **1000** | -26661 | -204 |
| **1100** | 7471 | 57 |
| **1200** | 43196 | 331 |
| **1300** | 80647 | 618 |

If these enthalpies are plotted against the temperature, a correlation can be obtained to calculate the specific enthalpy of tar (Temperature in ºC) (Figure II.1).

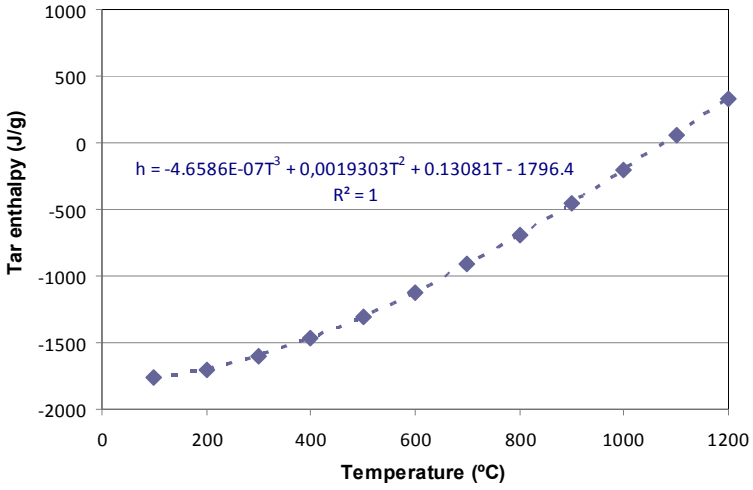


Figure II.1: Tar specific enthalpy as function of the temperature.

# Appendix III: Calculation of pyrolysis' yields correlations

Pyrolysis is not only an independent conversion technology but also part of the gasification process, which can be broadly separated into two main stages, solid devolatilization (pyrolysis) and char conversion (combustion and gasification). Devolatilization is a key conversion stage during gasification and combustion of biomass fuels. Pyrolysis of ligno-cellulosic biomass is a very complex process of interdependent reactions; nevertheless it can be reduced to the reaction illustrated in Figure III.1, universally known as the Broido-Shafizadeh mechanism (Broido, 1976; Varhegyi et al. 1994). Knowledge of yields and composition of volatiles is especially relevant for high volatile fuels such as biomass and waste. When biomass is devolatilized, light gases and tars represent 70–90 wt.% of the total mass fed, whereas only 10–30 wt.% is char (Neves et al., 2009).

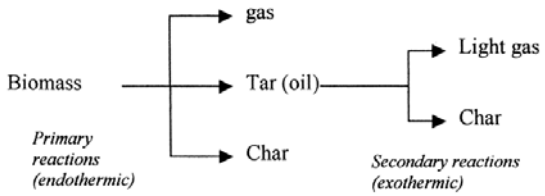


Figure III.1: Overall reaction mechanism of pyrolysis.

Secondary reactions are related to the thermal degradation of volatile tars. Strong interactions occur during secondary reactions. Thus, it is well established, that more solid char is formed if the volatile compounds constituting tar are confined within the solid matrix, by increasing the pressure or by slowing down the heating rate.

The distinction is commonly made between flash (or fast) pyrolysis and slow pyrolysis. Flash pyrolysis is performed on a finely-ground material at a high heating rate (500 to 1000ºC/min) and the yield in tar products can be as high as 60–70% without char formation. Slow pyrolysis is performed on a coarse material or at low heating-rates yielding a solid char of up to 35%.

Given a certain biomass, the ratio between the yields of solid char and volatile pyrolysis products depends on the particle size, temperature, pressure and heating rate (Nunn et al. 1985; Thunman et al., 2001). Char reactivity, in the second stage, is dependent upon the formation conditions (essentially temperature and heating rate) and the amount and composition of the inorganic content. In addition, the type of biomass (chemical composition and physical properties) also largely affects both biomass devolatilization and char conversión (Di Blasi, 1999). As a result of the many factors involved, theoretical prediction of devolatilization is complex. Recent reviews include detailed discussion of the various factors affecting the devolatilization behaviour of fuel particles in both lab devices (Neves et al., 2009; Di Blasi, 2008; Kersten et al., 2005, Gomez-Barea and Leckner, 2010) and commercial fluidized beds (Gomez-Barea and Leckner, 2010). Despite a considerable effort has been made on modeling of devolatilization processes (Chan et al., 1985; Agarwal et al., 1986; Peters and Bruch, 2003), an experimental approach is mostly used when facing the prediction of reactor performance in biomass combustion and gasification (Gomez-Barea and Leckner, 2010). Simplified (pseudo-empirical) models are used to estimate the time of complete devolatilization, the yields of char, tar and volatiles and the composition of volatiles, by empirical relations based on experimental data together with mass balances (Thunman et al., 2001).

Various types of laboratory equipments have been used, in the literature, to characterize devolatilization, including: packed bed furnace (Di Blasi et al., 2008), thermogravimetric apparatus (TGA) (Raveendran et al. 1996; Rao and Sharma, 1998), drop or FB (van den Aarsen, 1985; Jand and Foscolo, 2005; Jiang and Morey, 1992) and other devices such as tube reactor, heated-grid furnace, etc.

In order to obtain the correlations for predicting the yields of char, tar and volatiles produced during the pyrolysis and also to determine the composition of the light gas as a function of the pyrolysis temperature, the experimental data published by several authors has been reviewed. The data found in the literature for biomass pyrolysis can be generally classified in three groups: flash pyrolysis (usually in fluidised beds), conventional pyrolysis (slow or moderate heating rates / packed-bed) and pyrolysis in fluidised bed.

## III.1 CORRELATIONS FOR MODELLING BIOMASS FLASH PYROLYSIS

Generally, flash pyrolysis is used to maximize high-grade bio-oil production from biomass. After cooling and condensation, a dark brown mobile liquid is formed which has a heating value about half that of conventional fuel oil (Bridgwater, 2004). The essential principles to obtain high yields of bio-oils include moderate pyrolysis temperature (~500ºC), very high heating rates ($10^3$–$10^5$ºC/s), short vapour residence times (<2 s) to minimise secondary reactions and rapid quenching of pyrolysis (Qiang et al., 2009). A number of pyrolysis reactors have been developed that include bubbling fluidised bed, transport bed, circulating fluidised bed, rotating cone, vacuum pyrolysis reactor, ablative reactor, and screw reactor.

In Figure III.2 the yields (percentage of the initial solid biomass in dry basis) of char, gas and liquid/condensate (tars + water) produced during the flash pyrolysis of wood and reported by different authors are plotted (Scott et al., 1988; Toft, 1996; Horne and Williams, 1996; Beaumont and Schwob, 1984). Scott et al. (1988) pyrolysed eastern red maple sawdust (0.6 mm thick) in a fluidised bed in a temperature range of 450-900ºC and volatile residence times of about 0.5s. Horne and Williams (1996) pyrolysed mixed wood waste in a fluidised bed reactor in a temperature range between 400 and 550ºC with a residence time of the pyrolytic vapours in the hot reactor of about 2.5s at a pyrolysis temperature of 500ºC. Beaumont and Schwob (1984) pyrolysed beech wood sawdust in an experimental setup that allowed pyrolysis of wood particles in a gaseous sweeping steam. The plotted data from Toft (1996) corresponds to a compilation of published data for typical products from fast pyrolysis of wood.

From Figure III.2 it can be observed that the tendencies of data from different authors are in good agreement specially the ones from Scott et al. (1988) and Toft (1996). Maximum liquid yields are obtained at reaction temperatures around 500ºC. The char yield is reduced as the pyrolysis temperature increases. The char yields reported by Horne and Williams (1996) are higher than the others. This difference is probably due to the fact that a mixed wood waste was used in this work rather than a single known biomass feedstock. The decrease in the char yield with increasing temperature could be due either to greater primary decomposition of the wood at higher temperatures or to secondary decomposition of the char residue. The gaseous product yield increases with pyrolysis temperature. It is thought to be predominantly due to secondary cracking of the pyrolysis vapours at higher temperatures.

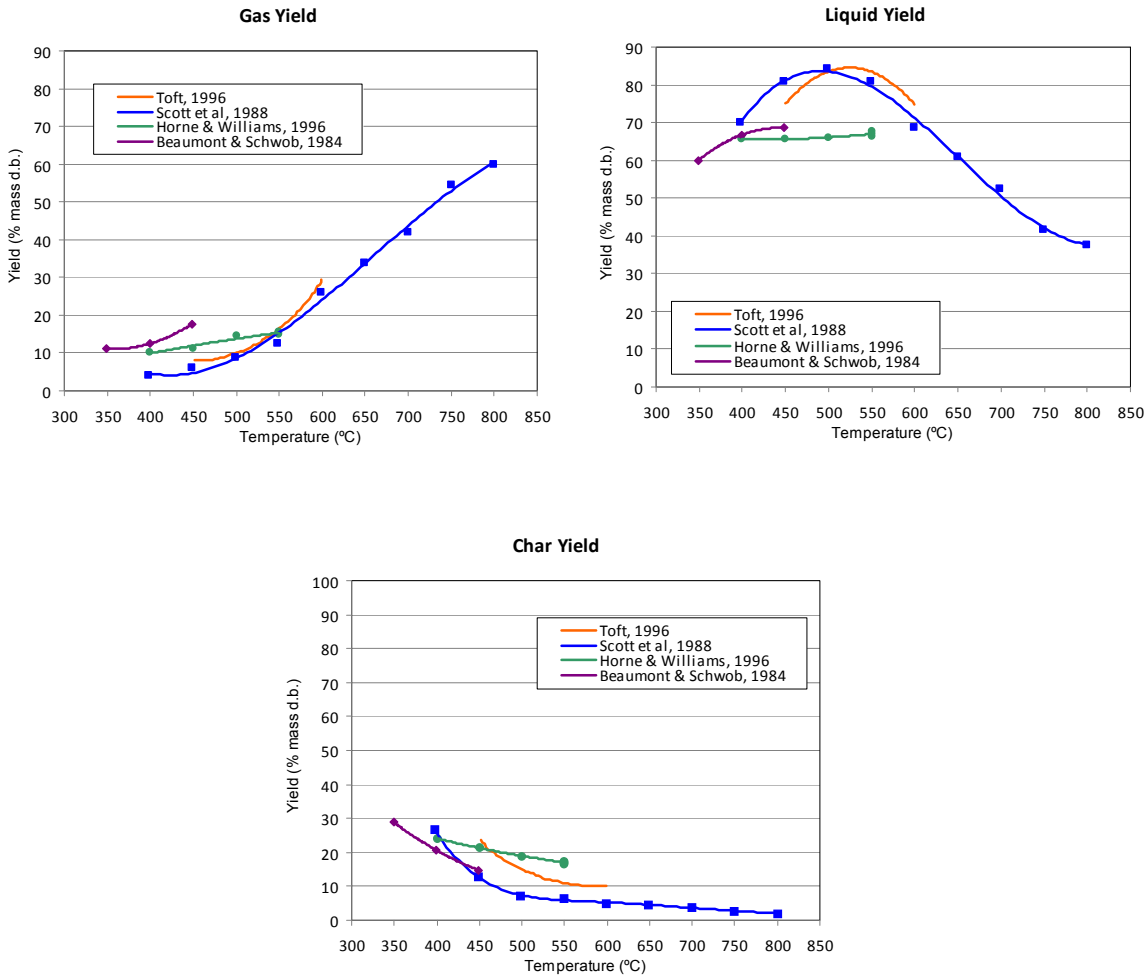


Figure III.2: Comparison data of wood chips flash pyrolysis from different authors (Scott et al., 1988; Toft, 1996; Horne and Williams, 1996; Beaumont and Schwob, 1984 ) for the gas, liquid and char yields as function of temperature.

## III.2 CORRELATIONS FOR MODELLING CONVENTIONAL PYROLYSIS (SLOW OR MODERATE HEATING RATES)

Slow pyrolysis is performed on a coarse material or at low heating-rates (typically 5–100ºC/min) and take place at temperatures typically between 300–700ºC and long residence times of the vapour phase products, which maximise the char yield (up to 35%). Such process conditions can be easily achieved in furnaces with various scales and shapes, such as fixed beds and rotary kilns.

In Figure III.3 the yields (percentage of the initial solid biomass in dry basis) of char, gas and liquid (tars + water) produced during slow or conventional pyrolysis of wood, and reported by different authors, are plotted (Di Blassi et al., 1999; Figueiredo et al., 1989; Fagbemi et al., 2001; Schröder, 2004). The experimental system of Di Blassi et al. (1999) established the conditions encountered by a thin ($4 \times 10^{-2}$ mm diameter) packed bed of fir wood chips particles suddenly exposed in a high-temperature environment in the range of 650-1000K. Figueiredo et al. (1989) pyrolysed holm-oak wood sawdust (0.40-2 mm diameter) with a range of temperatures between 300 and 900 °C in a fixed bed reactor. Fagbemi et al. (2001) pyrolysed wood cut into chips of 3 to 5 mm in thickness in a range of temperatures varying between 500 and 1000ºC. It can be observed that although the experimental conditions, i.e., wood type, particle size, heating rate and residence times, given in the literature for different studies are quite different, all of them are in good agreement. A rapid decrease of the char yield in the temperature range between 250 and 350ºC can be observed. Char, in this case, characterizes the unreacted or partially reacted solids remaining in the reactor. At temperatures above 350ºC, the char mass decreases more slowly. The decrease in mass results in an increase in tar and gases. At temperatures above 300ºC, the increase in tar yields becomes smaller than at lower temperatures. As it was observed for flash pyrolysis, the quantity of tar reaches a maximum value at about 500ºC then, drops with increasing temperature. At temperatures higher than 600ºC, the secondary reaction (i.e. tar cracking) prevails, leading to a larger amount of gas.

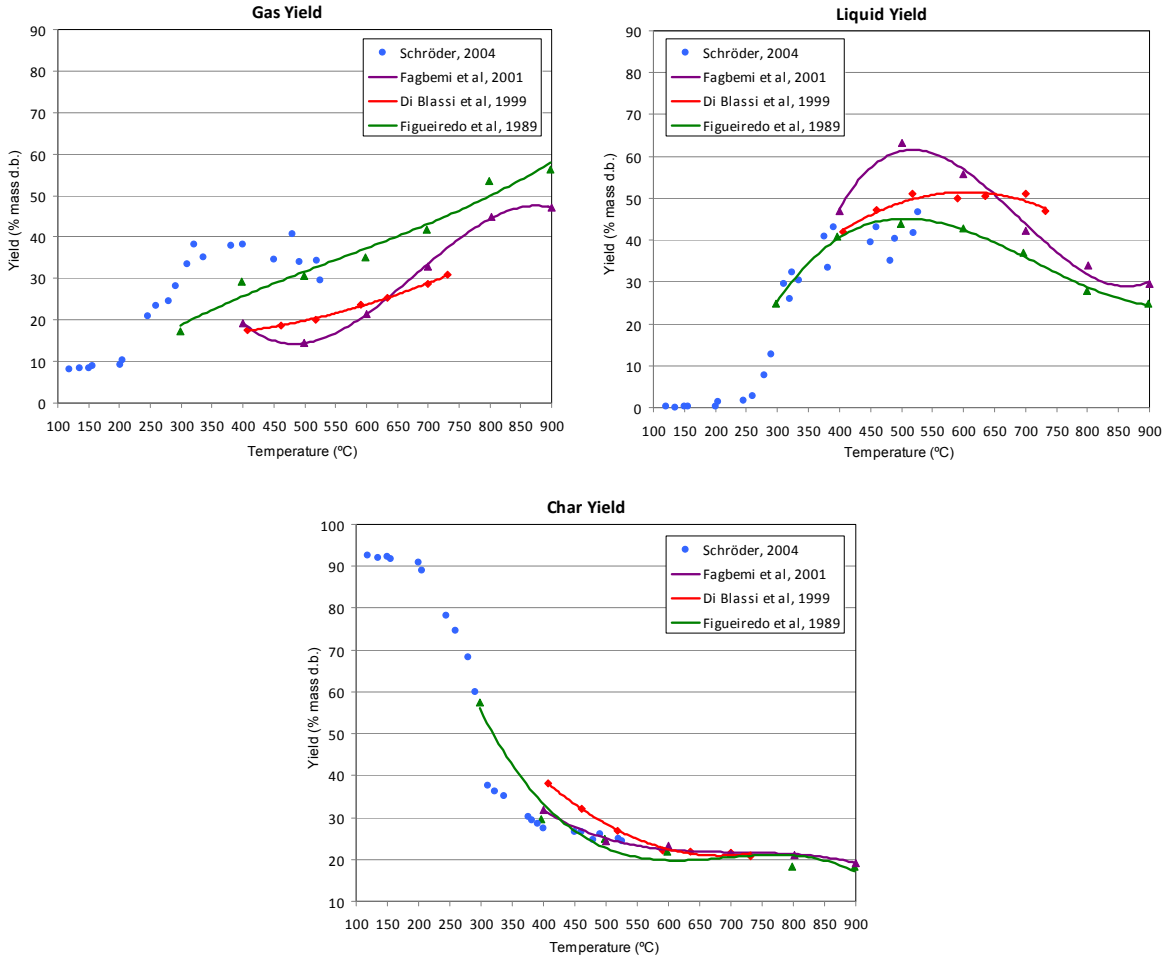


Figure III.3: Comparison data of wood chips conventional pyrolysis from different authors (Di Blassi et al., 1999; Figueiredo et al., 1989; Fagbemi et al., 2001; Schröder, 2004) for the gas, liquid and char yields as function of temperature.

Compared with Figure III.2, where product yields for flash pyrolysis are plotted, it can be seen that under flash pyrolysis conditions, liquid yields are maximised. This results from both primary volatile formation and secondary degradation of tar vapors becoming successively more favored by higher temperatures (Di Blasi et al., 1999).

Di Blasi et al. (1999) and Fabgemi et al. (2001) also studied the devolatilization behaviour of several agricultural residues typical of Mediterranean countries, such as olive husks, grape residues, wheat straw, and rice husks (Di Blasi et al.,1999) and coconut shell and straw (Fabgemi et al., 2001). The results obtained where compared with the ones for wood. For all of the biomasses, final product yields (expressed on a dry basis) as functions of temperature showed the same trends as those for wood, but

differences were quantitatively large. In comparison with wood, agricultural residues always gave rise to larger char yields. These findings were in qualitative agreement with previous studies, where the higher char yields observed for agricultural residues were attributed to the higher lignin (and carbon) contents (Zanzi et al., 1996) or to the presence of large amounts of inorganics which favour charring reactions (Scott et al., 1985). The maximum yield of tar product seems to depend greatly on the type of biomass. In both cases, the higher yield was for wood. According to Kosstrin (1980), the tar yield is closely related to the alphacellulose content of the material. Also in both studies, straw appears to yield more gas than the other tested bio-materials. The low thickness of the wall of the straw wisp, compared with the other bio-materials, results in higher heat-transfer, and hence a higher rate of pyrolysis, which is favourable to gas and tar production (Fagbemi et al., 2001).

In Figure III.4 the yields of the main gas components are plotted for the experimental data of Fagbemi et al. (2001) and Di Blassi et al. (1999). Both experimental data show similar tends. A regular decrease in $CO_2$ concentration with temperature occurs with a simultaneous increase in CO and $H_2$ concentration. High temperatures are known to favour the production of $H_2$ to the detriment of higher hydrocarbons (in C2, C3) which are dehydrogenated by thermal cracking. The evolution of CO and $CO_2$ concentrations are consistent particularly when considering the heterogeneous gas-solid reaction at thermodynamic equilibrium, i.e. $C+CO_2=2\ CO$; an increase in temperature results in a larger concentration in carbon monoxide (Fagbemi et al., 2001). The concentrations of $CH_4$ and $C_2H_x$ (not plotted) reached a maximum value at about 700ºC, that is in good agreement with the results of other investigators Déglise et al. (1980), who found values of $CH_4$ content of about 13–15% between 700 and 800ºC.

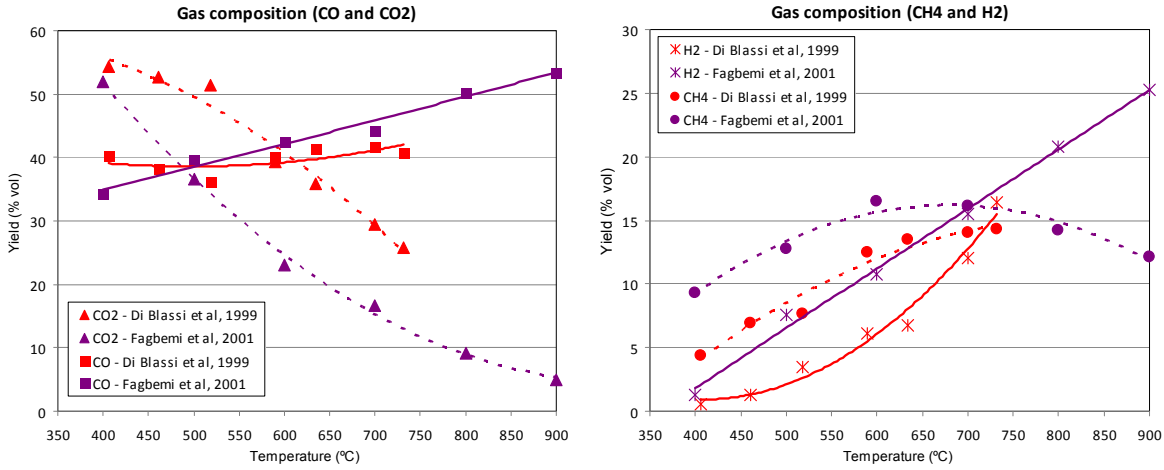


Figure III.4: Yields of the main gas components for wood chips conventional pyrolysis from different authors (Fagbemi et al., 2001; Di Blassi et al., 1999).

## III.3 CORRELATIONS FOR MODELLING BIOMASS PYROLYSIS IN A FLUIDISED BED

In order to predict the behaviour of FB gasifiers and combustors, pyrolysis and devolatilization data should be obtained at high temperature and heating rate using particle sizes in the range of the industrial application. Though, many studies have been undertaken in TGA, using low or moderate heating rates, or in applications of flash pyrolysis, where the heating rates are very high, and the temperature range of interest is from 300 to 700 °C (Neves, 2009; Di Blasi, 2008). In addition, in both cases the fuel particle size used for the experiments is fine, typically below 200 μm. In FB gasification and combustion, mm-sized particles are used, the temperature is higher (750–900 °C) than in flash pyrolysis and the heating rate may be higher than in TGA or other lab devices (100–1000°C/s). Therefore, when data are taken from TGA or flash pyrolysis to represent the behavior of biomass devolatilization in FB, some correction should be applied.

In their work, Gomez-Barea et al. (2010) studied the devolatilization behaviour of various biofuels (wood, meat and bone meal, compost and dried sewage sludge (DSS)) in a lab-scale fluidized bed between 750 and 900 °C. They determined the yields of char, condensate and light gas, the gas composition, as well as the time of conversion during devolatilization for the different fuels. The results obtained (Figure III.5), as expected (Jand and Foscolo, 2005; Hajaligol et al., 1982; Nunn et al., 1985;

Fagbemi et al., 2001), showed how the gas yield increases with temperature, whereas the condensate and char yield decrease for all fuels. Though, the char yields varied less with temperature than the condensate and gas yields. For wood, the decrease of the condensate yield with temperature was less pronounced than for the other materials, consistent with previous work (Di Blasi et al., 1999), arguing that the tar from wood is less reactive than tar from various agricultural residues.

The char yield from wood pellets was the highest, roughly 20 wt.%, whereas the MBM was the fuel with more gas release. For all the materials studied, the char yields obtained were close to the fixed carbon content (dry ash free basis) given by the proximate analysis. The char yield was expected to be closely related to the biomass composition, especially to the lignin content (Di Blasi et al., 1999; Antal et al., 2000) though, the presence of different inorganic species and physical properties, such as particle density and thermal conductivity, may also affect the product yields (Di Blasi, 1997). Concerning the volume fractions of the main species in the gas (Figure III.6) (CO, $CO_2$, $CH_4$ and $H_2$), wood gave higher CO concentrations and lower $CO_2$ concentrations in the gas than the other materials. These observations are in agreement with those given in (Di Blasi et al., 1999), where higher CO yields and lower $CO_2$ yields were measured for wood, compared to various agricultural residues. These authors also provided a simple way to numerically compute the char, tar and gas yields, as well as the individual yields of CO, $CO_2$, $CH_4$ and $H_2$ measured in this work by fitting these values to a quadratic function of temperature (T in °C).

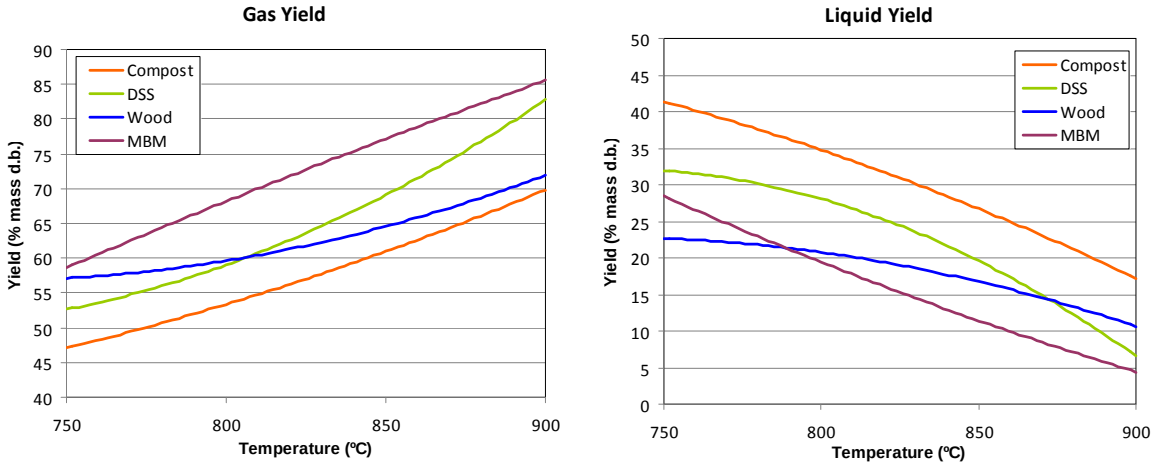

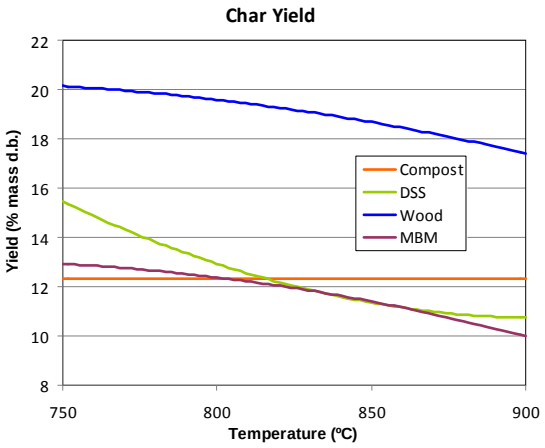


Figure III.5: Yields of char, liquid and gas obtained during the devolatilization of wood, MBM, DSS and compost in a fluidised bed (u=0.8m/s)

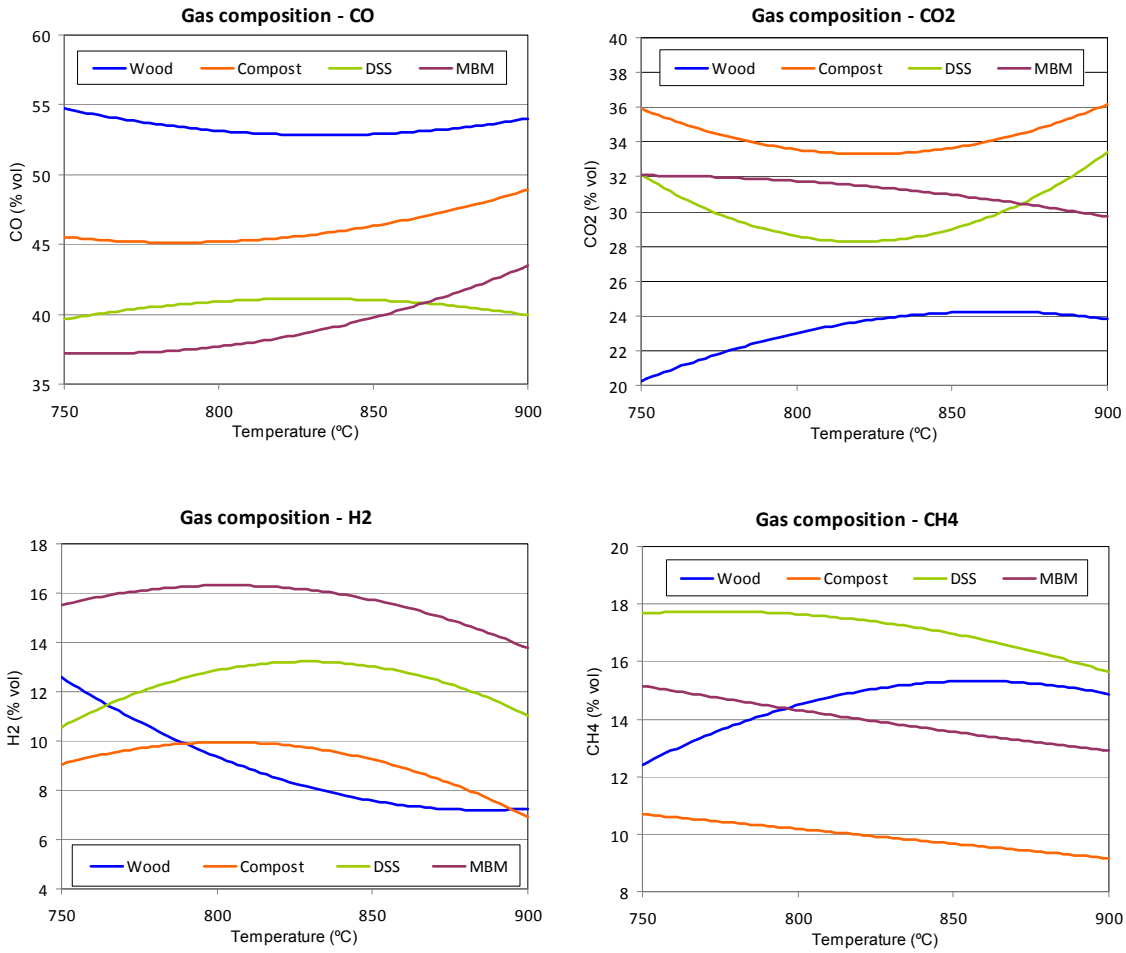


Figure III.6: Experimental composition of the main components in the gas (volume fraction): CO, $CO_2$, $CH_4$ and $H_2$ during the devolatilization of wood, MBM, DSS and compost in a fluidised bed (u=0.8m/s)

Once the review of different experimental data for biomass gasification has been done and due to the different yields on pyrolysis products obtained depending on the type of reactor and pyrolysis, at least two different kind of correlations have to be considered when modelling the pyrolysis unit. For this reason, in order to model the pyrolysis stage in a fixed bed reactor (downdraft, updraft…) the correlations obtained with the experimental data from Fagbemi et al. (2001) will be used. This experimental data has been selected because covers a wide range of temperatures and it is also in good agreement with the results obtained by the other authors.

If pyrolysis stage takes place in a fluidised bed, the correlations obtained by Gomez-Barea et al. (2010) will then be used. These correlations have been selected because they are the only ones for non-flash pyrolysis in fluidised bed that could be found in the literature. The model also gives the possibility not to use any of these correlations and to introduce the desired yields manually. It has also to be taken in account that only correlations for wood pyrolysis are considered in this model; however it is possible to extend the model including pyrolysis correlations for other kinds of biomass and agricultural residues.

The correlations used in the present unit are the following ones:

- Wood pyrolysis in a fluidised bed, correlations given by Gomez-Barea et al. (2010):

$$Gas\ yield(\text{mass\% d.b.}) = 311.10 - 351.45 \cdot \left(\frac{T_p}{T_{ref}}\right) + 121.43 \cdot \left(\frac{T_p}{T_{ref}}\right)^2$$

$$Char\ yield(\text{mass\% d.b.}) = -15.03 + 50.58 \cdot \left(\frac{T_p}{T_{ref}}\right) - 18.09 \cdot \left(\frac{T_p}{T_{ref}}\right)^2$$

$$Liquid\ yield(\text{mass\% d.b.}) = -196.07 + 300.86 \cdot \left(\frac{T_p}{T_{ref}}\right) - 103.34 \cdot \left(\frac{T_p}{T_{ref}}\right)^2 \qquad \text{Eq. III.1}$$

$$CO\ (\text{vol\%}) = 240.53 - 225.12 \cdot \left(\frac{T_p}{T_{ref}}\right) + 67.50 \cdot \left(\frac{T_p}{T_{ref}}\right)^2$$

$$CO_2(\text{vol\%}) = -206.86 + 267.66 \cdot \left(\frac{T_p}{T_{ref}}\right) - 77.50 \cdot \left(\frac{T_p}{T_{ref}}\right)^2$$

$$CH_4(\text{vol\%}) = -168.64 + 214.47 \cdot \left(\frac{T_p}{T_{ref}}\right) - 62.51 \cdot \left(\frac{T_p}{T_{ref}}\right)^2$$

$$H_2(\text{vol\%}) = 234.97 - 257.01 \cdot \left(\frac{T_p}{T_{ref}}\right) + 72.50 \cdot \left(\frac{T_p}{T_{ref}}\right)^2$$

Where $T_p$ is the pyrolysis temperature (ºC) and $T_{ref}$=500ºC

- Correlations for conventional pyrolysis of wood in a fixed bed reactor obtained from experimental data of Fagbemi et al. (2001):

$$Gas\ yield(\text{mass\% d.b.}) = -1.09 \cdot 10^{-6} \cdot T_p^{\,3} + 0.0022 \cdot T_p^{\,2} - 1.392 \cdot T_p + 288.534$$

$$Tar\ yield(\text{mass\% d.b.}) = 1.33 \cdot 10^{-6} \cdot T_p^{\,3} - 0.0028 \cdot T_p^{\,2} + 1.797 \cdot T_p - 339.139$$

$$Char\ yield(\text{mass\% d.b.}) = -6.6 \cdot 10^{-7} \cdot T_p^{\,3} + 0.00137 \cdot T_p^{\,2} - 0.93579 \cdot T_p + 230.5279$$

$$Water\ yield(\text{mass\% d.b.}) = 2.54 \cdot 10^{-7} \cdot T_p^{\,3} - 5.24 \cdot 10^{-4} \cdot T_p^{\,2} + 0{,}335 \cdot T_p - 40.883 \qquad \text{Eq. III.2}$$

$$CO(\text{vol\%}) = 0.0371 \cdot T_p + 19.961$$

$$CO_2(\text{vol\%}) = 0.000143 \cdot T_p^{\,2} - 0.27808 \cdot T_p + 139.948$$

$$H_2(\text{vol\%}) = 0.04694 \cdot T_p - 16.96286$$

# References

Agarwal, P.K.; Genetti, W.E.; Lee, Y.Y. (1986) Coupled drying and devolatilization of wet coal in fluidized beds. Chemical Engineering Science, 41: 2373–83.

Alanne, K.; Saari, A. (2004) Sustainable small-scale CHP technologies for buildings: The basis for multi-perspective decision-making. Renewable and Sustainable Energy Reviews, 8: 401-31.

Albers, J. (2002) TRNSYS type107-part load simulation of single staged absorption chillers in quasi steady states – contribution to a design tool for solar assisted air conditioning systems developed. In: IEA TASK25 Subtask B, Final Report. Forschungsbericht IEMB Nr. 2–67/2002 30. September 2002.

Albers, J.; Ziegler, F. (2008) Balancing the absorber and thermosyphon desorber capacity of a solar driven absorption chiller. International Sorption Heat Pump Conference, Seul, Korea, September 23-26, 2008.

Altafini, C.R.; Wander, P.R.; Barreto, R.M. (2003) Prediction of the working parameters of a wood waste gasifier through an equilibrium model. Energy Conversion and Management, 44: 2763-77.

Antal, M.J.; Allen, S.G.; Dai, X.; Shimizu, B.; Tam, M.S.; Grønli, M.G. (2000) Attainment of the theoretical yield of carbon from biomass. Industrial and Engineering Chemistry Research, 39: 4024–31.

Arena, U.; Di Gregorio, F.; Santonastasi, M. (2010) A techno-economic comparison between two design configurations for a small scale, biomass-to-energy gasification based system. Chemical Engineering Journal, 162: 580-90.

Aspen Plus – Aspen Technology, Inc., Cambridge, Massachusetts, USA.

Babu, B.V.; Sheth, P. (2005) Modeling & Simulation of Biomass Gasifier: Effect of Oxygen Enrichment and Steam-to-air Ratio. International Congress on Renewable Energy (ICORE-2005), Pune, India, January 20-22, 2005.

Babu, S.P. (2006) Work Shop No 1: Perspectives on Biomass Gasification. IEA Bioenergy Agreement. Task 33: Thermal Gasification of Biomass. May 2006.

Babu, B.V.; Sheth, P.N. (2006) Modeling and simulation of reduction zone of downdraft biomass gasifier: effect of char reactivity factor. Energy Conversion and Management, 47: 2602–11.

Bacon, D.W.; Downie, J.; Hsu, J.C.; Peters, J. (1982) Modeling of fluidized bed wood gasifiers. In: Overend, R.P.; Milne, T.A.; Mudge, L.K. (Eds.), Fundamentals of thermochemical biomass conversion. Elsevier, London, pp. 717–32.

Backham, L.; Croiset, E.; Douglas, P.L. (2003) Simulation of a coal hydrogasification process with integrated CO2 capture. Combustion Canada 2003;3A(4).

Bandi, A. (2003) Verfahrensübersicht – Gasreinigungsverfahren, FVS Fachtagung, 2003.

Baratieri, M.; Baggio, P.; Fiori, L.; Grigiante, M. (2008) Biomass as an energy source: Thermodynamic constrains on the performance of the conversion process. Bioresource Technology, 99: 7063-73.

Baratieri, M.; Baggio, P.; Bosio, B.; Grigiante, M.; Longo, G.A. (2009) The use of biomass syngas in IC engines and CCGT plants: a comparative analysis. Applied Thermal Engineering, 29: 3309-18.

Barker, R.E. (1983) ASPEN modeling of the tri-state indirect-liquefaction process. Oak Ridge National Laboratory, Oak Ridge, USA.

Basu, P. (2006) Combustion and gasification in fluidised beds. CRC Press – Taylor & Francis Group, Boca Raton, FO, USA.

Bauen A. (2004) Encyclopedia of energy, Biomass gasification. In: Cleveland, C.J. (Ed.) Elsevier.

Beaumont, O.; Schwob, Y. (1984) Influence of physical and chemical parameters on wood pyrolysis. Industrial and Engineering Process Design and Development, 23: 637-41.

Bentzen, J.D.; Gøbel, B. (1995) Dynamisk model af totrinsforgasningsprocessen, PE 95–13, Master Thesis, Department of Mechanical Engineering, Technical University of Denmark, Denmark.

Bentzen, J.D.; Brandt, P.; Gøbel, B.; Hansen, C.H.; Henriksen, U. (1998) 100kW Totrinsforgasningsanlæg på DTU Resultater til og med foråret 1998, ET-ES 98-11, Institut for Energiteknik, Technical University of Denmark, Denmark.

Bishop, C.M. (2002) Neural Networks for Pattern Recognition, Oxford University Press, New York, USA.

Brand, P.; Henriksen, U. (2000) Decomposition of tar in gas from updraft gasifier by thermal cracking. In: Kyritsis, S.; Beenackers, A.A.C.M.; Helm, P.; Grassi, A.; Chiaramonti, D. (Eds.) Proceedings of 1st World Conference and Exhibition on Biomass for Energy and Industry, 5-9 June 2000, Seville, Spain. James & James (Science Publishers) Ltd., London, UK.

Bridgwater, A.V. (1995) The technical and economic feasibility of biomass gasification for power generation. Fuel, 74: 631–53.

Bridgwater, A.V. (2002) Fast pyrolysis of biomass: Technical requirements for commercialisation. In Bridgwater, A.V. (Ed.) Pyrolysis and Gasification of Biomass and Waste. Proceedings of an Expert Meeting, CPL Press, Newbury, pp. 33 – 40.

Bridgwater, A.V. (2004) Biomass fast pyrolysis. Thermal Science, 8:21-49.

Broad (2004) Broad IX absorption chiller: model selection and design manual.

Broido A. (1976) Kinetics of solid-phase cellulose pyrolysis. In: Shafizadeh, F.; Sarkanen, K.V.; Tillman, D.A. (Eds.) Thermal uses and properties of carbohydrates and lignins. Academic Press, New York, pp. 19–35.

Brown, D.; Fuchino, T.; Marechal, F. (2006) Solid fuel decomposition modelling for the design of biomass gasification systems, In: Marquardt, W.; Pantelides, C. (Eds.) Computer Aided Chemical Engineering, Vol. 21, Part 2, 16th European Symposium on Computer Aided Process Engineering and 9th International Symposium on Process Systems Engineering, Elsevier, pp. 1661-66.

Brown, D.; Fuchino, T.; Marechal, F. (2007) Stoichiometric equilibrium modelling of biomass gasification: validation of artificial neural network temperature difference parameter regressions. Journal of Chemical Engineering of Japan, 40: 244-54.

Callaghan, C.A. (2006) Kinetics and catalysis of the water-gas-shift reaction: a microkinetic and graph theoretic approach. Ph.D. Thesis. Worcester Polytechnic Institute, Department of Chemical Engineering, Worcester, UK.

Campoy, M. (2009) Gasificación de biomasa y residuos en lecho fluidizado: estudios en planta piloto. Ph.D. Thesis. University of Seville, Seville, Spain.

Cardona, E.; Piacentino, A. (2005) Cogeneration: a regulatory framework toward growth. Energy Policy, 33: 2100-11.

Chan, W.-C.R.; Kelbon, M.; Krieger, B.B. (1985) Modelling and experimental verification of physical and chemical processes during pyrolysis of a large biomass particle. Fuel, 64: 1505–13.

Channiwala, S. A.; Parikh, P. P. (2002) A unified correlation for estimating HHV of solid, liquid and gaseous fuels. Fuel, 81: 1051-63.

Chee, C.S. (1987) The air gasification of wood chips in a gasifier bed. MSc Thesis, Kansas State University, USA.

Chen JS. (1987) Kinetic engineering modelling of co-current moving bed gasification reactors for carbonaceous material.Ph. D. thesis, Cornell University, New York, USA.

Chicco, G.; Mancarella, P. (2007) Trigeneration primary energy saving evaluation for energy planning and policy development. Energy Policy, 35: 6132-44.

Chinese, D.; Meneghetti, A.; Nardin, G. (2004) Diffused introduction of Organic Rankine Cycle for biomass-based power generation in an industrial district: a systems analysis. International Journal of Energy Research, 28: 1003-21.

Chinese, D.; Meneghetti, A. (2005) Optimisation models for decision support in the development of biomass-based industrial district-heating networks in Italy. Applied Energy, 82:228–54.

Cho, H.; Mago, P. J.; Luck, R.; Chamra, L. M. (2009). Evaluation of CCHP systems performance based on operacional cost, primary energy consumption, and carbon dioxide emisión by utilizing an optimal operation scheme. Applied Energy, 86: 2540-49.

Chua, H. T.; Toh, H. K.; Malek, A.; Ng, K. C.; Srinivasan, K. (2000) A general thermodynamic framework for understanding the behavior of absorption chillers. International Journal of Refrigeration, 23: 491-507.

Daubert, T.E. (1987) Chemical engineering thermodynamic. McGraw-Hill, Singapore.

de Souza-Santos, M. L. (1989) Comprehensive Modelling and Simulation of Fluidized-Bed Boilers and Gasifiers. Fuel, 68: 1507-21.

Déglise, X.; Richard, C.; Rolin, A.; François, H. (1980) Influence de la température et du taux d'humidité sur la pyrolyse-éclair des déchets lingno-cellulosiques. Revue Générale de Thermique, 19:871–80.

Demirbas, A. (2004) Combustion characteristics of different biomass fuels. Progress in Energy and Combustion Science; 30: 219-30.

Demirbas, A. (2006) Biomass gasification for power generation in Turkey. Energy Source Part A, 28: 433-45.

Demuth, H.; Beale, M.; Hagan, M. (2008) Neural Network Toolbox User's Guide. The Mathworks Inc. Available online at: http://homes.ieu.edu.tr/~tince/matlab%20nnet.pdf

Dennis, J.S.; Lambert, R.S.; Milne, A.J.; Scott, S.A.; Hayhurst, A.N. (2005) The kinetics of combustion of chars derived from sewage sludge. Fuel, 84: 117-26.

Desrosiers R. (1979) Thermodynamics of gas-char reactions. In: Reed, T.B. (Ed.) A survey of biomass gasification. Solar Energy Research Institute, Colorado, USA.

Detournay, M.; Hemati, M.; Andreux, R. (2011) Biomass steam gasification in fluidized bed of inert or catalytic particles. Comparison between experimental results and thermodynamic equilibrium predictions. Powder Technology, 208: 558-67.

Deydier, A.; Marias, F.; Bernada, P.; Couture, F.; Michon, U. (2011) Equilibrium model for a travelling bed gasifier. Biomas and Bioenergy, 35: 133 – 45.

Di Blasi, C. (1997) Influences of physical properties on biomass devolatilization characteristics, Fuel 76: 957–64.

Di Blasi, C.; Signorelli, G.; Di Russo, C.; Rea, G. (1999) Product distribution from pyrolysis of wood and agricultural residues, Industrial and Engineering Chemistry Research, 38: 2216–24.

Di Blasi (2000) Dynamic behaviour of stratified downdraft gasifiers. Chemical Engineering Science, 55: 2931-44.

Di Blasi, C. (2008) Modeling chemical and physical processes of wood and biomass pyrolysis, Progress in Energy and Combustion Science, 34: 47–90.

Doherty, W.; Reynolds, A.; Kennedy, D. (2008) Simulation of a Circulating Fluidised Bed Biomass Gasifier Using ASPEN Plus – A Performance Analysis. In Ziebik, A.; Kolenda, Z.; Stanek, W. (Eds.) Proceedings of the 21st International Conference on Efficiency, Cost, Optimization, Simulation and Environmental Impact of Energy Systems, 24-27 June 2008, Krakow, Poland.

Doherty, W.; Reynolds, A.; Kennedy, D. (2009) The effect of air preheating in a biomass CFB gasifier using Aspen Plus simulation. Biomass and Bioenergy, 33:1158-67.

Doherty, W.; Reynolds, A.; Kennedy, D. (2010) Computer simulation of a biomass gasification-solid oxide fuel cell power system using Aspen Plus. Energy, 35: 4545 – 55.

Double, J.M.; Smith, E.L.; Bridgwater, A.V. (1989) Computer modeling of fluidized bed gasifier. In: Ferrero, G.L.; Maniatis, K.; Buekens, A. (Eds.) Process and Gasification. Elsevier Applied Science, London, UK, pp. 651- 55.

Douglas, P.L.; Young, B.E. (1990) Modelling and simulation of an AFBC steam heating plant using ASPEN/SP. Fuel, 70: 145–54.

Drogu, M.; Howarth, C.R.; Akay, G.; Keskinler, B.; Malik, A.A. (2002) Gasification of hazelnut shells in a downdraft gasifier. Energy, 27: 415-27.

Ebeling, J.M.; Jenkins, B.M. (1985) Physical and chemical properties of biomass fuels. Transactions of the American Society of Agricultural Engineers, 28: 898-902.

EC - European Comission (2005) Biomass Green Energy for Europe. Available online at: http://ec.europa.eu/research/energy/pdf/biomass_en.pdf

EC (2004) Directive 2004/8/EC of the European Parliament and the Council of 11 February 2004 on the promotion of cogeneration based on a useful heat demand in internal energy market and amending Directive 92/42/EEC. Official Journal of the European Union, L 52/50, 21st February 2004.

EES (2010) “EES – Engineering Equation Solver”, Middleton, WI: F-Chart Software. Academic Professional Version V 8.649

EPA (U.S. Environmental Protection Agency) (2008) Catalog of CHP Technologies. Available online at: http://www.epa.gov/chp/documents/catalog_chptech_intro.pdf

EQTEC Iberia (2011) Brochure Movialsa Gasification Plant. Available online at: www.eqtec.es

Erlich, A.; Fransson, T.H. (2011) Downdraft gasification of pellets made of wood, palm-oil residues respective bagasse: Experimental Study. Applied Energy, 88: 899-908.

Esteban, L.S.; Carrasco, J.E. (2011) Biomass resources and costs: Assessment in different EU countries. Biomass and Bioenergy, doi:10.1016/j.biombioe.2011.03.045

Faaij A. (2007) Potential contribution of bioenergy to the world's future energy demand, IEA Bioenergy, ExCo: 2007:02. Available online at: http://www.idahoforests.org/img/pdf/PotentialContribution.pdf

Faaij, A.; van Ree, R.; Waldheim, L; Olsson, E.; Oudhuis, A.; van Wijk, A.; Daey-Ouwens, C.; Turkenburg, W. (1997) Gasification of biomass wastes and residues for electricity production. Biomass and Bioenergy, 12: 387 – 407.

Fagbemi, L.; Khezami, L.; Capart, R. (2001) Pyrolysis products from different biomasses: application to the thermal cracking of tar, Applied Energy, 69: 293–306.

Fermoso, J.; Arias, B.; Pevida, C.; Plaza, M.G.; Rubiera, F.; Pis, J.J. (2008) Kinetic models comparison for steam gasification of different nature fuel chars. Journal of Thermal Analysis and Calorimetry, 91: 779–86.

Figueiredo, J. L.; Valenzuela, C.; Bernalte, A.; Encinar, J.M. (1989) Pyrolysis of holm-oak wood: influence of temperature and particle size. Fuel 68: 1012-16.

Fiaschi D, Michelini M. (2001) A two-phase one-dimensional biomass gasification kinetic model. Biomass Bioenergy, 21:121-32.

Filho, P.A.; Badr, O. (2004) Biomass resources for energy in North-Eastern Brazil. Applied Energy, 77:51–67.

Flamos, A.; Georgallis, P.G.; Doukas, H.; Psarras, J. (2011) Using Biomass to Achieve European Union Energy Targets—A Review of Biomass Status, Potential, and Supporting Policies. International Journal of Green Energy, 8: 411-28

Fock, F.; Thomsen, K. (1999) Modellering af totrinsforgasser, ET-EP 99-10A. Institut for Energiteknik, Technical University of Denmark, Denmark.

Fock, F.; Thomsen, K. (2000) Optimering af koncepter for medstrømsforgasning, ET-EP 99-10B Institut for Energiteknik, Technical University of Denmark, Denmark.

Garson, G. D. (1991) Interpreting neural-network connection weights, AI Expert 6: 47–51.

Gautam, G. (2010) Parametric Study of a Commercial-Scale Biomass Downdraft Gasifier: Experiments and Equilibrium Modeling. Master's Thesis. Auburn University, Alabama, USA.

GE Jenbacher (2008) Technical specifications of cogeneration modules JMS 320 GS-S.L.; JMS 616 GS-S.L.; JMS 620 GS-S/N.L.

Gerber, S.; Behrendt, F.; Oevermann, M. (2010) An Eulerian modeling approach of wood gasification in a bubbling fluidized bed reactor using char as bed material. Fuel, 89: 2903-17.

Gil, J.; Aznar, M. P.; Caballero, M. A.; Francés, E.; Corella, J. (1997) Biomass Gasification in Fluidized Bed at Pilot Scale with Steam-Oxygen Mixtures. Product Distribution for Very Different Operating Conditions. Energy and Fuels, 11: 1109-18.

Giltrap, D.L.; McKibbin, R.; Barnes, G.R.G. (2003) A steady state model of gas–char reactions in a downdraft gasifier. Solar Energy, 74: 85–91.

Gøbel, B.; Bentzen, J.D. (1995) Dynamisk model af totrinsforgasningsprocessen, ET-PER 95-13, Laboratoriet for Energiteknik, Technical University of Denmark, Denmark.

Gøbel, B.; Bentzen, J. D.; Hindsgaul, C.; Henriksen, U.; Ahrenfeldt, J.; Fock, F.; Houbak, N.; Qvale, B. (2002) High Performance Gasification with the Two-Stage Gasifier. Proceedings of the 12th European conference on biomass for energy, industry and climate protection,17-21 June 2002, Amsterdam, The Netherlands, pp. 389-95.

Gøbel, B.; Henriksen, U.; Jensen, T.K.; Qvale, B.; Houbak, N. (2007) The development of a computer model for a fixed bed gasifier and its use for optimization and control. Bioresource Technology, 98: 2043–52.

Gomez, C.J.; Mitta, N.R.; Velo, E.; Puigjaner, L. (2007) Modelling and simulation of a biomass pyrolysis unit within a gasification-based plant. In: Plesu, V.; Agachi, P.S. Proceedings of the 17th European Symposium on Computer Aided Process Engineering, 27-30 May 2007, Bucharest, Romania, Elsevier.

Gómez, A.; Rodrigues, M.; Montañés, C.; Dopazo, C.; Fueyo, N. (2010a) The potential for electricity generation from crop and forestry residues in Spain. Biomass and Bioenergy 34: 703-19.

Gómez, A.; Zubizarreta, J.; Rodrigues, M.; Dopazo, C.; Fueyo, N. (2010b) An estimation of the energy potential of agro-industrial residues in Spain. Resources, Conservation and Recycling, 54: 972-84.

Gómez-Barea, A.; Leckner, B. (2010) Modeling of biomass gasification in fluidized bed. Progress in Energy and Combustion Science, 36: 444–509.

Gómez-Barea, A.; Nilsson, S.; Vidal Barrero, F.; Campoy, M. (2010) Devolatilization of wood and wastes in fluidized bed. Fuel Processing Technology, 91: 1624-33.

Gommed, K.; Grossman, G. (1990) Performance Analysis of Staged Absorption Heat Pumps: Water-Lithium Bromide Systems. ASHRAE Transactions 96 Part 1, 1590-98

Gordillo, E.D.; Belghit, A. (2011) A downdraft high temperature steam-only solar gasifier of biomass char: A modelling study. Biomass and Bioenergy, 35: 2034-43.

Gordon, J. M.; Ng, K. C. (1995) Predictive and diagnostic aspects of a universal thermodynamic model for chillers. International Journal of Heat and Mass Transfer, 38: 807-18.

Grace, J.R.; Li, X.T.; Lim, C.J. (2001) Equilibrium modelling of catalytic steam reforming of methane in membrane reactors with oxygen addition. Catalysts Today, 64: 141–49.

Gumz, W. (1950) Gas producers and blast furnaces. Wiley, New York, USA.

Guo, B.; Li, D.; Cheng, C.; Lu, Z.; Shen, Y. (2001) Simulation of biomass gasification with a hybrid neural network model. Bioresource Technology, 76: 77-83.

Hagan, M.T.; Menhaj, M.B. (1994) Training Feedforward Networks with the Marquardt Algorithm. IEEE Transactions on Neural Networks, 5: 989‐93.

Hajaligol, M.R.; Howard, J.B.; Longwell, J.P.; Peters, W.A (1982) Product compositions and kinetics for rapid pyrolysis of cellulose, Industrial and Engineering Chemistry Design and Development, 21: 457–65.

Hamzaoui, Y. El.; Hernandez,J.A.; Silva-Martinez,S.; Bassam, A.; Alvarez, A.; Lizama-Bahena,C. (2011) Optimal performance of COD removal during aqueous treatment of alazine

and gesaprim commercial herbicides by direct and inverse neural network. Desalination, 227: 325-37.

Hanaoka, T.; Minowa, T.; Miyamoto, A.; Edashige, Y. (2005) Effect of Chemicals property of waste biomass on air-steam gasification. Journal of the Japan Institute of Energy, 84: 1012-18.

Hannula, I; Kurkela, E. (2010) A semi-empirical model for pressurised air-blown fluidised-bed gasification of biomass. Bioresource Technology, 101: 4608 – 15.

Haryanto, A.; Fernando, S.D.; Pordesimo, L.O.; Adhikarid, S. (2009) Upgrading of syngas derived from biomass gasification: A thermodynamic analysis. Biomass and Bioenergy, 33: 882-89.

Heeb, R. (2010) B&W Vølund – Up-date on the Harboøre Technology. PowerPoint presentation given at course on thermal gasification of biomass at The Danish Society of Engineers (IDA), 10 May 2010, Copenhagen, Denmark.

Hellmann, H.M.; Ziegler, F. (1999) Simple Absorption Heat Pump Modules for System Simulation Programs. ASHRAE Transactions, 105: 780-87.

Hellmann, H.M.; Schweigler, C.; Ziegler, F. (1999) The characteristic equations of absorption chillers. Proceedings of the International Sorption Heat Pump Conference, 24-26 March 1999, Munich, Germany, pp. 169-72.

Highman, C.; Van der Burgt, M. (2008) Gasification 2nd Edition. Elselvier. USA

Hislop, D.; Hall, O. (1996) Biomass resources for gasification power plant, ETSU B/M3/00388/31/REP, Contractor: Energy For Sustainable Development Ltd, Kings College, University of London, UK.

Horne, P.A.; Williams, P.T. (1996) Influence of temperature on the products from the flash pyrolysis of biomass, Fuel: 75:1051-59.

Hornik, K. (1991) Approximation capabilities of multilayer feedforward networks. Neural Networks, 4: 251 - 57.

Huang, H.-J.; Ramaswamy, S. (2009) Modeling biomass gasification using thermodynamic equilibrium approach. Applied Biochemistry and Biotechnology, 154: 193-204.

Huang, Y.; Wang, Y.D.; Rezvani, S.; McIlveen-Wright, D.R.; Anderson, M.; Hewitt, N.J. (2011) Biomass fuelled trigeneration system in selected buildings. Energy Conversion and Management, 52: 2448-54.

IDAE (2005) Plan de Energías Renovables en España 2005-2010. Available online at: http://www.idae.es/index.php/mod.pags/mem.detalle/idpag.14/relcategoria.1153/relmenu.12

IDAE (2011) Plan de Acción Nacional en Materia de Energías Renovables (PANER 2011-2020) Draft version of the 26th July, 2011. Available online at: http://www.idae.es/index.php/id.670/mod.pags/mem.detalle

International Energy Agency (IEA) - www.iea.org.

International Energy Agency (IEA) (2007) Biomass for power generation and CHP. IEA Energy Technology Essentials, OECD/IEA, Paris, France, January 2007.

Jager-Waldau, A.; Ossenbrink, H. (2003) Progress of electricity from biomass, wind and photovoltaics in the European Union. Renewable and Sustainable Energy Reviews, 8:157–82.

Jand, N.; Foscolo, P.U. (2005) Decomposition of wood particles in fluidized beds, Industrial Engineering and Chemistry Research, 44: 5079–89.

Jarungthammachote, S.; Dutta, A. (2007) Thermodynamic equilibrium model and second law analysis of a downdraft waste gasifier. Energy, 32: 1660-69.

Jarungthammachote, S.; Dutta, A. (2008) Equilibrium modeling of gasification: Gibbs free energy minimisation approach and its application to spouted bed and spout-fluid bed gasifiers. Energy Conversion and Management, 49: 1345-56.

Jayah, T.H.; Aye, L.; Fuller, R.J.; Stewart, D.F. (2003) Computer simulation of a downdraft wood gasifier for tea drying. Biomass and Bioenergy, 25: 459-69.

Jenkins, B.M.; Baxter, L.L.; Miles, T.R.; Miles, T.R. (1998) Combustion properties of biomass, Fuel Processing Technology, 54: 17- 46.

Jiang, H.; Morey, R.V. (1992) Pyrolysis of corncobs at fluidization, Biomass and Bioenergy 3: 81–85.

Kaewluan, S.; Pipatmanomai, S. (2011) Potential of synthesis gas production from rubber wood chip gasification in a bubbling fluidized bed gasifier. Energy Conversion and Management, 52: 75-84.

Karamarkovic, R.; Karamarkovic, V. (2009) Exergy and energy analysis of biomass gasification at different temperatures. Energy, 35: 537-49.

Kersten, S.R.A.; Prins, W.; Van der Drift, A.; Van Swaaij, W.P.M. (2002) Interpretation of biomass gasification by “quasi”-equilibrium models. In: Palz, W.; Spitzer, J.; Maniatis, K.; Kwant, K.; Helm, P.; Grassi, A. (Eds.) Proceedings of the 12th European conference on biomass for energy, industry and climate protection,17-21 June 2002, Amsterdam, The Netherlands.

Kersten, S.R.A.; Wang, X.; Prins, W.; Van Swaaij, W.P.M. (2005) Biomass pyrolysis in a fluidized bed reactor. Part 1: Literature review and model simulations, Industrial and Engineering Chemistry Research, 44: 8773–85.

Khataee, A.R.; Mirzajani,O. (2010) UV/peroxydisulfate oxidation of C. I. Basic Blue 3: Modeling of key factors by artificial neural network. Desalination, 251: 64-69.

Kim, D.S.; Infante Ferreira, C.A. (2008) Analytic modelling of steady state single-effect absorption cycles. International Journal of Refrigeration, 31: 1012-20.

Kishore, V.V.N. (Ed.) (2008) Renewable Energy Engineering and Technology a knowledge compendium. The Energy and Resources Institute, New Delhi, India.

Klass, D.L. (1998). Biomass for renewable energy, fuels, and chemicals. Academic Press, San Diego, CA, USA.

Knack, O.; Barin, I. (1973) Thermodynamic properties of inorganic substances. Springer-Verlag, Berlin, Germany.

Knoef, H.A.M. (Ed.) (2005) Handbook biomass gasification. BTG biomass technology group B.V, Meppel, The Nederlands.

Kosstrin, H. (1980) Direct formation of pyrolysis oil from biomass. In Proceedings specialists workshop on fast pyrolysis of biomass. 19–22 October 1980, Copper Mountain, Colorado, pp. 105–21.

Kühn, A.; Ziegler, F. (2005) Operational Results of a 10 kW Absorption Chiller and Adaptation of the Characteristic Equation, Proceedings of the 1st International Conference Solar Air Conditioning, 6-7 October 2005, Bad-Staffelstein, Germany.

Kundsen, R.A.; Bailey, T.; Fabiano, L.A. (1982) Experience with ASPEN while simulating a new methanol plant. AIChE Symposium Series, 78: 214.

Kurkela, E. (2006) CHP plants based on biomass gasification – EU BIGPower project 2005-2008, VTT – Technical Research Centre of Finland. PowerPoint presentation, January 2006.

Kwant, K.W.; Knoef, H. (2004) Status of Gasification in countries participating in the IEA Bioenergy and GasNet activity. Available online at: http://www.energytech.at/pdf/status_of_gasification_08_2004.pdf

Labriet, M.; Cabal, H.; Lecho, Y.; Giannakidis, G.; Kanudia, A. (2010) The implementation of the EU renewable directive in Spain. Strategies and Challenges Energy Policy, 38: 2272–81.

Larminie, J.; Dicks, A. (2003) Fuel cell systems explained. 2nd Edition. John Wiley & Sons, Chichester, UK.

Larsen, E. (1999), Personal communication to F. Fock and K. Thomsen during the measurements of week 45, Risø DTU – National Laboratory for Sustainable Energy, July 1999.

Lecuona, A.; Ventas, R.; Venegas, M. C.; Zacarías, A.; Salgado, R. (2008) Temperatura de generación óptima en instalaciones de frío solar haciendo uso de la ecuación característica. Proceedings of the XIV Congreso Ibérico y IX Congreso Iberoamericano de Energía Solar, 17-21 June 2008, Vigo, Spain, pp. 351-356.

Lee, H.G.; Chung, K.M.; Kim, C.; Han, S.H.; Kim, H.T. (1992) Coal gasification simulation using ASPEN PLUS. In: US–Korea joint workshop on coal utilization technology, pages 447–74.

Levenberg, K. (1944) A Method for the Solution of Certain Non‐linear Problems in Least Squares. Quarterly of Applied Mathematics, 2: 164‐68.

Li, X. (2002) Biomass gasification in a circulating fluidised bed. Ph.D. Thesis. University of British Columbia, USA.

Li, X.; Grace, J.R.; Watkinson, A.P.; Lim, C.J.; Ergüdenler, A. (2001) Equilibrium modeling of gasification: a free energy minimization approach and its application to circulating fluidized bed coal gasifier. Fuel, 80: 195-207.

Li, X.T.; Grace, J.R.; Lim, C.J.; Watkinson, A.P.; Chen, H.P.; Kim, J.R. (2004) Biomass gasification in a circulating fluidized bed. Biomass and bioenergy, 26: 171-93.

Loha, C.; Chatterjee, P. K.; Chattopadhyay, H. (2011) Performance of fluidized bed steam gasification of biomass – Modeling and experiment. Energy Conversion and Management, 52: 1583 – 88.

Lucas, C.; Szewczyk, D.; Blasiak, W.; Mochida, S. (2004) High-temperature air and steam gasification of densified biofuels. Biomass and Bioenergy, 27: 563-75.

Lv, P.; Xiong, Z.H.; Chang, J.; Wu, C.; Chen, Y.; Zhu, J. (2004) An experimental study on biomass air–steam gasification in a fluidized bed. Bioresource Technology, 95: 95-101

Lv, P.; Yuan, Z.; Ma, L.; Wu, C.; Chen, Y.; Zhu, J. (2007) Hydrogen-rich gas production from biomass air and oxygen/steam gasification in a downdraft gasifier. Renewable Energy, 32: 2173-85.

Maniatis, K. (2001) Progress in biomass gasification: an overview. In: Bridgwater, A.V. (Ed.) Progress in thermochemical biomass conversion. Blackwell Science Ltd, Oxford, UK, pp. 1-31.

Maniatis, K.; Guiu, G.; Riesgo, J. (2002) The european commission perspective in biomass and waste thermochemical conversion. In: Bridgwater, A.V. (Ed.) Pyrolysis and Gasification of Biomass and Waste. Proceedings of an Expert Meeting, CPL Press, Newbury, October 2002, pp. 1 – 18.

Manohar, H.J.; Saravanan, R.; Renganarayanan, S. (2006) Modelling of steam fired double effect vapour absorption chiller using neural network. Energy Conversion and Management, 47: 2202-10.

Mansaray, K.G.; Al-Taweel, A.M.; Ghaly, A.E.; Hamdullahpur, F.; Ugursal, V.I. (2000a) Mathematical modeling of a fluidized bed rice husk gasifier: Part I Model Development. Energy Sources, 22: 83–98.

Mansaray, K.G.; Al-Taweel, A.M.; Ghaly, A.E.; Hamdullahpur, F.; Ugursal, V.I. (2000b) Mathematical modeling of a fluidized bed rice husk gasifier: Part II Model Sensitivity. Energy Sources, 22: 167-85.

Mansaray, K.G.; Al-Taweel, A.M.; Ghaly, A.E.; Hamdullahpur, F.; Ugursal, V.I. (2000c) Mathematical modeling of a fluidized bed rice husk gasifier: Part III Model Verification. Energy Sources, 22: 281-96.

Marquardt, D.W. (1963) An Algorithm for Least‐Squares Estimation of Nonlinear Parameters. Journal of the Society for Industrial and Applied Mathematics, 11: 431‐41.

Mathieu, P.; Dubuisson, R. (2002) Performance analysis of a biomass gasifier. Energy Conversion and Management, 43: 1291-99.

Matlab (2010) Matlab Neural Network Toolbox. Version 7.10.0.499 R2010a. MathWorks Inc.

McDonald, C.F.; Rodgers, C. (2008) Small recuperated ceramic microturbine demonstrator concept. Applied Thermal Engineering, 28: 60-74.

McKendry, P. (2002a) Energy production from biomass (part 1): Overview of biomass. Bioresource Technology, 83: 37-46.

McKendry, P. (2002b) Energy production from biomass (part 2): Conversion Technologies. Bioresource Technology, 83: 47-54.

McKendry, P. (2002c) Energy production from biomass (part 3): Gasification technologies. Bioresource Technology, 83: 55-63.

Melgar, A.; Pérez, J.F.; Laget, H.; Hornillo, A. (2007) Thermochemical equilibrium modelling of gasifying process. Energy Conversion and Management, 48: 59-67.

Meshram, J.R.; Mohan, S. (2007) Biomass power and its role in distributed power generation in India. In: 25 years of renewable energy in India. New Delhi: Ministry of New and Renewable Energy; p. 109-34.

Milligan, J.B. (1994) Downdraft gasification of biomass. Ph.D. thesis, Aston University, Birmingham, UK.

Mitta, N.R.; Ferrer-Nadal, S.; Lazovic, A.M.; Perales, J.F.; Velo, E.; Puigjaner, L. (2006) Modelling and simulation of a tyre gasification plant for synthesis gas production. Proceedings of 16th European Symposium on Computed Aided Process Engineering and 9th International Symposium on Process Systems Engineering, Garmisch-Partenkirchen, Germany, July 2006, pp. 1771-76.

MITYC - Ministerio de Industria Turismo y Comercio (2008). Registro administrativo de productores de electricidad en régimen especial (in Spanish). Available online at: http://www.mityc.es/energia/electricidad/RegimenEspecial/Paginas/Index.aspx.

MITYC – Ministerio de Industria Turismo y Comercio (2009). La Energía en España 2009 (in Spanish) Available online at: http://www.mityc.es/energia/balances/Balances/LibrosEnergia/Energia_2009.pdf

Moya, M. (2011) Sistemas avanzados de microtrigeneración con microturbinas de gas y enfriadoras por absorción con disipación por aire. Ph.D. Thesis. Mechanical Engineering Department. Rovira i Virgili University, Tarragona, Spain.

Narváez, I.; Orío, A; Aznar, M.P; Corella, J. (1996) Biomass gasification with air in an atmospheric bubbling fluidised bed. Effect of six operational variables on the quality of the produced raw gas. Industrial and Engineering Chemistry Research, 35: 2110-20.

Neves, D.; Thunman, H.; Seemann, M.; Ideias, P.; Matos, A.; Tarelho, L.; Gómez-Barea, (2009) A database on biomass pyrolysis for gasification applications, 17th European Biomass Conference, 29 June–3 July 2009, Hamburg, Germany.

Ng, K. C.; Chua, H. T.; Han, Q. (1997) On the modeling of absorption chillers with external and internal irreversibilities. Applied Thermal Engineering, 17: 413-25.

Ng, K. C.; Chua, H. T.; Han, Q. A.; Kashiwagi, T.; Akisawa, A.; Tsurusawa, T. (1999) Thermodynamic modeling of absorption chiller and comparison with experiments. Heat Transfer Engineering, 20: 42-51.

Nikoo, M.B.; Mahinpey, N. (2008) Simulation of biomass gasification in fluidized bed reactor using ASPEN PLUS. Biomass and Bioenergy, 32: 1245 – 54.

Nunn, T.R.; Howard, J.B.; Longwell, J.P.; Peters, W.A. (1985) Product compositions and kinetics in the rapid pyrolysis of sweet gum hardwood, Industrial and Engineering Chemistry Process Design and Development, 24: 836–844.

Nussbaumer, T.; Neuenschwander, P.; Hasler, P.; Bühler, R. (1997) Energie aus Holz - Vergleich der Verfahren zur Produktion von Wärme, Strom und Treibstoff aus Holz. Bundesamt für Energiewirtschaft, Bern, Switzerland.

Obernberger, I.; Carlsen, H.; Biedermann, F. (2003) State-of-the-art and future developments regarding smallscale biomass CHP systems with a special focus on ORC and Stirling engine technologies. In: International Nordic Bioenergy 2003 Conference of the Finnish Bioenergy Association, 2-5 September 2003, Jyvaeskylae, Finland, pp. 331-39.

Ortiga, J. (2010) Modelling environment for the design and optimization of energy polygeneration systems. Ph.D. thesis. Mechanical Engineering Department. Rovira i Virgili University, Tarragona, Spain.

Paviet, F.; Chazarenc, F.; Tazerout, M. (2009) Thermochemical equilibrium modelling of a biomass gasifying process using Aspen Plus. International Journal of Chemical Reactor Engineering, 7: A40.

Peters, B.; Bruch, C. (2003) Drying and pyrolysis of wood particles: experiments and simulation, Journal of Analytical and Applied Pyrolysis, 70: 233–50.

Peterson, D.; Haase, S. (2009) Market assessment of biomass gasification and combustion technology for small- and medium-scale applications. Technical Report NREL/TP-7A2-46190. National Renewable Energy Laboratory, Golden (CO), USA.

Phillips, J.N.; Erbes, M.R.; Eustis, R.H. (1986) Study of the off-design performance of integrated coal gasification. In: Combined cycle power plants, computer-aided engineering of energy systems, vol. 2—analysis and simulation, winter annual meeting of the American Society of Mechanical Engineers, Anaheim, CA, USA Conference.

Phyllis (2000) A database containing information on the composition of biomass and waste. ECN. Available online at: http://www.ecn.nl/phyllis.

Plis, P.; Wilk, R.K. (2011) Theoretical and experimental investigation of biomass gasification process in a fixed bed gasifier. Energy, 36: 3838-45.

Prins, M.J.; Ptasinski, K.J.; Janssen, F.J.J.G. (2003) Thermodynamics of gas-char reactions: first and second law analysis. Chemical Engineering Science, 58: 1003-11.

Prins, M.J.; Ptasinski, K.J.; Janssen, F.J.J.G. (2007) From coal to biomass gasification: comparison of thermodynamic efficiency. Energy, 32:1248–59.

Psichogios, D.C.; Ungar, L.H. (1992) A hybrid neural network-first principles approach to process modelling. AIChE Journal, 38: 1499 - 1511.

Puig-Arnavat, M.; López-Villada, J.; Bruno, J.C.; Coronas, A. (2010) Analysis and parameter identification for characteristic equations of single and double effect absorption chillers by means of multivariable regression. International Journal of Refrigeration, 33: 70-78.

Qiang, L.; Wen-Zhi, L.; Xi-Feng, Z. (2009) Overview of fuel properties of biomass fast pyrolysis oils. Energy Conversion and Management, 50: 1376-83.

Radmanesh, R.; Chaouki, J.; Guy, C. (2006) Biomass gasification in a Bubbling Fluidised Bed Reactor: Experiments and Modeling. AIChE Journal, 52: 4258-72.

Ramanan, M.V.; Lakshmanan, E.; Sethumadhavan, R.; Renganarayanan, S. (2008) Performance prediction and validation of equilibrium modelling for gasification of cashew nut shell char. Brazilian Journal of Chemical Engineering, 25: 585-601.

Rao, T.R.; Sharma, A. (1998) Pyrolysis rates of biomass materials, Energy, 23:973–78.

Rauch, R. (2003) Biomass gasification to produce synthesis gas for fuels and chemicals, report made for IEA Bioenergy Agreement, Task 33: Thermal Gasification of Biomass.

Raveendran, K.; Ganesh, A.; Khilar, K.C. (1996) Pyrolysis characteristics of biomass and biomass components, Fuel, 75: 987–98.

Reid, R.C.; Prausnitz, J.M.; Poling, B.E. (1987) The properties of gases and liquids 4th Edition. Mc-Graw Hill Inc.,New York, USA.

REN21. (2007) Renewables 2007, Global status report. Available online at: http://www.worldwatch.org/files/pdf/renewables2007.pdf.

Rentizelas, A.; Karellas, S.; Kakaras, E.; Tatsiopoulos, I. (2009) Comparative techno-economic analysis of ORC and gasification for bioenergy applications. Energy Conversion and Management, 50: 674-81.

Robinson, P.J.; Luyben, W.L. (2008) Simple dynamic gasifier model that runs in Aspen Dynamics. Industrial & engineering chemistry research. 47: 7784-92.

Roqueta, J.M.; Márquez, M. (2004) Trigeneración: el calor útil en la producción de frío. Cogen España, 2004.

Roshmi, A.; Murthy, J.; Hajaligol, M. (2004) Modeling of smoldering process in porous biomass fuel rod. Fuel, 83:1527-36.

Rotartica S.A. (2006) Catalogue available online at: http://andyschroder.com/rotartica.html Last accessed: August 2011.

Roy, P.C.; Datta, A.; Chakraborty, N. (2009) Modelling of a downdraft biomass gasifier with finite rate kinetics in the reduction zone. International Journal of Energy Research, 33: 833-51.

Royal Decree 661/2007 that regulates the electricity production in special regimen. (BOE-A-2007-10556) BOE num.126 of 26th of May 2007 pp. 22846-86.

Ruggiero, M.; Manfrida, G. (1999) An equilibrium model for biomass gasification processes. Renewable Energy, 16: 1106-09.

Sathyabhama, A.; Babu, T. P. A. (2008) Thermodynamic simulation of ammonia-water absorption refrigeration system. Thermal Science, 12: 45-53.

Schröder, E. (2004) Experiments on the pyrolysis of large beechwood particles in fixed beds. Journal of Analytical and Applied Pyrolysis, 71: 669–94.

Schuster, G.; Löffler, G.; Weigl, K.; Hofbauer, H. (2001) Biomass steam gasification: an extensive parametric modeling study. Bioresource Technology, 77:71-79.

Schwint, KT. (1985) Great plains ASPEN model development, methanol synthesis flowsheet. Final topical report, Scientific Design Co., Inc., USA.

Scott, D. S.; Piskorz, J.; Radlein, D. (1985) Liquid products from the continuous flash pyrolysis of biomass. Industrial and Engineering Chemistry Process Design and Development, 24: 581-88.

Scott, D. S.; Piskorz, J.; Bergougnou, M.A. (1988) The role of temperature in the fast pyrolysis of cellulose and wood. Industrial Engineering and Chemistry Research, 27: 8-15.

Sencan, A.; Yakut, K.A.; Kalogirou, S.A. (2006) Thermodynamic analysis of absorption systems using artificial neural network, Renewable Energy, 31: 29-43.

Senelwa, K. (1997) The air gasification of woody biomass from short rotation forests. Ph.D. Thesis, Massey University, New Zealand.

Sharma A.Kr. (2008) Equilibrium and kinetic modelling of char reduction reactions in a downdraft biomass gasifier: A comparison. Solar Energy, 52: 918-928.

Sheng, C.; Azevedo, J.L.T. (2005) Estimating the higher heating value of biomass fuels from basic analysis data. Biomass and Bioenergy, 28: 499-507.

Smith, W.R.; Missen, R.W. (1982) Chemical reaction equilibrium analysis: theory and algorithms. John Wiley & Sons, New York, USA.

Stassen, H.E.M.; Prins, W.; van Swaaij, W.P.M (2002) Thermal conversion of biomass into secondary products the case of gasification and pyrolysis. In: Palz, W.; Spitzer, J.; Maniatis, K.; Kwant, K.; Helm, P.; Grassi, A. (Eds.) Proceedings of the 12th European conference on biomass for energy, industry and climate protection,17-21 June 2002, Amsterdam, The Netherlands, pp. 38–44.

Steinbrecher, N.; Walter, J. (2001) Marktübersicht über dezentrale Holzvergasungsanlagen – Marktanalyse 2000 für Holzvergasungssysteme bis 5 MW, Ökoinstitut, April 2001, Darmstadt,Germany.

Stevens, D.J. (2001) Hot gas conditioning: Recent progress with large scale biomass gasification systems – Update and summary of recent progress. National Renewable Energy Laboratory, Subcontractor Report (NREL/SR-510-29952), Golden, CO, USA.

Sudiro, M.; Zanella, C.; Bressan, L.; Fontana, M.; Bertucco, A. (2009) Synthetic Natural Gas (SNG) from petcoke: model development and simulation. The 9th International Conference on Chemical and Process Engineering (ICheaP-9). 10-13 May 2009, Rome, Italy.

Sugiyama, S.; Suzuki, N.; Kato, Y.; Yoshikawa, K.; Omino, A.; Ishii, T.; Yoshikawa, K.; Kiga, T. (2005) Gasification performance of coals using high temperature air. Energy, 30: 399-413.

Sutton, D.; Kelleher, B.; Ross, J.R.H. (2001) Review of literature on catalysts for biomass gasification. Fuel Processing Technology, 73: 155-73.

TenWolde, A.; McNatt, J.D.; Krahn, L. (1988) Thermal properties of wood and wood panel products for use in buildings, DOE/USDA-21697/1, Oak Ridge National Laboratory, Oak Ridge, TN, USA.

Thunman, H.; Niklasson, F.; Johnsson, F.; Leckner, B. (2001) Composition of volatile gases and thermochemical properties of wood for modeling of fixed or fluidized beds, Energy and Fuels, 15: 1488–97.

Toft, A.J., (1996). A comparison of integrated biomass to electricity systems. Ph.D. thesis, Aston University, Birmingham, UK.

Traverso, A.; Magistri, L.; Scarpellini, R.; Massardo, A. (2003) Demonstration plant and expected performance of an externally fired micro gas turbine for distributed power generation. ASME Paper 2003-GT-38268.

Traverso, A.; Calzolari, F.; Massardo, A. (2005) Transient analysis of and control system for advanced cycles based on micro gas turbine technology. Journal of Engineering for Gas Turbines and Power, 127: 340-47.

van den Aarsen, F.G. (1985) Fluidised bed wood gasifier. Performance and modeling, PhD Thesis, University of Twente, The Netherlands.

van der Drift, A.; Van Doorn, J.; Vermeulen, J.W. (2001) Ten residual biomass fuels for circulating fluidized-bed gasification. Biomass and Bioenergy, 20: 45-46.

van der Meijden, C.M.; Veringa, H.J.; Rabou, L.P.L.M. (2010) The production of synthetic natural gas (SNG): A comparison of three wood gasification systems for energy balance and overall efficiency. Biomass and Bioenergy, 34: 302 – 11.

van Krevelen, D. W. (1950) Graphical-statistical method for the study of structure and reaction processes of coal. Fuel, 29: 269-284.

Varhegyi, G.; Jakab, E.; Antal, M.J. (1994) Is the broido-shafizadeh model for cellulose pyrolysis true? Energy and Fuels 8:1345–52.

Verma, S.P.; Andaverde, J.; Santoyo, E. (2006) Application of the error propagation theory in estimates of static formation temperatures in geothermal and petroleum boreholes. Energy Conversion and Management, 47: 3659–71.

Vincent, T.; Strenziok, R. (2007) The Micro Gas Turbine in Field Trials with Fermenter Biogas. Proceedings of the 15th European Biomass Conference & Exhibition. 7-11 May 2007, Berlin, Germany, pp. 2265-69.

Villanueva, A.L.; Gomez-Barea, A.; Revuelta, E.; Campoy, M.; Ollero, P. (2008) Guidelines for selection of gasifiers modelling strategies. Proceedings of the 16th European Biomass Conference and Exhibition, 2-6 June 2008, Valencia, Spain.

Wang, Y.; Kinoshita, C.M. (1993) Kinetic model of biomass gasification. Solar Energy, 51: 19-25.

Wang, W.; Cai, R.; Zhang, N. (2004) General characteristics of single shaft microturbine set at variable speed operation and its optimization. Applied Thermal Engineering, 24: 1851- 63.

Willis, M.J.; Di Massimo, C.; Montague, G.A.; Tham, M.T.; Morris, A.J. (1991) Artificial neural network in process engineering. IEE Proceedings-D, 138: 256–66 No.3

Wiltsee, G.; Emerson, H. (2003) Clean and Reliable Power and Heat from Digester Gas, in Anaerobic Digester Technology Applications in Animal Agriculture - A National Summit. 2003: Raleigh, North Carolina, USA.

Yan, H.M.; Rudolph, V. (2000) Modeling a compartmented fluidized bed coal gasifier process using ASPEN PLUS. Chemical Engineering Communication, 183:1–38.

Yang, Y.B.; Yamauchi, H.; Nasserzadeh, V. and Swithenbank, J. (2003) Effect of fuel devolatilization on the combustion of wood chips and incineration of simulated municipal wastes in packed bed. Fuel, 82: 2205-21.

Yang, W.; Ponzio, A.; Lucas, C.; Blasiak, W. (2006) Performance analysis of a fixed-bed biomass gasifier using high-temperature air. Fuel Processing Technology, 87: 235-45.

Yong, L. (2003) Introduction of Small-scale biomass gasification – electricity generation systems. International Conference on Bioenergy Utilization and Environment Protection 6th LAMNET Project Workshop, 24-26 September 2003, Dalian, China.

Yoshida, H.; Kiyon, F.; Tajima, H.; Yamasaki, A.; Ogasawara, K.; Masuyama, T. (2008) Two-stage equilibrium model for a coal gasifier to predict the accurate carbon conversion in hydrogen production. Fuel, 87: 2186–93.

Zainal, Z.A.; Ali, R.; Lean, C.H.; Seetharamu, K.N. (2001) Prediction of performance of a downdraft gasifier using equilibrium modeling for different biomass materials. Energy Conversion and Management 42: 1499-515.

Zainal, Z.A.; Ali, R.; Quadir, G.; Seetharamu, K.N. (2002) Experimental investigations of a downdraft biomass gasifier. Biomass and Bioenergy, 23: 283–89.

Zanzi, R.; Sjostrom, K.; Bjornbom, E. (1996) Rapid high-temperature pyrolysis of biomass in a free-fall reactor. Fuel, 75: 545-50.

Zhong, L. D.; Mei, W. H.; Hong, Z. (2009) Kinetic model establishment and verification of the biomass gasification fluidised bed. Proceedings of the 8th International Conference on Machine Learning and Cybernetics, 12-15 July 2009, Baoding, China.